Palaeoenvironmental reconstruction on the basis of Quaternary palaeo dune sequences on Fuerteventura

Dissertation

zur Erlangung des akademischen Grades

Doctor rerum naturalium (Dr. rer. nat.)

der Fakultät Umweltwissenschaften,

Technische Universität Dresden

vorgelegt von

Dipl.-Geogr. Christopher-Bastian Roettig

Gutachter & Betreuer:

Prof. Dr. Dr. Dominik Faust

Professur Physische Geographie
Institut für Geographie
Fakultät Umweltwissenschaften
TU Dresden

Gutachter:

Prof. Dr. Jürgen Heinrich

Professur für Physische Geographie und landschaftsbezogene Umweltforschung
Universität Leipzig

Gutachter:

Prof. h.c. Dr. Hartmut Heinrich

10°E maritime consulting
Hamburg

Übereinstimmungserklärung

Die Übereinstimmung dieses Exemplars mit dem Original der Dissertation zum Thema:

„Palaeoenvironmental reconstruction on the basis of
Quaternary palaeo dune sequences on Fuerteventura“

wird hiermit bestätigt.

Dresden, 01.03.2019
.....

Ort, Datum

Christopher-D. Daelly
.....

Unterschrift (Name, Vorname)

Abstract

The volcanic origin of the Canarian Archipelago widely determines the landscape of these islands. Partially in coastal near areas the volcanic rocks are covered by dune fields. The eastern Canary Islands show the largest areas of sand deposits. On northern Fuerteventura sandpits and deep incised gully systems allow broader insight into generations of these archives. The dune material originates from the shallow shelf. Hence, the mineral composition is dominated by calcite and aragonite. The outcrops show the layering of several generations of biogenic carbonate sands which are separated by palaeosurfaces. These surfaces suggest soil-forming processes by their (often) reddish colour. Generally, the occurrence of several palaeosurfaces promises a high potential of those Quaternary dune archives on northern Fuerteventura. Former studies focussed on just few quarries being situated in close distances. Differing formation concepts and contradicting chronologies (Middle to Late Pleistocene versus Late Pleistocene) suggest the need for further investigation of landward palaeo dune sections, resulting in a DFG funded project with regard to palaeo dune sequences within the catchments of two Barrancos on northern Fuerteventura. Firstly, the project called for defining representative sections of the two catchments for the purpose of working out a correlation and deducing a standard profile, both should be based on stratigraphic findings. IRSL dating shall contribute to finally establishing a chrono-stratigraphy. Besides the carbonate sands, the dune archives are influenced by the imprint of volcanic material (tephra, lapilli, and basaltic rock) and Saharan dust. Generally, the archives' composition and appearance raise several further questions: Are periods of surface formation dependent on reduced sand supply or on changes in climatic conditions? Which soil forming processes contribute to the characteristics of palaeosurface layers? How about the influence of Saharan dust? As dating of lava flows on northern Fuerteventura revealed Middle to Late Pleistocene ages, a further question refers to the relationship of dune formation and volcanic activity.

Mainly deduced from findings in the field but also by use of grain size distribution, elemental composition, content of $CaCO_3$, determination of Fe_d, measurements of rock magnetic parameters, analyses of gastropod associations, micromorphological analyses, determination of quartz content via Morphologi G3-ID measurements, XRD analyses, and IRSL dating, this thesis provides a chronostratigraphy of palaeo dune archives of northern Fuerteventura deduced from a correlation of sections close to the western coast and sections close to the eastern coast. The derived standard profile shows 15 units divided into 5 main sequences. These 5 sequences mainly differ in sand supply and accumulation, in

changing humidity, and in imprint of volcanic activity. The chrono-stratigraphy dates back to about 450 ka. Generally, the archives are very site-specific, because features of a stratigraphic layer often change within close distances, depending on connectivity to erosion pathways and distance to sand sources. Micromorphological analyses indicate soil forming processes which are restricted to de- and recalcification and recrystallisation of iron and manganese. Ultimately, the palaeosurfaces are primarily dominated by the characteristics of Saharan dust (silt dominated, yellow to red in colour, containing hematite and goethite). The archives indicate a cyclicity of predominant processes, starting with I) sand accumulation, followed by II) dust accumulation and weak soil formation, leading to III) water-induced relocation. On the basis of this cyclicity a conceptual approach of the archives' relationship to changes in sea level could be drawn. We assume highest sand supply during starting regression after sea level maxima. With dropping sea level, the distance between the studied sites and the sand source area (which are the gradually exposed shallow shelf areas) increases, leading to reduced sand accumulation. Starting transgression at the end of glacials suggests the lowest potential of sand accumulation. Furthermore, the concept is based on the assumption that with lower sea levels, more precipitation can reach the Canary Islands. Deduced from periods of lowest potential of sand accumulation in combination with periods of increased precipitation, best conditions for predominant dust accumulation and in-situ processes should be given at terminations. Generally, prevalence of palaeosurface formation is related to transgression periods. These periods are in good agreement with increased dust supply, which, in turn, seem to be affected by precession minima (according to Moreno et al., 2001). The predominance of dust accumulation and in-situ processes causes the fining of sediments, leading to reduced morphological resistance and, finally, water-induced relocation. Ultimately, site-specific sand availability seems to determine whether surfaces are exposed for longer durations, whereas the availability of precipitation (and dust) suggests determining the intensity of surface formation.

The studied sections indicate a strong relationship to local volcanic activity because lava flows are able to cut off sand pathways and cover former sand source areas. In combination with dated lava flows the findings point to three different periods of volcanic activity which ceased the sand supply gradually. A first period around 180-170 ka, a next period around 135 ka, and a third period after 100 ka but latest around 50 ka which, finally, completely stopped the sand supply. Regarding the northern part of Fuerteventura, the latest period has so far not been described.

Contents

List of figures

List of tables

List of abbreviations and units

Abbreviations

asl	above sea level
BCs	brood cells
ca.	circa
cf.	compare
c/f-ratio	coarse to fine ratio (according to Stoops, 2003)
COHMAP	cooperative Holocene mapping project
$\dot{D}$	dose rate
DFG	German research foundation
DWD	German Meteorological Service
E	east
e.g.	for example
ESR dating	electron spin resonance dating
et al.	and others
etc.	etcetera
Fe_d	pedogenic iron (soluble in dithionic acid)
Fe_t	total amount of iron
Fig.	figure
GFZ	German research centre for geoscience
HCl	hydrochloric acid
ICP-MS	inductively coupled plasma - mass spectrometry
ICP-OES	inductively coupled plasma – optical emission spectrometry
i.e.	in other words
IRSL	infrared stimulated luminescence
K-Ar dating	potassium–argon dating
N	north
NE	northeast
n.m.	not measured
NW	northwest
p.	page
PMIP	paleoclimate modelling intercomparison project
SAR	single aliquot regenerative-dose

SE	southeast
SL	sediment layer
sp.	species
SW	southwest
Tab.	table
TL	thermo luminescence
U-Th dating	uranium-thorium dating
W	west
XRD	X-ray diffraction
XRF	X-ray fluorescence
χ	magnetic susceptibility

Units

°	degree
°C	Celsius degree
%	percentage
cm	centimetre
d	day
g	gram
h	hour
ka	thousand years
kg	kilogram
km	kilometre
kW	kilowatt
l	litre
m	metre
Ma	million years
mm	milimetre
µm	micrometre
nm	nanometre
s	second
wt%	weight percentage
yr	year

Preliminary remarks

In the 2000s Prof. Faust (TU Dresden) and Prof. Zöller (University Bayreuth) discovered dune palaeosol sequences cropping out in diverse sand pits and gully systems on northern Fuerteventura. The vast number of different dune generations separated by more than eight intercalated palaeosols suggested high potential of those archives and led to a small-scale project, funded by the German Research Foundation (FA-239/15-1). As a result of that successfully completed small-scale project (the corresponding results are published in Faust et al., 2015), a large-scale project was granted (FA-239/18-1). The project, named "Aeolianite Soil Sequences of Fuerteventura and Central Spain – stadial/interstadial sequences and differing climatic zones", aimed to correlate loess archives of central Spain and dune palaeosol sequences of Fuerteventura. Accordingly, this project requested first reliable stratigraphies and standard profiles for both study areas. The here presented thesis addresses the palaeo dune archives of northern Fuerteventura the objectives to

I) develop a stratigraphic correlation of different sites within the dune fields and

II) derive a stratigraphic standard profile

define the key tasks of the here presented thesis (detailed objectives are given in Chapter 1.4). Both a correlation and a standard profile require deeper insight into the environmental system's behaviour. Since April 2014 several field trips to Fuerteventura have yielded new perspectives and led to an intense development within the working group of how to interpret the studied palaeo dune archives.

Statement of authorship

I hereby declare that as the author of the work presented here I assume full responsibility for all relevant decisions during the project. Thus, I was responsible for determining sampling sites, deciding on a sampling strategy and deciding which methods should be applied (of course within the framework of the approved project). Additionally, all of the main interpretations and conclusions are my responsibility. Nevertheless, I was supported throughout the study first and foremost by my supervisor, Prof. Dominik Faust, as well as the working group and numerous colleagues. Thus, I always had the possibility to discuss all decisions and to weigh up the preferable next step. Gratefully, and with all due to respect

to my supervisor, the members of the working group, and my discussion partners, this thesis is written in the plural form.

1 Introduction

1.1 Carbonate sands and carbonate aeolianites – a general perspective

Definition and distribution

In 1931 Sayles introduced the term "aeolianite" and defined it as every wind-blown sediment being lithified after deposition. Several decades later Fairbridge and Johnson (1978) established the definition of "aeolianite" as being restricted to consolidated carbonate sands. Accordingly, only lithification differentiates between aeolianites in the strict sense and unconsolidated carbonate sands. Since the term "aeolianite" archives is very common in the literature, thus an overview concerning both carbonate aeolianite and unconsolidated carbonate sands shall be included in this thesis.

According to Brooke (2001), carbonate aeolianites globally account for more than 80 % of all aeolianite archives between latitudes 20 and 40° in both hemispheres. In 1851 Darwin described aeolianite deposits on the island on St. Helena which he had investigated 15 years earlier. Daly continued Darwin's investigations on St. Helena in 1927 and Sayles (1931) studied outcrops on Bermuda. Pye and Tsoar (2009) listed Branner (1890), Agassiz (1895), Chapman (1900), and Evans (1900) as pioneers of aeolianite research. Following the very early studies in the subsequent decades, many researchers focussed on different "hotspots" of carbonate aeolinites around the globe. The investigations were mainly carried out in the Caribbean (e.g. Ball, 1967 and Ward, 1973), in Australia (e.g. Fairbridge & Teichert, 1953 and Warren, 1983), in the Mediterranean (e.g. Yaalon 1967), in southeast Africa (e.g. McCarthy 1967, Maud 1968) and in India (e.g. Sperling & Goudie, 1975).

Aside from sporadic Tertiary deposits most of those aeolianite deposits originating from the shallow shelf are largely of Quaternary age. In a global perspective, the Holocene dunes are characterised by unconsolidated deposits (carbonate sands), whereas most of the Pleistocene sections are consolidated (McKee and Ward, 1983). Carbonate sands become cemented and lithified over time under the influence of sea water and sea spray (Müller, 1964; Pye & Tsoar, 2009). The lithification is mainly caused by evaporitic precipitation of Calcite in intertidal unconsolidated carbonate sands. Moreover, red algal clasts are described to take part in this cementation process (Müller and Tietz, 1975).

Formation of carbonate sands

Biogenic carbonates originating from the shallow shelf are washed onshore by waves and subsequently blown by winds from the tidal flats inland (Short, 2005). Depending on the onshore relief, on quantities of sediment supply, prevailing wind directions, and wind strength, these carbonate sands are deposited as dunes close to the coastline or result in progradation further landwards.

With regard to the shallow shelf, Einsele (2000) described two main carbonate-producing communities differing in their associations: The tropical to subtropical carbonates derive from Chlorozoan association, whereas temperate to polar-subpolar carbonates originate from Foramol association. The latter one mainly consists of foraminifera, molluscs, and bryozoans, and can also include calcareous red algae, echinoderms, brachiopods, corals and barnacles. By contrast, the tropical to subtropical Chlorozoan association is dominated by green algae and hermatypic corals (whereby also foraminifera, molluscs, bryozoans, calcareous red algae, and barnacles can be added). High siliciclastic imprint into the shallow shelf area generally lowers the production of carbonates. Thus, in the tropics, best carbonate-producing conditions are found on island sites and reefs due to the tropics' humidity and the resulting high runoff at continental margins (Einsele, 2000). Globally, best conditions for those communities are given in the arid to semiarid regions of the subtropical zone. That explains the above mentioned main distribution between 20 and 40° of the northern and southern hemispheres (Brooke, 2001).

1.2 The Canary Islands

The Canary Islands belong with respect to their original biogeographical environment to the volcanic islands of Macaronesia, which also comprises the Azores, Madeira, the Cape Verde Islands and the "Marrocan enclave" according to Sunding (1979). Del Arco Aguilar and Rodríguez Delgado (2018) follow the bioclimatic classification of Rivas-Martínez (2009) who classified this area into four floristic regions, whereby the Canarian-Madeiran subregion is part of the Mediterranean region. The Canarian archipelago encompasses thirteen islands, of which eight are populated (Rothe, 2008). Medwenitsch (1970) named Humboldt as the first person to investigate these islands, inspiring L. v. Buch to study the archipelago in 1815. These first investigations entailed a great number of scientists. For example, C. Lyell and G. Hartung, W. Reiss, G. A. Sauer or C. Gagel researched the Canary Islands during the 19th century. At the beginning of the 20th century, Spanish

geologists S. Calderón and Arana began their studies, followed in 1908 by L. Fernandez Navarro. For further detail please refer to the remarks by Medwenitsch (1970, page 166).

Over the last decades different hypotheses have contributed to an explanation concerning the origin of the archipelago. Anguita and Hernán (1975) confronted a hot spot model with a propagating fracture model. The latter explains the connection to the Atlas Mountains via a megashear system, as this relation has been discussed before by several researchers (e.g. MacFarlane and Ridley, 1969 or Dash and Bosshard, 1969). Araña and Ortiz (1986) ascribed the formation of the islands to compressive tectonics causing the uplift of several blocks. In 2000 Anguita and Hernán presented a model which unified these three approaches (I. hot spot, II. uplift and III. fracture). Accordingly, a sheet shaped mantle thermal anomaly under North Africa represents the source of magma for the volcanism in both the Canary Islands and the Atlas Mountains. The uplift is caused by transpressive shears and the fractures are well developed from the Atlas Mountains to the Canary Islands with the exception of the area between the archipelago and the African continent caused by its very thick sedimentary deposits. Accordingly, the islands differ strongly in their ages.

The eastern Canary Islands are the oldest of the whole Archipelago. Balogh et al. (1999) reported ages of about 70 Ma of the basal complex. According to Ferrer-Valero et al. (2019) the subaerial emissions on Fuerteventura started around 22.6 Ma. The western islands of the archipelago, on the other hand, are much younger (on Tenerife the subaerial phase started around 7.5 Ma and around 2 Ma on La Palma). Consequently, there are clear differences in the island-specific duration of subaerial erosional activity (Ferrer-Valero et al., 2019). The resulting diverse morphology due to the different duration of erosion causes a wide range of climatic conditions within the Canarian archipelago as, in general, the

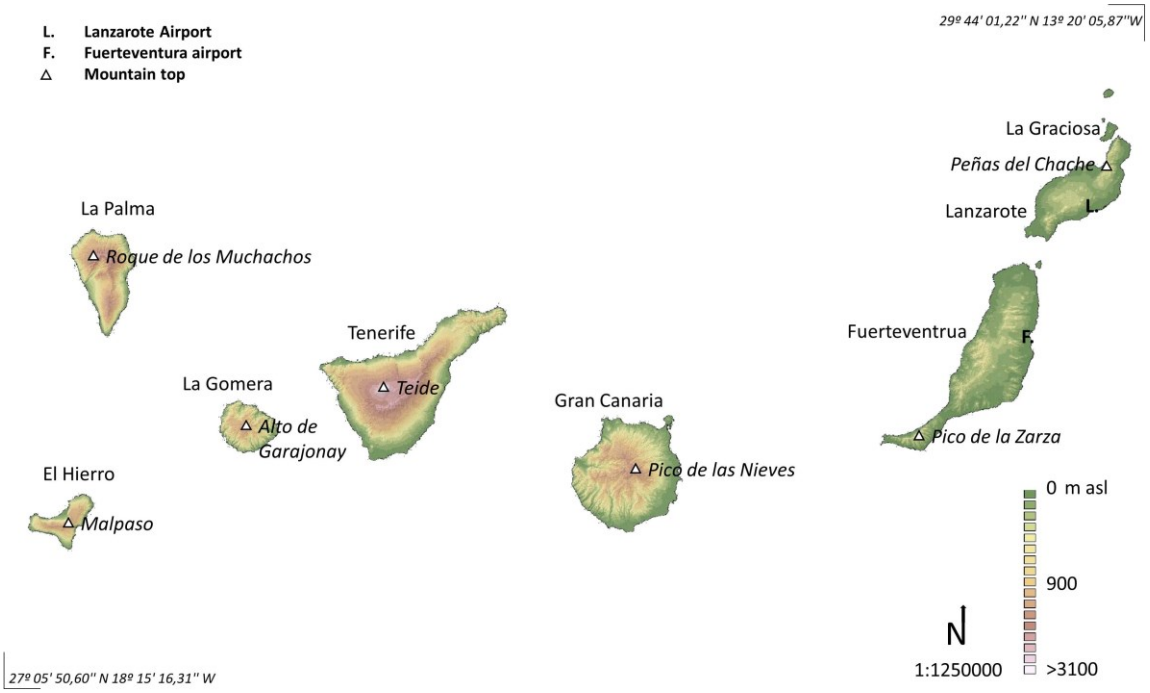

Fig. 1.1. Relief map of the Canary Islands, based on IDE Canarias (2019), modified.

Canary Islands are dominated by orographic rainfall (Rothe, 2008). Thus, under prevailing trade winds the different altitudes affect island-specific annual precipitation values.

The western Canary Islands (see Fig. 1.1) are characterised by higher altitudes (on La Palma up to 2426 m asl (Roque de los Muchachos), on El Hierro 1500 m asl (Malpaso), on Tenerife up to 3718 m asl (Teide), on La Gomera up to 1487 m asl (Alto de Garajonay), on Gran Canaria up to 1949 m asl (Pico de las Nieves). These higher altitudes result in increased orographic rainfall. The DWD (German Meteorological Service) provide mean values based on measurements of the period 1961 – 1990 (DWD, 2019). Accordingly, the annual precipitation at Los Rodeos (617 m asl) on Tenerife averaged 619 mm per year. In contrast the eastern Canary Islands are much lower and flatter. The maximum altitude on Fuerteventura is given by the Pico de la Zarza (807 m asl), on Lanzarote by the Peñas del Chache (671 m asl) and La Graciosa is just up to 266 m asl in its maximum elevation (Las Agujas Grandes). Hence, the eastern Canary Islands are less influenced by orographic rainfall due to their leveled relief. The United Nations provides mean precipitation values based on data of the period from 1973 to 1990. Accordingly, the location of Lanzarote airport ("L." in Fig. 1.1) close to Arrecife shows an annual mean value of 112 mm. Generally, the eastern Canary Islands Fuerteventura, Lanzarote, and La Graciosa are characterised by annual precipitation values of 90 to 150 mm (Zarei, 1989). The mean value of annual precipitation during the period 1961 – 1990 (measured at Fuerteventura Airport at 30 m asl; "F." in Fig. 1.1) yielded 90 mm. In the recent past, the year 2017 showed an extremely low annual precipitation of 31 mm. In accordance with the mentioned values the eastern Canary Islands' climate is classified as "hot desert climate (BWh)", according to the classification by Köppen and Geiger (Beck et al., 2018).

1.3 Carbonate sands on Fuerteventura

The carbonate sands of Fuerteventura are dominated by the middle sand fraction and feature $CaCO_3$ content of more than 80 % (Faust et al., 2015). Müller and Tietz (1975) described the following composition of carbonate sands (average values of 18 samples, Playa Blanca, located close to the airport of Fuerteventura; see Fig. 1.2): coralline algae (51 %), foraminifera (19 %), molluscs (16 %), bryozoans (3 %), echinoderms (1 %), and 10 % unidentifiable material.

On Fuerteventura a larger deposit of carbonate sands is located close to the southern tip of the island. Alcántara-Carrío et al. (2010) described Tertiary, Pleistocene, and Holocene dune generations as characterising those dune archives at the Isthmus de la Pared.

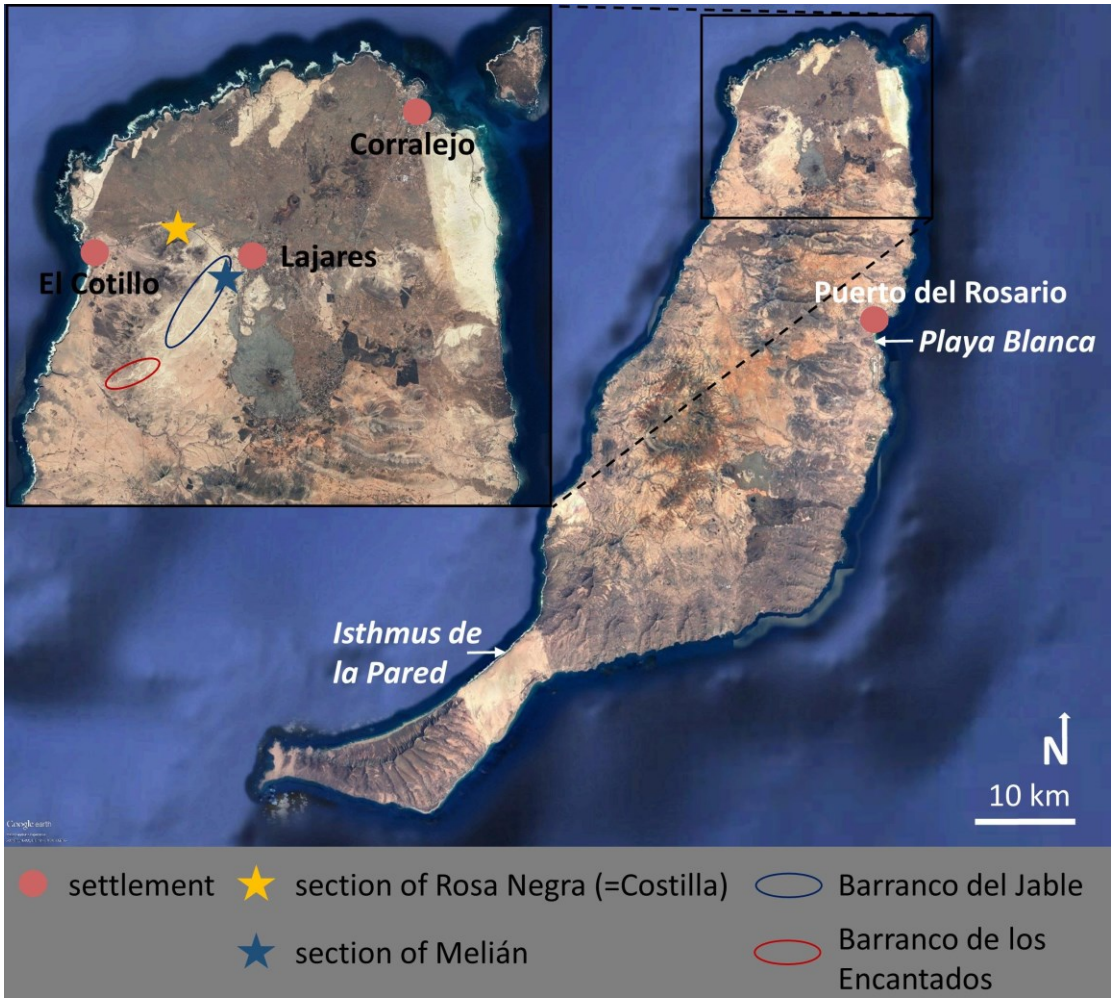

Fig. 1.2. Site locatings on Fuerteventura, based on Google earth (2019), modified

They doubted a predominant remobilisation of Pliocene carbonate sediments postulated by Meco (1993) and Meco et al. (2008). According to Meco et al. (1993 and 2008) the formation of shallow shelf carbonates was restricted to the Tertiary. After landward deposition a massive crust (Caliche) covered and fixed the carbonate sands. Since 1 Ma the crust has been partially eroded and allows the material to be remobilised, propagating further landwards (cf. Apendix Fig 6.1). As an equivalent to the deposits at the southern tip of the island, there are larger areas of dune deposits in the northern part which are built up by generations of carbonate sand layers with intercalated palaeosurfaces. In 1988 Coudé-Gaussen and Rognon presented a concept concerning the formation of the palaeo dune archives on Fuerteventura.

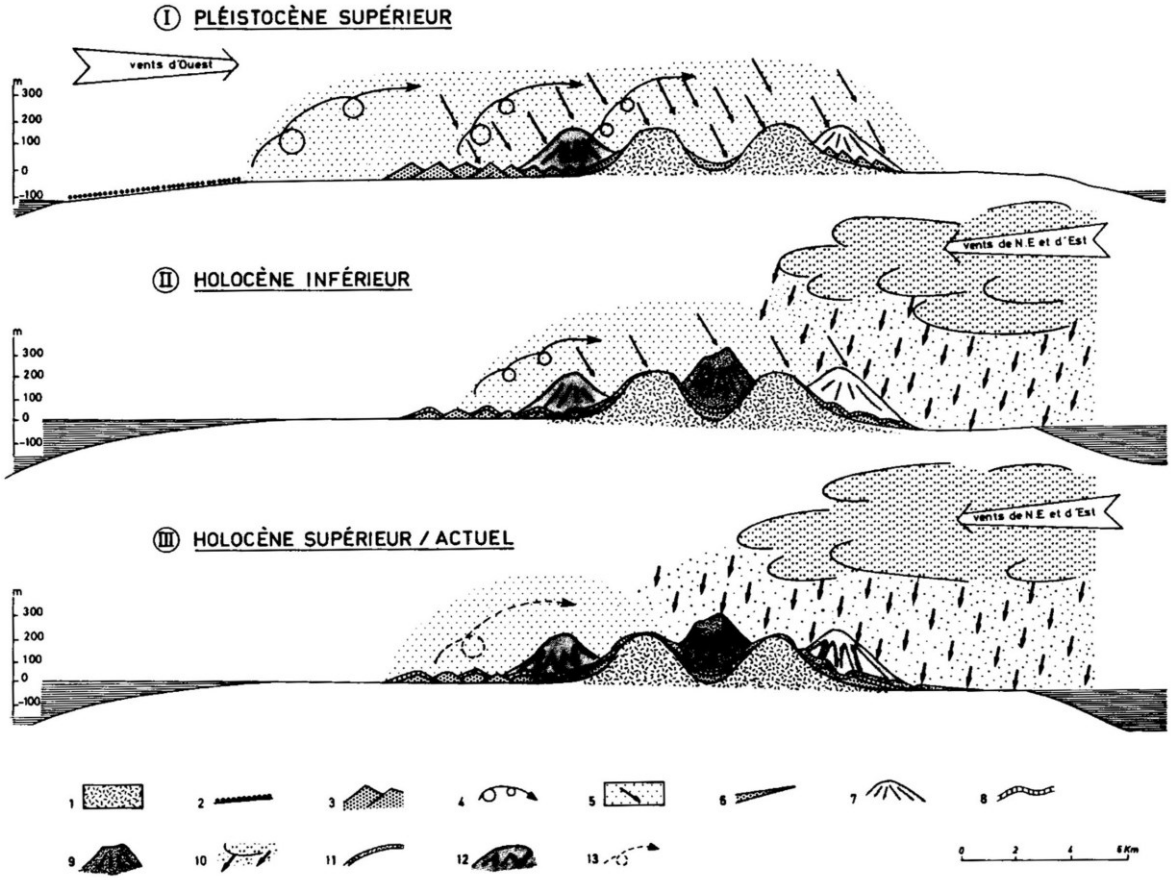

Upper Pleistiocene: 1. volcanic substratum; 2. emerged platform during glacio-eustatic regression, covered by bioclastic material; 3. loose dunes with bioclastic material of marine origin; 4. carbonate dust mobilization after aeolian comminution and sorting of dune materials; 5. fallout of "local" carbonate dusts; 6. sheets of wind-blown bioclastic sands on the slopes; 7. pre-Holocene volcano.
Lower Holocene: 8. calcrete on stable dunes and volcanic rocks (wet period); 9. late strombolian cone (Lower Holocene); 10. Fallout of Saharan dusts.
Upper Holocene until present day: 11. deposit of aeolian allochthonous silts; 12. carbonate deposit on slopes of scoria cones; 13. occasional contributions of carbonate aerosols by local aeolian reworking.

Fig. 1.3. Dune formation concept according to Coudé-Gaussen and Rognon (1988), modified

Thereby, they defined three main formation stages (Fig. 1.3),

I. Upper Pleistocene (Fig. 1.3, 1 – 7): Westerlies carried vast amounts of sand onshore accompanied by depositions of "local" carbonate dust.

II. Early Holocene (Fig. 1.3, 8 – 10): Wet conditions led to calcrete formation, additionally with increased supply of Saharan dust carried by easterly to northeasterly winds. III. Late Holocene until present day (Fig. 1.3, 11 – 13): Allochthonous dust material (carried by eastern to northeastern winds) was occasionally deposited, and carbonates are reworked locally.

Meco et al. (2011) proposed another concept with a time frame that is based on K-Ar dated volcanic eruptions: This concept describes a succession of

I) a full-glacial period characterised by aridity and cold conditions, favouring dune accumulation,
II) an early interglacial period, punctuated by humid and temperate phases, forming palaeosols,
III) warm and humid conditions during interglacial sea level high stand, which turned into
IV) an arid and temperate climate forming pedogenic calcretes.

The first geochronological framework (OSL-dating) carried out in palaeo dune archives on northern Fuerteventura was done by Bouab and Lamothe (1995), resulting in 181 +/- 27 ka sampled 2 m below the present surface and 183 +/- 27 ka in 5.5 m below present surface of the section of Rosa Negra (for locating see Fig. 1.2). The lowermost part of dune layers underlain by basaltic rock, dated 318 +/- 45 ka. Edwards and Meco (2000) presented a K-Ar age of 185 ka performed on Lapilli deposits embedded into dune generations 1 m below the present surface in the sandpit of Melián (see Fig. 1.2). Additionally, they measured U-Th ages of snail shells of 229 +/- 7.5 ka (sampled 3 m depth below the present surface) and of 241 +/- 4.9 ka (sampled 8 m below present surface). Faust et al. (2015) presented a correlation of four dune palaeosol sequences based on stratigraphic findings and OSL dating, spanning the last 280 ka, approximately. OSL dating revealed an age of 228 +/- 33.0 ka within the quarry of Costilla (identically equal to "Rosa Negra") in comparable stratigraphic position of the aforementioned dating of 183 +/- 27 ka according to Bouab and Lamothe (1995).
A first correlation of palaeo dune sections on the eastern Canary Islands was based on amino acid racemisation dating (Ortiz et al., 2006). The study revealed an age of 47.2 +/- 4.6 ka of the lowermost part of the Rosa Negra section. This age is in a comparable stratigraphic position to the aforementioned IRSL age of 318 +/- 45 ka by Bouab and Lamothe (1995). Meco et al. (2011) discussed strong underestimation of amino acid racemisation dating generally referring to Ortiz et al. (2006). In 2008 Meco et al. presented diverse ages based on different dating methods performed on material of the sections of Rosa Negra (Fig. 1.4) and Melián (see Apendix Fig. 6.2).

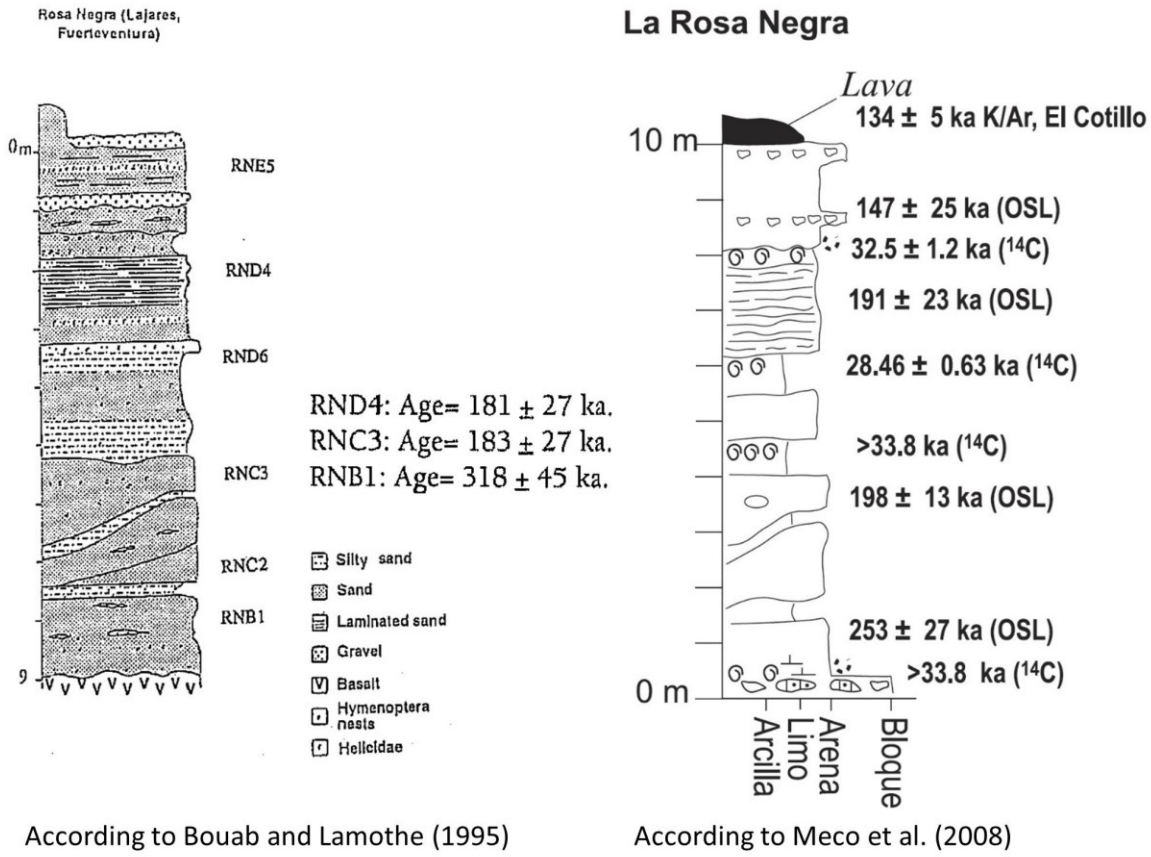

Fig. 1.4. Rosa Negra section according to Bouab and Lamothe (1995), modified and according to Meco et al. (2008)

^{14}C ages performed on shell material resulted in much younger ages by contrast with U-Th and OSL ages. Thus ^{14}C dating and those ages based on acid racemisation contradict OSL, U-Th, and K-Ar dating. Criado and Naranjo (2011) discussed this discrepancy. With reference to Meco et al. (2008) they tended towards higher reliability of OSL, U-Th, and K-Ar dating, since these higher ages fit much better into the geomorphological context. Von Suchodoletz et al. (2013) led a similar discussion against the background of additional ESR datings and resulted in the same statement, since the ESR dating also partly indicates Middle Pleistocene age. Finally, in view of contradictory data, Meco et al. (2011) concluded that there is still a lack of investigation of landward aeolian sand sections.

1.4 Motivation and objectives

The contradictive formation concepts and dating results point to unclear interpretability of palaeo dune archives on Fuerteventura. So far, only few landward sections have been studied and dated. The thesis aims to contribute to the long lasting history of researchers working on the eastern Canary Islands as the dune archives of Fuerteventura are promising against the backdrop of being located within the arid zone and of being formed as coastal dunes as well. The arid conditions implicate the archives' sensitivity against changes in moisture conditions (Reynolds et al., 2007) and the coastal zone links these archives to global pattern by their implied relation to sea level changes (Pye and Tsoar, 2009). Thus, the dune generations of Fuerteventura suggest high sensitivity against changing environmental conditions on a regional scale (changes in moisture conditions) as well as on a global scale (sea level changes). The open questions and the need for investigation result from the stratigraphic work that has been missing so far. Sandpits and deeply incised gully systems allow insight into wider areas of the Barranco de los Encantados and the Barranco del Jable. Thus, best conditions are given for deeper geomorphological and stratigraphical insight into the dune archives on Fuerteventura.
The following objectives and project questions underlie the here presented thesis:

Initial Objectives/Aims

- To work out a stratigraphy of dune palaeosurface sequences of the Barranco del Jable and for the Barranco de los Encantados. Is it possible to correlate the dune archives of the Barranco del Jable with the sequences of the Barranco de los Encantados? (with reference to Chapter 2)
- To derive a standard profile from the stratigraphic correlation. (with reference to Chapter 2)

As the thesis is embedded into the DFG-funded project (FA-239/18-1), the following questions concerning periods of soil formation are extracted from the application:

- When did soil formation (within glacial cycles) take place? (with reference to Chapter 3)
- Are these periods dominated by decreasing sand supply or by changing climatic conditions? (with reference to Chapter 3)

As time progressed, deeper insights into the dune archives raised further questions.

Additional Objectives/Aims:

- Concerning palaeosurface layers: Which characteristics of palaeosurfaces are related to soil forming processes? (with reference to Chapter 3)
- What does the deposition of sand depend on? (with reference to Chapter 3)
- Is it possible to extend the stratigraphic correlation to a palaeo dune field which does not directly border the dune field of Barranco del Jable and Barranco de los Encantados? (with reference to Chapter 4)
- How about the influence of local volcanism on archives of aeolianite palaeosurface sequences? (with reference to Chapter 3 and 4)

1.5 Thesis format

This cumulative thesis encompasses three submitted (Chapters 2–4) and partly already accepted (Chapters 2–4) manuscripts. All of the three journals (Palaeogeography, Palaeoclimatology, Palaeoecology; Quaternary Research and Geomorphology) guarantee an international peer review processing. Within this thesis each manuscript provides an individual list of references. The three manuscripts are embedded into a general introductory part and an extended summary (including a synthesis). For Chapter 1 (Introduction), Chapter 5 (Extended Summary) and Chapter 6 (Apendix) there is a separate list of references (7 References). The style of the reference lists was partly revised (to avoid journal-specific formats) in order to present a uniform format within the thesis. Similarly, some terms have been adapted, as the thesis is written in British English (e.g. “paleosol” adjusted to British English “palaeosol”). Numbering of figures and tables has been adjusted in the context of presenting a consecutive order within the thesis. For the benefit of the reader, and to improve flow, the positioning of tables and figures within already published manuscripts has been partially adjusted. As each manuscript has to be understandable on its own, overlapping of contents could not be avoided.

2 Complexity of Quaternary aeolian dynamics (Canary Islands)

C-B. Roettig[a], T. Kolb[b], D. Wolf[a], P. Baumgart[a], C. Richter[a], A. Schleicher[c], L. Zöller[b] & D. Faust[a]

[a]Dresden University of Technology
[b]University of Bayreuth
[c]GFZ German Research Centre for Geoscience

Publication history: submitted 31.08.2016 / accepted January 2017 / published (online) January 2017 / printed 2017 - Palaeogeography, Palaeoclimatology, Palaeoecology 472, 146–162.

2.1 Abstract

Carbonate aeolianites are important Quaternary archives at the point of intersection between marine and terrestrial systems. Since they are composed of alternating aeolian sediments and several palaeosol units, these sequences are highly suitable to reconstruct palaeoenvironmental conditions. In northern Fuerteventura, at least five different areas are characterised by successions of different dune generations and palaeosols. Few studies have addressed the stratigraphic order of individual dune areas. Therefore, a comprehensive consideration spanning several dune fields is needed. Here, we aim to present a detailed stratigraphy of two different dune areas and to identify the contribution of different materials (shelf origin, dust origin, volcanic origin) along with processes (accumulation, soil formation, erosion/preservation) that build up these archives. Four key sections were selected and sampled for laboratory analyses (texture, elemental composition, $CaCO_3$ content, palaeoenvironmental magnetics, luminescence dating, and gastropod assemblages). Based on main stratigraphic features, five major sedimentary sequences were identified indicating differences in prevailing sediment supply, humidity, and volcanic activity. First luminescence dating (IRSL) of the sequences revealed sedimentation ages between 360 ka and 15 ka. Finally, we are able to demonstrate that different dune areas show comparable stratigraphic patterns, but each studied site is defined by certain characteristics depending on the respective features of the closer surrounding. The knowledge of these peculiarities and the underlying background is

essential in order to correlate different sites and to attempt an appropriate environmental interpretation of the sedimentary sequences.

Keywords: Fuerteventura, palaeosol sequence, dune, luminescence dating, stratigraphy

2.2 Introduction

Most carbonate aeolianites of the mid latitudes are important archives of Quaternary climate and environmental changes, because the deposition of dune material seems to be linked to varying sea level and/or to climate change, whereas discontinuities between several generations of dunes are often marked by palaeosols (Brooke, 2001). Appropriate deposits are situated in northern Fuerteventura. In the last decade, most studies conducted across the Canary Islands focused on composition of Saharan dust (Engelbrecht et al., 2014; López-García et al., 2013; Menéndez et al., 2007, 2013), discussed the importance of dust availability (Moreno et al., 2001; Perez-Marrero et al., 2002), or pointed to the influence of dust input in soils (von Suchodoletz et al., 2010, 2013). Yanes et al. (2007, 2011, 2013) focused on the significance of land snails for reconstructing palaeoclimatic conditions. Beyond the theories of the volcanic origin of the island (Abdel-Monem et al., 1971; Anguita and Hernán, 2000), Coudé- Gaussen and Rognon (1988) described sediment deposition which originates from shelf and dust input as one of the main parent materials in dune fields. Similar coastal stratigraphical studies aimed to date aeolian and volcaniclastic deposits (Bouab and Lamothe, 1995; Damnati et al., 1996; Meco, 2008; Ortiz et al., 2006), but only one study (Faust et al., 2015) examined sand palaeosol sequences in four adjacent sites. In 2011, Meco et al. reported a lack of age control in landward aeolian sand sections. The investigations of (Faust et al., 2015) act as a starting point for examinations in a much wider area of palaeo dunes and sand sheets. Hence, it remains a challenge to work out stratigraphic sequences from different parts of the island to establish a standard profile for northern Fuerteventura. Two catchments were investigated by the study in hand. Of more than one hundred prospected sites, we chose four sampling sites which we present in order to correlate them, and also to correlate them to the sequences presented in (Faust et al., 2015). We aim to present a detailed stratigraphy of alternating aeolianite and palaeosol sequences from northern Fuerteventura. Furthermore, this stratigraphy is based on a conceptual attempt that considers the spatial distribution pattern of materials and processes participating in dune formation. Finally, we present a standard profile with 13 sediment units which we classify into five main

stratigraphic sequences. These sequences are characterised by different forcing factors including sediment supply, differing humidity, and changes in volcanic activity.

2.3 Geographical setting

Today, Fuerteventura is characterised by arid conditions with an annual precipitation of 147 mm Edwards and Meco (2000), and with wind direction dictated by the northeasterly trade winds. The northern part of Fuerteventura is mainly characterised by Tertiary and Pleistocene volcanism, Pliocene and Quaternary aeolian deposits in the form of palaeo dune fields, and sand sheets (Fig. 2.1) (Criado et al., 2004; Edwards and Meco, 2000).

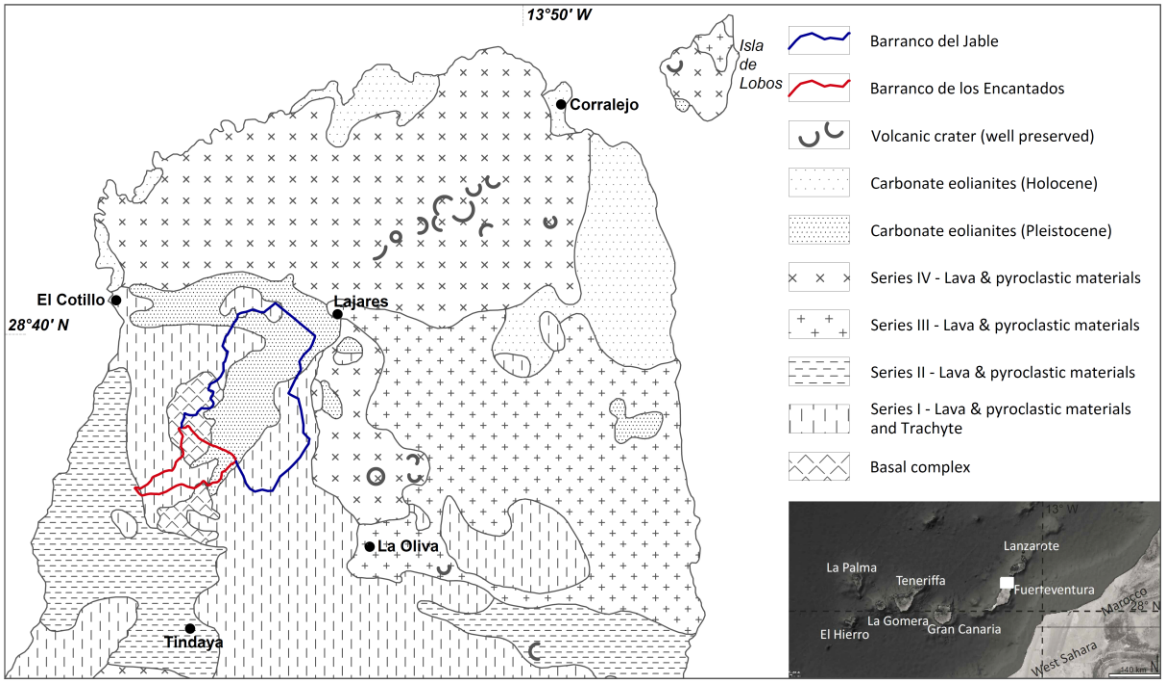

Fig. 2.1. Location map and major geological units of northern Fuerteventura (Rothe, 1996, modified) and the two catchments of the study area.

The Oligocene-Pliocene age volcanic rocks, the so called 'Basal complex', are exposed near to the western coast and in the central part of the island (Ancochea et al., 1996; Balogh et al., 1999; Coello et al., 1992). These volcanoes are classified into four basaltic series (Fúster et al., 1968; Rothe, 1996): The 'Basal complex' and the volcanism of Series I are of Miocene age. The post-Miocene Series II is mainly represented in the centre of Fuerteventura. Some volcanoes of Series III (Pleistocene age) are located in the east, for example the Montana Roja, dated to 1.7 Ma (Ibarrola et al., 1989), near the eastern coast. The youngest eruptions of Series IV are of middle to late Quaternary age (Fúster et al., 1968; Rothe, 1996) and are mainly located in northern Fuerteventura (Fig.2.1). The Montana de la Arena and the volcanic chain of the Calderon Hondo are examples of these

volcanic activities. Several dune fields and sand sheets are embedded into this volcanic landscape. A Holocene dune field of barchans and transverse dunes is located along the eastern coast close to Corralejo (Criado et al., 2004) (Fig. 2.1). The sedimentary environment of the palaeo dune fields is characterised by coarse grained biogenetic sandy shelf material ('carbonate aeolianites' according to Brooke (2001), Coudé-Gaussen and Rognon (1988), and Edwards and Meco (2000)) and Saharan dust (Menéndez et al., 2007). Volcanic ashes and lapilli fragments are admixed. Menéndez et al. (2007) reported dust accumulation rates of 17–79 g m^{-2} yr^{-1} on average on Gran Canaria, based on measurements in 2002 and 2003. Misota and Matsuhisa (1995) and Menéndez et al. (2007) described high amounts of quartz within the mineral composition of dust. Von Suchodoletz et al. (2013) mentioned that all quartz on Lanzarote is of aeolian origin. Even though the Basal Complex on Fuerteventura contains SiO_2, Alcántara-Carió et al. (2010) describe Saharan dust as the main source of quartz in the sediments of Fuerteventura. The study area includes the southern catchment of the Barranco de los Encantados and the northern catchment of the Barranco del Jable (Fig. 2.2). The watershed between the northern and the southern catchment is located in the SE of Montana Blanca. The catchment of Barranco de los Encantados is deeply incised by gully systems, and its middle reaches are dominated by huge whitish sand deposits. The catchment of Barranco del Jable comprises three tributaries which coalesce in the centre of the catchment (Fig. 2.2). The lower reaches of the three tributaries are characterised by lower relief energy and reduced gully incision, while the area of the middle and higher reaches shows higher relief intensity and deeply incised gully systems (Fig. 2.2(b)). All three tributaries were investigated, but detailed analytic work was carried out only in the central gully system. The richness of alternating palaeosol aeolianite sequences and the given accessibility of lower parts, caused by incision, make the area highly suitable for the here presented study. The Encantado section (28.63915° N / 13.978792° W) is located close to the watershed between the catchment of the Barranco de los Encantados and the Barranco del Jable (Fig. 2.2(a)) in the area of deeply incised gullies. The profile is developed within slope sediments of the SE-facing flank of the Montana Blanca. Jable 1 (28.643783° N / 13.974378° W) is situated within the centre of the Barranco del Jable catchment, to the east of its thalweg, where gullies incised up to 10 m deep. Jable 2 (28.647389° N / 13.9773° W) is also situated within the central part of the Barranco del Jable catchment, but to the west of the thalweg. Around this site, slopes are steeper and the gullies are less broad in comparison to the site of Jable 1. The quarry of Melián (28.669258° N / 13.953765° W) and Lajares III (28.664184° N /

13.936153° W) are situated to the south of the village of Lajares. There are four pit walls of the subrectangular sandpit of Melián.

Fig. 2.2. (a) Northern catchment of Barranco del Jable (blue), southern catchment of Barranco de los Encantados (red) and the four sampled sites. Based on google earth (modified); (b)Barranco del Jable, (close to site Jable 2) – northeastern direction of view.

located on the NE, SE, SW, and NW side. The quarry is located to the east of the thalweg of the Barranco del Jable. Some remnants of a former gully system remain on the upper slope positions to the east of the sandpit.

2.4 Methods

2.4.1 Fieldwork

Four sampling locations were selected after a thorough investigation of the study area. The selected profiles were then described for soil formations, accompanying features, and sediment composition.

2.4.2 Grain size distribution

The grain size distributions were measured with the Horiba LA-950 laser diffraction particle sizer at GFZ Potsdam. The air-dried samples were suspended with sodium pyro phosphate for 24 h. Neither calcium carbonate nor organic material was removed. Each sample was measured consecutively 5 times. The plotted values are the medians of 80 classes between 0.058 and 2500 µm. The grain size plots were created with the software R. Grain size distribution was plotted as heatmaps (Schulte et al., 2016) representing percentage of each class. The attribution of colour is logarithmic for three single matrices (see at the bottom of the grain size Figures 2.3–2.6). The first matrix represents the clay fraction and ranges from 0.058 to 1.981 µm. The second matrix represents the silt fraction and ranges from 1.981 to 58.953 µm. The third matrix contains the grain sizes from 58.953 to 2500 µm and represents the sand fraction. The cumulated percentage of the three matrices (per sample) is presented at the top of the grain size figures (Figs. 2.3–2.6).

2.4.3 Magnetic susceptibility

Rock magnetic measurements were performed at the Laboratory for Palaeo- and Environmental Magnetism at the University of Bayreuth. The dried sample material was carefully ground to a homogeneous structure and compressed into standardised plastic boxes (6.4 cm^3). The mass normalised value of χ (in $10^{-8} m^3\ kg^{-1}$)was determined in a magnetic AC field of 300 A m−1 using a MAGNON VSFM susceptibility bridge (sensitivity N5 × 10−6 SI) with a frequency of 300 Hz.

2.4.4 Elemental composition and $CaCO_3$ content

The elemental composition for Fe, Al, K, Na, Mg, Mn, Sr, Zn, and Ca was measured after pressure digestion with concentrated nitric and hydrofluoric acid by atomic adsorption spectrometry, whereas the pedogenic iron content (Fe_d) was measured after dithionite extraction using atomic adsorption spectrometry (Schlichting et al., 1995) at the Geographic Laboratory of the TU Dresden. The content of $CaCO_3$ was determined by treating the samples with hydrochloric acid and measuring them in a Scheibler apparatus (Schlichting et al., 1995). SiO_2 (wt%) was determined by X-ray fluorescence (XRF) analysis using a PANalytical AXIOS Advanced machine at the GeoForschungsZentrum Potsdam (GFZ). Powdered sample material was fused to a glass disc, and the specific elements were analysed with an End-window Rh x-ray tube SST-mAX with 4 kW output.

2.4.5 Gastropods

Gastropod analysis was carried out on 26 samples from the Encantado profile and 27 samples were taken from the quarry of Melián. Each sample comprised 10 l of sediment. The reference unit is litres because density fluctuations between layers could cause significant influence on weight and consequently on the size of the sample. All samples were wet sieved to the fraction bigger than 1 mm to extract the shells. To keep an effective mode of operation for the analysis process, samples with very high mollusc abundances were split and reduced to a half, quarter, or sometimes an eighth of the original volume. For this purpose, a partitioning procedure was applied, keeping a representative sample. The mollusc countings of split samples were extrapolated to their original volume of 10 l. Consequently, with these samples, there is an increased risk that rare species are under-represented or missed out. Qualitative and quantitative analysis was conducted using a MÜLLER MTX-4c stereomicroscope with accessory lens providing a magnification of 5 to 20 times. After identification (Bank et al., 2002; Ibáñez et al., 2003; Welter-Schultes, 2012), complete shells and unique fragments (apices, umbilicuses, and apertures) were counted and subsequently quantified (Ložek, 1964; Moine et al., 2005). Therefore, fragments which could belong to the same individual were set off against each other.

2.4.6 Colours

Colours were determined using the Munsell scale. The colours were identified in dry and wet conditions of each sample. For all descriptions in the text we use the colours of the wet condition.

2.4.7 Profile figures

The profile figures were created through AutoCAD Civil software. The bar plots of elemental composition as well as the heatmap images of grain size distributions were created using the software R and transferred to AutoCAD Civil 2015. The height of a single bar corresponds to the representative section which was determined in the field.

2.4.8 Luminescence dating

Sixteen samples for infrared stimulated luminescence (IRSL) dating were collected from the sites of Encantado (5 samples), Jable 1 (3 samples), Jable 2 (2 samples), and Melián (6 samples) using light-tight bags (an appropriate table is available in the Supplementary material). Due to the high amount of carbonates, at least 3 kg of material had to be collected

for each sample. All samples were prepared under subdued red-light conditions (640 +/- 20 nm). After wet sieving to grain sizes <38 μm, carbonates and organic material were dissolved by using 10% HCl and 10% H_2O_2, respectively. The polymineral fine grain fraction (4–11 μm) was separated by settling the remaining material in Atterberg cylinders applying specific settling times according to Stoke's law. All luminescence measurements were carried out in the luminescence laboratory of the University of Bayreuth using an automated Risø-Reader TL/OSL-DA-15, equipped with a 90Y/90Sr β-source for artificial irradiation and infrared light LEDs (875+/- 80 nm) for stimulation. The luminescence signal was detected using a Thorn-EMI 9235 photomultiplier, combined with a 3-mm Chroma Technology D410/ 30x interference filter, restricting the detection window to the blue wavelength band. Possible age underestimations due to anomalous fading in feldspars were minimised by using a modified single aliquot regenerative- dose (SAR) protocol for equivalent dose estimation (Faust et al., 2015; Huot and Lamothe, 2003; Preusser, 2003; Rother et al., 2010). Thereby, high temperatures of 270 °C for 120 s were used for both the preheat and the cutheat step of the SAR protocol. Additionally, a resting period of 20 min was added to the SAR protocol between each preheat/cutheat step and the subsequent IRSL readout. For equivalent dose determination, the first 5 s of the measured IRSL signal was used after subtracting a background derived from the last 20 s. The IRSL data were analysed with the Analyst software (Version 4.31.7) by applying a single exponential function for the construction of the dose response curve. All aliquots which were not able to pass the rejection criteria were excluded. Thus, only aliquots with a recycling ratio of 0.9–1.1, a recuperation of ≤5% of the natural sensitivity corrected signal intensity (Murray and Wintle, 2000), and a signal not lower than 3 times the background were accepted for equivalent dose calculation. For dose rate (Ḋ) determination, the U- and Th-concentrations were detected by thick source α-counting, and the K-contents of the samples were measured by ICP-MS. The conversion factors given by Guerin et al. (2011) were used. Cosmic dose rates were calculated according to (Prescott and Hutton, 1994). Interstitial water contents of 10 +/- 5% for Melián and Jable 1 and 5 +/- 5% for Enamorados and Jable 2 were assumed to be representative for the burial period, derived from measurements of the present day water contents and considering both sedimentological properties of the specific samples and differences in the geographical settings of the locations. A common a-value of 0.1 +/- 0.02 was used for calculating the alpha effectiveness of all samples. This value was calculated as a mean value derived from a-value measurements that were performed for 16 samples originating from the four investigated locations.

2.5 Results

An important finding based on the field work refers to the high variability of soil characteristics within short distances. For instance, a palaeosol can be preserved in the form of a reddish clayey soil accompanied by strong decalcification features combined with a high abundance of gastropods and brood cells (BCs), the latter have been attributed to soil nesting bees (Edwards and Meco, 2000), locusts (Meco et al., 2010, 2011), or coleopterans (Genise et al., 2013). However, within a short distance of several tens of metres, the same 'soil' shows just a few gastropods and no further pedogenic indications. For this reason we have to mention that, of course, some of the described soils within the sampled sections (Figs. 2.3–2.6; Tables 2.1–2.4) were not ideally developed/ preserved.

2.5.1 Encantado section

The characteristics of each sediment layer of the Encantado section (Fig. 2.3) are given in Tab. 2.1.

SL16	homogeneous soil sediment, reddish yellow (7.5 YR 6/6), 60% sand, 45% $CaCO_3$, maximum values of mass specif. susceptibility, contains basaltic fragments; strong palaeosol on top, strong brown colour (7.5 YR 4/6), <25% sand, 40 % $CaCO_3$, high values of elemental composition
SL 15	pure shelf material, yellow (10 YR 8/6), >90% sand, >80% $CaCO_3$, consists mainly of Ca, Sr, Mg and Na, very low mass specif. susceptibility, some volcanic impurities, IRSL age of 366,3 +/- 34,0 ka; very weak palaeosol on top, reddish yellow (7.5 YR 7/6), 80% sand
SL 14	mainly shelf material, reddish yellow (7.5 YR 7/6), >90% sand, 70% $CaCO_3$, low mass specif. susceptibility; on top features of relocation, reddish yellow (7.5 YR 6/6), impurities of mafic minerals
SL 13	pure shelf material, reddish yellow (7,5 YR 6/6), >75% sand, 70% $CaCO_3$, low mass specif. susceptibility, strong palaeosol on top, reddish yellow (7.5 YR 6/6), 60% sand, 55% $CaCO_3$, coated BCs, high abundance of *Cochlicella sp.*
SL 12	mainly shelf material, pink (7,5 YR 8/4), >95% sand, 85% $CaCO_3$,consists mainly of Ca, Sr, Mg and Na, very low mass specif. susceptibility, palaeosol on top, strong brown (7.5 YR 5/6), 60% sand, 60% $CaCO_3$, coated BCs, several *Cochlicella sp.* & *Pomatias lanzarotensis*

SL 11	soil sediment, reddish yellow (7,5 YR 6/6), >80% sand, <65% $CaCO_3$, low mass specif. susceptibility; very strong palaeosol on top, strong brown (7.5 YR 4/6), 30% sand, 60% $CaCO_3$, coated BCs, high content of SiO_2, high abundance of *Pomatias lanzarotensis*
SL 10	pure shelf material, very pale brown (10 YR 8/4), >95% sand, >85% $CaCO_3$,consists mainly of Ca, Sr, Mg and Na, very low mass specif. susceptibility; weak palaeosol on top, reddish yellow (7,5 YR 6/6), 85% sand, <75% $CaCO_3$, impurities of mafic minerals
SL 9	mainly shelf material, pink (7,5 YR 7/4), >95% sand, 85% $CaCO_3$,consists mainly of Ca, Sr, Mg and Na, low mass specif. susceptibility, dominated by features of relocation
SL 8	mainly shelf material, reddish yellow (7.5 YR 7/6), <80% sand, <80% $CaCO_3$; very strong palaeosol on top, strong brown (7.5 YR 4/6), 25% sand, <20% $CaCO_3$, highest values of elemental composition, much impurities of mafic minerals, coated BCs, highest content of SiO_2
SL 7	relocated sediment, reddish yellow (7.5 YR 6/6), <25% sand, maximum clay content (>45%), >50% $CaCO_3$, on top relocation features (even fragments of $CaCO_3$-crust)
SL 6	shelf material with volcanic imprint, very pale brown (7.5 YR 5/6), <75% sand, 60% $CaCO_3$; very weak palaeosol on top, strong brown (7,5 YR 5/6), <55% sand, 60% $CaCO_3$, higher mass specif. susceptibility, many impurities of mafic minerals
SL 5	shelf material, reddish yellow (7.5 YR 6/6), 70% sand, >65% $CaCO_3$, several BCs
SL 4	shelf material, reddish yellow (10 YR 8/6), >75% sand, >80% $CaCO_3$, consists mainly of Ca, Sr, Mg and Na
SL 3	mainly shelf sediment, reddish yellow (7.5 YR 7/6), <75% sand, >70% $CaCO_3$, abundance of coated BCs,
SL 2	shelf sediment, reddish yellow (7.5 YR 6/6), >60% sand, >60% $CaCO_3$, palaeosol on top, strong brown (7.5 YR 4/6), <25% sand, <25% $CaCO_3$, several mafic minerals
SL 1	colluvial layer, reddish yellow (7.5 YR 6/6), >75% sand, <60% $CaCO_3$

Tab. 2.1 Results of the Encantado section (for detailed description and profound insight into gastropod results, we refer to the Supplementary materials: "Stratigraphic results – Detailed Description").

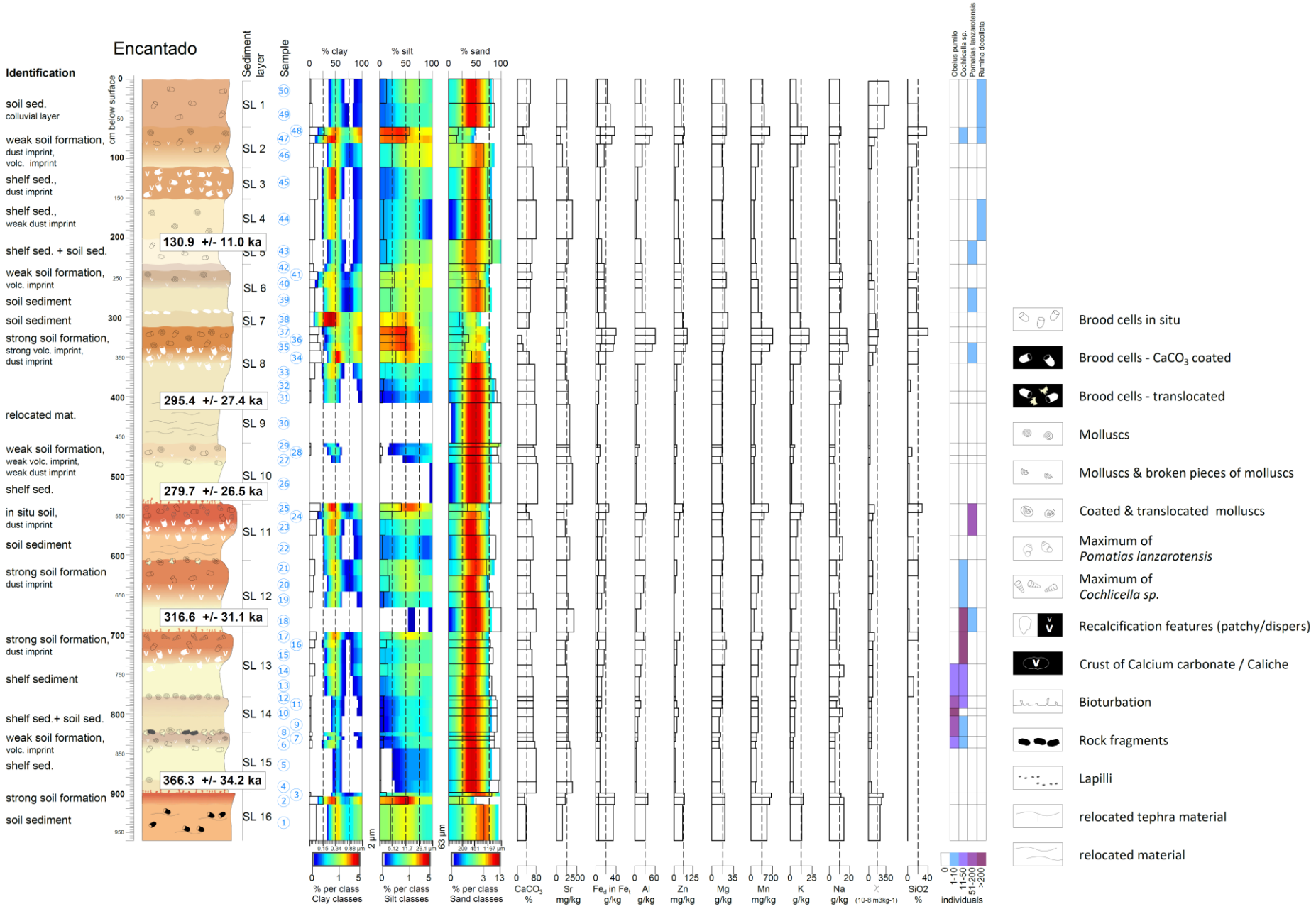

Fig. 2.3. Profile figure of Encantado section.

2.5.2 Jable 1 section

The characteristics of each sediment layer of Jable 1 (Fig. 2.4) are given in Tab. 2.2.

SL 12	shelf material, pink (10 YR 8/4), >95% sand, >85% $CaCO_3$,consists mainly of Ca, Sr, Mg and Na, very low mass specif. susceptibility, very weak palaeosol on top, reddish yellow (7,5 YR 6/6), 80% sand, 75% $CaCO_3$
SL 11	soil sediment, reddish yellow (7,5 YR 6/6), <75% sand, <70% $CaCO_3$, low mass specif. susceptibility; strong palaeosol on top, strong brown (7.5 YR 5/8), 50% sand, <55% $CaCO_3$, coated BCs, abundance of coated BCs
SL 10	relocated material, reddish yellow (7.5 YR 6/6), >90% sand, 80% $CaCO_3$, consists mainly of Ca, Sr, Mg and Na in the lower part, very low mass specif. susceptibility
SL 9	soil sediment, reddish yellow (7.5 YR 6/8), >75% sand, <75% $CaCO_3$, low mass specif. susceptibility, dominated by features of relocation; strong palaeosol on top, strong brown (7.5 YR 5/8), <55% sand, <65% $CaCO_3$, high abundance of coated BCs
SL 8	soil sediment, reddish yellow (7.5 YR 6/6), <75% sand, <75% $CaCO_3$; on top dominated by features of relocation
SL 7	relocated sediment, reddish yellow (7.5 YR 6/6), <70-90% sand, <65% $CaCO_3$, impurities of mafic minerals; on top very weak palaeosol, reddish yellow (7.5 YR 7/6), <90% sand, 70% $CaCO_3$
SL 6	shelf material, very pale brown (10 YR 8/4), 100% sand, >85% $CaCO_3$, , consists mainly of Ca, Sr, Mg and Na, low mass specif. susceptibility, several mafic minerals, features of relocation on top
SL 5	shelf material with light volcanic imprint, very pale brown (10 YR 7/4), >95% sand, >80% $CaCO_3$, impurities of mafic minerals; very weak palaeosol on top, reddish yellow (7.5 YR 6/6), >90% sand, 80% $CaCO_3$
SL 4	shelf material, very pale brown (10 YR 8/4), 100% sand, >85% $CaCO_3$, very low mass specif. susceptibility; features of recalcification and relocation on top, broken coated BCs, impurities of mafic minerals
SL 3	shelf sediment, reddish yellow (7.5 YR 7/6), <70% sand, >70% $CaCO_3$,
SL 2	mainly shelf sediment, reddish yellow (7.5 YR 6/6), >75% sand, >70% $CaCO_3$, impurities of mafic minerals
SL 1	colluvial layer with remnants of Caliche, reddish yellow (7.5 YR 6/6), >75% sand, 70% $CaCO_3$

Tab. 2.2 Results of Jable 1 (for detailed description and profound insight into gastropod results, we refer to the Supplementary materials: “Stratigraphic results – Detailed Description”).

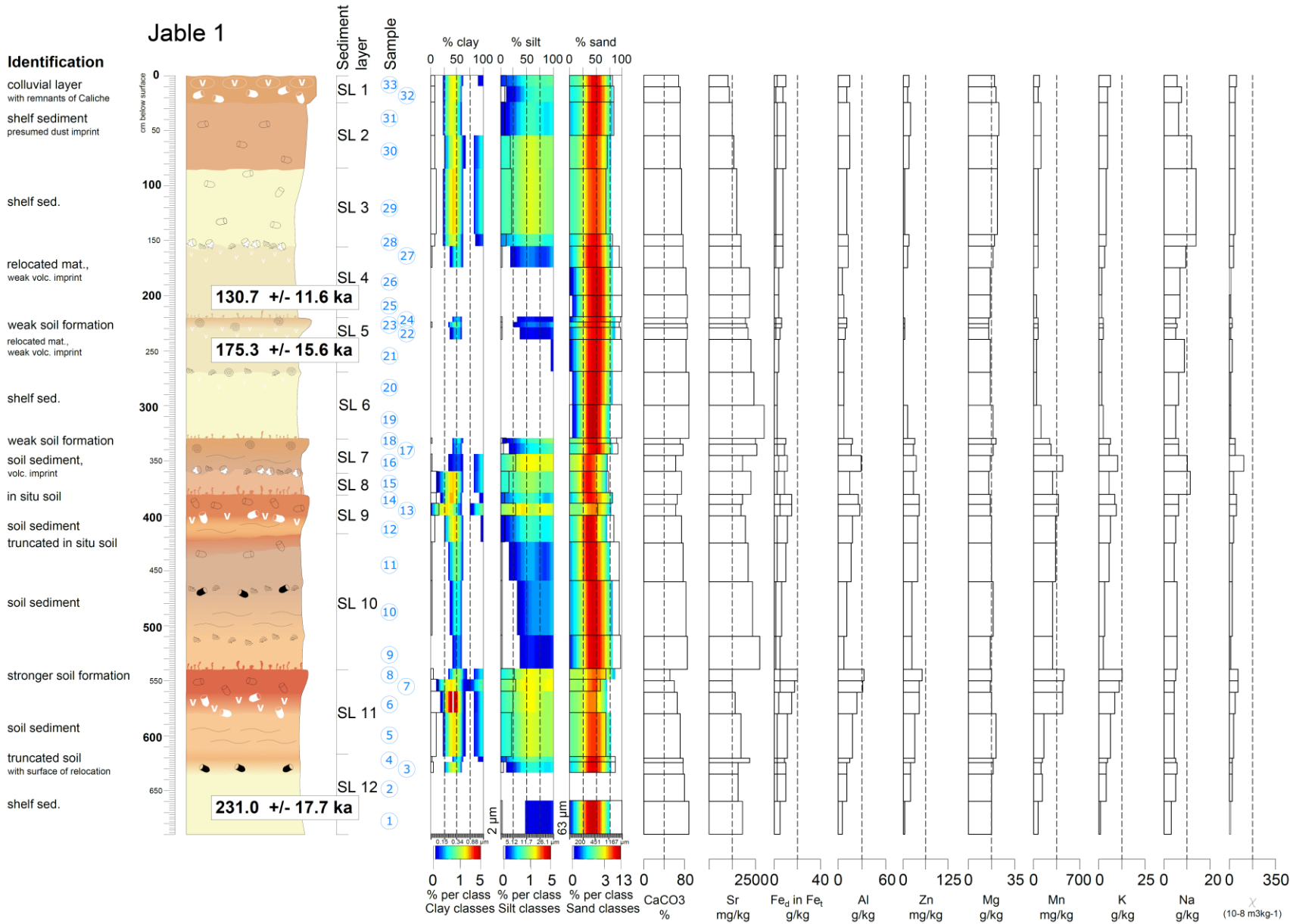

Fig. 2.4. Jable 1 section; see Fig. 2.3 for key.

2.5.3 Jable 2 section

The characteristics of each sediment layer of Jable 2 section (Fig. 2.5) are given in Tab. 2.3.

SL 12	very strong palaeosol in soil sediment, strong brown (7.5 YR 4/6), <30% sand, <25% $CaCO_3$, highest mass specif. susceptibility, black coated BCs, high values of Fe_d & Mn
SL 11	shelf material, very pale brown (10 YR 7/4), >95% sand, >85% $CaCO_3$, , consists mainly of Ca, Sr, Mg and Na, very low mass specif. susceptibility; very weak palaeosol on top, several BCs and gastropods, some mafic impurities
SL 10	shelf material, very pale brown (10 YR 7/4), >95% sand, >85% $CaCO_3$, , consists mainly of Ca, Sr, Mg and Na, very low mass specif. susceptibility; strong palaeosol on top, strong brown (7.5 YR 5/6), <75% sand, <55% $CaCO_3$
SL 9	soil sediment, reddish yellow (7.5 YR 6/6), >75% sand, >65% $CaCO_3$,; strong palaeosol on top, reddish yellow (7.5 YR 6/6), <55% sand, 60% $CaCO_3$, abundance of BCs
SL 8	soil sediment, reddish yellow (7.5 YR 6/6), >75% sand, <60% $CaCO_3$; on top dominated by features of relocation (broken coated BCs, rock fragments)
SL 7	soil sediment with volcanic imprint, reddish yellow (7.5 YR 6/6), >75% sand, <60% $CaCO_3$, impurities of mafic minerals; on top very weak palaeosol, reddish yellow (7.5 YR 6/6), 75% sand, <65% $CaCO_3$, local maximum of mass specif. susceptibility
SL 6	shelf material, very pale brown (10 YR 8/4), 100% sand, >85% $CaCO_3$, , consists mainly of Ca, Sr, Mg and Na, very low mass specif. susceptibility, features of relocation on top (broken coated BCs, rock fragments)
SL 5	shelf material with volcanic imprint, reddish yellow (7.5 YR 6/6), >90% sand, 70% $CaCO_3$, impurities of mafic minerals; weak truncated palaeosol on top, reddish yellow (7.5 YR 6/6), <80% sand, <65% $CaCO_3$
SL 4	relocated material, reddish yellow (7.5 YR 6/6), >80% sand, 70% $CaCO_3$, broken gastropods

SL 3	relocated material, reddish yellow (7.5 YR 6/6), 75% sand, >60% $CaCO_3$; truncated palaeosol on top, strong brown (7.5 YR 5/6), <50% sand, >40% $CaCO_3$, abundance of coated BCs, contains remnants of Caliche on top
SL 2	palaeosol, strong brown (7.5 YR 5/6), <45% sand, <25% $CaCO_3$, impurities of mafic minerals, several BCs
SL 1	colluvial layer, strong brown (7.5 YR 5/6), >50% sand, <30% $CaCO_3$, high values of Fe_d & Mn

Tab. 2.3 Results of Jable 2 section (for detailed description and profound insight into gastropod results, we refer to the Supplementary materials: "Stratigraphic results – Detailed Description").

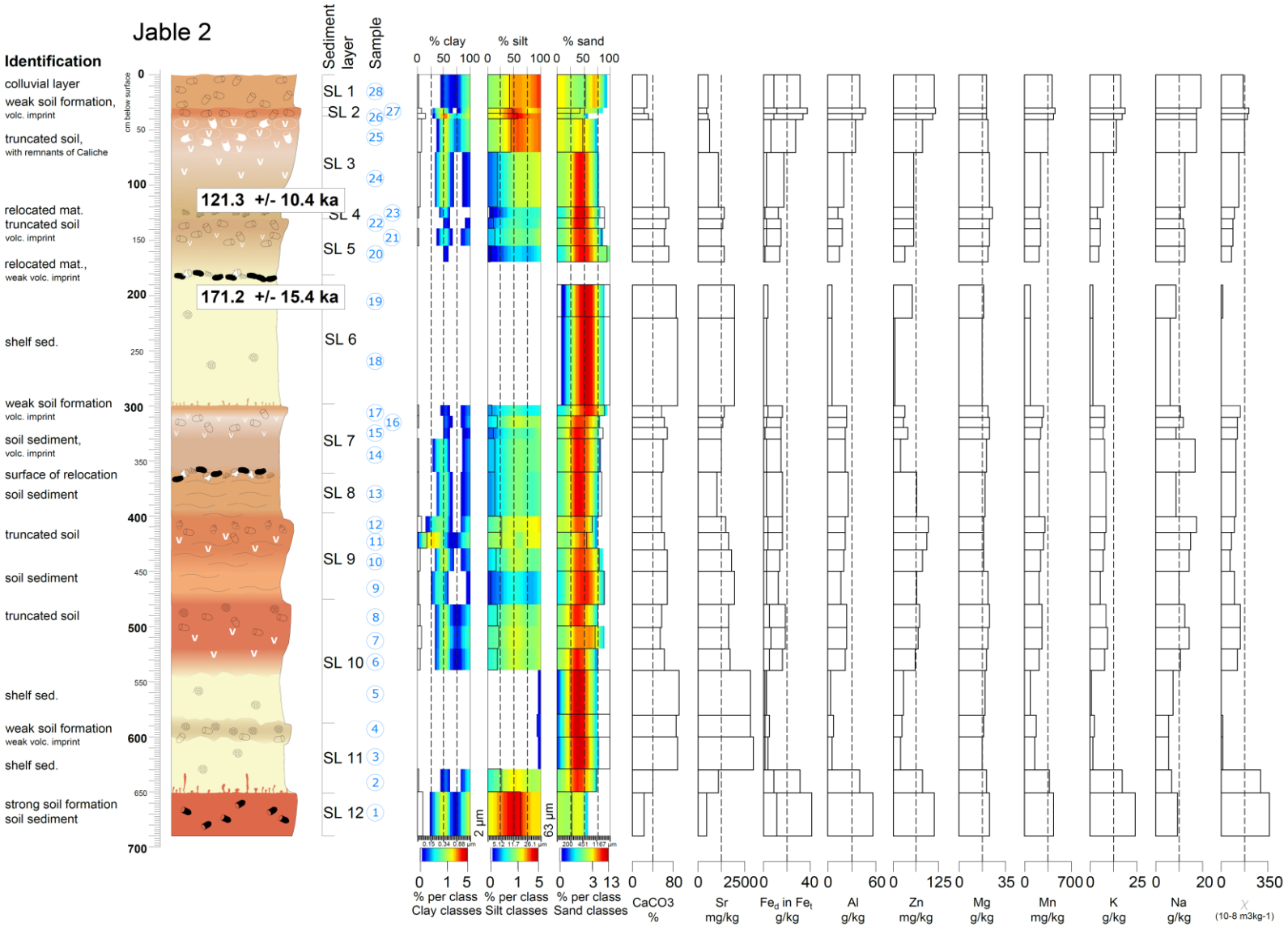

Fig. 2.5. Jable 2 section; see Fig. 2.3 for key.

2.5.4 Melián section

All of the four pit walls were investigated. Finally, three different sequences were sampled to work out a composite profile (Fig. 2.6). For the lower parts of the section, (Faust et al., 2015) already gave a comprehensive description. Consequently, we add a more detailed description for the upper younger parts of the section. A summary of the results of the Melián section are given in Tab. 2.4.

SL 18	relocated material, sandy, channels filled by basaltic gravel; truncated palaeosol on top
SL 17	relocated material, sandy, in lower parts kinds of stone pavements, in the upper parts channels filled by basaltic gravel; truncated palaeosol on top
SL16	relocated sediment, reddish yellow (7.5 YR 6/6), >75% sand, >60% $CaCO_3$, , contains basaltic gravel, very high mass specif. susceptibility; weak palaeosol on top, reddish yellow (7.5 YR 6/6), >80% sand, >60% $CaCO_3$, maximum values of mass specif. susceptibility
SL 15	shelf material, yellow (7.5 YR 7/6), >75% sand, >65% CaCO3, lower part much basaltic gravel+ high mass specif. susceptibility, upper part less basaltic fragments + middle mass specif. susceptibility, weak palaeosol on top, reddish yellow (7.5 YR 7/6), <65% sand, <70% CaCO3, impurities of mafic minerals
SL 14	mainly shelf material, reddish yellow (7.5 YR 7/6), >90% sand, 70% $CaCO_3$, low mass specif. susceptibility, even features of relocation; palaeosol on top, reddish yellow (7.5 YR 6/6), <75% sand, <60% $CaCO_3$, coated BCs, high abundance of *Cochlicella sp*
SL 13	relocated material, reddish yellow (7,5 YR 7/6), >95% sand, 75% $CaCO_3$
SL 12	relocated material with truncated palaeosol (7,5 YR 7/6), >75% sand, >70% $CaCO_3$
SL 11	soil sediment, reddish yellow (7,5 YR 6/6), >75% sand, 70% $CaCO_3$, high abundance of relocated coated BCs; truncated palaeosol on top, reddish yellow (7.5 YR 6/6), >75% sand, 60% $CaCO_3$, high abundance of coated BCs, within that section the only occurrence of *Pomatias lanzarotensis*
SL 10	relocated material, brownish yellow (10 YR 6/6), >95% sand, >85% $CaCO_3$, contains a lot of Lapilli; very weak palaeosol on top, reddish yellow (7,5 YR 6/6), <95% sand, <80% $CaCO_3$, impurities of mafic minerals and Lapilli

SL 9	mainly shelf material, reddish yellow (7,5 YR 6/6), >90% sand, >75% $CaCO_3$, low mass specif. susceptibility; palaeosol on top, strong brown (7,5 YR 5/8), <70% sand, <45% $CaCO3_3$, highest values of elemental composition, in the upper parts admixture of tephra with ongoing soil formation above transition into relocation, brownish yellow (10 YR 6/6), 75% sand, 70% $CaCO_3$
SL 8	mainly shelf material, yellow (10 YR 7/6), >95% sand, >85% $CaCO_3$; very weak palaeosol on top, yellow (10 YR 7/6), >90% sand, <80% $CaCO_3$, impurities of mafic minerals
SL 7	mainly shelf material, brownish yellow (10 YR 6/6), >90% sand, >80% $CaCO_3$; impurities of mafic minerals; very weak palaeosol on top, brownish yellow (10 YR 6/6), >90% sand, 80% $CaCO_3$, impurities of mafic minerals
SL 6	mainly shelf material, yellow (10 YR 7/6), 100% sand, 85% $CaCO_3$; very strong truncated palaeosol on top, strong brown (7,5 YR 4/6), <100% sand, 55% $CaCO_3$, a lot of Lapilli, high abundance of coated BCs, in the upper part remnants of Caliche
SL 5	relocated material, consists of tephra material, yellowish brown (10 YR 5/6)
SL 4	truncated palaeosol in relocated material, yellowish brown (10 YR 5/6), >75% sand, <55% $CaCO_3$, abundance of coated BCs
SL 3	relocated material with volcanic imprint, strong brown (7.5 YR 5/6), >75% sand, <45% $CaCO_3$, a lot of mafic minerals; weak palaeosol on top, dark yellowish brown (10 YR 3/6), <20% sand, <35% $CaCO_3$, contains tephra
SL 2	relocated material, light yellowish brown (10 YR 6/4), >75% sand, >65% $CaCO_3$, very weak palaeosol on top, strong brown (7.5 YR 5/6), <50% sand, 60% $CaCO_3$, contains tephra
SL 1	relocated material, yellowish brown (10 YR 5/6), >75% sand, >65% $CaCO_3$

Tab. 2.4. Results of Melián section (for detailed description and profound insight into gastropod results, we refer to the Supplementary materials: "Stratigraphic results – Detailed Description").

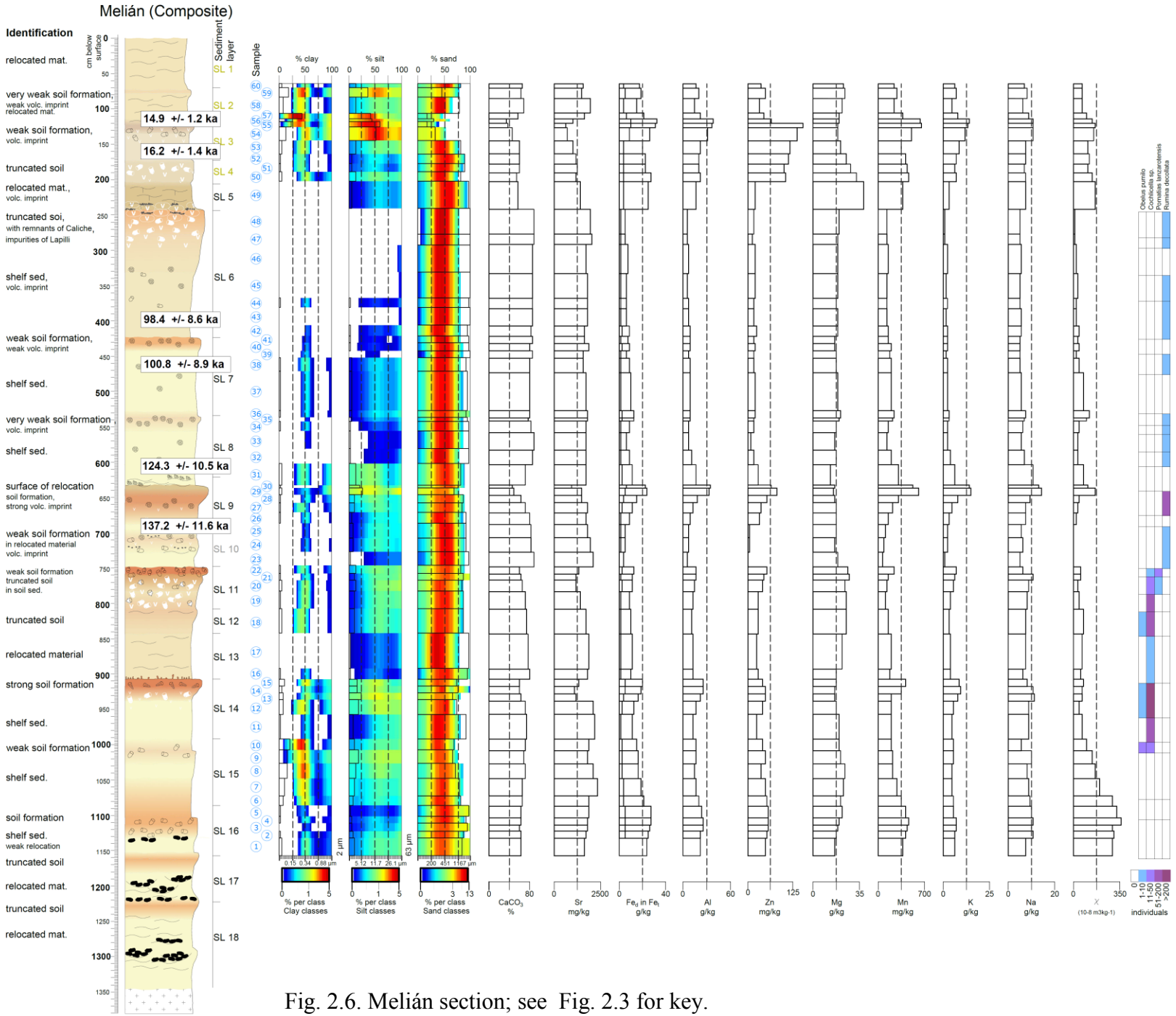

Fig. 2.6. Melián section; see Fig. 2.3 for key.

2.5.5 Lajares III section

The main reason for including Lajares III is to correlate the new sections with an important site documented in (Faust et al., 2015). Consequently, for this section we refer to the published work of (Faust et al., 2015). Although we also studied this site, we only have to contribute a small piece to the existing description of Lajares III:
(Faust et al., 2015) described a 'marker soil' (Fig. 2.9 at 450 cm below surface) with an underlying 'sand layer'. The new insight presents features of relocation within this 'sand layer', even containing pieces of relocated *Cochlicella sp.* and further pieces of gastropods and rock fragments. Because of this soil sediment, we assume a hiatus below the 'marker soil'.

2.6 Discussion

2.6.1 Spatial stratigraphic features

Even though each studied site seems to be unique, the general system dynamics in the course of dune and sand sheet formation are consistent and distinctive. To get an idea how to integrate each site into a general stratigraphic pattern, some characteristic bedding conditions of palaeo dunes and sand sheets of the study area are shown in Fig. 2.7.

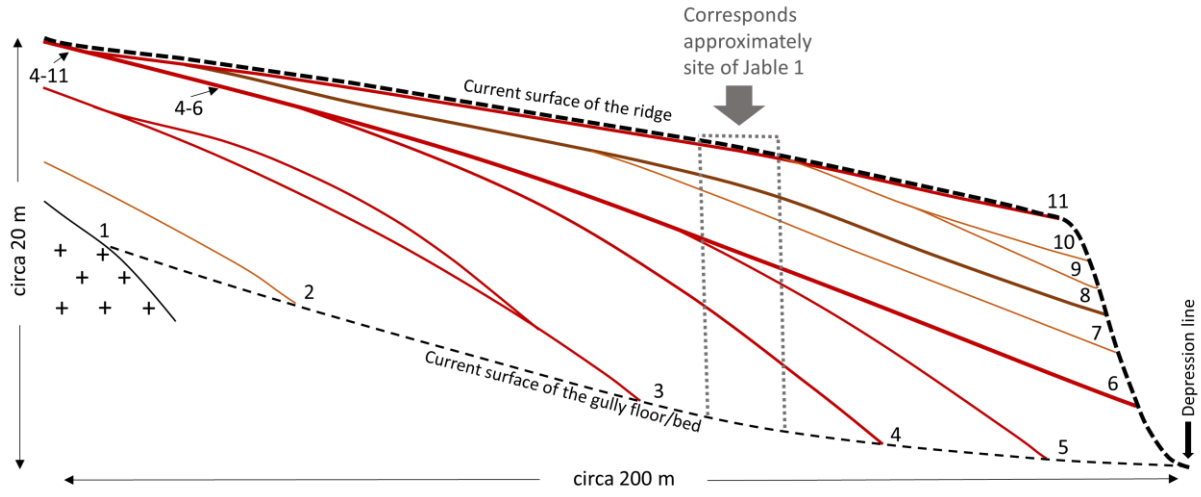

Fig. 2.7. Sand deposits and palaeosurfaces. The schematic sketch is based on the closer surrounding of the site of Jable 1.

The sediment layers cover the slope of a volcanic mountain (on the left side) and are oriented towards the main depression line of the Barranco del Jable catchment (on the right side). In down slope direction (from left to right), palaeosurfaces (e.g. Fig. 2.7 No. 1–3) of the lower parts are dipping into the gully bed/floor, whereas in the upper parts several palaeosurfaces (e.g. Fig. 2.7 No. 6–10) firstly become recognisable further downslope. This results in a very heterogeneous pattern of stratigraphic successions dependent on the specific location of the profile sections. There are two important features to distinguish between relocated soil material and in situ soil formations on Fuerteventura. First, the sequence of an in situ soil starts from below with the appearance of BCs, followed by the occurrence of snail shells and BCs upwards, and is closed up with an obvious increase of molluscs towards the top of the soil (see Fig. 2.8).

Fig. 2.8. Melián (NE pit wall): SL 9 of Melián shows soil formation with BCs & gastropods coated by $CaCO_3$, covered by a tephra layer and ongoing soil formation. On top of the tephra admixture the characteristics transition into features of (low energy) relocation.

This sequence seems to occur in different intensities (different number of individuals) according to the intensity of soil formation. We often detected a mixture of this clear succession and a more chaotic arrangement of molluscs and brood cells, which indicates soil formation within relocated soil sediment. Furthermore the BCs occur in different "stages" of coating. On the one hand, there are non-coated brood cells in in-situ positions (Edwards and Meco, 2000) which are very fragile and could not be transported. On the other hand $CaCO_3$- coated BCs are comparatively robust against transport and may serve as an indicator of relocation especially when they are in chaotic order. Furthermore, broken

coated BCs are abundant in soil sediments. In addition, the occurrence of several rhizoconcretions (compare McKee and Ward (1983) and Pye and Tsoar, (2009)) within the same level indicate palaeosurfaces. Surprisingly, the gastropod results give reason to assume a relationship between the occurrence of certain species and their stratigraphic position (as shown in Figs. 2.3 and 2.6). Four assemblages, which are specified by a certain species, were identified as mutually exclusive in large parts. In stratigraphical order, the four assemblages are specified by I. *Obelus pumilio* (Dillwyn, 1817), II. *Cochlicella sp.* (Yanes et al., 2004), III. *Pomatias lanzarotensis* (Wollaston, 1878), and IV. *Rumina decollata* (Linnaeus, 1758). We observed the coexistence of a maximum of two immediately consecutive species (e.g. coexistence of *Obelus pumilio* and *Cochlicella sp.*), whereas the maxima of the species correspond to a stratigraphical order. Therefore, we use these species as a corroborating feature to correlate the sites.

2.6.2 An attempt towards a stratigraphic correlation of the different catchments

The study in hand aims to attempt a correlation (Fig. 2.9) of all hitherto sampled sites (including a site investigated by Faust et al., 2015). Thirteen units have been identified so far.

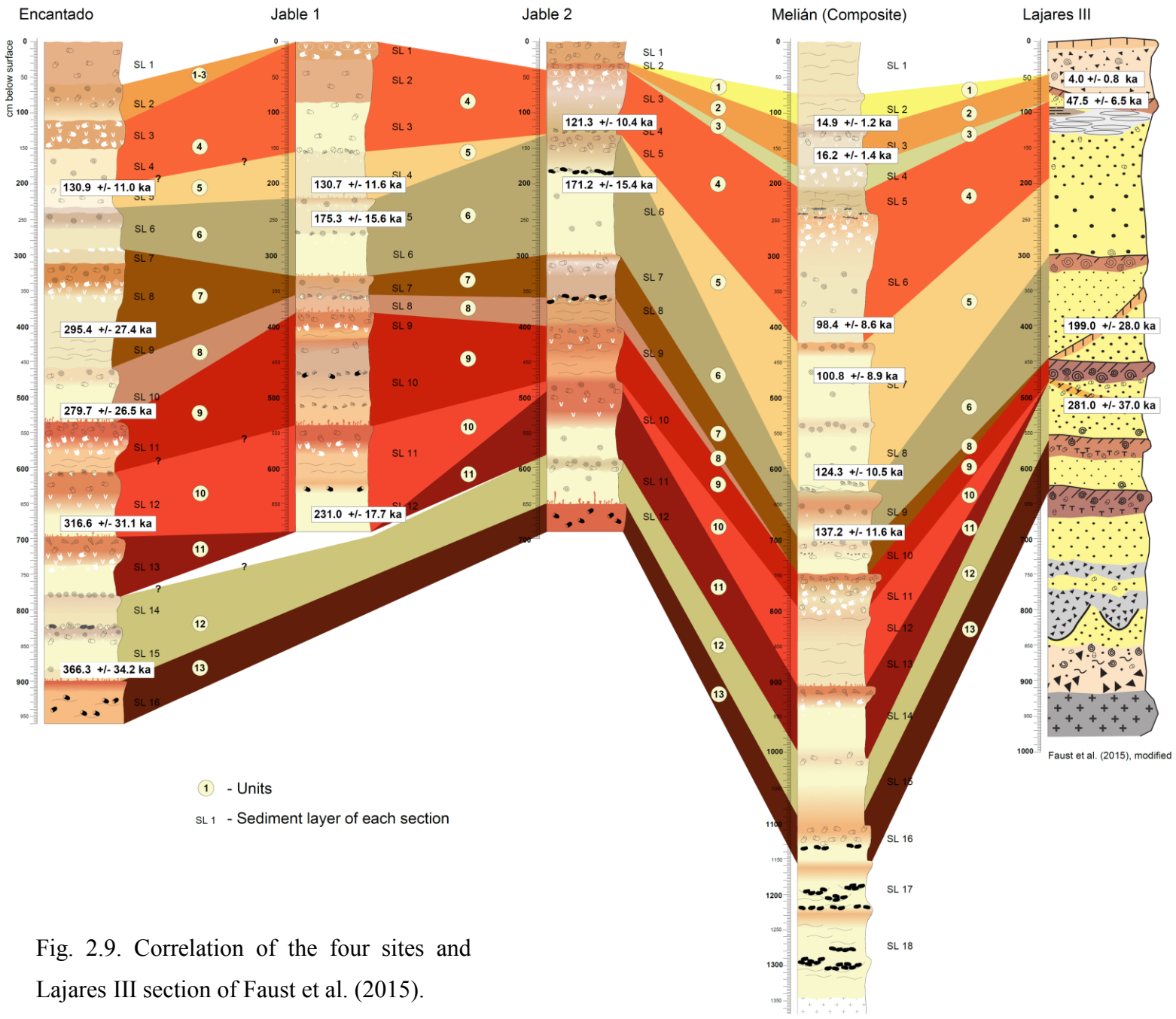

Fig. 2.9. Correlation of the four sites and Lajares III section of Faust et al. (2015).

Unit 13

A strong reddish brown soil that is developed in brownish soil sediments in the lowermost part of Encantado (SL 16) is also present at Jable 2 (SL 12) and Melián (SL 16). The two most important features of Unit 13 are the homogenous colour and the abundance of basaltic rock fragments that assumedly cause the highest values in mass-specific susceptibility at all sites. At Encantado and Jable 2, this soil sediment rests directly on basaltic rock. While at Melián Unit 13 is above several metres of relocated material. Based on our findings in the field (features of relocation like broken pieces of *Cochlicella sp.*), we assume the 'soil sediment' below the 'marker soil' described by (Faust et al., 2015) to be the respective sediment layer of Unit 13. For the Melián section we cannot exclude that SL 17 and SL 18 are also parts of Unit 13. A similar situation applies for Lajares III where sediment deposits below the correlated palaeosol may also be attributed to Unit 13.

Unit 12

Unit 12 marks a layer that is related to weak soil formation and a palaeosurface characterised by features of slight relocation. Furthermore, this unit contains tephra material. We suppose that this unit belongs to SL 15 and possibly SL 14 at Encantado section, SL 11 at Jable 2 section, and SL 15 at Melián section. A corroborating feature is the occurrence of *Obelus pumilio* at the sites of Encantado and Melián. Again, this correlation should be interpreted with caution, but it is supported by the occurrence of mafic minerals, increased Zn content at Encantado, Jable 2, and Melián, and by higher values of magnetic susceptibility at Encantado and Mélian, all of which are further evidence for the imprint of tephra material. Two ages are available: the IRSL age of 366.3 +/- 34.2 ka at Encantado and the 281.0 +/- 37.0 ka age of Lajares III by (Faust et al., 2015). The IRSL ages may fit together in their margins of error. Another explanation is connected to the new insight of Lajares III with a soil sediment below the 'marker soil' described by (Faust et al., 2015). The position of the IRSL sample which resulted in an age of 281.0 +/- 37.0 ka is not clear. It could be placed above, below, or directly within the soil sediment (placed below the soil sediment in Fig. 2.9). Hence, instead of an association with SL 15 of Encantado, the dated sediment of Lajares III could be linked to SL 14 or even SL 13 of Encantado.

Unit 11

At Encantado (SL 13), Unit 11 shows a strong soil developed in pale pure shelf material. In chronological order it is the first palaeosol that is characterised by a gastropod assemblage dominated by *Cochlicella sp.*, and thus it signifies an important stratigraphic marker. This is the only soil showing such high abundance of *Cochlicella sp.* that reaches 672 individuals/10 kg sediment within the Encantado section. As already mentioned, likewise the soil formation related to Unit 10 contains several individuals of *Cochlicella sp.*, but thereafter the occurrence stops abruptly. At Melián, the distribution of *Cochlicella sp.* is much more scattered in the lower sediment units. Here, *Cochlicella sp.* occurs in several horizons, which are mainly characterised by relocation. Clear maximum proportions of *Cochlicella sp.* (1180 individuals/10 kg sediment) occur precisely within the soil of Unit 11 (Melián SL 11). At Jable 1, the soil associated with the high abundance of *Cochlicella sp.* extends several metres to the east of the sampled section and should thus be stratigraphically located below the exposed base of the profile. At Jable 2 the respective SL (between SL 10 and SL 11 of Jable 2) seems to be eroded. It is the same to Lajares III, where a hiatus is assumed.

Unit 9 & 10

This complex comprises up to three soil formations (up to two of Unit 9 and one of Unit 10). Given that a minimum of two of these soils have been converged, they often generate a morphologically resistant surface level, which is exposed within the current gully system. Unit 10 is represented by SL 12 at the Encantado section, SL 11 & 12 at Jable 1, as well as SL 10 at Jable 2, and SL 12 & 13 at Melián. At Lajares III it is eroded and therefore assumed to be absorbed by the aforementioned hiatus. Unit 10 seems to be a transitional link between the gastropod assemblages of *Pomatias lanzarotensis* and the one of *Cochlicella sp.*, as analysed in the Encantado and Melián sections. In chronological order, Unit 10 is the first formation that contains individuals of *Pomatias lanzarotensis*, and simultaneously the last one, which contains individuals of *Cochlicella sp*. Subsequent to the formation of Unit 10, this species is considered to be extinct. The whole succession of Unit 9 and 10 does not indicate volcanic admixtures. Perhaps the marked age of 316.6 +/- 31.1 ka at the Encantado section is overestimated, because another studied section (in the course of the study in hand) very close to the Encantado site showed a preliminary age of 249.3 +/- 22.0 ka (produced in the course of this study) at the same stratigraphic position. A contamination of older sediments (e.g. by bioturbation) could be a reason for

overestimation. Hence, the age of 231.0 +/- 17.7 ka of Jable 2 seems more realistic. Usually, the two palaeosols of Unit 9 are converged, only in the surrounding of the Jable 1 section did we find them separated. This soil complex points to a very high abundance of coated BCs and high de- and recalcification intensities. Another characteristic feature is the gastropod assemblage with occurrence of *Pomatias lanzarotensis*. The complex of Unit 9 and 10 is characterised by strong red colours, caused by soil formation in relocated material. If the palaeosols are separated, they show relocated sediments and soil sediments in between. At the Melián section the complex is represented by an abundance of calcified relocated BCs, which we suppose to be the equivalent of Unit 9. On top of this thick accumulation, a soil in Unit 9 is developed characterised by in situ BCs with an abundance of *Pomatias lanzarotensis* which is represented by 30 individuals/10 kg sediment.

Unit 8

Unit 8 shows features of weak soil formation inside a sediment pointing to relocation at all sites. Again, the Encantado section (SL 10) reveals the best preservation of that unit, showing an IRSL age of 279.7 +/- 26.5 ka. In Jable 1 (SL 8) and Jable 2 (SL 8), we assume the equivalent to Unit 8 to be reflected by a marked erosive surface. At all sites, features of volcanic impact could be observed that create a greasing effect typical of amorphous clay minerals like allophanes which have been formed from volcanic glasses (Kirkman and McHardy, 1980). Hence, this unit fixes a starting point for more intensive volcanic activity, because in almost all sections volcanic impurities were detected to a greater extent in the layers above. On most pitwalls of the quarry of Melián we observed only remnants of Unit 8, at the sampling site it seemed to be admixed on top of Unit 9. The age of 279.7+/-26.5 ka at Encantado seems to be overestimated, and it is possible that stronger bioturbation of the strong palaeosol formation below leads to a wider contamination of laying sediments into this unit.

Unit 7

In chronological order, Unit 7 is the first layer, indicating a very strong influence of volcanic activity, represented by high values of mass-specific susceptibility. In addition, it represents a period of intense soil formation. We suppose that the lowest $CaCO_3$ content in the Encantado section is caused by a combination of the high contribution of volcanic material and the comparably strong soil formation. At Encantado, Unit 7 is represented by a strong soil formation with maximum amounts of SiO_2. We relate this high SiO_2 content

to dust input as well as the incorporation of volcanic material, whereas the latter is additionally supported by maximum values of nearly all measured elements. At Jable 1 & 2, Unit 7 is mainly represented by a mixture of soil sediment and volcanic material accompanied by weak soil formation on top of this soil sediment. Although the two sites bear such strong relocation features in Unit 7, we measured the highest values of mass-specific susceptibility, which we assume to be caused by strong volcanic imprint. Perhaps the high clay values and fragments of a $CaCO_3$ crust at Encantado can be explained by the relocation period. Melián Unit 7 shows an admixture of lapilli and strong relocation features (like chaotic bedding, broken pieces of gastropods, and rock fragments). The IRSL ages of Unit 7 at Encantado (295.4+/-27.4 ka) and the ages of the layers above Unit 7 in Melián (137.2+/-11.6 ka) point to a gap. We assume the age of Encantado is much too old, and it is possibly based on contamination by older sediments caused by translocation processes (seems probable, because of the strong features of relocation of this sediment layer at Encantado). Taking all IRSL ages of Encantado into account, the data suggest that there are methodological problems in dating the deposition of the sediments (which are marked by features of relocation). The ages of Encantado show inverse sequences, perhaps a datable limit of the sediments is exceeded, as described by Wolf and Faust (2013). In sum, 295.4 +/- 27.4 ka does not seem credible.

Unit 6

At Encantado, Unit 6 is dominated by volcanic imprint (mafic minerals and lapilli) and by weak de- and recalcification features. Therefore, we suppose that the local maximum of mass-specific susceptibility is mainly caused by the input of volcanic material. At Jable 1, a weak palaeosol, also accompanied by volcanic impurities, completes an accumulation of sediments of shelf origin. At Jable 2 these sediments of shelf origin are interrupted by relocation features with a palaeosol above, showing stronger volcanic imprint with weak de- and recalcification features. At Melián, Unit 6 gives detailed insights into a sequence of soil formation, volcanic influence, and relocation: Here, at the beginning, soil formation took place in parent material dominated by sediments of shelf origin, followed by the accumulation of tephra material. Finally, ongoing soil formation affected this mixture of tephra and shelf material, before relocation was initiated (compare Fig. 2.8). The Lajares III section also presents a weak soil formation with apparent volcanic imprint (impurities of lapilli and mafic minerals).

Unit 5

Only in the quarry of Melián is Unit 5 clearly differentiated. Here, a huge accumulation (SL 8 & 9) of shelf material is interrupted by a palaeosurface, dominated more by volcanic imprint than by weak pedo features. Most notably, this soil is framed by medium to coarse-grained shelf material above and below. Only at Encantado is Unit 5 characterised by a pale silty sand layer. At Jable 1we assume SL 4 to represent Unit 5, although we have to interpret this correlation with caution in view of the highly dynamic system and the weak stratigraphic features. Perhaps the SL 4 of Jable 1 is part of the Unit 4 above. At Jable 2 we could not identify Unit 5, perhaps it is admixed in the overlying stratum. At Melián we assume that Unit 5 is represented by SL 8 and 9. The IRSL dating present ages of 130.9 +/- 11.0 ka at Encantado, 130.7 +/- 11.6 ka at Jable 1, a minimum (preliminary) age of 121.3 +/- 10.4 ka at Jable 2, and at Melián 124.3 +/- 10.5 ka for the lower parts and 100.8 +/- 8.9 ka for the upper parts of Unit 5.

Unit 4

In the entire study area Unit 4 is mostly characterised by a huge crust of $CaCO_3$, often in combination with incorporated lapilli in the upper parts or relocated tephra material on top of the crust. Regularly, this position is characterised by intense cementations of $CaCO_3$, but as soon as the respective layer is exposed, a massive laminated crust is formed on top by rinsing processes. As (Faust et al., 2015) already assumed, the associated soil could have been eroded. The interpretation comprises a strong soil formation with a subsequent erosion phase, disturbed by volcanic activity. The material of volcanic origin was relocated immediately after deposition. At most studied sites this unit also presents a high abundance of relocated coated BCs. At the Encantado section as well as Jable 1 & 2,we observed a huge accumulation of relocated $CaCO_3$ coated BCs in a reddish yellow silty matrix. At Melián, Unit 4 shows different appearances: We found incorporated lapilli at the SW pit wall, and thick layers of relocated tephra material were found at the NW pit wall. At different sites of the Barranco del Jable (also at Lajares III), we identified incorporated lapilli and a $CaCO_3$ crust in the respective stratigraphic position. At Melián, the IRSL age of 98.4 +/- 8.6 ka of this unit and the age of 100.8 +/- 8.9 ka of the underlying stratum underline the assumption of a shorter period of geomorphic stability to form weak soil before the accumulation of Unit 4 sediments started. All upper parts (above Unit 7) of Encantado are hard to correlate with SLs of the other sites. Examining the low thickness of sediments in the upper parts of Encantado together with less evidence of erosion

features, it is possible that a change in sediment supply and hence less deposition hamper a differentiation of the uppermost parts therefore the layers and units are less definable.

Unit 1-3

Only at Melián are the first three units differentiated. An accumulation of coated BCs, which we interpret as a remnant of an eroded palaeosol, characterises Unit 3 at the northwestern pit wall of Melián. Unit 2 shows a weak palaeosol developed in tephra material that is characterised by less intense de- and recalcification. First IRSL datings showed a period of 1 ka (16.2 +/- 1.4 ka to 14.9 +/- 1.2 ka) for this palaeosol. Unit 1 is the youngest sediment unit and hosts seemingly the weakest palaeosol of the whole stratigraphic sequence. It is interbedded in relocated cross-bedded material. Fine impurities of mafic minerals indicate volcanic influence. At Encantado we assume all three units are incorporated into SL 2, which presents a higher content of elemental composition (including Fe_d), higher silt content, and features of de- and recalcification. This uppermost palaeosol is covered by a silty colluvial layer that we tentatively relate to anthropogenic land use (because we observed lynchets close to the sites of Encantado and Jable 2).

2.6.3 Local forcing factors affecting the stratigraphy

As an important statement, a comparison of the studied sites indicates certain similarities but also obvious differences in the appearance of specific stratigraphic positions. If these differences are brought into a spatial context, certain regularities may appear to relate to palaeo dune and sand sheet dynamics. Within one and the same period, there may be obvious discrepancies between different sites with respect to sedimentary and pedogenetic features. For instance, in the quarry of Melián, Unit 9 indicates strong soil formation but the parent material has been largely relocated. In contrast, at Encantado the same unit is represented by strong reddish in situ soil formations. We assume that such differences between sites are generally caused by spatially different intensities of accumulation processes, preservation, and relocation/erosion. Accumulation is primarily dependent on sediment supply. In the study area, north facing slopes of volcanoes are covered by climbing dunes. According to Coudé-Gaussen and Rognon (1988), shelf material has been mainly transported by westerlies during sea level low stands under arid conditions. Contrastingly, Criado et al. (2004) postulated that sediments of shelf origin have been blown out by palaeowinds from the same direction as present day north-easterly trade winds which, for example, build up the Holocene dune field of Corralejo. Alcántara- Carió

et al. (2010) postulated dominating trade winds alternating with easterly winds during the development of the oldest dunes. However, the sandy shelf material, which builds up the dunes, is transported by saltation and creeping processes. These processes indicate comparatively short transport distances. Hence, this kind of sediment supply is dependent on distance and connectivity to the shelf area (see Fig. 2.10).

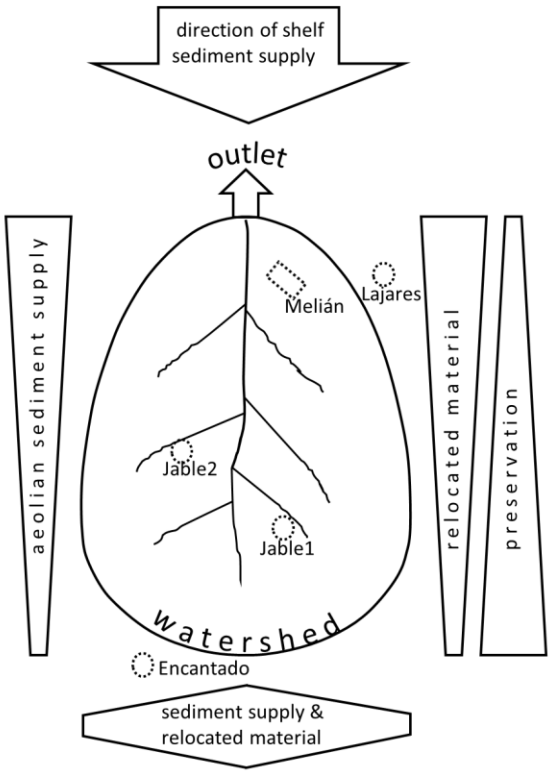

Fig. 2.10. Generalised spatial patterns of sediment supply, relocation, and preservation conditions within a catchment of the study area (derived from Barranco del Jable). According to these patterns, we located the positions of the sites within the sketch.

In contrast to the accumulation of shelf material that is the main process for dune and sand sheet formation, the accumulation of dust is assumed to be ubiquitously distributed. Concerning the accumulation of shelf sediments, we observed an apparent difference between the Melián section (also Lajares III section) and the section of Encantado that mainly becomes obvious in the upper parts of the profiles. In fact, Mélian and Lajares show thick accumulations of sand sediments above Unit 7, whereas these deposits are much thinner in Encantado. Furthermore, sediments in Encantado show higher silt contents. We suppose that these differences are also caused by the relationship between the distance of sediment transport and the direction to the source. Hence, the observation allowed us to assume a much shorter distance between Melián and the shelf area (in comparison to the distance to Encanctado), accompanied by a sediment supply from a northern direction. At the very least we observed lower thicknesses of shelf material in comparison to Melián and Lajares III concerning the parts above Unit 7. The processes of preservation, relocation, and erosion are primarily dependent on vegetation cover, the permeability of the shallow subsurface, as well as on the slope gradient (Schumm, 1956). Furthermore, each site shows some specific characteristics regarding the efficiency of erosion. In this context, the concept of (dis)connectivity describes in how far a certain location is linked to a network of erosion

pathways that appear throughout the catchment (Brierley et al., 2006). Along these erosive pathways, different types of obstacles may strongly influence the connectivity that finally characterises the operation of sediment cascades (Fryirs et al., 2007). Therefore, the connectivity of a location affects processes of relocation/erosion and vice versa the state of preservation. Taking one single site within the study area and simplifying all the complex relations within an individual catchment, the following regularities (compare Fig. 2.10) may arise for the studied palaeo dune systems:

I. The closer the sediment source, the higher the sediment supply and deposition.
II. The closer the outlet of the catchment (base level of erosion), the stronger the sediment relocation over the whole time (compare Wolf and Faust, 2013).
III. The closer the former channel system, the stronger the sediment relocation.
IV. The closer the water divide, the better the sediment preservation conditions.
V. The higher the slope angles, the stronger the sediment relocation.

Melián (as well as Lajares III) features the strongest relocation, especially within the lower parts that are characterised by the occurrence of *Cochlicella sp.* According to the above mentioned concept, we suppose the best connectivity for those sites that are in accordance with its position close to the (former) outlet of the Barranco del Jable catchment. Even the strong inclination of the observed palaeosurfaces over the whole profile support this relationship. In contrast, the site of Encantado shows the best sediment preservation conditions, which assumingly is due to its position close to the watershed (Fig. 2.2) accompanied by a much smaller drainage area, hence less surface runoff and therefore lower connectivity. We suppose that these differences in connectivity are key to explaining the well preserved soils in Encantado, whereas Melián is mainly characterised by relocation features during the corresponding periods. Likewise, the partially stronger preservation of dust within the Encantado section (e.g. in Unit 7) further illustrates reduced erosion activity at that location. The sites of Jable 1 and Jable 2 appear to vary in their connectivity characteristics during different periods. At both sites, Units 7–10 refer to relocation processes, but Jable 2 indicates a stronger influence of relocation compared to Jable 1. This may be due to the much larger drainage area of Jable 2, which is further intensified by much steeper slope gradients that have been observed as related to palaeo-surfaces in Jable 2. Based on this conceptual model, we observe a north-south gradient of decreasing accumulation and sediment supply as well as vulnerability to erosion and of better preservation conditions (Fig. 2.10).

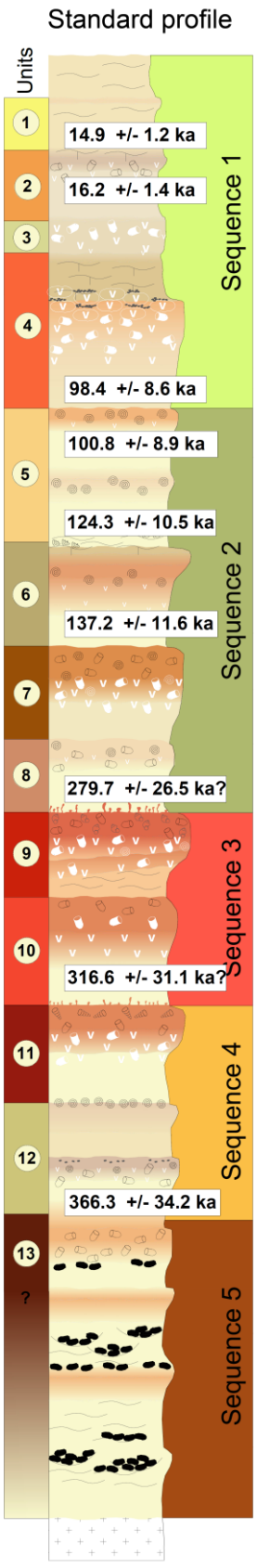

Fig. 2.11. Standard profile.

Within the succession of 13 units of correlation that have been described, we can distinguish five characteristic sequences (Fig. 2.11). Sequence 5 comprises Unit 13 and the parts below. The latter present obvious features of strong relocation induced by water in the quarry of Melián. The deposits of the whole of Sequence 5 contain a lot of basaltic rock fragments. Unit 13 represents very high amounts of iron and the maximum values of mass-specific susceptibility. This sequence is older than 360 ka. Sequence 4 corresponds to Unit 11 and Unit 12 and encompasses roughly 50 ka, from 60 ka to 310 ka, and is characterised by the thickest preserved deposits at the Barranco de los Encantados. Shelf material with a total thickness of several metres has been deposited. In general, the deposits show fewer features of relocation induced by water. Unlike in the channels in the lowest parts of Melián (Sequence 5), there are no channels, and there are no strong recalcification features, $CaCO_3$ coatings, or truncated parts as presented by the upper parts of Sequence 3. Hence we assume more arid conditions and a long lasting exposure of the surface on top of Sequence 4 in order to form such an intensive soil. Unit 12 indicates volcanic imprint. Sequence 3 comprises Unit 9 and 10. The latter represents to some extent a shifting period between the former Unit 11 and the subsequent Unit 9. In the whole study area we note high sediment supply of shelf material with embedded strong reddish soil formations. The high content of pedogenic iron (Fe_d), the features of intercalated strong relocation periods, and observed truncated palaeosols (on top of Unit 9 at Melián) indicate more humid conditions. There is no evidence of volcanic activity. Sequence 3 started approximately 310 ka and did not end before 280 ka. We interpret the IRSL dating (especially from Encantado) with caution, because they may suggest sediments that are too old. Enhanced uncertainties could be caused by the transport

cascades of the dated sediments (seems natural against the backdrop of the described strong relocation features) and the admixture of older sediments by bioturbation. Sequence 2 corresponds to Units 5–8. Given the dating of Melián and Encantado, we know that Sequence 2 started before 140 ka and ended approximately at 100 ka. Within Unit 8 we observed severe volcanic imprint, with a clear increase within Unit 7 and Unit 6 and a weaker but ongoing volcanic influence in the subsequent Unit 5. The northern part (sites of Melián and Lajares III) shows thick aeolian deposits, hence the supply of shelf sediment continued, whereas in the southern part (Encantado) we note thin deposits. Fewer features of relocation are recognisable, hence eroded sediments are improbable and severely restricted sediment supply is more likely. Sequence 1 encompasses Units 1–4 and encompasses the last 100 ka. In chronological order Unit 4 represents a clear increase of humidity, represented by the formation of a $CaCO_3$ crust. We also observed strong volcanic imprint (deposits of lapilli as well as tephra material). The subsequent Units 3, 2, and 1 show further volcanic imprint with decreased humidity that temporally led to weak soil formation features, but also to severe relocation. Unit 2 marks a short period of a thousand years at 16 to 15 ka. The high values of element proportions might be caused by impurities of volcanic material or by anthropogenic influence, for example indicated by lynchets in the closer surrounding of Encantado and Jable 2. Units 1–3 are characterised by a severely restricted or even stopped deposition of aeolian sediment of shelf origin.

2.6.4 Source differentiation and processes

As stated above, the sediments that form dunes and sand sheets in northern Fuerteventura mainly consist of material originating from three different sources:

i. shelf origin

ii. volcanic origin (tephra, lapilli, and rock fragments)

iii. dust origin

Fig. 2.12 shows a simplified conceptual model of sediment components and different sediment pathways within the dune fields on Fuerteventura. We distinguish different sediment sources and processes by geochemical characteristics (e.g. Fe, Sr, Ca content) and prominent features (e.g. de- and recalcification, configuration of bee nests, silt content, etc.).

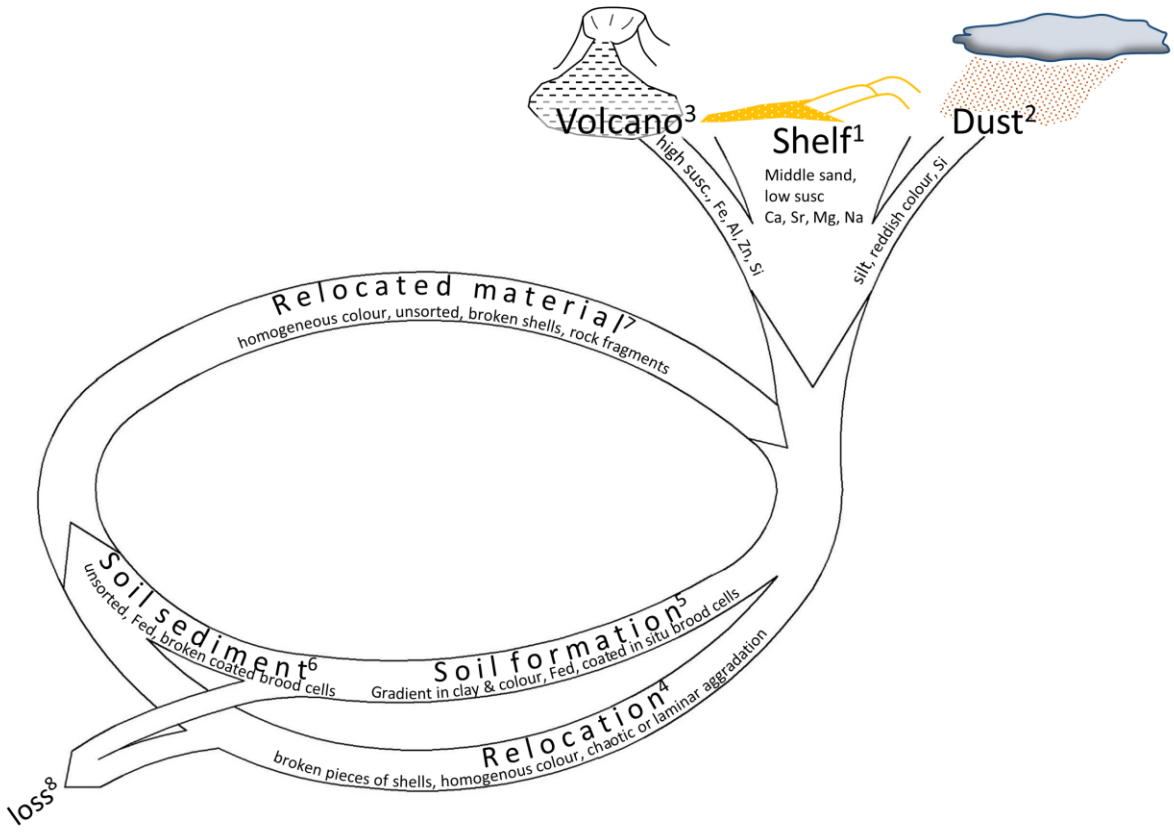

Fig. 2.12. The schematic sketch traces the participating materials and possible pathways of the different sediment mixtures and their indications. Thus, the figure sums up different possibilities for origin and history of each sediment within a profile.

Dunes and reworked dune sands on Fuerteventura are mainly formed by shelf material (Fig. 2.12, indicated by No. 1) that is described by (Brooke, 2001) as shallow-marine biogenic carbonate sediment. These aeolianites only consist of Ca, Sr, Na, and Mg, and they are characterised by a dominance of the middle to coarse-grained sand fraction, a very pale brown colour, and by very low values of mass-specific susceptibility.

Varying quantities of dust are admixed to the formation of dune palaeosol sequences (Fig. 2.12 compare No. 2). This dust is generally of Saharan origin (Menéndez et al., 2009) and is characterised by markedly higher silt content and a higher content of SiO_2 bearing minerals due to the high amounts of quartz and feldspar (and mica). The amount of quartz is considered to be the best indicator of dust input on the Canary Islands (Misota and Matsuhisa, 1995; von Suchodoletz et al., 2013). Hence, for this $CaCO_3$ dominated area (poor in silicates), the concentration of SiO_2 can be taken as an indicator of dust input (Moreno et al., 2002; Muhs, 2013). Furthermore, dust on the Canary Islands also consists of up to 6% hematite (Menéndez et al., 2013), therefore likewise the reddish colour can be taken as an indicator of dust input. In the case of sediment accumulation, we have to add

that the conceptual approach of sedimentation rate dependent intensity of soil formation by (Faust et al., 2015) has to be extended. The appearance of soil formation is also dependent on sediment properties. Therefore, the input of Saharan dust does not dilute the colours of soil formation, but could instead intensify the colour appearance.

Materials of volcanic origin (tephra, lapilli, and rock fragments) are indicated by higher values of susceptibility and darker colour, because of impurities of mafic minerals (Fig. 2.12 see No. 3). The basaltic material related to volcanism on Fuerteventura causes higher values of Fe, Al, and Mg content (compare Rothe, 1996), and also Zn seems to be enriched by input of basaltic material (Faust et al., 2015). Also, the amounts of volcanic glasses that may be subject to allophane weathering play an important role in providing elements like Si or Al for mineral neogenesis (Ming Huang et al., 2011; Shoji et al., 1993).

With respect to sediment supply, deflation of shelf material is seen as the most important process. After the deposition of dunes and sand sheets, a first relocation of short distance took place that led to sediment dominated by shelf material in which basaltic fragments, tephra material, and (broken) mollusc shells are admixed (Fig. 2.12, compare No. 4). This process is followed by a short period of exposure. In this context, sediments are not necessarily transported directly to the outlet of the catchment, but instead they pass a cascade of different sedimentary sinks starting from foot slope position, through tributary channels, and finally to the main channel. Such relocated material that has not been subject to longer exposition is characterised by features like (i) an unsorted mixture of different grain sizes, (ii) a homogenous light colour, (iii) impurities of several rock fragments and pieces of mollusc shells, and (iv) often by laminar deposition features.

Another possible step may lead via longer duration of sediment exposure to more dust input and soil formation (Fig. 2.12, see No. 5). Indications of in situ soil formation in our study area are (i) de- and recalcification features that are regularly reflected by different intensities of coatings of BCs in in situ position (compare Edwards and Meco, 2000), (ii) an enrichment of clay, (iii) higher colour intensities, and (iv) higher values of Fe_d as well as of K and Mg. As already mentioned, dust input is evidenced by a higher content of silt, iron oxide, and SiO_2.

Subsequently, the soil material may be relocated in a similar way as described above, forming a colluvial layer of soil sediments in footslope position (Fig. 2.12, see No. 6). During each relocation process, slope material such as basalt debris, lapilli, but also transported BCs and mollusc shells may be incorporated into the sediment. After deposition, these relocated soil sediments are characterised by (i) coated BCs that are

reworked, (ii) broken pieces of coated BCs, (iii) a certain abundance of mainly broken mollusc shells, (iv) medium to high values of susceptibility and Fe_d, (v) unsorted fine grained sediments, and (vi) often by a reddish always homogenous colour. This mixture of different materials finally generates our sedimentary archives (Fig. 2.12, No. 7), or alternatively can be removed from the system (Fig. 2.12, No. 8). The column "Identification" of the profile figures (Figs. 2.3–2.6) is based on these concepts.

2.7 Conclusion

This study presents an attempt to correlate sequences of alternating aeolian deposition and palaeosol formation within a highly dynamic system of palaeo dunes and sand sheets. For the first time, a universal stratigraphy for different catchments could be presented. The position related to relief and the connectivity to erosion pathways within the catchment determines the sedimentary characteristics and respective features of each site. The soil colour, which in many other terrestrial archives is a useful proxy to differentiate between different intensities of soil formation, turned out to be highly variable, and thus less suitable to identify soil formation intensities. This is mainly caused by the dominance of very pale parent material (shelf sediments) and the imprint of coloured dust as well as of volcanicmaterial that contain considerable amounts of iron oxides and fast weathering minerals. Nevertheless, colour is still useful to distinguish between the different participating materials (biogenic shelf material, dust, or volcanic material). Instead, differences in decalcification and recalcification features proved to be the most reliable indicators to distinguish between different intensities of soil formation in dune fields in northern Fuerteventura. Especially $CaCO_3$ coatings in combination with the occurrence of BCs, and the different stages of $CaCO_3$ coating of these brood cells, are evidence of surface stability and soil formation. In general, a typically developed soil formation in dune sands on Fuerteventura shows a characteristic succession of gastropods and brood cells, starting with in situ BCs, followed by a combination of BCs and gastropods, and completed by an abundance of gastropods on top. We observed four land snail assemblages which give reason to assume a relationship between their occurrence and their stratigraphic position. The order of maxima of *Obelus pumilio*, *Cochlicella sp.*, *Pomatias lanzarotensis*, and *Rumina decollata* correspond to a stratigraphical order. Moreover, during phases of soil formation the amounts of elemental SiO_2 within the upper soil horizons are enriched due to dust accumulation. This has likewise been confirmed by former studies, although we found the highest values of SiO_2 linked to dust input in combination with imprint of

volcanic material. We identified five major sedimentary sequences that differed in thickness of deposits, prevailing humidity, and volcanic activity. Soil formation and (water induced) erosion are primarily controlled by humidity, hence more humid climate conditions might be able to initiate both processes. Which process takes place seems to be dependent on the connectivity to erosion pathways of each site and the steepness of slopes. In phases of higher sediment supply, a palaeosurface can be covered by new dune material depending on the distance to the source area of shelf sediment. On the other hand, during more humid periods soil formation can be (but must not be) interrupted by surface erosion, which in turn depends on the characteristics of each site (connectivity within the catchment, steepness). Hence, considering the whole range of geomorphic processes, the simple division into periods of geomorphological stability and geomorphological activity seems not really appropriate for the studied dune systems. Rather, phases of morphodynamic activity, characterised by a large supply of shelf material, may only take place locally and alternate with more humid phases which in turn may be characterised by further morphodynamic activity in terms of water-induced erosion. In a next step, intense dating will be realised in order to achieve a chronological resolution that enables a detailed ecological interpretation of the sequences.

2.8 Acknowledgments

We are extremely grateful to Maria Tarquis Gongora and Don Manuel Gutierrez Ruiz who always permit access to important study sites. Many thanks to Michael Zech, Rico Hübner, Hans von Suchodoletz, and Sascha Meszner for intensive discussions. Special thanks to Michael Dietze for coordinating the grain size measurements at the GFZ Potsdam and for supportive ideas. Many thanks for all advices from Assist. Prof. Dr. Yurena Yanes (University of Cincinnati), and to Beate Winkler who did the measurements at the laboratory of the TU Dresden. We would like to thank the two anonymous reviewers for all comments and advice. Special thanks to Elizabeth Kelly for proofreading. This work was supported by the German Research Foundation (FA 239/18-1).

2.9 References

Abdel-Monem, A.,Watkins, N.D., Gast, P. W., 1971. Potassium-argon ages: volcanic stratigraphy and geomagnetic polarity history of the Canary Islands. Am. J. Sci. 271, 490–521.

Alcántara-Carió, J., Fernández-Bastero, S., Alonso, I., 2010. Source area determination of

aeolian sediments at Jandia Isthmus (Fuerteventura, Canary Islands). J. Mar. Syst. 80, 219–234.

Ancochea, E., Brändle, J. L., Cubas, C. R., Hernán, F., Huertas, M. J., 1996. Volcanic complexes in the eastern ridge of the Canary Islands: the Miocene activity of the island of Fuerteventura. J. Volcanol. Geotherm. Res. 70, 183–204.

Anguita, F., Hernán, F., 2000. The Canary Islands origin: a unifying model. J. Volcanol. Geotherm. Res. 103, 1–26.

Balogh, K., Ahijado, A., Casillas, R., Fernández, C., 1999. Contributions to the chronology of the Basal Complex of Fuerteventura, Canary Islands. J. Volcanol. Geotherm. Res. 90, 81–101.

Bank, R. A., Groh, K., Ripken, T. E. J., 2002. Catalogue and bibliography of the non-marine Mollusca of Macaronesia. In: Falkner, M., Groh, K., Speight, M.C.D. (Eds.), Collectanea Malacologica. Conchbooks, Hackenheim, pp. 89–235.

Bouab, N., Lamothe, M., 1995. Geochronological framework for the Quaternary paleoclimate record of the Rosa Negra section (Fuerteventura – Canary Islands, Spain). Clim. Past 2-7 (1995), 37–42.

Brierley, G., Fryirs, K., Jain, V., 2006. Landscape connectivity: the geographic basis of geomorphic applications. Area 38 (2), 165–174.

Brooke, B., 2001. The distribution of carbonate eolianite. Earth Sci. Rev. 55, 135–164.

Coello, J., Cantagrel, J.-M., Hernán, F., Fúster, J.-M., Ibarrola, E., Ancochea, E., Casquet, C., Jamond, C., Diaz de Téran, J.-R., Cendrero, A., 1992. Evolution of the eastern volcanic ridge of the Canary Islands based on new K-Ar data. J. Volcanol. Geotherm. Res. 53, 251–274.

Coudé-Gaussen, G., Rognon, P., 1988. Origine Eolienne de Certains Encroutements Calcaires sur l'ile de Fuerteventura (Canaries Orientales). Geoderma 42, 271–293.

Criado, C., Guillo, H., Hansen, A., Hansen, C., Lillo, P., Torres, J. M., Naranjo, A., 2004. Geomorphological evolution of Parque Natural de Las Dunas de Corralejo (Fuerteventura, Canary Island). In: Benito, G., Díez Herrero, A. (Eds.), Contribuciones Recientes sobre Geomorfología. SEG y CSIS, Madrid.

Damnati, B., Petit-Maire, N., Fontugne, M., Meco, J., Williamson, D., 1996. Quaternary paleoclimates in the Eastern Canary Islands. Quat. Int. 31, 37–46.

Edwards, N., Meco, J., 2000.Morphology and palaeoenvironment of brood cells of Quaternary ground-nesting solitary bees (Hymenoptera, Apidae) from Fuerteventura, Canary Islands, Spain. Proc. Geol. Assoc. 111, 173–183.

Engelbrecht, J. P., Menéndez, I., Derbyshire, E., 2014. Sources of PM2.5 impacting on Gran Canaria, Spain. Catena 117, 119–132.

Faust, D., Yurena, Y., Willkommen, T., Roettig, C., Richter, Dan., Richter, Dav., Suchodoletz, H.v., Zöller, L., 2015. A contribution to the understanding of late Pleistocene dune sand- palaeosol-sequences in Fuerteventura (Canary Islands). Geomorphology 246, 290–304.

Fryirs, K. A., Brierley, G. J., Preston, N. J., Kasai, M., 2007. Buffers, barriers and blankets: the (dis)connectivity of catchment-scale sediment cascades. Catena 70, 49–67.

Fúster, J. M., Hernandez-Pacheco, A., Munoz, M., Badiola, E. R., Cacho, L. G., 1968. Geology and volcanology of the Canary Islands. Internat. Symposium Volcanology.

Genise, J. F., Alonso-Zarza, A. M., Verde, M., Meléndez, A., 2013. Insect trace fossils in aeolian deposits and calcretes from the Canary Islands: Their ichnotaxonomy, producers, and palaeoenvironmental significance. Palaeogeogr. Palaeoclimatol. Palaeoecol. 377, 110–124.

Guerin, G., Mercier, N., Adamiecz, G., 2011. Dose rate conversion factors update. Ancient TL 29, 5–8.

Huot, S., Lamothe, M., 2003. Variability of infrared stimulated luminescence properties from fractured feldspar grains. Radiat. Meas. 37, 499–503.

Ibáñez, M., Alonso, M. R., Groh, K., Hutterer, R., 2003. The genus *Obelus* Hartmann, 1842 (Gastropoda, Pulmonata, Helicoidea) and its phylogenetic relationships. Zool. Anz. 242, 157–167.

Kirkman, J. H., McHardy, W. J., 1980. A comparitive study of the morhology, chemical composition and weathering of rhyolitic and andesitic glass. Clay Miner. 15, 165–173.

López-García, P., Gelado-Caballero, M. D., Santana-Castellano, D., de Tangil, M. S., Collado-Sánchez, C., Hernández-Brito, J.J., 2013. A three-year time-series of dust deposition flux measurements in Gran Canaria, Spain: a comparison of wet and dry surface deposition samplers. Atmos. Environ. 79, 689–694.

Ložek, V., 1964. Quartärmollusken der Tschechoslowakei. Rozpravy Ústøedního ústavu geologického. 31 Prag.

McKee, E. D., Ward, W. C., 1983. Eolian. In: Scholle, P. A., Bebout, D. G., Moore, C. H. (Eds.), Carbonate Depositional Environments. AAPG Memoir 33.

Meco, J. (Ed.), 2008. Historia geológica del clima en Canarias (Las Palmas de Gran

Canaria).

Meco, J., Petit-Maire, N., Ballester, J., Betancort, J. F., Ramos, A. J. G., 2010. The Acridian plagues, a new Holocene and Pleistocene palaeoclimatic indicator. Glob. Planet. Chang. 72, 318–320.

Meco, J., Muhs, D. R., Fontugne, M., Ramos, A. J. G., Lomoschitz, A., Patterson, D., 2011. Late Pliocene and Quaternary Eurasian locust infestations in the Canary Archipelago. Lethaia 44, 440–454.

Menéndez, I., Díaz-Hernández, J. L., Mangas, J., Alonso, I., Sánchez-Soto, P. J., 2007. Airborne dust accumulation and soil development in the North-East sector of Gran Canaria (Canary Islands, Spain). J. Arid Environ. 71, 57–81.

Menéndez, I., Cabrera, L., Sánchez-Pérez, I., Mangas, J., Alonso, I., 2009. Characterisation of two fluvio-lacustrine loessoid deposits on the island of Gran Canaria, Canary Islands. Quat. Int. 196, 36–43.

Menéndez, I., Pérez-Chacón, E., Mangas, J., Tauler, E., Engelbrecht, J. P., Derbyshire, E., Cana, L., Alonso, I., 2013. Dust deposits on La Graciosa Island (Canary Islands, Spain): texture, mineralogy and a case study of recent dust plume transport. Catena 117, 133–144.

Misota, C., Matsuhisa, Y., 1995. Isotopic evidence for the eolian origin of quartz and mica in soils developed on volcanic materials in the Canary Archipelago. Geoderma 66, 313–320.

Ming Huang, P., Li, Y., Sumner, M.E., 2011. Handbook of Soil Sciences, Second Edition (Two Volume Set): Handbook of Soil Sciences: Properties and Processes. CRC Press.

Moine, O., Rousseau, D., Antoine, P., 2005. Terrestrial molluscan records of Weichselian Lower to Middle Pleniglacial climatic changes from the Nussloch loess series (Rhine Valley, Germany) - the impact of local factors. Boreas 34, 363–380.

Moreno, A., Targarona, J., Henderiks, J., Canals, M., Freudenthal, T., Meggers, H., 2001. Orbital forcing of dust supply to the North Canary Basin over the last 250 kyr. Quat. Sci. Rev. 20, 1327–1339.

Moreno, A., Nave, S., Kuhlmann, H., Canals, M., Targarona, J., Freudenthal, T., Abrantes, F., 2002. Productivity response in the North Canary Basin to climate changes during the last 250 000 yr: a multi-proxy approach. Earth Planet. Sci. Lett. 196, 147–159.

Muhs, D. R., 2013. The geologic records of dust in the Quaternary. Aeolian Res. 9, 3–48.

Murray, A. S.,Wintle, A.G., 2000. Luminescence dating of quartz using an improved single aliquot regenerative dose protocol. Radiat. Meas. 32, 57–73.

Ortiz, J. E., Torres, T., Yanes, Y., Castillo, C., de la Nuez, J., Ibáñez, M., Alsonso, M. R., 2006. Climatic cycles inferred from the aminostratigraphy and aminochronology of Quaternary dunes and palaeosols from the eastern islands of the Canary Archipelago. J. Quat. Sci. 21, 287–306.

Perez-Marrero, J., Llinás, O., Maroto, L., Rueda, M. J., Cianca, A., 2002. Saharan dust storms over the Canary Islands during winter 1998 as depicted from the advanced very highresolution radiometer. Deep-Sea Res. II 49, 3465–3479.

Prescott, J. R., Hutton, J. T., 1994. Cosmic ray contribution to dose rates for luminescence and ESR dating: large depths and long-term time variations. Radiat. Meas. 23, 497–500.

Preusser, F., 2003. IRSL dating of K-rich feldspars using the SAR protocol: comparison with independent age control. Ancient TL 21, 17–23.

Pye, K., Tsoar, H., 2009. Aeolian Sand and Sand Dunes. Springer-Verlag, Berlin Heidelberg.

Rothe, P., 1996. Kanarische Inseln. Sammlung Geologische Führer 81. Gebrueder Borntraeger, Stuttgart.

Rother, H., Shulmeister, J., Rieser, U., 2010. Stratigraphy, optical dating chronology (IRSL) and depositional model of pre-LGM glacial deposits in the Hope Valley, New Zealand. Quat. Sci. Rev. 29, 576–592.

Schlichting, E., Blume, H.-P., Stahr, K., 1995. Bodenkundliches Praktikum. Blackwell, Berlin, Wien.

Schulte, P., Lehmkuhl, F., Steininger, F., Loibl, D., Lockot, G., Protze, J., Fischer, P., Stauch, G., 2016. Influence of HCl pretreatment and organo-mineral complexes on laser diffraction measurement of loess– palaeosol-sequences. Catena 137, 392–405.

Schumm, S. A., 1956. Evolution of drainage systems and slopes in badlands at Perth Amboy, New Jersey. Geol. Soc. Am. Bull. 67, 597–646.

Shoji, S., Nanzyo, M., Dahlgren, R., 1993. Volcanic ash soils genesis, properties and utilization. Developments in Soil Science. 21, pp. 1–288.

Von Suchodoletz, H., Oberhänsli, H., Faust, H., Fuchs, M., Blanchet, C., Goldhammer, T.,

Zöller, L., 2010. The evolution of Saharan dust input on Lanzarote (Canary Islands) - influenced by human activity in the Northwest Sahara during the early Holocene. The Holocene 20 (2), 169–179.

Von Suchodoletz, H., Glaser, B., Thrippleton, T., Broder, T., Zang, U., Eigenmann, R., Kopp, B., Reichert, M., Zöller, L., 2013. The influence of Saharan dust deposits on La Palma soil properties (Canary Islands, Spain). Catena 103, 44–52.

Welter-Schultes, F. W., 2012. European Non-marine Molluscs, a Guide for Species Identification. Planet Poster Editions, Göttingen.

Wolf, D., Faust, D., 2013. Holocene sediment fluxes in a fragile loess landscape (Saxony, Germany). Catena 103, 87–102.

Yanes, Y., Castillo, C., Hutterer, R., De la Nuez, J., Quesada, M., Torres, T., Ortiz, J. E., Alonso, M. R., Ibáñez, M., 2004. Valoración patrimonial de las formaciones dunares cuaternarias del Barranco de los Encantados y Cantera de Melián de la isla de Fuerteventura (Islas Canarias). Geogaceta 36, 195–198.

Yanes, Y., Kowalewski, M., Ortiz, J. E., Castillo, C., de Torres, T., de la Nuez, J., 2007. Scale and structure of time-averaging (age mixing) in terrestrial gastropod assemblages from Quaternary eolian deposits of the eastern Canary Islands. Palaeogeogr. Palaeoclimatol. Palaeoecol. 251, 283–299.

Yanes, Y., Yapp, C. J., Ibáñez, M., Alonso, M. R., de-la-Nuez, J., Quesada, M. L., Castillo, C., Delgado, A., 2011. Pleistocene–Holocene environmental change in the Canary Archipelago as inferred from the stable isotope composition of land snail shells. Quat. Res. 75, 658–669.

Yanes, Y., García-Alix, A., Asta, M. P., Ibáñez, M., Alonso, M. R., Delgado, A., 2013. Late Pleistocene–Holocene environmental conditions in Lanzarote (Canary Islands) inferred from calcitic and aragonitic land snail shells and bird bones. Palaeogeogr. Palaeoclimatol. Palaeoecol. 378, 91–102.

2.10 Supplementary material

2.10.1 Stratigraphic results – detailed description

Concerning 2.5.1. Encantado section

The lowermost part of the profile is characterised by a homogeneous soil sediment of strong brown colour (7.5 YR 4/6, sample 2). The sediment layer 16 (SL 16) contains basaltic fragments and shows high values of mass specific susceptibility, ranging from 193.06 (sample1) to 210.69 (sample 2). The highest values (232.49 in sample 3) of the whole section Encantado belong to a palaeosol that is developed in the uppermost part of SL 16. The next overlying stratum (SL 15) is characterised by nearly pure shelf material (7.5 YR 7/6; sample 5) with some impurities of mafic minerals of volcanic origin. The shelf material only consists of Ca, Sr, Mg and Na, lacking all other measured elements. The IRSL dating resulted 366.3 +/- 34.2 ka (Tab. 2.5, No. BT 1426) of SL 15.

Laboratory code	^{238}U [ppm][a]	^{232}Th [ppm][a]	^{40}K [%][b]	$\dot{D}_{cosmic}$ [Gy/ka][c]	Total Dose rate $\dot{D}$ [Gy/ka]	Equivalent Dose ED [Gy]	Luminescence Age [ka]
Melián							
BT 1340	1.55 ± 0.08	0.91 ± 0.23	0.12 ±0.01	0.16 ± 0.02	1.07 ± 0.08	108.01 ± 4.54	100.8 ± 8.9
BT 1341	1.45 ± 0.07	0.88 ± 0.23	0.15 ±0.02	0.15 ± 0.02	1.04 ± 0.08	102.79 ± 4.34	98.4 ± 8.5
BT 1342	1.40 ± 0.13	2.51 ± 0.42	0.41 ±0.04	0.14 ± 0.01	1.46 ± 0.11	200.50 ± 8.51	137.2 ± 11.6
BT 1343	1.59 ± 0.14	2.71 ± 0.45	0.48 ±0.05	0.13 ± 0.01	1.62 ± 0.12	201.39 ± 8.46	124.3 ± 10.5
BT 1344	1.81 ± 0.16	3.48 ± 0.52	0.86 ±0.09	0.13 ± 0.01	2.15 ± 0.15	32.14 ± 1.37	14.9 ± 1.2
BT 1345	1.70 ± 0.09	1.22 ± 0.28	0.29 ±0.03	0.14 ± 0.01	1.31 ± 0.10	21.33 ± 0.92	16.2 ± 1.4
Encantado							
BT 1421	1.24 ± 0.06	1.02 ± 0.19	0.20 ±0.02	0.17 ± 0.02	1.10 ± 0.08	144.00 ± 6.35	130.9 ± 11.0
BT 1423	1.49 ± 0.08	0.52 ± 0.24	0.10 ±0.01	0.13 ± 0.01	1.00 ± 0.08	295.98 ± 12.44	295.4 ± 27.4
BT 1424	1.54 ± 0.08	0.52 ± 0.24	0.08 ±0.01	0.12 ± 0.01	1.00 ± 0.08	278.92 ± 11.56	279.7 ± 26.5
BT 1425	1.91 ± 0.07	0.11 ± 0.18	0.05 ±0.01	0.10 ± 0.01	1.07 ± 0.10	337.87 ± 14.00	316.6 ± 31.1

BT 1426	1.22 ± 0.10	1.18 ± 0.32	0.16 ±0.02	0.09 ± 0.01	0.98 ± 0.08	359.78 ± 14.82	366.3 ± 34.2
Laboratory code	**^{238}U [ppm][a]**	**^{232}Th [ppm][a]**	**^{40}K [%][b]**	**$\dot{D}_{cosmic}$ [Gy/ka][c]**	**Total dose rate $\dot{D}$ [Gy/ka]**	**Equivalent Dose ED [Gy]**	**Luminescence Age [ka]**
Jable 1							
BT 1514	1.33 ± 0.08	1.26 ± 0.25	0.13 ± 0.01	0.16 ± 0.02	1.08 ± 0.08	141.80 ± 5.91	130.7 ± 11.6
BT 1515	1.30 ± 0.03	1.37 ± 0.01	0.11 ± 0.01	0.13 ± 0.01	0.99 ± 0.07	172.68 ± 8.35	175.3 ± 15.6
BT 1518	1.90 ± 0.03	0.35 ± 0.01	0.06 ± 0.01	0.06 ± 0.01	1.53 ± 0.09	354.18 ± 16.61	231.0 ± 17.7
Jable 2							
BT 1525	1.31 ± 0.06	0.80 ± 0.19	0.18 ± 0.02	0.19 ± 0.02	1.10 ± 0.08	132.83 ± 6.37	121.3 ± 10.4
BT 1526	1.34 ± 0.06	0.69 ± 0.17	0.10 ± 0.01	0.17 ± 0.02	1.00 ± 0.08	170.86 ± 8.13	171.2 ± 15.4

[a] Determined by thick source α-counting.
[b] Determined by ICP-MS.
[c] Cosmic dose rate calculated according to Prescott & Huttton (1994).

Tab. 2.5.: Analytic results and luminescence ages.

In the topmost part of SL 15, a very weak truncated palaeosol (sample 6-8) is characterised by high amounts of gastropods with mafic mineral content. The parent material of SL 14 again is dominated by pure shelf material (7.5 YR 7/6; sample 9) with a palaeosurface on top with the maximum of *Obelus pumilio* (248 individuals/10 litres of sediment, Tab. 2.6). The uppermost part is characterised by relocation features (sample 11-12). Again the SL 13 is of sandy material accompanied by very low mass-specific susceptibility, showing only contents of Ca, Mg, Sr and Na. SL 13 ends up with a marked soil with a high abundance of *Cochlicella sp.* (Tab.5.) and higher amounts of BCs (brood cells). The sandy sediment of SL 12 (sample 18) shows values of 85.5 % of $CaCO_3$ and 2135 mg/kg of Sr (as well as 17.26 g/kg of Mg and 7.12 g/kg of Na). This sediment with an IRSL age of 316.6 +/- 31.1 ka (Tab. 2.5, No. BT 1425) is the parent material of the subsequent palaeosol (samples 19 - 21), which contains a gastropod assemblage with several individuals of *Pomatias lanzarotensis* as well as some individuals of *Cochlicella sp.* SL 11 represents a reddish yellow (7.5 YR 6/6; sample 22) soil sediment, which again represents an elemental composition of Sr, Mg, Mn and Na. It ends up with a strong brown (7.5 YR 4/6; sample 25) palaeosol showing the maximum of *Pomatias lanzarotensis* (70 individuals/10 litres

of sediment) as well as an abundance of BCs and high SiO_2 values (samples 24 - 25) within the whole section of Encantado. The relatively low value of 40% $CaCO_3$ indicates a more intensive decalcification, and hence a higher intensity of soil formation. This palaeosol (dominated by the colour of hematite – 7/5 YR 4/6) has a high geomorphological significance, because its palaeosurface has a relatively high resistance against erosion and shapes a significant height level within the gully system. The overlying stratum (SL 10) is characterised by shelf material relating to the coarse and middle sand fraction, only showing higher values of $CaCO_3$, Sr, Mg, Mn and Na. It is dated to an age IRSL age of 279.7 +/- 26.5 ka (Tab. 2.5, No. BT 1424). A soil formation with a certain amount of mafic minerals (sample 28) and a reddish yellow colour (7.5 YR 6/6) completes that unit. The sediments above (SL 9) shows marked features of relocation such broken pieces of molluscs and rock fragments. That relocated material resulted an IRSL age of 295.4 +/- 27.4 ka (Tab. 2.5, No. BT 1423). In combination with a switch in grain size distribution, SL 9 (of pure sand fraction) is delimited against SL 8, which is characterised by a broader spectrum of grain sizes. On top of SL 8 a strong brown (7.5 YR 4/6, sample 37) soil with a higher content of mafic minerals is developed. This palaeosol represents the highest values of SiO_2, Fe_t and Fe_d as well as the highest contents of Al, Mn, and K of the whole section Encantado. It likewise possesses the highest values in mass specific susceptibility, the lowest values of $CaCO_3$, and a very high proportion of silt-sized particles. The overlying strata (SL 7) presents the highest amount of clay and a maximum in Mg content (26.99 mg/kg). Although the reddish yellow (7.5 YR 6/6) colour does not indicate soil formation, the comparable low amount of 51.6% of $CaCO_3$ could be an evidence of decalcification. Moreover, numerous fragments of a carbonate crust together with basaltic rubble document a former erosion surface on top of SL 7. Also the subsequent sediments of SL 6 show features of relocation, while in the upper part samples 40 to 42 document a weak soil formation and some content of mafic minerals. A very broad spectrum of grain size distribution and a broad spectrum of elemental composition characterise SL 5, with comparably lower $CaCO_3$ values. The sediments of SL 5 are IRSL dated to an age of 130.9 +/- 11.0 ka (Tab. 2.5, No. BT 1421). SL 4 points to a strong contribution of shelf material again and is mainly characterised by amounts of $CaCO_3$, Sr, Mg, Mn and Na. It is the first layer containing *Rumina decollata*. SL 3 shows a reddish yellow (7.5 YR 7/6; sample 45) sediment with a high abundance of coated in situ BCs as well as calcified relocated ones. In the uppermost part of the profile there is at least one soil developed (SL 2, samples 47 - 48) with a small number of *Rumina decollata* accompanied by features of relocation.

Finally the section is topped by a sandy silty reddish yellow (7.5 YR 6/6; sample 49&50) colluvial layer (SL 1).

Sediment layer	*Canariella plutonia*			*Candidula ultima*			*Caracolina lenticula*			*Cochlicella sp.*			*Cryptella auriculata*			*Ferussacia fritschi*			*Hemicycla flavistoma*			*Hemicycla sarcostoma*			*Granopupa granum*			*Monilearia monolifera*			*Obelus nov. cf. discogranulatus*			*Obelus pumilio*			*Pomatias lanzarotensis*			*Rumina decollata*			*Theba indet.*			*Xerotricha lancerottensis*			*Snail eggs*		*sp. Monilearia/ Xerotricha (apeces)*
	Entire ind.	Broken ind.	**Total**	Entire ind.	Broken ind.	**Total**	Entire ind.	Broken ind.	**Total**	Entire ind.	Broken ind.	**Total**	Entire ind.	Broken ind.	**Total**	Entire ind.	Broken ind.	**Total**	Entire ind.	Broken ind.	**Total**	Entire ind.	Broken ind.	**Total**	Entire ind.	Broken ind.	**Total**	Entire ind.	Broken ind.	**Total**	Entire ind.	Broken ind.	**Total**	Entire ind.	Broken ind.	**Total**	Entire ind.	Broken ind.	**Total**	Entire ind.	Broken ind.	**Total**	Entire ind.	Broken ind.	**Total**	Entire ind.	Broken ind.	**Total**	Broken ind.	**Total**	**Total**
SL 1	-	-	-	-	-	-	-	-	-	-	-	-	-	-	-	-	-	-	-	6	**2**	-	-	-	-	-	-	14	8	**22**	-	-	-	-	-	-	-	-	-	-	12	**8**	56	56	**112**	-	-	-	-	**8**	-
SL 2	-	-	-	-	-	-	-	-	-	-	2	**2**	-	2	**2**	-	-	-	-	-	-	-	-	-	-	-	-	2	16	**18**	-	-	-	-	-	-	-	-	-	-	12	**6**	10	14	**24**	-	-	-	-	**4**	-
SL 2	-	-	-	-	-	-	-	-	-	-	-	-	-	-	-	-	-	-	-	1	**1**	-	-	-	-	-	-	-	1	**1**	-	-	-	-	-	-	-	-	-	-	-	-	15	4	**19**	-	-	-	-	-	-
SL 4	-	-	-	4	4	**8**	-	-	-	-	-	-	-	-	-	-	-	-	-	-	-	-	-	-	4	-	**4**	24	28	**52**	-	-	-	-	-	-	-	-	-	-	2	**2**	56	184	**240**	2	10	**12**	-	-	-
SL 5	-	4	**4**	-	8	**8**	-	-	-	-	-	-	-	-	-	-	-	-	-	4	**2**	-	-	-	-	-	-	6	36	**42**	-	-	-	-	-	-	-	2	**2**	-	-	-	28	130	**158**	-	-	-	-	-	-
SL 6	-	-	-	-	-	-	-	-	-	-	-	-	-	-	-	-	-	-	-	-	-	-	-	-	-	-	-	-	-	-	-	-	-	-	-	-	-	-	-	-	-	-	-	-	-	-	-	-	-	-	-	-
SL 6	-	-	-	-	8	**6**	-	-	-	-	-	-	-	-	-	-	2	**2**	-	-	-	-	-	-	-	-	-	6	12	**18**	-	-	-	-	-	-	-	2	**2**	-	-	-	44	50	**94**	-	-	-	-	-	-
SL 8	-	-	-	-	-	-	2	-	**2**	-	-	-	-	-	-	-	-	-	2	2	**4**	-	-	-	-	-	-	4	2	**6**	-	-	-	-	-	-	-	-	-	-	-	-	40	30	**70**	-	-	-	-	-	-
SL 8	-	-	-	-	6	**6**	-	-	-	-	-	-	-	-	-	-	-	-	-	14	**6**	-	-	-	-	-	-	6	8	**14**	-	-	-	-	-	-	4	6	**10**	-	-	-	76	58	**134**	-	-	-	-	-	-
SL 8	-	-	-	-	2	**2**	-	-	-	-	-	-	-	-	-	-	-	-	-	-	-	-	-	-	-	-	-	6	2	**8**	-	-	-	-	-	-	-	-	-	-	-	-	128	84	**212**	-	-	-	-	-	-
SL 8	-	-	-	-	-	-	-	-	-	-	-	-	-	-	-	-	-	-	-	-	-	-	-	-	-	-	-	20	30	**50**	-	-	-	-	-	-	-	-	-	-	-	-	108	152	**260**	-	-	-	-	-	-
SL 9	-	-	-	-	-	-	-	-	-	-	-	-	-	-	-	-	-	-	-	-	-	-	-	-	-	-	-	-	-	-	2	-	**2**	-	-	-	-	-	-	-	-	-	2	40	**42**	-	-	-	-	-	-
SL 10	-	-	-	-	-	-	-	-	-	-	-	-	-	-	-	-	-	-	-	-	-	-	-	-	-	-	-	-	-	-	-	-	-	-	-	-	-	-	-	-	-	-	237	549	**786**	-	-	-	-	-	-
SL 10	-	-	-	-	-	-	-	-	-	-	-	-	-	-	-	-	-	-	-	-	-	-	-	-	-	-	-	12	8	**20**	-	-	-	-	-	-	-	-	-	-	-	-	300	442	**742**	-	-	-	-	-	-
SL 10	-	-	-	-	-	-	-	-	-	-	-	-	1	1	**2**	-	-	-	-	-	-	-	-	-	-	-	-	8	8	**16**	-	-	-	-	-	-	-	-	-	-	-	-	81	158	**239**	-	-	-	-	-	-
SL 11	4	10	**10**	-	-	-	-	-	-	-	-	-	14	10	**22**	-	-	-	-	14	**4**	-	-	-	-	-	-	-	-	-	-	-	-	-	-	-	-	14	56	**70**	-	-	-	100	64	**164**	-	-	-	-	-	-
SL 11	-	-	-	-	-	-	-	-	-	-	-	-	-	-	-	-	2	**2**	-	-	-	-	-	-	-	-	-	7	10	**17**	-	-	-	-	-	-	-	-	-	-	-	-	5	49	**54**	-	-	-	-	-	-
SL 12	-	-	-	-	-	-	-	-	-	-	8	**8**	-	8	**6**	-	4	**4**	-	50	**18**	-	-	-	-	-	-	10	18	**28**	-	-	-	-	-	-	-	-	-	-	-	-	400	516	**916**	2	4	**22**	-	-	-
SL 12	-	8	**6**	-	-	-	-	-	-	-	620	**620**	-	2	**2**	-	4	**4**	-	6	**2**	-	-	-	-	-	-	-	-	-	-	-	-	-	-	-	-	2	**2**	-	-	-	6	200	**206**	-	-	-	-	-	**10**
SL 13	2	2	**4**	-	-	-	-	-	-	-	672	**672**	62	24	**86**	-	14	**14**	2	8	**6**	**2**	2	**4**	-	-	-	40	56	**96**	-	-	-	-	-	-	-	-	-	-	-	-	218	362	**580**	-	12	**12**	-	-	-
SL 13	-	-	-	-	-	-	-	-	-	-	36	**36**	-	4	**4**	-	-	-	-	-	-	-	-	-	-	-	-	-	2	**2**	-	2	**2**	-	20	**20**	-	-	-	-	-	-	152	244	**396**	2	-	**2**	-	-	-
SL 13	-	-	-	-	-	-	-	-	-	-	20	**20**	-	6	**6**	-	-	-	-	-	-	-	-	-	-	-	-	4	10	**14**	-	-	-	-	94	**94**	-	-	-	-	-	-	110	222	**332**	-	-	-	-	-	-
SL 14	-	-	-	-	-	-	-	-	-	-	-	-	2	-	**2**	-	-	-	-	-	-	-	-	-	-	-	-	2	2	**4**	-	-	-	76	172	**248**	-	-	-	-	-	-	288	174	**462**	-	-	-	-	-	-
SL 14	-	-	-	-	-	-	-	-	-	-	6	**6**	6	-	**6**	-	-	-	-	-	-	-	-	-	-	-	-	6	2	**8**	-	-	-	60	80	**140**	-	-	-	-	-	-	144	266	**410**	-	-	-	-	-	-
SL 14	-	-	-	-	-	-	-	-	-	-	4	**4**	2	2	**4**	-	-	-	-	-	-	-	-	-	-	-	-	2	2	**4**	-	-	-	-	20	**20**	-	-	-	-	-	-	196	324	**520**	-	-	-	-	-	-
SL 15	-	-	-	-	-	-	-	-	-	-	-	-	-	4	**2**	-	-	-	-	-	-	-	-	-	-	-	-	2	14	**16**	-	-	-	-	-	-	-	-	-	-	-	-	276	422	**698**	-	-	-	-	-	-
SL 16	-	6	**2**	-	-	-	-	-	-	-	-	-	-	14	**10**	-	-	-	-	-	-	-	-	-	-	-	-	-	2	**2**	-	-	-	-	-	-	-	-	-	-	-	-	74	200	**274**	-	4	**4**	-	-	-

Tab. 2.6 Gastropod results of Encantado section

Concerning 2.5.2. Jable 1 section

The lowermost part (SL 12) of the Jable 1 (Fig. 2.4) section is composed of a very pale brown (10 YR 8/4; sample 1) sediment, dominated by sand relating to the middle and coarse fraction. SL 12 is dated to an (preliminary) age of 231.0 +/- 17.7 ka (Tab. 2.5, No. BT 1518). The overlying soil sediment (SL 11) presents features of relocation and shows increased clay and silt contents as well as a homogenous reddish yellow colour (7.5 YR 6/6; sample 5). In the upper part, (sample 7&8) a strong brown (7.5 YR 5/8) palaeosol is accompanied by a $CaCO_3$ content of 52%, indicating a high $CaCO_3$ mobilisation. Again, relocated sediments and predominantly relocated soil material occur in the overlying strata (SL 10). On top of that sediment two palaeosols of strong brown colour (7.5 YR 5/8; sample 21) containing *Pomatias lanzarotensis* (only results of field work) lie very densely on top of each other and confluence into one soil a bit further along the profile wall (SL 9). Above, a reddish yellow coloured (7.5 YR 6/6, sample 15) relocated material is cut by a surface of relocation features, as broken pieces of molluscs and of BCs (SL 8). Even SL 7 is characterised by features of relocation and is completed by a weak soil evidenced by in situ brood cells (sample 17 - 18). This sequence comprises mafic minerals. With a value of 108.34 (10^{-8} m^3kg^{-1}), sample 18 shows a comparably high value of mass-specific susceptibility within the whole profile. The subsequent part consists of an accumulation of very pale brown (10 YR 8/4, sample 19&20) material of SL 6, characterised by persistently high values of $CaCO_3$, Sr, Mg, and Na. A palaeosurface characterised by of relocation (broken pieces of molluscs and coated BCs as well as rock fragments) completes SL 6. The overlaying stratum (SL 5) shows a very pale brown (10 YR 7/4; sample 21) sediment, which shows a preliminary age of 175.3 +/- 15.6 ka (Tab. 2.5, No. BT 1515). On top of SL 5 a weak reddish yellow (7.5 YR 6/6; sample 24) palaeosol is developed, showing slightly higher values of silt and clay. Again a very pale brown (10 YR 8/4; sample 25&26) sediment (SL 4) continues the sequence. That sediment is dated to a preliminary age of 130.7 +/- 11.6 ka (Tab. 2.5, No. BT 1514). The layer is completed by a truncated weak soil, which on top is characterised by features of relocation. The reddish yellow (7.5 YR 7/6; sample 5) sediment of SL 3 shows higher silt and clay contents and is dominated in general by amounts of $CaCO_3$, Sr, Mg and Na (sample 29). SL 2 represents higher values of Fe_t as well as Fe_d. Within SL 2 there is a slight shift in grain size distribution, from higher silt values (sample 30) to lower silt content (sample 31). That layer shows a reddish yellow (7.5 YR 6/6; sample 30&31) colour. The whole sequence is completed by remnants

of Caliche on top of the profile (SL 1). Approximately 30 m uphill of the sampled site, we found a palaeosol with a gastropod assemblage pointing to a high abundance of *Cochlicella sp.* But several metres to the east of the sampled site this palaeosol dips into the gully floor, and thus runs below the sequence described in Jable 1.

Concerning 4.3. Jable 2 section

Close to the gully floor a strong brown (7.5 YR 4/6; sample 1) palaeosol containing basaltic rock fragments is exposed (SL 12). This palaeosol indicates the highest mass-specific susceptibility values of 358.63 (10^{-8} m^3kg^{-1}). Above a very pale brown (10 YR 7/4; sample 3) sediment is deposited (SL 11), with a very weak soil on top, indicated by some BCs, accompanied by slight volcanic imprint. SL 10 again shows a very pale brown (10 YR 7/4; sample 5) sediment characterised by grain sizes of nearly 100 % sand fraction and an elemental composition dominated by contents of Ca, Sr, Mg and Na as seen in all these carbonate aeolianites of Northern Fuerteventura. On top of that pale sequence there is a strong brown (7.5 YR 5/6; samples 7&8) palaeosol developed, indicating decalcification and relatively high values of Fe_t and Fe_d. The overlying stratum (SL 9) is dominated by features of relocation such as broken pieces of coated BCs, basalt fragments and incorporated brownish soil aggregates. This layer ends up with a palaeosol containing *Pomatias lanzarotensis*. Subsequently, relocated material (SL 8) is completed by a palaeo-surface evidenced containing basaltic fragments and broken BCs. SL 7 completes this sequence of relocated sediments and is characterised by higher values of mass-specific susceptibility (sample 16 – 17). Here, mafic minerals and features of weak decalcification might indicate a weak palaeosol. There is a clear change to the overlying stratum (SL 6), which consists of mainly medium to coarse-grained very pale brown (10 YR 8/4) material, dominated by higher contents of $CaCO_3$, Sr, Mg and Na. That sediment is dated to a preliminary age of 171.2 +/- 15.4 ka (Tab. 2.5, No. BT 1526). SL 6 ends up with a temporary palaeosurface evidenced by debris and broken BCs. Above, a weak palaeosol (sample 21-22) with mafic minerals concludes SL 5. A small band with an abundance of broken molluscs and a reddish yellow (7.5 YR 6/6; sample 23) sediment characterises SL 4. That part shows a preliminary age of 121.3 +/- 10.4 ka (Tab. 2.5, No. BT 1525). The uppermost part of the section is comprised of strongly relocated sediments with coated BCs and basalt debris (SL 3) that are cemented by carbonate in the lower part (sample 24). Assumingly SL 3 shows a truncated soil, evidenced by remnants of a $CaCO_3$ crust. These

remnants are topped by a strong brown (7.5 YR 5/6; sample 26&27) soil enriched in silt and clay (SL 2). Finally, a colluvial silty layer completes the whole sequence (SL1).

Concerning 2.5.4 Melián section

The lowermost part is directly based on basaltic rock. SL 18 is characterised by very pale brown sediments with a lot of basalt fragments (up to 10 or even 20 cm), which are accumulated in horizontal lines or in palaeo channels. A brownish palaeosol completes SL 18. SL 17 seems to repeat the sequence of SL 18, even if it presents more palaeo-channels filled with basalt gravels. Also SL 16 shows relocated basalt fragments with a palaeosol on top, which presents the highest values in mass-specific susceptibility (sample 4) of the entire section of Melián. SL 15 shows a relative enrichment of Fe_t and Fe_d (up to sample 10) and ends up with a reddish yellow coloured (7.5 YR 7/6; sample11) layer with several impurities of mafic minerals. The succession from sample 4 of SL 16 to sample 10 of SL 15 shows consequently decreasing values of mass-specific susceptibility accompanied by decreasing contents of basalt rock fragments. SL 15 presents the maximum of *Obelus pumilio*, beside several indiviuals of *Cochlicella sp.* Above, SL 14 is characterised by grain sizes of up to 90% of sand fraction and a very low Fe_d-value. This unit ends with a reddish yellow (7.5 YR 6/6; sample 15) palaeosol, which contains a gastropod assemblage with the maximum of *Cochlicella sp.* (Tab. 2.7.). Above the sediments (SL 13) are dominated by features of relocation. Except a small number of *Cochlicella sp.*, there are no gastropods at all. SL 12 represents remnants of a truncated palaeosol, which is overdrawn by recalcification features from above. Even this part contains several individuals of *Cochlicella sp.* The truncated palaeosol of SL 11 presents the maximum of *Pomatias lanzarotensis* (at the same time it is a single occurrence within the whole section) and a very high abundance of relocated coated BCs. Above a brownish yellow (10 YR 6/6) sediment (SL 10) ends up with a weak soil formation in reworked sediments with several impurities of lapilli. SL 10 shows the first occurrence of *Rumina decollata*. In SL 9 the number of that species raise its maximum. This layer is characterised by a strong brown (7.5 YR 5/8; sample 29) palaeosol, which is interrupted by a tephra accumulation (samples 30). In view of pedogenic features the soil formation outlasted the tephra accumulation, since on top the tephra material leads over into features of relocation. The tephra layer shows the highest contents of Al, Zn, Mn, K and Na, as well as the second highest content of Fe_t. Furthermore, sample 29 provides a conspicuous local maximum in mass-specific susceptibility that amounts to 126.56 (10^{-8} m^3kg^{-1}). The parent material of SL 9 is dated to

an age of 137.2 +/- 11.6 ka (Tab. 2.5, No. BT 1342). Above the tephra, a thick accumulation of medium to coarse-grained shelf material (SL 8) is mainly characterised by high contents of $CaCO_3$, Sr, Mg and Na and resulted an IRSL age of 124.3 +/- 10.5 ka (Tab. 2.5, No. BT 1343). A very weak soil with a slight mafic mineral content is embedded in that shelf material containing a small number of *Rumina decollata*. Despite only weak soil forming intensity, which is indicated by weak decalcification features, the mass-specific susceptibility shows again a local maximum (120.73 10^{-8} m^3kg^{-1}) that is most probably linked to the mafic mineral content. A slightly more intense yellow (10 YR 7/8; sample 40) colour belongs to the soil on top of SL 7. But again, decalcification can hardly be certified. The mass-specific susceptibility shows slightly raised values (sample 40) in comparison to the over- and underlying strata. The parent material of SL 7 show an age of 100.8 +/- 8.9 ka (Tab. 2.5, No. BT 1340). In the upper part of the profile, the sediments of SL 6 show just a small number of BCs and broken snail shells that can be seen as an indication of low energy sediment redistribution. The sediments are dated to an IRSL age of 98.4 +/- 8.6 ka (Tab. 2.5, No. BT 1341). The lowest and the most upper parts of SL 6 present a small number of *Rumina decollata*. On top of that sediment layer strong $CaCO_3$ cementations and remnants of a huge Caliche horizon are developed within a yellow (10 YR 7/6) coloured layer that indicates remnants of a strong soil formation. SL 5 is characterised by features of relocation with larger amounts of lapilli within small rinsing channels. The lapilli is directly embedded on top of the Caliche crust. The next part shows a truncated soil (SL 4), which is represented by calcified BCs. Above, SL 3 shows strong brown (7.5 YR 5/6; samples 52&53) relocated material, which is dated to an age of 16.2 +/- 1.4 ka (Tab. 2.5, No. BT 1345). Subsequently, a further strong brown (7.5 YR 4/6; sample 55) soil is characterised by high silt contents and is covered by dark yellowish brown (10 YR 3/6, sample 56) tephra material. The final sediment layer (SL 2&1) consists of transported and/or relocated yellowish brown (10 YR 5/6; sample 60) material that is up to 4 m thick. Within that thick deposit a very weak soil on top of SL2 is developed. The relocated sediment of SL 2 is dated to 14.9 +/- 1.2 ka (Tab. 2.5, No. BT 1344). The subsequent sediments show an alternate layering of sands and several impurities of lapilli. The Nebka dunes at the today's surface document recent aeolian activity.

Sediment layer	*Canariella plutonia*			*Candidula ultima*			*Caracolina lenticula*			*Cochlicella sp.*			*Cryptella auriculata*			*Ferussacia fritschi*			*Hemicycla flavistoma*			*Hemicycla sarcostoma*		
	Entire ind.	Broken ind.	Total	Entire ind.	Broken ind.	Total	Entire ind.	Broken ind.	Total	Entire ind.	Broken ind.	Total	Entire ind.	Broken ind.	Total	Entire ind.	Broken ind.	Total	Entire ind.	Broken ind.	Total	Entire ind.	Broken ind.	Total
SL 6	-	-	-	-	-	-	-	2	2	-	-	-	-	-	-	-	-	-	-	-	-	-	-	-
SL 6	-	-	-	-	-	-	-	-	-	-	-	-	-	-	-	-	-	-	-	-	-	-	-	-
SL 6	-	-	-	-	-	-	-	-	-	-	-	-	-	-	-	-	-	-	-	1	1	-	-	-
SL 6	-	-	-	-	-	-	-	-	-	-	-	-	-	-	-	-	-	-	-	-	-	-	-	-
SL 6	-	-	-	-	-	-	-	-	-	-	-	-	-	-	-	-	-	-	-	-	-	-	-	-
SL 7	-	-	-	-	-	-	-	-	-	-	-	-	-	-	-	-	-	-	-	-	-	-	-	-
SL 7	-	-	-	-	-	-	-	-	-	-	-	-	-	-	-	-	-	-	-	-	-	-	-	-
SL 7	-	-	-	-	-	-	-	-	-	-	-	-	-	-	-	-	-	-	-	-	-	-	-	-
SL 8	-	-	-	-	-	-	-	-	-	-	-	-	-	-	-	-	-	-	-	-	-	-	-	-
SL 8	-	-	-	-	-	-	-	-	-	-	-	-	-	-	-	-	-	-	-	-	-	-	-	-
SL 8	-	-	-	-	-	-	-	-	-	-	-	-	-	-	-	-	-	-	-	-	-	-	-	-
SL 8	-	-	-	-	-	-	-	-	-	-	-	-	-	-	-	-	-	-	-	-	-	-	-	-
SL 9	-	-	-	-	-	-	-	-	-	-	-	-	-	-	-	-	-	-	-	-	-	-	-	-
SL 9	-	-	-	-	-	-	8	32	40	-	-	-	-	-	-	-	-	-	-	-	-	-	8	8
SL 9	-	-	-	-	-	-	-	-	-	-	-	-	-	-	-	-	-	-	-	-	-	-	-	-
SL 10	-	-	-	-	-	-	-	1	1	-	-	-	-	-	-	-	2	2	-	-	-	-	4	1
SL 11	-	4	2	-	-	-	-	-	-	-	10	4	-	-	-	-	-	-	-	-	-	-	4	2
SL 11	-	-	-	4	4	8	-	-	-	-	30	22	2	6	8	-	-	-	-	6	2	-	-	-
SL 11	-	-	-	14	8	22	-	-	-	2	254	108	2	2	4	-	-	-	-	2	2	-	-	-
SL 12	-	-	-	2	26	26	-	6	6	-	178	134	-	20	14	-	-	-	-	-	-	-	-	-
SL 13	2	-	2	-	12	10	-	-	-	-	18	8	2	2	4	-	-	-	-	2	2	-	-	-
SL 14	-	2	2	14	-	14	-	4	4	36	1298	1180	18	24	40	-	12	12	-	6	4	-	-	-
SL 14	-	-	-	-	-	-	-	4	4	-	168	148	-	10	8	-	-	-	-	2	2	-	-	-
SL 15	-	-	-	-	-	-	-	-	-	-	18	16	2	-	2	-	-	-	-	-	-	-	-	-
SL 15	-	-	-	-	-	-	-	-	-	-	-	-	-	2	2	-	-	-	-	-	-	-	-	-
SL 16	-	-	-	-	-	-	-	-	-	-	-	-	-	4	2	-	-	-	-	-	-	-	-	-
SL 16	-	-	-	-	-	-	-	-	-	-	-	-	-	4	4	-	-	-	-	-	-	-	-	-

Sediment layer	*Granopupa granum*			*Monilearia monolifera*			*Obelus nov. cf. discogranulatus*			*Obelus pumilio*			*Pomatias lanzarotensis*			*Rumina decollata*			*Theba indet.*			*Xerotricha lancerottensis*			*Snail eggs*		*sp. Monilearia/ Xerotricha (apeces)*
	Entire ind.	Broken ind.	Total	Entire ind.	Broken ind.	Total	Entire ind.	Broken ind.	Total	Entire ind.	Broken ind.	Total	Entire ind.	Broken ind.	Total	Entire ind.	Broken ind.	Total	Entire ind.	Broken ind.	Total	Entire ind.	Broken ind.	Total	Broken ind.	Total	Total
SL 6	-	-	-	-	11	11	-	-	-	-	-	-	-	-	-	-	4	2	2	201	203	-	-	-	-	-	-
SL 6	-	-	-	4	17	21	-	-	-	-	-	-	-	-	-	-	1	1	36	219	255	6	11	17	-	1	-
SL 6	-	-	-	-	-	-	-	-	-	-	-	-	-	-	-	-	-	-	-	109	109	-	-	-	-	-	8
SL 6	-	-	-	22	84	106	-	-	-	-	-	-	-	-	-	-	4	4	82	638	720	2	8	10	-	-	-
SL 6	-	-	-	8	11	29	-	-	-	-	-	-	-	-	-	-	2	2	44	285	329	11	21	32	-	-	-
SL 7	-	-	-	-	-	-	-	-	-	-	-	-	-	-	-	-	-	-	283	702	985	19	57	76	-	-	-
SL 7	-	-	-	2	52	54	-	-	-	-	-	-	-	-	-	-	2	2	90	694	784	-	-	-	-	-	-
SL 7	-	-	-	8	42	50	-	-	-	-	-	-	-	-	-	-	-	-	244	438	682	-	-	-	-	-	-
SL 8	-	-	-	18	82	100	-	-	-	-	-	-	-	-	-	-	2	2	152	812	964	-	-	-	-	-	-
SL 8	-	-	-	30	124	154	-	-	-	-	-	-	-	-	-	-	8	8	132	804	936	-	-	-	-	-	-
SL 8	-	-	-	-	44	44	-	-	-	-	-	-	-	-	-	-	3	3	1	414	415	-	-	-	-	-	-
SL 8	-	-	-	212	560	772	-	-	-	-	-	-	-	-	-	-	4	4	792	2516	3308	32	124	156	-	-	-
SL 9	-	-	-	-	-	-	-	-	-	-	-	-	-	-	-	-	-	-	-	-	-	-	-	-	-	-	-
SL 9	16	16	24	208	696	744	-	-	-	-	-	-	-	-	-	8	192	144	1408	4016	5424	24	264	288	-	176	-
SL 9	-	-	-	18	26	44	-	-	-	-	-	-	-	-	-	-	-	-	237	168	405	-	-	-	-	1	-
SL 10	-	-	-	2	25	27	-	-	-	-	-	-	-	-	-	-	5	3	4	277	281	-	-	-	-	1	-
SL 11	-	-	-	2	6	8	-	-	-	-	-	-	2	28	30	-	-	-	74	100	174	-	-	-	-	-	-
SL 11	-	-	-	2	-	2	-	-	-	-	-	-	-	2	2	-	-	-	86	64	150	-	-	-	-	-	-
SL 11	-	-	-	8	2	10	-	-	-	-	-	-	-	-	-	-	-	-	164	132	296	-	-	-	-	-	-
SL 12	-	-	-	-	30	30	-	-	-	-	2	2	-	-	-	-	-	-	236	618	854	30	50	80	-	-	-
SL 13	-	-	-	2	22	24	-	-	-	-	-	-	-	-	-	-	-	-	414	378	792	6	28	34	-	-	-
SL 14	4	-	4	50	118	168	-	-	-	-	2	2	-	-	-	-	-	-	698	1656	2354	226	490	716	-	-	-
SL 14	-	-	-	30	64	94	-	-	-	-	-	-	-	-	-	-	-	-	518	628	1146	38	26	64	-	-	-
SL 15	-	-	-	-	12	12	-	-	-	-	40	32	-	-	-	-	-	-	726	634	1360	2	10	12	-	-	-
SL 15	-	-	-	4	6	10	-	-	-	-	-	-	-	-	-	-	-	-	68	90	158	-	-	-	-	-	-
SL 16	-	-	-	-	2	2	-	-	-	-	-	-	-	-	-	-	-	-	24	58	82	-	2	2	-	-	-
SL 16	-	-	-	12	26	38	-	-	-	-	-	-	-	-	-	-	-	-	104	202	306	2	2	4	-	-	-

Tab. 2.7. Gastropod results of Melián section

3 Characteristics, nature, and formation of palaeosurfaces within dunes on Fuerteventura

C-B. Roettig[a], G. Varga[b], D. Sauer[c], T. Kolb[d], D. Wolf[a], V. Makowski[a], J. M. Recio Espejo[e], L. Zöller[d], D. Faust[a]

[a]Dresden University of Technology
[b]Hungarian Academy of Sciences
[c]University of Göttingen
[d]University of Bayreuth
[e]University of Cordoba

Publication history: received 15.09.2017 / accepted April 2018 / published (online) Oktober 2018 / printed 2019 - Quaternary Research Volume 91, Issue 1, 4-23.

3.1 Abstract

The appearances of palaeosurfaces intercalated into palaeo-dune fields on Fuerteventura are multifaceted. Although reddened layers in these dune sediments might suggest that strong soil-formation processes have taken place, the combination of aridity and parent material, namely biogenic carbonate sand of shelf origin, reveals that strong soil formation seems unlikely. These sediments rather represent de- and recalcification processes only. Solely in the case of admixed material of volcanic origin and dust deposits further soil-forming processes seem to be possible. Hematite-rich Saharan dust contributes to reddish colouration of the palaeosurfaces. In addition, $CaCO_3$-coated iron particles appear to be ingredients of dust being leached after deposition and transformed to hematite. Overall, we propose much weaker soil-forming processes during the Pleistocene than previously postulated. Our findings support the relevance of local environments. Carbonate sands of shelf origin hinder strong soil formation and the reddish layers separating dune generations are palaeosurfaces, which mainly consist of Saharan dust. After deposition of allochthonous material, these layers are overprinted by weak soil-forming processes. The formation of palaeosurfaces primarily depends on morphodynamically stable periods during limited sand supply. Our data suggest a cyclicity of processes in the following order:

(1) sand accumulation, (2) dust accumulation and weak soil formation, and (3) water-induced erosion. For the Canary Islands, we support the assumption of glacial maxima being periods of increased levels of moisture. In combination with rising sea level, we propose that favorable conditions of surface stability occur immediately after glacial maxima during periods of starting transgression, whereas regression periods immediately after sea-level high stands seem to yield the highest sand supply for the study area.

Keywords: palaeosol; Pleistocene; aeolianite; soil formation; Canary Islands

3.2 Introduction

Palaeo dune fields comprised of unconsolidated carbonate aeolianites seem to be highly suitable for reconstructing palaeoenvironmental conditions because of their direct linkage to global sea-level change. Studies of the Bahamas (Ball, 1967; White and Curran, 1988), Australia (Ward et al., 1979; Warren, 1983; James and Bone, 2017), Mexico (Inman, et al., 1966; Fryberger et al., 1990) or Sri Lanka (Singhvi et al., 1986) show the capability and the persistent interest in these lowerlatitude systems located close to the coast. Different generations of carbonate aeolianites are often separated by palaeosols, as discussed, for instance, by Williamson and Yaalon (1977), who worked in the eastern Mediterranean, or by Kruse and Meyer (1970), who studied Moroccan dune fields. Fuerteventura possesses a long history of studies focusing on volcanic origin (Rothe, 1966; Fúster et al., 1968; Ibarrola, 1969; Abdel-Monem et al., 1971; Casquet et al., 1980; Coello et al., 1992; Muñoz et al., 2005; Troll and Carracedo, 2016), but the island has also been of interest due to carbonate aeolianites (Müller, 1965;Müller and Tietz, 1975; Coudé-Gaussen et al., 1988; Coudé-Gaussen and Rognon, 1988; Criado et al., 2004; Ortiz et al., 2005; Alcántara-Carrió et al., 2010; Alonso et al., 2011; Faust et al., 2015; Roettig et al., 2017). More recently, several studies (Criado and Dorta, 2003; Menéndez et al., 2007, 2013; López-García et al., 2013; von Suchodoletz et al., 2013; Huerta et al., 2015) have focused on the accumulation of African dust material preserved on these aeolianites sections. Thereby, the Canary Islands are an ideal setting to study temporal variations of dust accumulation because of their close position to the Sahara, which encompasses some of the largest dust sources at global scale (most prominent is the Bodelé Depression; Scheuvens et al., 2013). So far, studies explaining mechanisms of dune formation and especially the formation of intercalated palaeosurfaces on Fuerteventura (Coudé-Gaussen and Rognon, 1988; Criado et al. 2004, 2011, 2012; Meco et al., 2011) have not considered all of the three main stages: (1) dune formation, (2) dust imprint, and (3) soil-forming

processes. The present study aims to contribute to the understanding of the evolution of coastal dune systems in the Canary Island, and other comparable low-latitude regions. Four main questions are addressed in the present study:

(1) What soil-forming processes can potentially take place in a subtropical environment primarily consisting of carbonate sands?

(2) What measurable physical and chemical features documented on palaeosurfaces reflect dust imprint rather than soil formation?

(3) Is it possible to distinguish among periods of soil formation, dust imprint and supply, and accumulation of carbonate sands?

(4) What do features of palaeosurfaces in dune fields on Fuerteventura tell us about the processes responsible for creating these characteristics?

To assess these questions, the present research integrates published and new field stratigraphy combined with data on physical and chemical properties extracted from several Pleistocene dune-palaeosol sequences on Fuerteventura.

3.3 Geographical and environmental setting

Nowadays, Fuerteventura is characterised by an annual precipitation of 147mm (Edwards and Meco, 2000). The arid conditions on the island result from the influence of the trade winds in combination with reduced topography. The highest mountain on Fuerteventura is the Pico de la Zarza (~800m above mean sea level). Different periods of volcanism are decisive for the geological structure of the island (Fig. 3.1). Remnants of the Cretaceous submarine "Basal Complex" is exposed in the center and the northwestern part of Fuerteventura (Coello et al., 1992). Close to the western coast, ultra alkalines of Oligocene age and remains of Miocene volcanism are preserved (Muñoz et al., 2005). On the eastern coast, the Montaña Roja (~1.7 Ma) represents the middle Pleistocene period of volcanism (Criado et al., 2004). Several cones and lava flows depict significant Late Pleistocene volcanism, dominating the morphology of the northern part of the island. Prominent examples related to this period are Montaña de los Saltos or the chain of volcanoes of Calderon Hondo and Bayuyo (Rothe, 1996; Meco et al., 2002). Montaña de la Arena was first interpreted as a ~ 185-ka old volcano (Edwards and Meco, 2000), but later work concluded that this volcano is Holocene in age, thus representing the youngest volcanic activity on the island (Rando et al. , 2008; Criado and Naranjo, 2011).

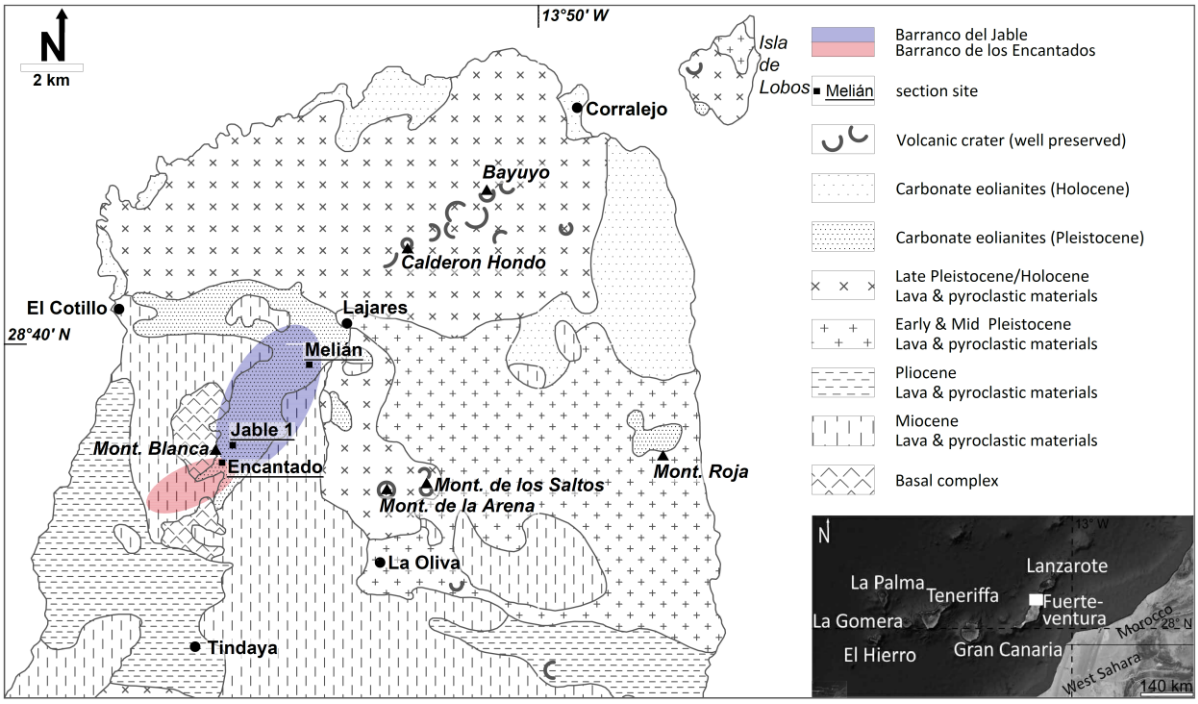

Fig. 3.1. Main geological units of northern Fuerteventura and location of sites (adapted from Rothe, 1996 in Roettig et al., 2017, modified).

Several Pleistocene dunes and sand sheets (e.g., south of Lajares) and dunes of Holocene age (e.g., dune field of Corralejo) cover the rough volcanic landscape of Fuerteventura. The dune sediments consist of middle to coarse sandgrained unconsolidated carbonate aeolianites from the shallow shelf (Criado et al., 2012; Roettig et al., 2017). Up to 80% of these sediments are biogenic carbonates (Meco et al., 2011) containing both aragonite and calcite minerals (Coudé-Gaussen and Rognon, 1988). Studies by Coudé-Gaussen et al. (1987), Edwards and Meco (2000), Criado and Dorta (2003), and Menéndez et al. (2007, 2009, 2013) pointed out the accumulation of aeolian dust as a persistent process on the Canary Islands. The silty material is mainly Saharan in origin and consists of up to 40% $CaCO_3$ (Criado and Dorta, 2003; Menéndez et al., 2007; von Suchodoletz et al., 2009) and contains significant amounts of quartz and feldspars. Quartz minerals are only found in the submarine "Basal Complex" in the eastern Canary Islands and feldspars are also rare on the island. Accordingly, quartz is an established indicator of Saharan-dust imprint in the eastern Canary Islands (Misota and Matsuhisa, 1995; Alcántara-Carió et al., 2010; von Suchodoletz et al., 2013). On Lanzarote, von Suchodoletz et al. (2010) showed the imprint of Saharan dust in valley floor sediments alternating with loess-like deposits. Regarding the Corralejo dune field, on the northeastern coast of Fuerteventura (Fig. 3.1), Criado et al. (2012) described sequences of alternating carbonate sand layers and dust deposits. Regarding soil-forming processes on Fuerteventura, so far Pomel et al. (1985) have studied

Late Pleistocene Rhodoxeralfs near Pajara (cf. Fig. 3.9) and Faust et al. (2015) have described Holocene aridisols and entisols of dune fields in northern Fuerteventura. To summarise, palaeo dune fields in northern Fuerteventura are composed of three main different parent materials: (1) carbonate sands of shelf origin ("carbonate aeolianites" [Brooke et al., 2001, p. 135.] or "unconsolidated carbonate dune sands" [Pye and Tsoar, 2009, p. 362]); (2) dust of Saharan origin; and (3) material of volcanic origin (Lapilli, Tephra; Coudé-Gaussen and Rognon, 1988; Meco et al., 2011; Roettig et al., 2017) as admixture in some stratigraphic positions.

3.4 Study area

The present study focuses on three different sections that are located in the Barranco del Jable and Barranco de los Encantados (northern Fuerteventura). Barranco del Jable is a south-north-oriented Wadi system, south of the village of Lajares (Fig. 3.1 and 3.8). The upper reaches of this system are incised by gullies of up to 10m in depth. Barranco de los Encantados (Fig. 3.1 and 3.8) is situated in the south next to the Barranco del Jable catchment. The lower reaches of this barranco are free of sedimentary archives, whereas the middle reaches present remnants of huge accumulations of carbonate sands. The upper reaches are characterised by a gully system deeply incised into these carbonate sands (Fig. 3.2).

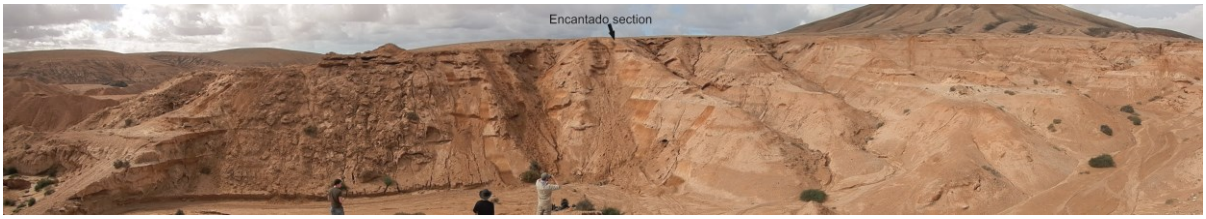

Fig. 3.2. Barranco de los Encantados, view to the southwest.

Currently, it is an active system of ongoing incision. The depth of incision reaches up to 30m. The watershed between Barranco de los Encantados and Barranco del Jable runs from the Montaña Blanca in an easterly direction (Fig. 3.1). Finally, both catchments belong to the same palaeo dune field, which is captured by two fluvial systems from a northerly direction by Barranco del Jable and a southern to southwestern direction by Barranco de los Encantados). The Encantado section (28.63915°N, 13.978792°W) is situated in the upper reaches of Barranco de los Encantados on the southeastern flank of the Montaña Blanca. The Melián section (28.669258°N, 13.953765°W) is located in the lower reaches of Barranco del Jable, close to the village of Lajares. Naturally, remnants of gullies are

observable only on the upper slope position, right at the back of the site in an eastern direction. Nowadays low Nebkha dunes cover the surrounding surface. The El Jable section (28.643783°N, 13.974378°W) is situated in the upper reaches of Barranco del Jable. The gullies here are not as deep (roughly 10 m), but are therefore wider than the gullies of Barranco de los Encantados. So far, Roettig et al. (2017) presented the oldest age of 366.3+/- 34.2 ka for the Encantado section and the youngest age of 14.9+/-1.2 ka for the Melián section.

3.5 Methods

The Encantado and Jable 1 sections presented in this study are already described in detail by Roettig et al. (2017). The Melián section was reported by Edwards and Meco (2000), Faust et al. (2015), and Roettig et al. (2017). This study extends former results (section-wise grain size medians and elemental composition of clay fraction) and adds new data (quartz contents, micromorphological analyses, and x-ray diffraction [XRD]).

3.5.1 Fieldwork

The three sections Encantado, Melián, and Jable 1 (Fig. 3.1) were selected for sampling with regard to micromorphological analyses, XRD measurements, and determination of quartz and iron content. The profiles were studied and described based on features of palaeosurfaces and respective sediment composition of parent material, features of relocation, and mineralogical composition.

3.5.2 Colours

Colours were determined by using the Munsell (1975) scale. The colour of each sample was identified in wet conditions.

3.5.3 Determination of quartz contents

Automated static image analysis procedure

Granulometric and chemical analysis data were obtained from automatic static image analysis with a Malvern Morphologi G3-ID at the Geographical Institute of Research Centre for Astronomy and Earth Sciences, Hungarian Academy of Sciences. Seven mm3 of sedimentary particles were dispersed with an instantaneous, 10 ms pulse of 4 bar compressed air with a 60 s settling time onto a flat glass. Size and shape data of ~ 50,000

individual particles were automatically recorded for each sample from the captured highresolution images. At the same time, the mean light intensity measured after transmission through each particle was automatically recorded by the system as a proxy of optical properties of the material, thus providing further information. Mean intensity values are dependent on chemical composition and/or thickness of the particles, while standard deviations of intensities are linked to heterogeneity of particle constitution and surface morphology. Image analysis-based measurements were organised into a number-based database. All of the particles have their own identity number (ID), which is the primary key in the data matrix. A large number of measured particles ensures a statistically robust and objective insight into the granulometric characteristics of the investigated samples. For grain size distribution, the individual circle-equivalent diameter data were classified into grain size bins. Chemical analysis was performed by using the Raman spectrometer of the Malvern Morphologi G3-ID. Spectra were acquired from several hundreds of targeted individual particles. These were compared with library spectra, and correlation calculations were performed to determine the chemical nature of the targeted sedimentary grains. The overwhelming majority of particles were classified as quartz particles and carbonates.

Curve fitting

Image analysis were mathematically partitioned by applying the parametric curve fitting method. The measured curves were approximated by the summary of three, three-parameter Weibull functions by using an iterative numerical method as a least-square problem to assess the appropriate goodness of fit of measured data and calculated size distributions of mathematically constructed subpopulations. According to our assumption, the finest (W1) subpopulation can be regarded as the product of accumulation of far-travelled Saharan dust material subpopulations (for further details, see Supplementary Material).

Identification of quartz particles

Besides the relatively time-consuming Raman spectroscopy measurements, the acquired intensity values of image analysis procedure were also used. We found that the quartz particles are lighter in comparison to carbonates. Based on these findings, it was possible to determine the volumetric amount of possible quartz particles.

3.5.4 Micromorphological analyses

Micromorphological analyses were performed on 22 thin sections (10 from the Encantado section and 12 from the Melián section). The locations of thin sections are marked in Figures 3.3 and 3.4. We used Viscovoss N 55 S for preparation in combination with Araldite 2020. All thin sections were described following Stoops (2003) using a Leica DMLP and Kappa Zelos-655C camera.

3.5.5 Grain-size distribution

Grain-size distribution was measured at GFZ Potsdam using the Horiba LA-950 laser diffraction particle sizer. The samples (air-dried) were suspended with sodium pyrophosphate for 24 hours. In accordance with the origin of the samples (dominance of sediments of shelf origin), no calcium carbonate or organic material was removed. The samples were measured consecutively five times. The plotted values correspond to the medians of 80 classes between 0.058 and 2500 μm. All grain-size plots were created using the software "R." The respective distributions were plotted as heatmaps (Schulte, 2016) representing the percentage of each class. According to Roettig et al. (2017), the attribution of colour is logarithmic for three single matrices: first matrix, the clay fraction (0.058 to 1.981 μm); the second matrix, the silt fraction (1.981 to 58.953 μm); and the third matrix, the sand fraction (58.953 to 2500 μm). Cumulated percentages of each matrix are presented at the top of the grain size figures (section- wise).

3.5.6 Measured Fe contents

After pressure digestion with concentrated nitric and hydrofluoric acid by atomic adsorption spectrometry, the Fe contents were measured. Similarly, selected samples were measured to quantify the elemental composition of the clay fraction (treated with HCl and untreated). The clay fraction was extracted by means of the gravitational Köhn method (using Atterberg cylinders). $CaCO_3$ content was determined using Scheibler apparatus by treating the samples with hydrochloric acid (Schlichting, 1995).

3.5.7 XRD analysis

The determination of clay minerals of the selected samples was carried out at the University of Cordoba. Mineralogical clay fraction analysis by XRD was performed using an XRD Siemens diffractometer with a copper lamp. The range of scan was 2–17°, and 1º per minute. Clay minerals were classified according to the Brindley and Brown (1980)

method, identified and semi-quantified according to Montealegre Contreras (1976) using peak areas and relative index reflection of each clay mineral.

3.6 Results

3.6.1 Encantado section

Carbonate sands

In general, this section (Fig. 3.3) is composed of different generations of accumulated carbonate sands and corresponding palaeosurfaces on top of each generation. Because they are of shelf origin, carbonate sands offer a high proportion of $CaCO_3$, up to >90 %. The almost pure material of shelf origin ranges in colour from very pale brown (10 YR 8/4), to yellow (10 YR 8/6) or reddish yellow (7.5 YR 6/6). These middle sand-dominated carbonate sands are almost free of quartz and have a very low iron content. For example, Unit 11 shows values of 5.42 g/kg Fe_t and 0.97 g/kg Fe_d. Consequently, these layers also present very low Si contents.

Soil sediments

Occasionally, soil sediments replace carbonate sands as parent material, with a $CaCO_3$ content of 40–70 %. Accordingly, Units 9 and 13 of the Encantado section are reddish yellow (7.5 YR 6/6), showing a minimum content of 70 % sand, up to 25 % silt, and 10 % clay. The amount of Fe_t in these soil sediments varies between 12.38 % (Unit 9) and 33.69% (Unit 13). The amount of silicon reaches 11.1 wt% (Unit 9). The highest clay value (>45 %) of the whole section is related to the soil sediment in the uppermost part of Unit 7.

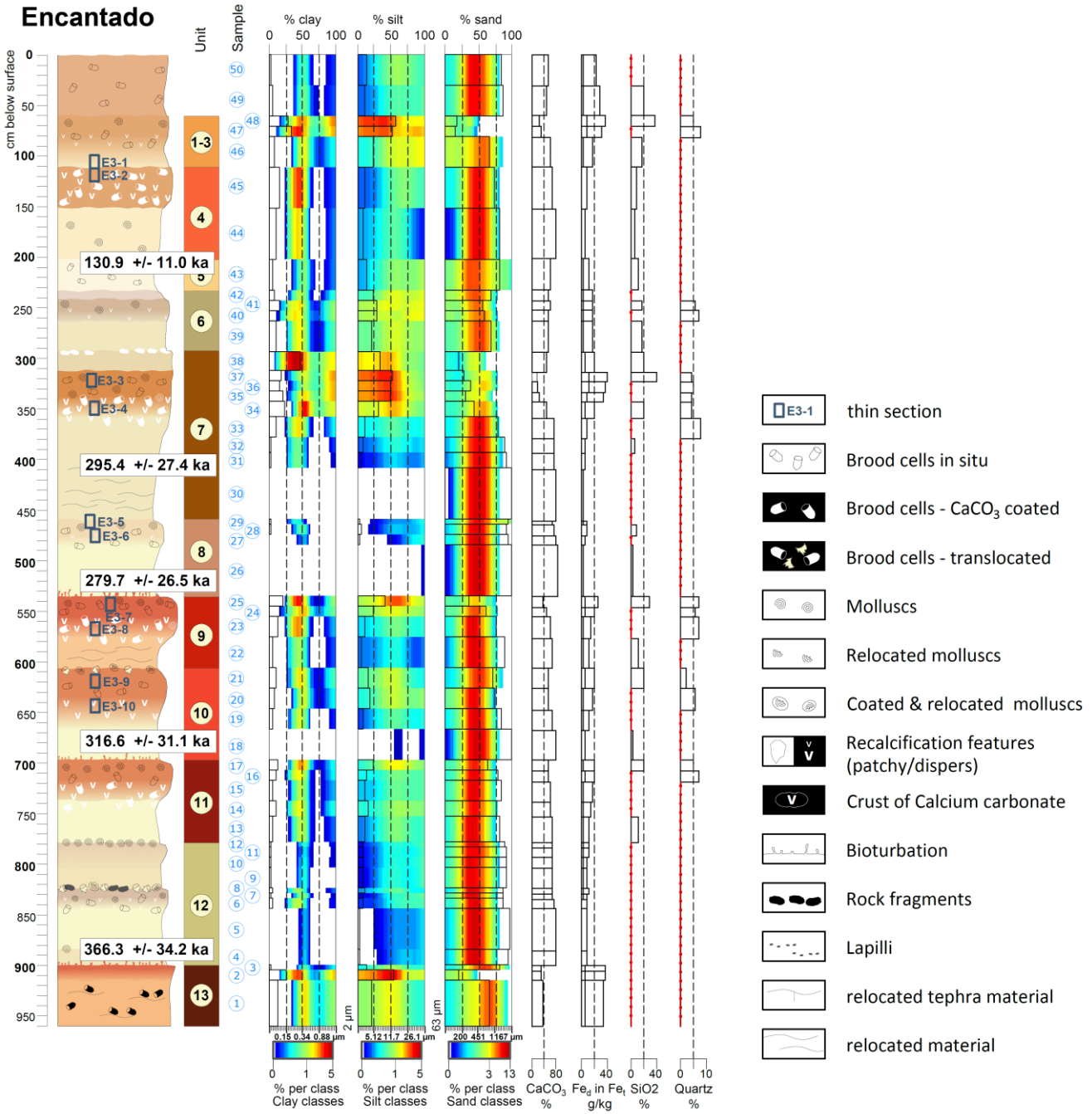

Fig. 3.3. Encantado section with key including analytical data sample-wise. Sequences with no available data indicated by red lines (according to Roettig et al., 2017, modified).

Palaeosurfaces

The palaeosurfaces differ in their characteristics, as maybe expected. The lowest $CaCO_3$ value of 16 % is related to Unit 7 (strong brown colour [7.5 YR 4/6]). The highest value reaches almost 75 % $CaCO_3$ (Unit 8), in combination with a reddish yellow (7.5 YR 6/6) colour. The silt content in layers of palaeosurfaces reaches 40–50 % (Units 1–3, 7, 9, and 13); clay content shows a maximum of 25 % (Unit 13). The highest Fe_t content is 20–40 g/kg (Units 1–3, 7, 9–11, and 13). Silicon values of palaeosurfaces normally range between 20 and 41 wt%, and calculated quartz content reaches more than 7 % (e.g., Unit 9). In agreement, the thin section E3-7 (Unit 9) shows the highest amount of quartz (Tab. 3.1). The lowest value yields roughly 2 % of quartz (uppermost part of Unit 10). Additionally, some parts consist of materials of volcanic origin. Thus, Unit 12 presents constituents of Lapilli, the same way Units 6–8 feature mafic minerals/tephra material. Of course, many parts show admixtured basaltic rock fragments, but these are related to relocation processes originating from the basaltic surrounding instead of concurrent volcanic activity. The combination of palaeosurfaces and volcanic imprint means that iron content can reach up to 40.69 g/kg Fe_t and 11.91 g/kg Fe_d. The thin sections (Tab. 3.1) support the imprint of volcanic material, e.g., volcanic glasses as observed in Units 4, 7, and 8. As reported by Roettig et al. (2017), the infrared-stimulated luminescence (IRSL) data classify the lower parts of this section in ages older than 366.3+/-34.2 ka. The youngest age of this section (130.9+/-11.0 ka) is linked to Unit 5.

Sample	**Microstructure**	**Porosity**	**c/f-ratio**	**Mineral and organic constituents**
E3-1 (Unit 1–3)	upper part: vughy lower part: pellicular grain- u. intergrain	upper part: 5–10%, lower part: 60–70%	upper part: 1:3, lower part: 1:2	quartz, feldspar, fragments of volcanic origin (even volc. glass)
E3-2 (Unit 4)	intergrain, vughy	30%	1:3	feldspar, muscovite, volc. glass, various rock fragments, quartz (sized)
E3-3 (Unit 7)	intergrain, vughy	30–40%	1:4	fragments of volcanic origin, quartz (lower part: sized)
E3-4 (Unit 7)	intergrain, pellicular grain	20%	1:3 bis 1:4	volcanic glass, various rock fragments, quartz

E3-5 (Unit 8)	single grain, partially pellicular grain	70%	clear of fine material	volcanic glass, various rock fragments
E3-6 (Unit 8)	pellicular and intergrain	20–30%	2:1, lower part 3:1	quartz
E3-7 (Unit 9)	pellicular and intergrain	30–40%	3-4:1, lower part 2:1	fragments of volcanic origin, quartz (many)
E3-8 (Unit 9)	bridged, pellicular and intergrain	50–60%	1:1	feldspar, fragments of volcanic origin
E3-9 (Unit 10)	pellicular and intergrain	70%	1:1	fragments of volcanic origin, muscovite
E3-10 (Unit 10)	pellicular and intergrain	upper part 50–60%, lower part: 10–20%	1:1	feldspar, muscovite, volcanic glass, various rock fragments

Tab. 3.1. Micromorphological features of the Encantado section. See Figure 3.3 for sample location.

3.6.2 Melián section

Carbonate sands

In the Melián section, the middle to coarse sand grained carbonate sands of shelf origin are characterised by a $CaCO_3$ content of up to 86.6 % (e.g., Unit 5, lower part). These sediments are a reddish yellow (7.5 YR 7/6; Unit 14) and yellow (10 YR 7/6; Units 6–8) colour. Iron content can be up to 11.54 g/kg Fe_t and 2.22 g/kg Fe_d.

Soil sediments

Just the parent materials of Unit 9 and 10 (Fig. 3.4) are linked to soil sediments. Both Units are characterised by a succession of different layers featuring relocated molluscs. The soil sediment of Unit 10 is reddish yellow (7.5 YR 7/6) in colour, showing 75.4 % $CaCO_3$ with 11.21 g/kg Fe_t and 1.95 g/kg Fe_d.

Palaeosurfaces

The palaeosurfaces of the Melián site feature 40–80 % $CaCO_3$, the lowermost is related to Unit 6. Accordingly, Fe_t values reach their maximum in Unit 6, offering 23.56 g/kg combined with 5.40 g/kg Fe_d, whereas the quartz content of Unit 6 reaches only 5%. Units 1 and 2 show higher amounts of quartz of 6 to ~ 10 %. The thin sections M-SW 8, 9, and 10 indicate highest quartz content in Units 9 and 11. In stratigraphic order, Unit 7, Unit 6,

and Unit 5 are the first units clearly featuring volcanic imprint. They are characterised by impurities of mafic minerals.

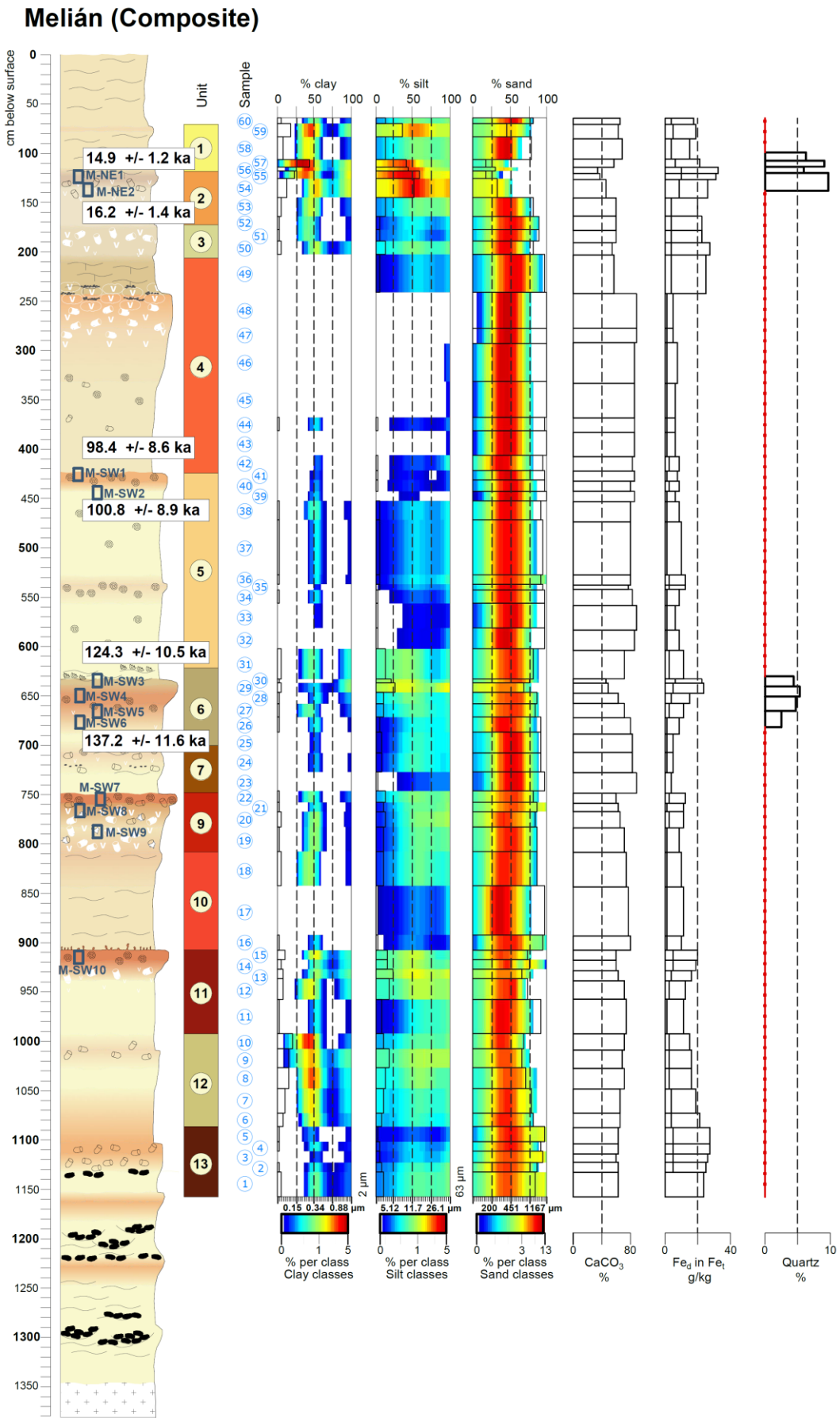

Fig. 3.4. Melián section including analytical data sample wise. Sequences with no available data indicated by red lines (according to Roettig et al., 2017, modified). See Figure 3.3 for key.

Correspondingly, thin sections M-SW 2 (Unit 5) and M-SW 6 (Unit 6) show the admixture of volcanic glasses (Tab. 3.2). Additionally, the upper most part of Unit 4 shows volcanic imprint by accumulation of tephra material. Units 1–3 also feature several impurities, supported by thin section M-NE 2, showing a significantly high proportion of fragments of volcanic origin. Unit 6 is dated 137.2+/- 11.6 ka. The palaeosurface on top of Unit 5 is dated to roughly 100 ka. The youngest dated palaeosurface is underlain by sediments aged 16.2+/- 1.4 ka and overlain by deposits aged 14.9+/- 1.2 ka.

Sample	**Microstructure**	**Porosity**	**c/f -ratio**	**Mineral constituents**
M-NE 1 (Unit 2)	single and intergrain, partially bridged grain	70%	2:1	mica, quartz (sparse), fragments of volcanic origin
M-NE 2 (Unit 2)	intergrain	upper part: 70%, lower part: 60%	1:1	fragments of volcanic origin, feldspar, muscovite, quartz
M-SW 1 (Unit 5)	single grain	30%	sparse fine material	feldspar, quartz (sparse and rounded), fragments of volcanic origin
M-SW 2 (Unit 5)	upper part: pellicular grain lower part: pellicular and bridged grain	20%	50:1	volcanic glass, feldspar (few), quartz (few), fragments of volcanic origin
M-SW 3 (Unit 6)	single grain, seldomly pellicular	50%	sparse fine material	quartz (few) feldspar (few)
M-SW 4 (Unit 6)	upper part: single grain central part: single and intergrain, lower part: complex	30–40%	2:1	weathered quartz, feldspar and mica, fragments of volcanic origin
M-SW 5 (Unit 6)	bridged. upper part: add. vughy lower part: add. intergrain	40%, (10% in dense material)	1:2 to 1:3	biotite (few), quartz (few), feldspar (few), fragments of volcanic origin (few)
M-SW 6 (Unit 6)	single and intergrain, lower part: add. bridged	40–50%	1:2	volcanic glass, biotite, quartz,

				feldspar, fragments of volcanic origin
M-SW 7 (Unit 9)	pellicular and intergrain, channel: single grain, pellicular grain, intergrain	10–15%	1:1	fragments of volcanic origin (many), quartz, feldspar
M-SW 8 (Unit 9)	upper part: intergrain, vughy, central part: intergrain lower part: vughy	20%, brood cell: <5%	1:1	quartz, volcanic glass, various rock fragments
M-SW 9 (Unit 9)	intergrain, pellicular grain	30%, brood cell: 0-<5%	1:2	quartz muscovite, volcanic glass, fragments of volcanic origin
M-SW 10 (Unit 11)	single and intergrain	40–60% (irregular)	3:1	quartz, feldspar, volcanic glass, muscovite (few), fragments of volcanic origin (sized)

Tab. 3.2. Micromorphological features of the Melián section. See Figure 3.4 for sample location.

3.6.3 Jable 1 section

Carbonate sands

The carbonate sands range in colour from pink (10 YR 8/4), very pale brown (10 YR 8/4 and 7/4), to reddish yellow (7.5YR 7/6). Dominated by the sand fraction (up to >95 %), they feature very low amounts of iron. Fe_t content shows a maximum of 8.14 g/kg and Fe_d content a maximum of 1.89 g/kg (Fig. 3.5, Unit 4).

Soil sediments

The central part of this section is dominated by soil sediments (Units 7–9 and the upper part of Unit 10) consisting of about 70 % to >83 % $CaCO_3$. These sediments are reddish yellow (7.5 YR 6/6) in colour and contain up to 25 % silt and 10 % clay (e.g., upper part of Unit 10). The amounts of iron reach a maximum of 11.76 g/kg Fe_t and 3.34 g/kg Fe_d (Unit 10, upper part).

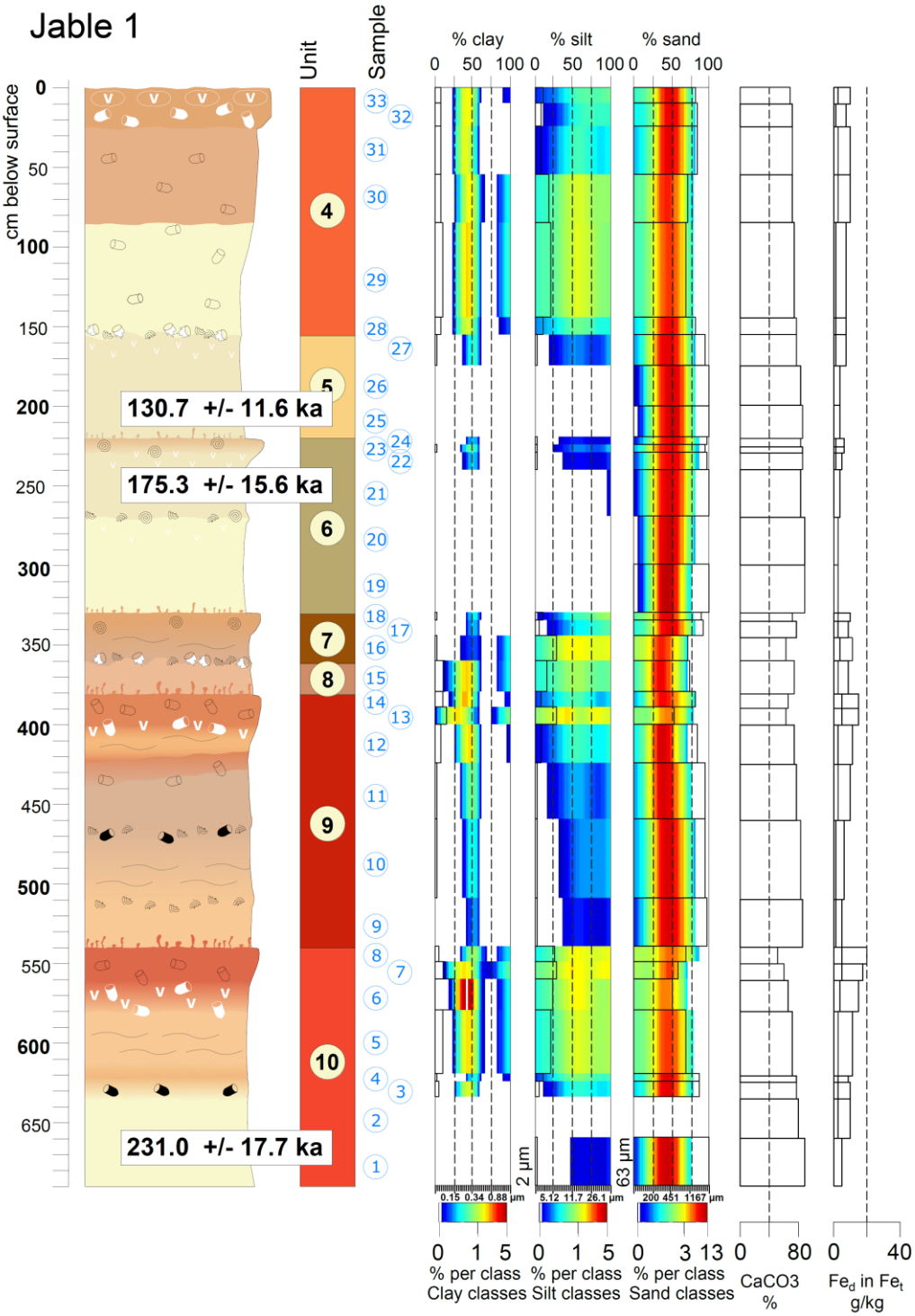

Fig. 3.5. Jable 1 section including analytical data sample wise (according to Roettig et al., 2017, modified). See Figure 3.3. for key.

Palaeosurfaces

The $CaCO_3$ content of different palaeosurfaces of this section presents values between 52% (Unit 10) and 80% (Unit 6). Unit 10 presents the highest clay content (25%) of the whole

section. The colours of the different palaeosurfaces range from strong brown (7.5 YR 5/8; Units 9 and 10) to reddish yellow (7.5 YR 6/6 and 7/6; Units 6 and 7). Thus, the Fe_t content reaches its maximum of 20.18 g/kg and Fe_d content of 5.42 g/kg related to Unit 10. Units 6–8 show volcanic influence featured by impurities of mafic minerals (tephra material). The section is dated to 231.0 +/-17.7 ka in the lowermost part. On top (2m below current surface), the sediment was dated to 130.7 +/-11.6 ka. For a more detailed description of the sections, refer to the study by Roettig et al. (2017).

3.7 Discussion

3.7.1 Soil formation versus imprint of dust

Soil-forming processes

Our micromorphological analyses (Fig. 3.6, Tables 3.1 and 3.2) indicate that the weakest in-situ soil formation (e.g., Unit 5, Melián section) in carbonate sands on Fuerteventura is characterised only by features of very weak de- and recalcification. These processes seem to take place within very short distances (excluding root casts), thereby they are not comparable to those decalcification processes like those reported from mid-European loess sections that reveal a marked nearhorizontal boundary of a late glacial and Holocene decalcification front (Meszner et al. 2013).

In carbonate sands, voids and pores are favored areas of recalcification (cf. Fig. 3.6A thin section E3-7, central part). These processes take place in an environment with more than 75 % $CaCO_3$ (e.g., Unit 6 of the Encantado section). In these calcareous carbonate sands, features of de- and recalcification show a patchy distribution. Further features of weak in-situ soil formation are concretions of manganese and iron (Fig. 3.6B, thin section E3-3, upper part). It seems to be impossible that these concretions have been relocated. The outer rims of the manganese-coated grains are irregular and must be autochthonous. One special feature is presented by the upper part of Unit 4 of the Encantado section that indicates clay illuviation (Fig. 3.6C, thin section E3-2, upper part) incorporated in large fragments and aggregates, perhaps related to former soil formation. Hence, clay illuviation took place prior to reworking, and it is unclear if the respective soil formation took place directly in carbonate sands. So far, on Fuerteventura solely Pomel et al. (1985, p. 59) described a section close to the village of Pajara including a palaeosol (Rhodoxeralf, “sol brun-rouge calcifère”) featuring cutanes, as an indicator of in-situ clay illuviation. Pal et al. (2003)

described the illuviation of clay and the formation of pedogenic $CaCO_3$ as two concurrent processes concerning alfisols of the semi-arid part of the Indo-Gangetic Plain.

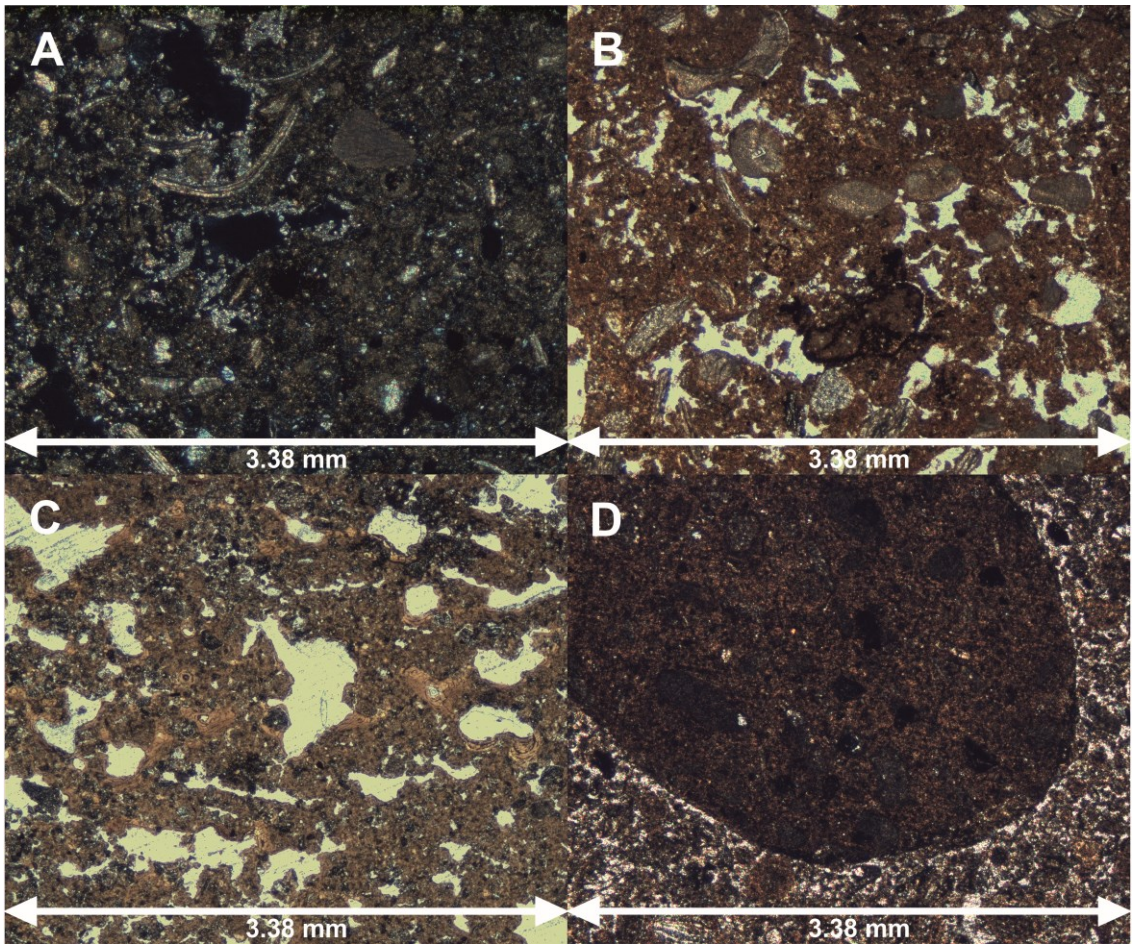

Fig. 3.6. Thin sections showing features of: (A) de- and recalcification (sample E3-7, central part of thin section, not HCl treated: partially decalcified, secondary carbonates around voids and weathered ash grains); (B) oxidation of manganese (samples E3-3, upper part of thin section, not HCl-treated: besides silt-sized quartz grains, irregular autochthonous impregnation of Manganese); (C) relocated aggregates including fragments of clay illuviation (sample E3-2, upper part of thin section, not HCl-treated: large fragments of former soil containing illuvial clay); and (D) rounded reworked material (sample M-SW7, lower part of thin section, not HCl-treated: rounded reworked aggregates often consist of dense brown fine material of a much more intensively developed soil). For sample location, please see Figs. 3.3. and 3.4.

Albeit, Unit 4 is characterised by a $CaCO_3$ content of more than 70% without featuring any indicative decalcification. Thus, from our findings on Fuerteventura, we do not consider these clay coatings and aggregates as in-situ features because they were detected in reworked material still containing a very high amount of $CaCO_3$. Thin section E3-4 (Unit 7 of the Encantado section) indeed shows coatings (clay and iron oxides) of coarser grains, but the rounded rims clearly suggest relocated sediments. We did not observe characteristic

structures like alignments of clay enrichment, which one would expect from clay illuviation in such sandy material. In combination with detecting only in-situ concretions of iron and manganese (Fig. 3.6B, thin section E3-3, upper part), our study is in line with Kruse and Meyer (1970), who did not find evidence of further pedogenetic processes other than decalcification and oxidation of iron in sequences in Moroccan coastal dunes.

Formation of clay minerals

Micromorphological analyses did not support neo- or transformation of clay minerals. The autochthonous minerals of volcanic origin should transform to smectites (Jahn, 1988; Zarei, 1989), but only under hydromorphic conditions (von Suchodoletz et al., 2009). The free drainage conditions on Fuerteventura did not facilitate any in-situ smectite formation (Tab. 3.3). As formation of kaolinite is almost impossible in settings of calcareous parent material, we assume that all measured illite and kaolinite (Tab. 3.3) are allochthonous and reached the system from Saharan dust, as reported by Criado and Dorta (2003) and von Suchodoletz et al. (2009).

Encantado section	**Illite (%)**	**Kaolinite (%)**	**Verm./Clorite (%)**
sample 20	95	5	
sample 21	82	18	
sample 23	90	10	
sample 24	92	8	
sample 25	84	16	
sample 35	81	19	traces
sample 36	81	19	
sample 37	81	19	

Tab. 3.3. Results of X-ray diffraction analysis.

Fine material

Unit 9 of the Encantado section (Fig. 3.3) is characterised by decreasing values of $CaCO_3$ and increasing amounts of clay and silt from the bottom to the top of the section. At the Encantado section silt content can be up to 40–50 % (e.g., Units 7 and 9). Higher silt content suggests increased dust imprint (von Suchodoletz et al., 2009; Muhs et al., 2010; Scheuvens et al., 2013); however, increased clay content should indicate more intense soil formation due to a lower c/f-ratio. Yet, despite a lower content of fine material (clay and silt), thin section E3-8 (Tab. 3.1) features a lower c/f-ratio (1:1) in comparison to thin section E3-7 characterised by a c/f-ratio of 4:1 to 3:1. Firstly, due to a higher silt and clay content, E3-7 (the uppermost part of Unit 9) seems to be dominated by dust imprint.

Secondly, this suggests more intense soil formation in E3-8 than in E3-7. Assuming more intense soil formation related to dune fields on Fuerteventura involves notable de- and recalcification processes and oxidation of iron and manganese. Fuerteventura soils are not comparable, however, to intense soil-formation processes of tropical regions, for instance.

Imprint of dust

In addition to the aforementioned features, the quartz content is also a convincing marker of dust imprint in the eastern Canary Islands (Misota and Matsuhisa, 1995; Menendez et al., 2007; von Suchodoletz et al., 2013). Except for one sample (~2% quartz, uppermost part of Unit 10 of Encantado), the quartz content of layers related to palaeosurfaces is quite similar (ca. 4–7 %), whereas layers of middle to coarse sand-dominated biogenic carbonate sands are almost free of quartz. The similar quartz content suggests aggrading soils due to a relatively steady dust accumulation. We assume that increasing Si values are mainly related to increased volcanic imprint. Faust et al. (2015) proposed a hypothesis to explain sediment-accumulation dependent soil-forming intensity on Fuerteventura. Less accumulation of sediment would result in higher soil-forming intensity indicated by soil reddening. We cannot rule out the possibility of reddening caused by higher accumulation rates of dust including hematite as a constituent, however, in accordance with zu Leiningen (1915), Dan and Yaalon (1966, 1968), Dan (1990), and Yaalon (1997). Similarly, Jahn (2010) identified iron oxides of higher crystallinity besides quartz, kaolinite, and illite as indicators of dust material on Lanzarote, and Menéndez et al. (2013) measured up to 6 % of hematite as a constituent of dust material. Therefore, adding to the interpretation by Faust et al. (2015), even higher dust-accumulation rates could contribute to the reddening of the sediments. Hence, more intense reddening is not necessarily caused by more intense soil formation. Kruse and Meyer (1970) reported autochthonous $CaCO_3$-coated primary iron exposed by decalcification in Moroccan dune deposits. Subsequently, the primary iron was oxidised and reddened the material. This process is called “Entkalkungsrötung” (“decalcification reddening”). Ultimately, it is hard to determine and distinguish between the contribution of dust (i.e., by the content of hematite) and the influence of in-situ reddening. Thus, the most plausible hypothesis supports that dust accumulation and in-situ reddening are two concurrent processes. Hence, we have to mention the combination of dust imprint and in-situ reddening as an in-situ soil-forming process. Extending the study by Kruse and Meyer (1970) we assume, $CaCO_3$-coated primary iron as constituents of dust, which are leached after deposition and transform into hematite (Andreucci et al., 2012).

Our analyses of elemental composition of the clay fraction (comparing the results of pretreated [HCl] and non-pretreated samples, see Tab. 3.4) support the assumption of $CaCO_3$-coated iron particles.

Encantado section	Clay pretreated Fe (g/kg)	Clay non-pretreated Fe (g/kg)	Bulk sample pretreated Fe (g/kg)	Bulk sample non-pretreated Fe (g/kg)
Sample 16	47.55	21.73	49.55	20.76
sample 17	49.29	n. m.	50.38	20.80
sample 20	59.20	n. m.	50.94	17.74
sample 21	57.10	n. m.	52.84	19.81
sample 23	48.82	0.20	52.17	15.72
sample 24	54.40	4.19	51.61	20.83
sample 25	54.07	n. m.	n. m.	26.42
sample 33	43.44	n. m.	n. m.	8.31
sample 34	57.18	n. m.	n. m.	21.84
sample 35	60.61	n. m.	n. m.	33.66
sample 36	60.93	n. m.	n. m.	38.70
sample 37	57.02	n. m.	n. m.	40.69
sample 40	45.25	n. m.	n. m.	18.07
sample 41	36.67	n. m.	n. m.	17.28
sample 47	59.25	n. m.	n. m.	31.81
sample 48	57.94	n. m.	n. m.	38.21

Tab. 3.4. Measured Fe-contents of clay fraction and bulk samples (pretreated and non-pretreated; n.m., not measured)

The values of measured pretreated samples are many times higher than the values of non-pretreated samples. Considering the results from measured elements, the values of pretreated samples show higher iron contents. For example, sample 24 of Unit 9 (Encantado section) features 4.19 g/kg Fe (clay fraction, non-pretreated) versus 54.4 g/kg Fe (clay fraction, pretreated). In addition, results of the respective bulk sample (clay + silt + sand) show 51.61 g/kg Fe (pretreated). This implies that all of the iron is linked to the clay fraction. The high $CaCO_3$ content (52 % in Unit 9 of the Encantado section, sample 24) suggests an incomplete leaching of $CaCO_3$, but possibly a noteworthy contribution to reddening by $CaCO_3$-coated iron particles as constituents of dust.

3.7.2 Determination of periods of palaeosurface formation

Remarkably, we recurrently observed the following sequence of layering (from the bottom to the top of each stratigraphic sequence) at different aeolian sections:
(1) pure carbonate sands (unconsolidated aeolianites); (2) material influenced by dust imprint and soil formation; (3) soil sediment (relocated by water-induced erosion) or

(1) pure carbonate sands (unconsolidated aeolianites); (2) soil sediment (relocated by water-induced erosion); and (3) material influenced by dust imprint and soil formation. In contrast, we rarely observed carbonate sands (without the influence of dust imprint, soil formation, or volcanic imprint) relocated by water-induced erosion. This allows us to assume a simplified alternation of sand supply, soil formation including dust imprint, and finally water-induced erosion and reworking (Fig. 3.7).

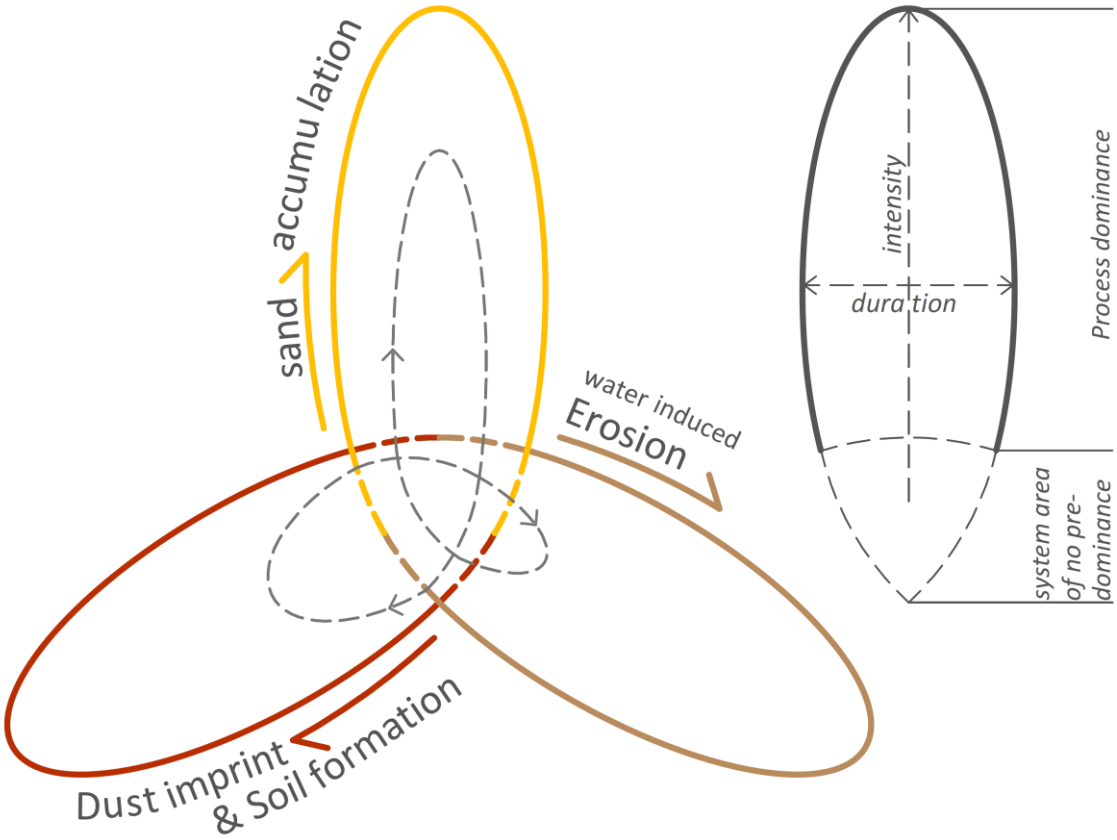

Fig. 3.7. Process cyclicity. Sectors of predominance of "sand accumulation" (yellow), "dust imprint and soil formation" (red), and "water-induced erosion" (greyish-brown) result in process cyclicity. The grey line shows an example of one cycle. The idealised sequence starts with sediment supply (grey line in yellow sector, following the direction of the arrow) taking place within a relatively short period but being of high intensity of supply (please see markings of "duration" and "intensity" on the right side), followed by a longer lasting but less intense period of dust imprint and soil formation, making the sediment vulnerable to waterinduced erosion, finally (following the grey line: short period of water-induced erosion of low intensity). This example is derived from interpretation of Unit 11.

Occasionally, this sequence is followed by further dust imprint and soil formation. Thus, we suggest morphological resistance as a main reason for the mentioned succession of processes, i.e., the unconsolidated aeolianites are characterised by middle to coarse-

grained sand. Coarse grain size is related to a value of water permeability of almost 250–675 cm/d (dependent on bulk density; Ad-hoc Arbeitsgruppe Boden, 2005). The high permeability causes a high morphological resistance to water-induced erosion. Similarly, this is reflected in recent dune fields, where development and preservation of depression lines and discharge pathways is strongly inhibited. Additionally, during periods of predominant sand supply, the surface is subject to strong aeolian dynamics, which continuously rework the sediments. Finally, the sand supply has to decrease to simultaneously facilitate stable surface conditions and the development of depression lines. In case of decreasing sand supply, the prevalence of dust accumulation and soil-forming processes causes the fining of near-surface sediments, resulting in decreased water permeability and reduced morphological resistance. Thus, vulnerability to water-induced erosion increases. Furthermore, Jahn (2010) proposed an increasing water-storage capacity caused by the substrates' fining due to dust imprint. Indeed, this coupling leads to the self-enhancement of stable surfaces and dust imprint, leading to soil-forming processes and at least changing successively the value of water permeability in the course of admixture of fine material. Consequently, sand supply seems to be the primary control quantity in allowing site-specific geomorphic stability, related to dust accumulation and soil-forming processes, in view of forming palaeosurfaces. On Fuerteventura, we mainly consider three possible drivers controlling the supply of carbonate sands of shelf origin: (1) changing wind directions, (2) volcanic activity, and (3) changing sea level.

Wind direction

In general, it is conceivable that the supply of carbonate sands may depend on a particular dominant wind direction. On the case of Fuerteventura, Coudé-Gaussen and Rognon (1988) hypothesised a westerly wind direction during periods of sand supply. In contrast, Alcántara-Carió et al. (2010) suggested more intense trade winds alternating with easterly winds during periods of favored sand supply. Criado et al. (2004) postulated wind directions similar to northeast trade winds seen nowadays. Roettig et al. (2017) suggested that the archives of aeolianite palaeosol sequences indicate northerly wind directions during periods of prevalent sand supply. Two facts support the latter suggestion. First, the assumption that the coarser the material the closer the sediment source is wellsupported by the distribution of grain sizes within the three studied sections. Figure 3.8 provides the grain- size medians of each section in relation to the grain-size median of the whole area (median of all sections).

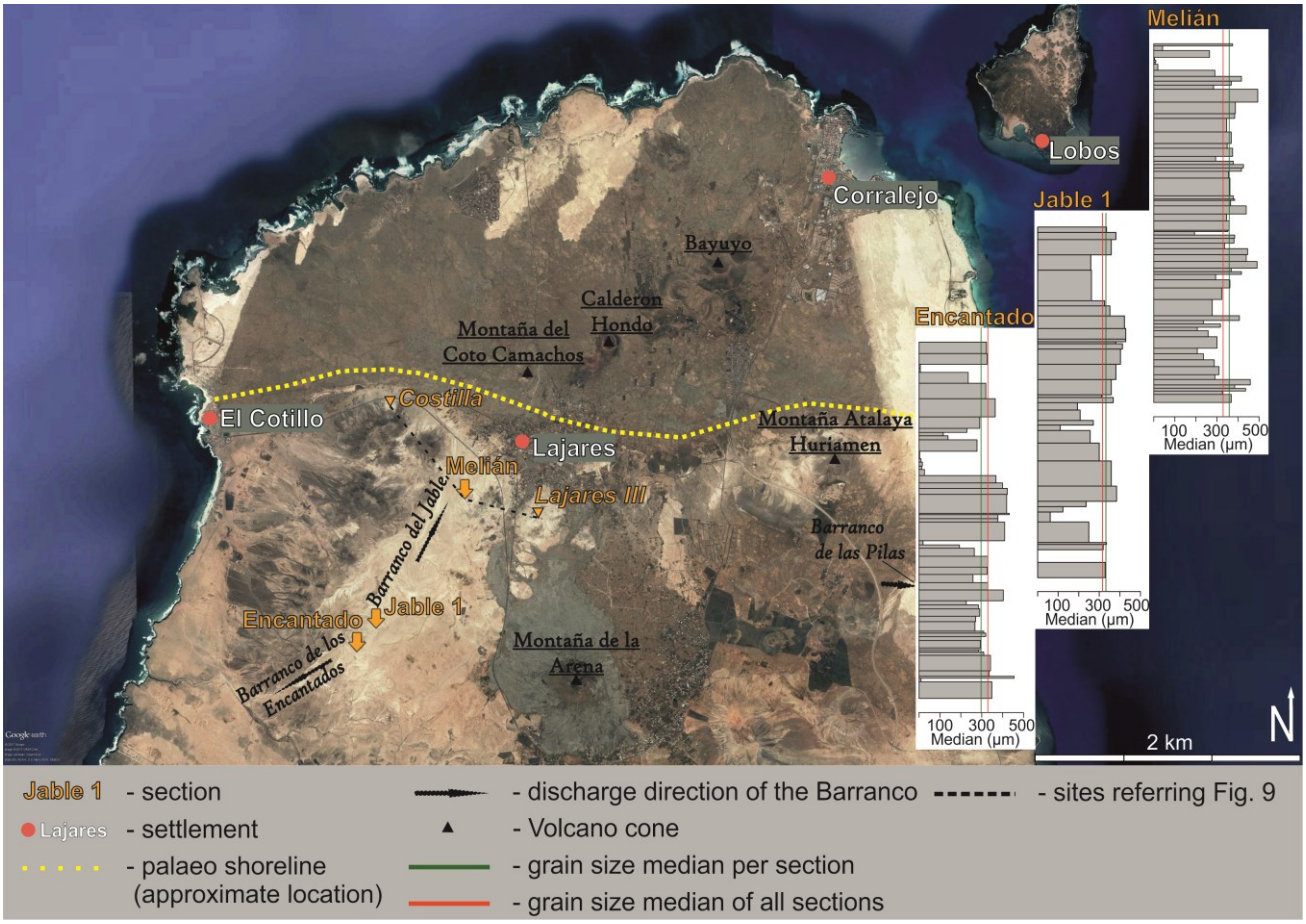

Fig. 3.8. Satellite image of the study area, including grain-size median plots of the Encantado, Jable 1, and Melián sections including the approximate location of a former coastline, described by Ruiz et al. 2011 (based on Google Earth, modified).

The southernmost Encantado section shows a median of 294.7 µm, whereas the northernmost Melián section presents a tendency to coarser material with a median of 355.7 µm, and Jable 1, located in between Melián section and Encantado section, reveals a grain-size median of 331.4 µm. This trend could be influenced by the site-specific preservation conditions and therefore more preserved finer material. Nevertheless, we observed the same tendency comparing distinct correlated sand layers (respective Units). For example, the parent material of Unit 5 shows the following median values: 290.7–363.6 µm (sample 43–44, Encantado), 421.2– 350.0 µm (samples 25–26, Jable 1), 344.3–437.6 µm (samples 32–33, Melián), or, in the case of the carbonate aeolianites of Unit 11, 267.9 µm (samples 13, Encantado) versus 300.4 µm (samples 11, Melián). This coarsening of grain sizes towards a northern direction suggests a sand supply related to northerly wind directions. The second aspect refers to the distribution of carbonate sands taking the whole island of Fuerteventura into account. Apart from the palaeo dune fields in our study area,

we can outline the following areas of accumulated dune sediments (Fig. 3.9): (1) Llano del Cotillo o Angustura (on the southern tip of the island); (2) Istmo de la Pared and El Jable between the settlements of Jandia and La Pared; (3) Jable de las Salinas and Jable de Vigocho 5 km southwest of Pajara; (4) sand sheets in the north of El Cotillo (Los Lagos)

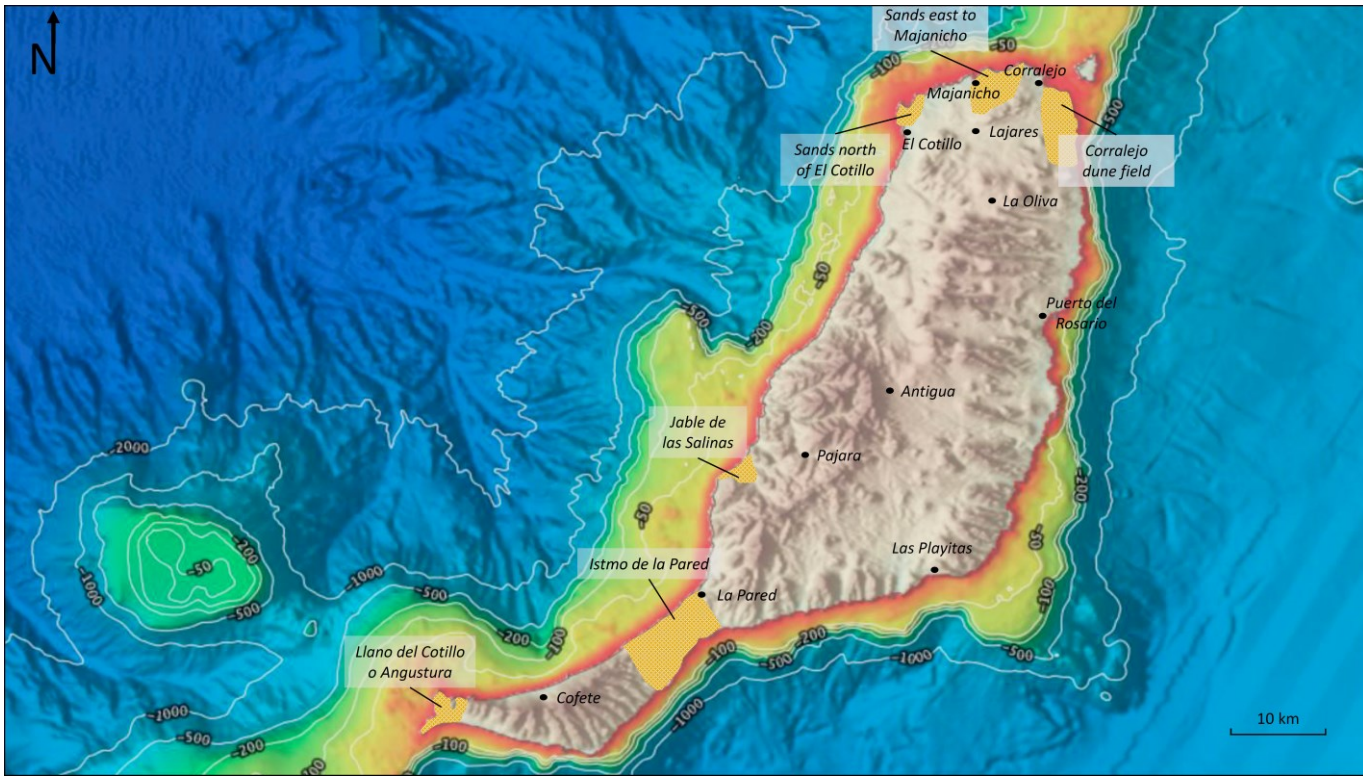

Fig. 3.9. Bathymetric data showing areas of shallow shelf around Fuerteventura with marked accumulation areas of carbonate sands of shelf origin (orange/black; based on EMODnet, modified).

and to the east of Majanicho; and (5) the Holocene dune field of Corralejo.

All these areas are characterised by palaeo dune fields fed by a shallow shelf area in a northern direction. We did not find remnants of palaeo dunes to the north of Las Playitas, despite a respective/corresponding shallow shelf offshore. Here, we have to point out that the potential source area offshore is located in a southeastern direction. Another counterexample is the area close to the village of Cofete on the southern tip of the island. Here, the coastline is exposed to a northern direction, but, unfortunately, we found only a very narrow shallow shelf area offshore. Again, there are no noteworthy accumulations of carbonate aeolianites. Ultimately, we can assume a source area exposed northward in terms of a wide shallow shelf offshore as prerequisites to generate an accumulation of unconsolidated carbonate aeolianites on Fuerteventura.

3.7.3 Volcanism

Volcanic activity is an important local controlling factor for dune accumulation. Hereby, the main influence on sand supply is exercised via interruptions of sediment cascades. Our study area is a perfect example to investigate the impact of volcanic activity on the formation of aeolianite sequences. Based on stratigraphic findings, Roettig et al. (2017) assumed a change in sediment delivery around 185 ka and again at 135 ka. These time periods coincide with volcanic eruptions reported byMeco et al. (2002, 2011) and Criado et al. (2004).Moreover, Ruiz and Cabrera (2011) suggested an old shoreline running from El Cotillo to Lajares to Montaña Atalaya Huriamen (Fig. 3.8, yellow dotted line). This corresponds with the distribution of palaeo dune fields and sand sheets (Barranco del Jable and Barranco de los Encantados, Barranco de las Pilas), and with the huge basaltic lava sheet covering the northern part of the island. At its center there is a chain of volcanoes. Calderon Hondo and Bayuyo are included in this chain of volcanoes, and both are dated 135 ka (Meco et al., 2002; Ruiz and Cabrera, 2011). Montaña de la Arena first erupted 185 ka (Edwards and Meco, 2000). These volcanic eruptions are assumed responsible for a major change in sediment supply, delivery, and accumulation. Accordingly, the Melián site shows a change in its sediment preservation.We suggest that the upper part of this section (starting with Unit 7) would have never been preserved without a change in the local characteristics. Until the mentioned volcanic events, the Melián site was characterised by high morphodynamics, situated close to the outlet of the catchment of Barranco del Jable (Roettig et al., 2017). The volcanic activity caused a change in the base level of erosion by blocking the former outlet of the Barranco del Jable. We assume this change is responsible for better preserving conditions of the sediments of Units 1–7 at the Melián site. The assumption is supported by the IRSL age of 137.2 +/- 11.6 ka, related to Unit 6 of Melián. Also, we observed a change, namely a lack of further sedimentation, in the same stratigraphic position at the site of Encantado. We suggest that the lava flow inhibited further sediment supply because the vast lava field covered former dune fields, which, in turn, hindered the transportation of sand material. Differences in site-specific preservation conditions cannot be completely excluded, but there is no field evidence indicating that preservation and erosion are responsible for this feature at the Encantado section. Surprisingly, the Melián section features no cutoff from sediment accumulation (but better preservation conditions in the upper sequence as mentioned before). Faust et al. (2015) investigated the Costilla section (the same as “Rosa Negra” in the literature; e.g., Damnati et al., 1996). This section is located on the northern slope of the outcrops of

Miocene volcanism (Fig. 3.8). Therefore, the section is located between the villages of Lajares and El Cotillo, just 2.5 km northwest of the Melián section. Faust et al. (2015) described Costilla in detail, but the thickness of the upper part of the section was underestimated. They reported an age of 228 +/- 33 ka of the sediments below the so-called "marker horizon." The "marker horizon" is equivalent to Unit 9 according to Roettig et al. (2017). Bouab and Lamothe (1997) dated the sediments above Unit 9 as 181 +/- 27 ka and 183 +/- 27 ka. Hence, in combination with our own investigation, we can conclude a

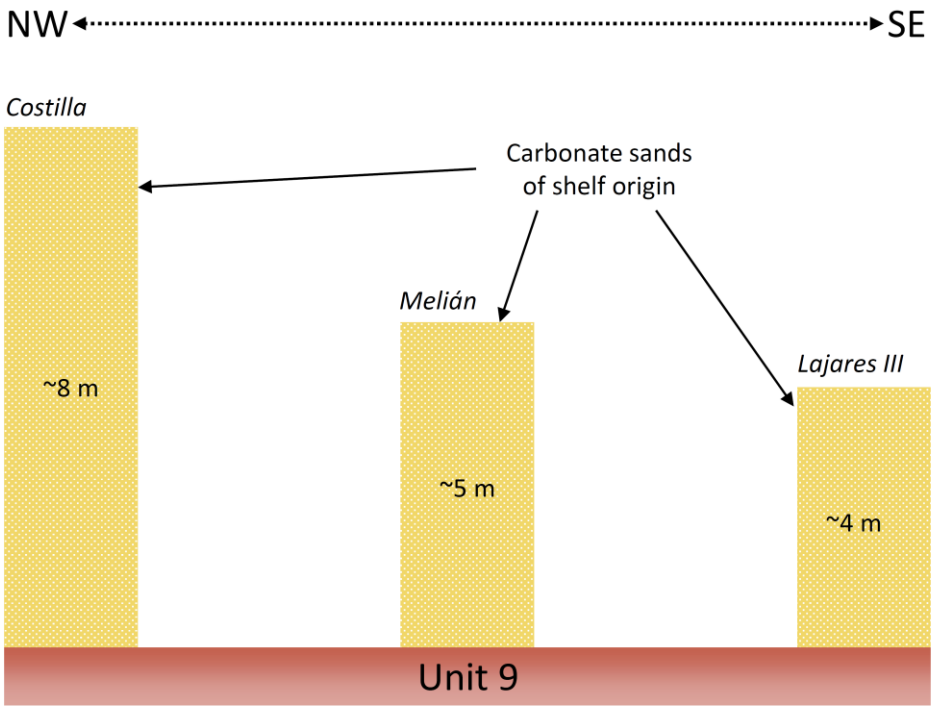

Fig. 3.10. Simplified illustration of sediment thicknesses overlying Unit 9 of the Costilla, Melián, and Lajares III sections. For location of sections, please see Fig. 3.8.

possible relation to the period of volcanic activity. At Costilla, the sediments above Unit 9 are up to 8m thick, whereas the respective sediments at Melián are approximately 5m thick (Fig. 3.10).

In turn, at the Lajares III section (also described by Faust et al., 2015) approximately only 4m has accumulated. To summarize, in agreement with the volcanic activity at 185 ka and at 135 ka, we observed a lack of sediment accumulation at Encantado, and decreasing thickness of sand layers at Jable 1, whereas sedimentation continued at the sites of Costilla, Melián, and Lajares. The last three mentioned sites present a gradient of decreasing accumulation in an eastern direction. This leads to the assumption that the volcanic events at 185 ka and at 135 ka caused a cutoff from sediment delivery from a northern to

northeastern direction. Correspondingly, mainly derived from the gradient of sediment accumulation at Costilla, Melián, and Lajares, we assume ongoing sediment delivery from a northwestern direction. The leeward positioning behind the basal complex of the site of Encantado inhibited its supply of sediment from a northwestern direction. Possibly, a further eruption, maybe related to the chain of volcanoes of the Calderon Hondo or to the Montaña del Coto Camachos, situated further west (see Fig. 3.8), completed the basaltic barrier/lava sheet, as observed nowadays, and blocked off the western-to-northwestern sediment pathway. The archives of Melián, Lajares, and Costilla show a respective complete cutoff before 50 ka (47.5 +/- 6.5 ka at Lajares; Faust et al., 2015) and after 100 ka (98.4 +/- 8.4 ka; Roettig et al., 2017). After this point in time (>50 ka), none of the sites (Encantado, Melián, Jable 1, Costilla, and Lajares III) experiences additional accumulation of sediments directly delivered from the shelf area. A period of volcanic activity around 51 ka is also supported by Pomel et al. (1985), who described volcanism near to Pajara. The sites of Melián, Lajares, and Costilla, however, indicate clear features of volcanic activity, such as lapilli in respective stratigraphic position.

3.7.4 Sea level

Meco et al. (2011) presented a curve of middle Pleistocene to Holocene ice volume (reverse sea level) combined with information related to marine deposits, palaeosols, and dune accumulations on the Canary Islands. According to these authors, palaeosols (indicated by “locust infestations”; Meco et al., 2011) are early indicators of interglacials, whereas sand supply took place during glacial sea-level low stands. Similarly, in their model of landscape evolution on Fuerteventura, Coudé-Gaussen and Rognon (1988) designated glacials of lowered sea level as periods of sand supply. Undoubtedly, there is an effect of sea-level changes on supply of sediment of shelf origin. Pye and Tsoar (2009) summarised different approaches of linking sea-level fluctuations to sediment supply and landward migration of coastal dune systems. A first model, developed by Sayles (1931), describes the possibility of sediment supply during sea-level low stand in accordance with the assumptions of Meco et al. (2011) and Coudé-Gaussen and Rognon (1988). An alternative approach suggests sand supply during sealevel high stands (Bretz, 1960), and a third model by Schofield (1975) describes the relevance of falling sea level for sediment supply and dune formation. According to the aforementioned approach, the spreading of dune systems is seen to be approximately proportional to the net fall of sea level during one specific sea-level fluctuation (cf. Fig. 3.11). This implies that sea-level low stands

would not correspond to periods of sediment supply. Instead, periods of falling sea level appear to be much more relevant. According to the data reported by Roettig et al. (2017), dune sediments in northern Fuerteventura were dated around 171.2 +/-15.4 and 175.3+/-15.6 ka, respectively. Other periods of sand supply took place around 137.2 +/-11.6, 130.9 +/-11.0, 130.7 +/-11.6, and 124.3+/- 10.5 ka. An additional period of significant sand supply dated to 100.8+/- 8.9 and 98.4 +/-8.6 ka. In the context of presented IRSL ages with a +/-10% error, it seems inappropriate to support or exclude any of these proposed models linking sea-level changes with periods of sand supply. From a dating perspective, younger sediments should be much more useful. Unfortunately, because of the previously mentioned cutoff from supply of sediments of shelf origin no later than ca. 50 ka caused by volcanic activity, younger sediments are non-existent in the investigated aeolianite sections. Aside from the dating error, the ages reported by Roettig et al. (2017) least contradicts the concept (Schofield, 1975) of predominant sediment supply during falling sea level. If we take a look at the current conditions of the dune field close to Corralejo (cf. Fig. 3.1), we observe persistent but less intense sediment supply during a phase of sea-level high stand, which is in accordance with Bretz (1960). Less intense sediment supply means a sediment supply just high enough to form barchans and sand sheets (compare Criado and Naranjo, 2011). Derived from this observation and with regard to the process cyclicity presented in Figure 3.7, less intense sediment supply should be followed by high availability of sediment during falling sea level.

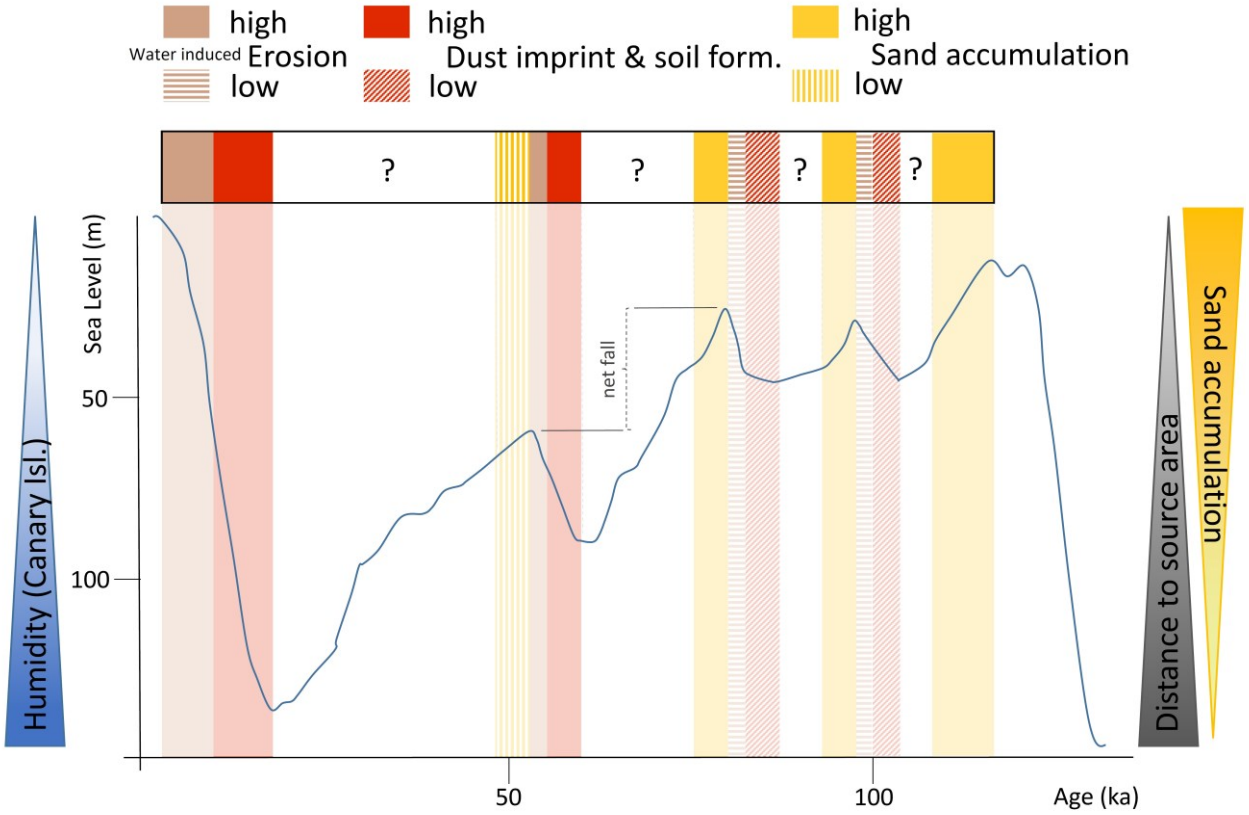

Fig. 3.11. Conceptual approach of process relation to sea-level fluctuation.

Here, in turn, it is important to consider the distance between the dune field (and our current archives) and the source area. Continually falling sea level is accompanied by strictly retreating shoreline in shallow shelf areas. Accordingly, the newly exposed areas as main sources of sand move away from the dune field, initially resulting in decreasing sand supply. This relationship is illustrated in the conceptual idea in Figure 3.11. In contrast to Coudé-Gaussen et al. (1987) and Meco et al. (2011), who suggested dune formation during arid glacial maxima, we assume a short period of high availability of coarse sand, with subsequent landward migration at the beginning of falling sea level. In our study sites, we often observed more sand sheet-like deposits of sediments instead of real dune accumulation. This could be caused by the long distance from the source area. Perhaps the material was just too coarse or the wind transport capacity was too low, thus resulting in a sand sheet-like accumulation.

3.7.5 Variations in humidity

Besides the great influence of sediment supply on the development of palaeosurfaces, changes in humidity should also be taken into consideration. In contrast to the global tendency toward more arid conditions during glacials, the Canary Islands seem to have

experienced more moist conditions (Yanes et al., 2011, 2013). Correspondingly, Rognon and Coudé-Gaussen (1996) assumed western wind directions for the last glacial maximum in latitudes between 28° to 35°N, including the Canary Islands. Equally, von Suchodoletz et al. (2010), who worked on loess-like deposits on Lanzarote, concluded increased humidity during glacial periods, possibly caused by stronger westerly winds. The Cooperative Holocene Mapping Project (COHMAP) members (1988) already pointed out that glacial periods are accompanied with a southward displacement of the westerlies, causing increased moisture in northwest Africa. Accordingly, Bush and Philander (1999) described weakened easterly and stronger westerly winds near the African west coast (20°N). Furthermore, stronger northerly winds were calculated concerning the latitudes beyond 20°N (>20°). In the case of the Canary Islands, a northern-to-northwestern wind direction could be assumed. Similarly, the PMIP-2-scenarios support the assumption of the mentioned southward displacement of westerlies, such as those stated by Laîne et al. (2009), whereby a southward shift and an eastward extension of the storm track for the Northern Hemisphere was reported. Based on these ideas, we assume a simplified pattern for the eastern Canary Islands. The lower the sea level, the more humid conditions prevail over the eastern Canary Islands. Consequently, the potential for soil formation increases with falling sea level (see Fig. 3.11).

3.8 Conclusion

Generally, soil-forming processes in palaeo dune fields of Fuerteventura are of weak intensity. They are usually constrained to processes of de- and recalcification and processes of recrystallization of iron and manganese. In the individual case Unit 4 of the Encantado section, relocated material illuviation features of former soil formation were detected, but composition of parent material related to the former soil formation remains unknown. Hematite as a constituent of dust is assumed to contribute to the reddening of palaeosurfaces in these archives. In general, decalcification reddening is also considered an important process of soil formation. This implies that the combination of dust and in-situ reddening as possible jointly operating processes. As a result, we assume Saharan $CaCO_3$-coated iron particles were leached after deposition, transformed to hematite, and intensified the colour of palaeosurface layers. Based on the high morphological resistance of pure unconsolidated carbonate aeolianites, we propose a cyclicity model describing subsequent phases of: (1) sand accumulation; (2) dust imprint and soil formation, and (3) waterinduced erosion. On Fuerteventura, sand supply and accumulation seem to be a main

controlling factor for the development of persistently exposed palaeosurfaces. In turn, changing wind direction, causing periods dominated by sediment supply/ accumulation could be excluded. The palaeowinds within the last ~ 400 ka seem to be linked to northern directions (northwestern to northeastern). Regarding the study area, periods of predominant sand accumulation are assumed to occur right after sea-level maxima during periods of falling sea level. The higher the baseline value of sea level, the more sand could have accumulated at our study sites. This assumption is supported by a simple function of falling sea level and an increasing distance between study sites and source area of carbonate sands. Thus, the lower the sea level, the greater the distance between source area and current sediment archives. Volcanic eruptions massively modified the supply and availability of carbonate sands of shelf origin. A complex history of blocking situations by lava flows largely controlled the sediment supply on northern Fuerteventura. This happened primarily in two ways: (1) sediment pathways were closed by lava flows; and (2) source areas (i.e., shallow shelf areas) were covered by lava flows. Apart from volcanic periods around 180 and 135 ka, the sedimentary archives point to further volcanic activity no later than ca. 50 ka. After that point in time, all studied sections were cutoff from supply of sediments of shelf origin. By this period, the study area became a palaeo dune field. Hence, it seems inappropriate to link the accumulation, or lack thereof, of carbonate sands of shelf origin to only one factor (e.g., sea level). Apart from sand supply and accumulation, humidity is suggested to have been higher during glacial periods, increasing the potential of surface stability of dust accumulation and soil-forming processes. Thus, we conclude that the best conditions for surface stability occur immediately after glacial maxima during periods of starting transgression. Further IRSL data will enable us to gain a deeper understanding of landscape evolution as registered in the sedimentary archives of northern Fuerteventura.

3.9 Acknowledgements

We are very thankful to Maria Tarquis Gongora and Don Manuel Gutierrez Ruiz, who supported us and always permitted access to important study sites. Special thanks to Michael Dietze for coordinating the grain-size measurements and to Anja Schleicher for coordinating the XRF measurements at the GFZ Potsdam. Many thanks to Sascha Meszner and Michael Zech for intensive discussions. Special thanks to BeateWinkler, who did the measurements at the laboratory of the TU Dresden. We are very thankful for all ideas and advices from the two anonymous reviewers and the editors. Many thanks to Elizabeth

Kelly for proofreading. This work was supported by the German Research Foundation (FA 239/18-1). Support of the National Research, Development and Innovation Office (NKFI) under contract NKFI K120620 (for G. Varga) is gratefully acknowledged.

3.10 References

Abdel-Monem, A., Watkins, N. D., Gast, P. W., 1971. Potassiumargon ages, volcanic stratigraphy, and geomagnetic polarity history of the Canary Islands: Lanzarote, Fuerteventura, Gran Canaria and La Gomera. American Journal of Science 271, 490–521.

Ad-hoc Arbeitsgruppe Boden. 2005. Bodenkundliche Kartieranleitung KA 5. E. Schweizerbartsche Verlagsbuchhandlung, Hannover. Alcántara-Carió, J., Fernández-Bastero, S.,Alonso, I., 2010. Source area determination of aeolian sediments at Jandia Isthmus (Fuerteventura, Canary Islands). Journal of Marine Systems 80, 219–234.

Alonso, I., Hernández, L., Alcántara-Carrió, J., Cabrera, L., Yanes, A., 2011. Los grandes campos de dunas actuales de Canarias. In: Sanjaume, E., Gracia, J. (Eds.), Las dunas en España. Sociedad Espanola de Geomorfología, Puerto Real, Cádiz, pp. 103–118.

Andreucci, S., Bateman, M. D., Zucca, C., Kapurs, S., Aksit, I., Dunalko, A., Pascucci, V., 2012. Evidence of Saharan dust in upper Pleistocene reworked palaeosols of North-west Sardinia, Italy: palaeoenvironmental implications. Sedimentology 59, 917–938.

Ball, M. M., 1967. Carbonate sand bodies of Florida and the Bahamas. Journal of Sedimentary Petrology 37, 556–591.

Bouab, N., Lamothe, M., 1997. Geochronological framework for the Quaternary palaeoclimate record of the Rosa Negra section (Fuerteventura – Canary Islands, Spain). In: Meco, J., Petit-Maire, N. (Eds.), Climates of the Past: Proceedings of the CLIP Meeting held June 2–7, 1995 — Lanzarote und Fuerteventura (Canary Islands, Spain). IUGS-UNESCO, Las Palmas de Gran Canaria, pp. 37–42.

Brindley, G. W., Brown, G., 1980. Crystal Structures of Clay Minerals and Their X-Ray Identification. Mineralogical Society No. 5, London, pp. 495. Bretz, J.H., 1960. Bermuda, a partially drowned, late mature, Pleistocene karst. Geological Society of America Bulletin 71, 1729–1754.

Brooke, B., 2001. The distribution of carbonate eolianite. Earth- Science Reviews 55, 135–

762 164.

Bush, A. B. G., Philander, S. G. H., 1999. The climate of the Last Glacial Maximum: results from a coupled atmosphere-ocean general circulation model. Journal of Geophysical Research 104, 24509–24525.

Casquet, C., Ibarrola, E., Fúster, J. M., Ancochea, E., Cantagrel, J. M., Jamond, C., Cendrero, A., Diaz de Teran, J. R., Hernan, F., 1989. Cronología de la Serie I de Fuerteventura. 130–131. In: Araña, V. (coordinador). Esf Meeting on Canarian Volcanism (Lanzarote, November–December 1989). European Science Foundation, Madrid. 367 pages.

Coello, J., Cantagrel, J.-M., Hernan, E., Foster, J. M., Ibarrola, E., Ancochea, E., Casquet, C., Jamond, C., Diaz De Teran, J.-R., Cendrero, A., 1992. Evolution of the eastern volcanic ridge of the Canary Islands based on new K-Ar data. Journal of Volcanology and Geothermal Research 532, 251–274.

Cooperative Holocene Mapping Project (COHMAP) Members, 1988. Climatic Changes of the Last 18,000 Years: observations and Model Simulations. Science 241, 1043–1052.

Coudé-Gaussen, G., Rognon, P., 1988. Origine eolienne de certains encroutements calcaires sur l'ile de Fuerteventura (Canaries Orientales). Geoderma 42, 271–293.

Coudé-Gaussen, G., Rognon, P., Bergametti, G., Gomes, L., Strauss, B., Gros, J. M., Le Coustumer, M. N., 1987. Saharan dust on Fuerteventura Island (Canaries): Chemical and mineralogical characteristics, air mass trajectories, and probable sources. Journal of Geophysical Research 92, 9753–9771.

Criado, C., Dorta, P., 2003. An unusual blood rain on the Canary Islands: the storm of January 1999. Journal Arid Environment 55, 765–783.

Criado, C., Guillo, H., Hansen, A., Hansen, C., Lillo, P., Torres, J. M., Naranjo, A., 2004. Geomorphological evolution of Parque Natural de Las Dunas de Corralejo (Fuerteventura, Canary Island). In: Benito, G., Díez Herrero, A. (Eds.), Contribuciones recientes sobre geomorfología. Sociedad Espanola de Geomorfología, Madrid.

Criado, C., Naranjo, A., 2011. Geomorfología y Paisaje en La Oliva. In: Lobo Cabrera, M. (Ed.), La Oliva Historia de un pueblo de Fuerteventura. Ayuntamiento de La Oliva, La Oliva, Spain, pp. 13–44.

Criado, C., Torres, J. M., Hansen, A., Lillo, P., Naranjo, A., 2012. Intercalaciones de polvo

sahariano en paleodunas bioclásticas de Fuerteventura (Islas Canarias). Cuaternario y Geomorfología 26, 73–88.

Criado, C., Yanes, A., Hernández, L., Alonso, I., 2011. Origen y formación de los depósitos eólicos en Canarias. In: Sanjaume, E., Gracia, F. J. (Eds.), Las dunas en España. Sociedad Española de Geomorfología, Zaragoza, Spain, pp. 447–465.

Damnati, B., Petit-Maire, N., Fontugne, M., Meco, J., Williamson, D., 1996. Quaternary paleoclimates in the Eastern Canary Islands. Quaternary International 31, 37–46.

Dan, J., 1990. The effect of dust deposition on the soils of the Land of Israel. Quaternary International 5, 107–113.

Dan, J., Yaalon, D. H., 1966. Trends of soil development with time in the mediterranean environment of Israel. In: Transactions of the International Conference on Mediterranean Soils, Madrid, Spain, pp. 139–145.

Dan, J., Yaalon, D. H., 1968. Formation and distribution of the soils and landscape in the Sharon. K'tavim 18, 69–94.

Edwards, N., Meco, J., 2000. Morphology and palaeoenvironment of brood cells of Quaternary ground-nesting solitary bees (Hymenoptera, Apidae) from Fuerteventura, Canary Islands, Spain. Proceedings of the Geologists' Association 111, 173–183.

Faust, D., Yurena, Y., Willkommen, T., Roettig, C., Richter, Dan., Richter, Dav., Suchodoletz, H. V., Zöller, L., 2015. A contribution to the understanding of late Pleistocene dune sand-paleosol-sequences in Fuerteventura (Canary Islands). Geomorphology 246, 290–304.

Fryberger, S. G., Krystinik, L. F., Schenk, C. J., 1990. Tidally flooded back barrier dunefield, Guerrero Negro area, Baja California, Mexico. Sedimentology 37, 23–43.

Fúster, J. M., Cendrero, A., Gastesi, P., Ibarrola, E., López Ruiz, J., 1968. Geology and Volcanology of Canary Islands, Fuerteventura. Instituto Lucas Mallada, Consejo Superior de Investigaciones Científicas, Madrid.

Huerta, P., Rodríguez-Berriguete, A., Martín-García, R., Martín- Pérez, A., La Iglesia Fernández, A., Alonso-Zarza, A. M., 2015. The role of climate and aeolian dust input in calcrete formation in volcanic islands (Lanzarote and Fuerteventura, Spain). Palaeogeography, Palaeoclimatology, Palaeoecology 417, 66–79.

Ibarrola, E., 1969. Variation trends in basaltic rocks of the Canary Islands. Bulletin of Volcanology 33, 729–777.

Inman, D. L., Ewing, G. C., Corliss, J. B., 1966. Coastal sand dunes of Guerro Negro, Baja California, Mexico. Bulletin of the Geological Society of America 77, 787–802.

Jahn, R., 1988. Böden Lanzarotes. PhD dissertation, University Stuttgart, Stuttgart-Hohenheim, Germany.

Jahn, R., 2010. Impact of aeolian sediments on pedogenesis – examples from the fringe area of the Saharan desert. 19th World Congress of Soil Science. In: Proceedings of the International Union of Soil Science, Wageningen. Brisbane, Australia.

James, N. P., Bone, Y., 2017. Quaternary aeolianites in south-east Australia – a conceptual linkage between marine source and terrestrial deposition. Sedimentology 64, 1005–1043.

Kruse, W., Meyer, B., 1970. Untersuchungen zum Prozeß der Rubefizierung (Entkalkungsrötung) mediterraner Böden am Beispiel kalkhaltiger marokkanischer Küsten - Dünen. Göttinger Bodenkundlichen Berichte 13, 77–140.

Laîné, A., Kageyama, M., Salas-Mélia, D., Voldoire, A., Rivière, G., Ramstein, G., Planton, S., Tyteca, S., Peterschmitt, J. Y., 2009. Northern hemisphere storm tracks during the last glacial maximum in the PMIP2 ocean-atmosphere coupled models: energetic study, seasonal cycle, precipitation. Climate Dynamics 32, 593–614.

López-García, P., Gelado-Caballero, M. D., Santana-Castellano, D., Suárez de Tangil, M., Collado-Sánchez, C., Hernández-Brito, J. J., 2013. A three-year time-series of dust deposition flux measurements in Gran Canaria, Spain: A comparison of wet and dry surface deposition samplers. Atmospheric Environment 79, 689–694.

Meco, J., Guillou, H., Carracedo, J-C., Lomoschitz, A., Ramos, A. J. G., Rodríguez-Yánez, J.J., 2002. The maximum warmings of the Pleistocene world climate recorded in the Canary Islands. Palaeogeography, Palaeoclimatology, Palaeoecology 185, 197–210.

Meco, J., Muhs, D. R., Fontugne, M., Ramos, A.J.G., Lomoschitz, A., Patterson, D., 2011. Late Pliocene and Quaternary Eurasian locust infestations in the Canary Archipelago. Lethaia 44, 440–454.

Menéndez, I., Cabrera, L., Sánchez-Pérez, I., Mangas, J., Alonso, I., 2009. Characterisation of two fluvio-lacustrine loessoid deposits on the island of Gran Canaria, Canary Islands. Quaternary International 196, 36–43.

Menéndez, I., Díaz-Hernández, J. L., Mangas, J., Alonso, I., Sánchez-Soto, P. J., 2007. Airborne dust accumulation and soil development in the north-east sector of Gran Canaria (Canary Islands, Spain). Journal of Arid Environments 71, 57–81.

Menéndez, I., Pérez-Chacón, E., Mangas, J., Tauler, E., Engelbrecht, J. P., Derbyshire, E, Cana, L., Alonso, I., 2013. Dust deposits on La Graciosa Island (Canary Islands, Spain): texture, mineralogy and a case study of recent dust plume transport. Catena 117, 133–144.

Meszner, S., Kreutzer, S., Fuchs, M., Faust, D., 2013. Late Pleistocene landscape dynamics in Saxony, Germany: paleoenvironmental reconstruction using loess-paleosol sequences. Quaternary International 296, 94–107.

Misota, C., Matsuhisa, Y., 1995. Isotopic evidence for the eolian origin of quartz and mica in soils developed on volcanic materials in the Canary Archipelago. Geoderma 66, 313–320.

Montealegre Contreras, L., 1976. Mineralogía de sedimentos y suelos de la depresión del Guadalquivir. PhD dissertation, Universidad de Granada, Granada, Spain.

Muhs, D. R., Budahn, J., Skipp, G., Prospero, J. M., Patterson, D., Bettis, E. A. III, 2010. Geochemical and mineralogical evidence for Sahara and Sahel dust additions to Quaternary soils on Lanzarote, eastern Canary Islands, Spain. Terra Nova 22, 399–410.

Müller, G., 1964. Frühdiagenetische allochthone Zementation mariner Küsten-Sande durch evaporitische Calcit-Ausscheidung im Gebiet der Kanarischen Inseln. Beitr. z. Mineralogie u. Petrographie 10, 125–131.

Müller, G., Tietz, G., 1975. Regressive diagenesis in Pleistocene eolianites from Fuerteventura, Canary Islands. Sedimentology 22, 485–496.

Muñoz, M., Sagredo, J., de Ignacio, C., Fernández-Suárez, J., Jeffries, T. E., 2005. New data (U-Pb, K-Ar) on the geochronology of the alkaline-carbonatitic association of Fuerteventura, Canary Islands, Spain. Lithos 85, 140–153.

Ortiz, J. E., Torres, T., Yanes, Y., Castillo, C., De La Nuez, J., Ibáñez, M., Alonso, M.R., 2005. Climatic cycles inferred from the aminostratigraphy and aminochronology of Quaternary dunes and palaeosols from the eastern islands of the Canary Archipelago. Journal of Quaternary Science 21, 287–306.

Pal, D. K., Srivastava, P., Bhattacharyya, T., 2003. Clay illuviation in calcareous soils of the semiarid part of the Indo-Gangetic Plains, India. Geoderma 115, 177–192.

Pomel, R. S., Miallier, D., Fain, J., Sanzelle, S., 1985. Datation d'un sol brun rouge calcifère par une coulée volcanique d'âge Würm ancien (51 000 ans) à Fuerteventura (Iles Canaries). Méditerranée, troisième série 56, 59–68.

Pye, K., Tsoar, H., 2009. Aeolian Sand and Sand Dunes. Springer- Verlag, Berlin.

Rando, J. C., Alcover, J. A., Navarro, J. F., García-Talavera, F., Hutterer, R., Michaux, J., 2008. Chronology and causes of the extinction of the Lava Mouse, Malpaisomys insularis (Rodentia: Muridae) from the Canary Islands. Quaternary Research 70, 141–148.

Roettig, C-B., Kolb, T., Wolf, D., Baumgart, P., Richter, C., Schleicher, A., Zöller, L., Faust, D., 2017. Complexity of aeolian dynamics (Canary Islands). Palaeogeography, Palaeoclimatology, Palaeoecology 472, 146–162.

Rognon, P., Coudé-Gaussen, G., 1996. Paleoclimates off northwest Africa (28°–35°N) about 18,000 yr B.P. based on continental eolian deposits. Quaternary Research 46, 118–126.

Rothe, P., 1966. Zum Alter des Vulkanismus auf den östlichen Kanaren. Societas Scientiarum Fennica, Communications in Mathematical and Physics 31, 1–80.

Rothe, P., 1996. Kanarische Inseln. Sammlung Geologische, Führer 81, Gebrueder Borntraeger, Stuttgart.

Ruiz, R. C., Torres Cabrera, J.M., 2011. Inventario de recursos vulcanológicos de Fuerteventura. Cabildo de Fuerteventura, Fuerteventura.

Sayles, R. W., 1931. Bermuda during the Ice Age. Proceeding of the American Academy of Arts and Sciences 66, 381–468.

Scheuvens, D., Schütz, L., Kandler, K., Ebert, M., Weinbruch, S., 2013. Bulk composition of northern African dust and its source sediments—a compilation. Earth-Science Reviews 116, 170–194.

Schlichting, E., Blume, H.-P., Stahr, K., 1995. Bodenkundliches Praktikum. Blackwell, Berlin.

Schofield, J. C., 1975. Sea level fluctuations cause periodic post-glacial progradation, South Kaipara barrier, North Island, New Zealand. New Zealand Journal of Geology and Geophysics 18, 295–316.

Schulte, P., Lehmkuhl, F., Steininger, F., Loibl, D., Lockot, G., Protze, J., Fischer, P., Stauch, G., 2016. Influence of HCl pretreatment and organo-mineral complexes on laser diffraction measurement of loess–paleosol-sequences. Catena 137, 392–405.

Singhvi, A. K., Deraniyagala, S. U., Sengupta, D., 1986. Thermoluminescence dating of Quaternary red sand beds: a case study of coastal dunes in Sri Lanka. Earth and Planetary Science Letters 80, 139–144.

Stoops, G., 2003. Guidelines for Analysis and Description of Soil and Regolith Thin Sections. Soil Science Society of America, Madison.

Troll, V., Carracedo, J.C., 2016. The Geology of the Canary Islands. Dunedin Academic Press, Edinburgh.

Von Suchodoletz, H., Glaser, B., Thrippleton, T., Broder, T., Zang, U., Eigenmann, R., Kopp, B., Reichert, M., Zöller, L., 2013. The influence of Saharan dust deposits on La Palma soil properties (Canary Islands, Spain). Catena 103, 44–52.

Von Suchodoletz, H., Kühn, P., Hambach, U., Dietze, M., Zöller, L., Faust, D., 2009. Loess-like and palaeosol sediments from Lanzarote (Canary Islands/Spain)—indicators of palaeoenvironmental change during the Late Quaternary. Palaeogeography, Palaeoclimatology, Palaeoecology 278, 71–87.

Von Suchodoletz, H., Oberhänsli, H., Hambach, U., Zöller, L., Fuchs, M., Faust, D., 2010. Soil moisture fluctuations recorded in Saharan dust deposits on Lanzarote (Canary Islands) over the last 180 ka. Quaternary Science Reviews 29, 2173–2184.

Ward, W. T., Little, I. P., Thompson, C. H., 1979. Stratigrapy of two sandrocks at Rainbow Beach, Queensland, Australia, and a note on humate composition. Palaeogeography, Palaeoclimatology, Palaeoecology 26, 305–316.

Warren, J. K., 1983. On pedogenic calcrete as it occurs in the vadose zone of Quaternary calcareous dunes in coastal South Australia. Journal of Sedimentary Petrology 53, 787–796.

White, B., Curran, H. A., 1988. Mesoscale physical sedimentary structures and trace fossils in Holocene carbonate eolianites from San Salvador Island, Bahamas. Sedimentary Geology 55, 163–184.

Williamson, C., Yaalon, D.H., 1977. An experimental investigation of reddening in dune sand. Geoderma 17, 181–191.

Yaalon, D. H., 1997. Soils in the Mediterranean region: what makes them different? Catena 28, 157–169.

Yanes, Y., García-Alix, A., Asta, M. P., Ibáñez, M., Alonso, M.R., Delgado, A., 2013. LatePleistocene–Holocene environmental conditions in Lanzarote (Canary Islands) inferred from calcitic and aragonitic land snail shells and bird bones. Palaeogeography, Palaeoclimatology, Palaeoecology 378, 91–102.

Yanes, Y., Yapp, C.J., Ibáñez, M., Alonso, M. R., de-la-Nuez, J., Quesada, M. L., Castillo, C., Delgado, A., 2011. Pleistocene– Holocene environmental change in the Canary Archipelago as inferred from the stable isotope composition of land snail shells. Quaternary Research 75, 658–669.

Zarei, M., 1989. Verwitterung und Mineralneubildung in Böden aus Vulkaniten auf

Lanzarote (Kanarische Inseln). Edition B. Schulz, Berlin.

Zu Leiningen, W. G., 1915. Über die Einflüsse von äolischer Zufuhr auf die Bodenbildung. (Mit besonderer Berücksichtigung der Roterde). Österreichische Geologische Gesellschaft, Vienna, Austria.

3.11 Supplementary material

3.11.1 Concerning 3.5.3. Determination of quartz contents

Subpopulations

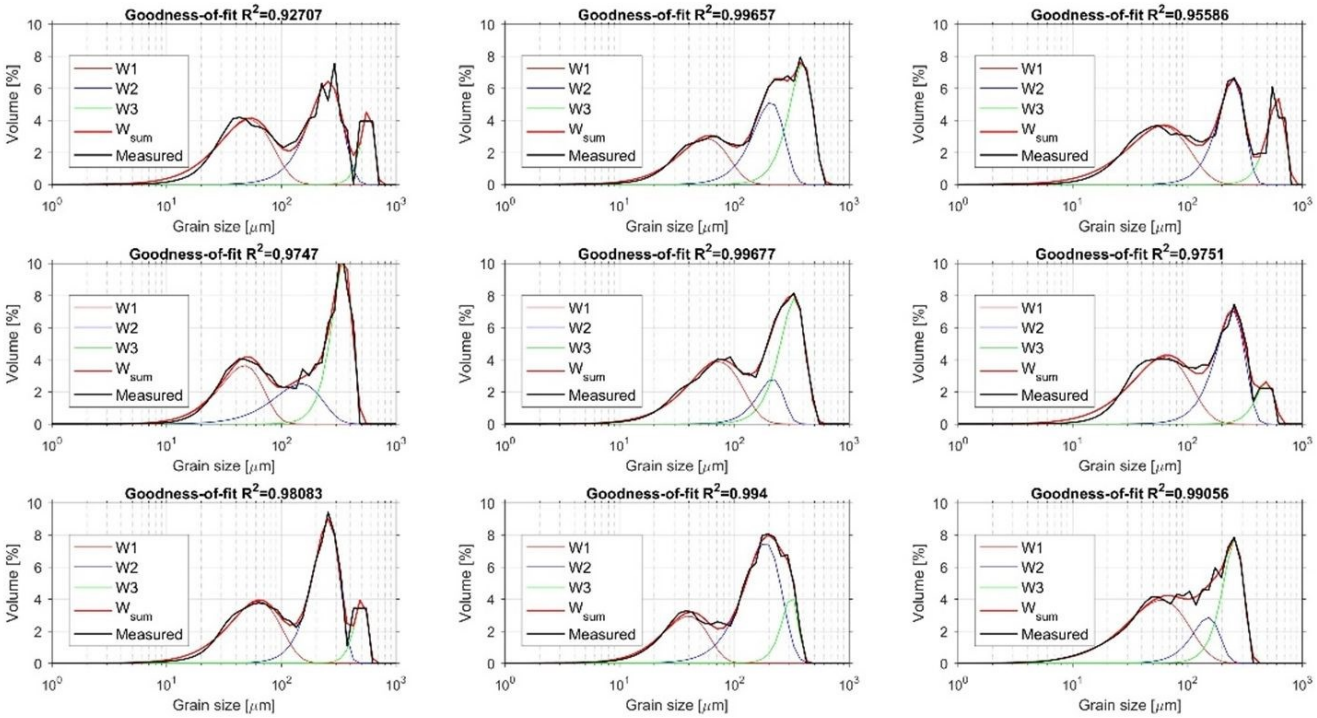

Fig. 3.12. Measured grain size distribution curves of samples and results of parametric curve-fitting decomposition. W1 subpopulations are regarded as the product of accumulation of far-travelled Saharan dust material.

The fine-grained subpopulation (decomposed by using parametric curve fitting as W1) of measured grain size distributions are regarded as Saharan dust. Previous studies dealing with grain size distributions of aeolian dust deposits reported similar particle size values of deposited Saharan dust material on Canary Islands (e.g. Menéndez et al., 2007, 2014; von Suchodoletz et al., 2013). The coarse silt-sized sedimentary material (with small proportion of fine sand) can be transported during dust storms several hundred kilometres from the source areas (Prins et al., 2007; Vandenberghe, 2013; Varga et al., in press). Varga et al. (2014) reported washout of coarse silt-sized Saharan dust material even further, from Central Europe.

Intensity

Mean grayscale intensity and standard deviation of particles were measured as the bottom light transmits through the particles. White light intensity of each pixel of particles is recorded on a scale from 0 to 255, where zero is the black, 255 is white. The automatically

recorded dimensionless values serve as a proxy of optical properties. Mean intensity values are dependent on chemical composition, mineralogy and particle thickness, while standard deviations of intensities are controlled by the heterogeneity of particle constitution and surface morphology.

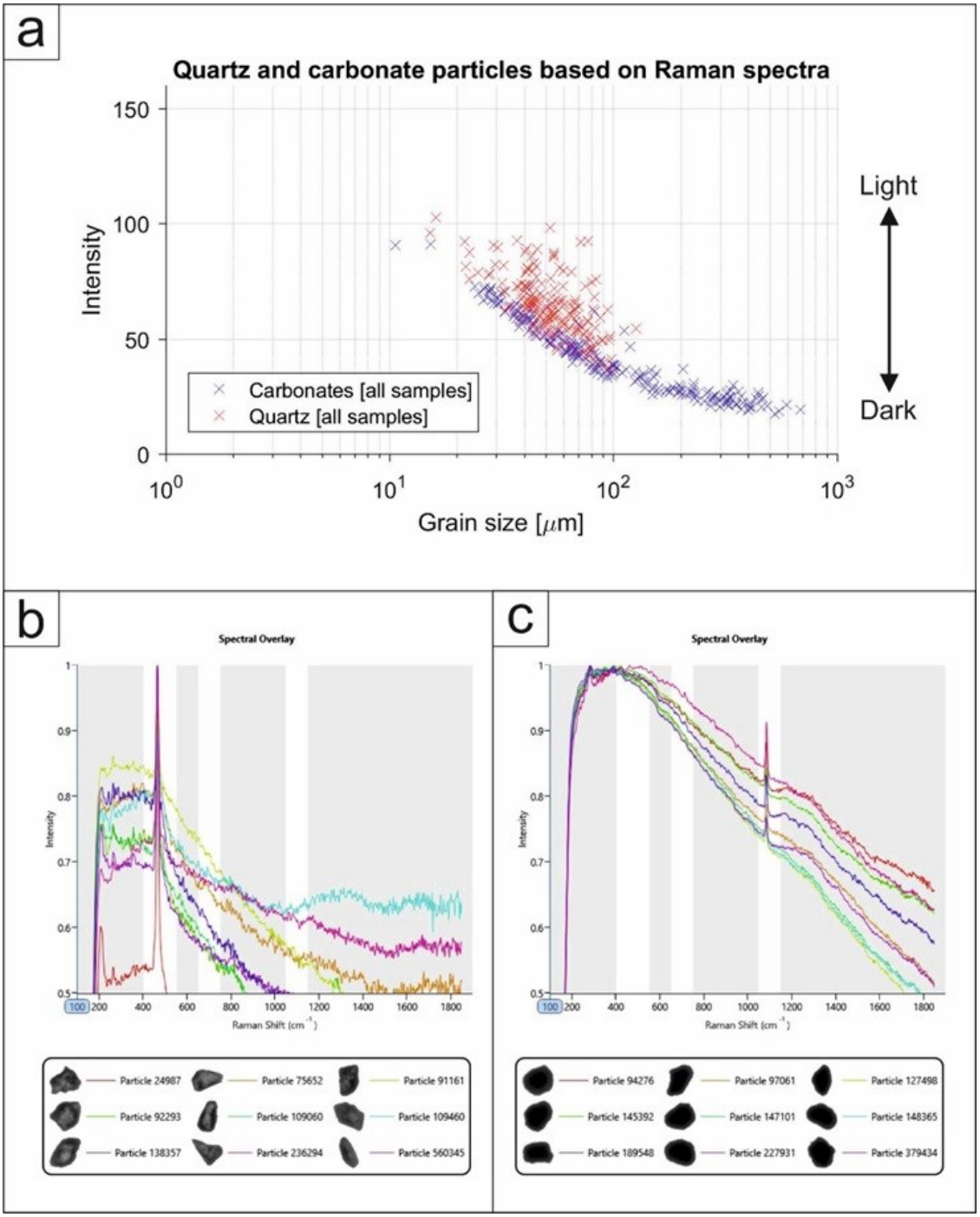

Fig. 3.13. Relationship among grain size, grayscale intensity and mineral composition of particles: (a) grains size vs. intensity scatter plot of quartz and carbonate particles; (b) Raman spectra and micrographs of typical silt-sized quartz particles; (c) Raman spectra and micrographs of typical silt- sized carbonate particles.

The comparison of acquired Raman spectra and mean grayscale intensities of particles indicated that there were two distinct group of mineral grains. In a given size-class the grayscale intensities of quartz grains were higher (meaning brighter, lighter) particles, while carbonates were darker with lower intensity values.

3.11.2 References

Menéndez, I., Díaz-Hernández, J. L., Mangas, J., Alonso, I., Sánchez-Soto, P. J., 2007. Airborne dust accumulation and soil development in the North-East sector of Gran Canaria (Canary Islands, Spain) Journal of Arid Environments 71, 57-81.

Menéndez, I., Pérez-Chacón, E., Mangas, J., Tauler, E., Engelbrecht, J. P., Derbyshire, E., Cana, L., Alonso, I., 2014. Dust deposits on La Graciosa Island (Canary Islands, Spain): Texture, mineralogy and a case study of recent dust plume transport. Catena 117, 133-144.

Prins, M. A., Vriend, M., Nugteren, G., Vandenberghe, J., Lu, H., Zheng, H., Weltje, G. J., 2007. Late Quaternary aeolian dust input variability on the Chinese Loess Plateau: inferences from unmixing of loess grain-size records. Quaternary Science Reviews 26, 230-242.

Von Suchodoletz, H., Glaser, B., Thrippleton, T., Broder, T., Zang, U., Eigenmann, R., Kopp, B., Reichert, M., Zöller, L.. 2013. The influence of Saharan dust deposits on La Palma soil properties (Canary Islands, Spain). Catena 103, 44-52.

Vandenberghe, J., 2013. Grain size of fine-grained windblown sediment: A powerful proxy for process identification. Earth-Science Reviews 121, 18-30.

Varga, Gy., Cserháti Cs., Kovács, J., Szeberényi, J., Bradák, B., 2014. Unusual Saharan dust events in the Central European Carpathian Basin in 2013 and early 2014. Weather 69, 309-313.

Varga, Gy., Újvári, G., Kovács, J. (in press). Interpretation of sedimentary (sub)populations extracted from grain size distributions of Central European loess-paleosol series. Quaternary International

4 A detailed chrono-stratigraphical record of Canarian dune archives - interplay of sand supply and volcanism

C-B. Roettig[a], T. Kolb[b], L. Zöller[b] & D. Faust[a]

[a]*Dresden University of Technology*
[b]*University of Bayreuth*

Publication history: submitted 04.03.2019

4.1 Abstract

Volcanic activity on Fuerteventura has often been the subject of research and debate, but the influence of volcanism on sediment pathways has never been discussed in detail. Biogenic carbonate sands originating from the shallow shelf migrate landwards, building up the archives of dune generations which are separated by palaeosurfaces. Recent investigation of the Montaña Roja dune field located on the eastern coast indicates a relationship between local volcanism and the supply of carbonate sands, because lava flows are able to cut off the dune fields from sand supply. Up to now, investigations have focused on the palaeo dunes of the western part of northern Fuerteventura, but there is still a lack of stratigraphic correlation across the island from the western to the eastern sections. This study aims to fill that gap by presenting an extended chrono-stratigraphical correlation spanning from the middle reaches of the Barranco de los Encantados to the dune field on the northern flanks of the Montaña Roja.

In terms of luminescence dating, the standardly used carbonate sands show only small amount of datable minerals, whereas the palaeosurface material contains increased amounts of quartz and feldspar reaching the island by dust transport. Hence, this material enabled a comparison between luminescence datings performed on dune layers and datings performed on palaeosurface material. The datings performed on palaeosurface material seem to reveal standardly underestimated IRSL ages. Generally, the results are suitable to extend the correlation of aeolianite palaeosurface sequences on northern Fuerteventura and suggest two older units. Findings in the field and IRSL dating indicate accumulation of unconsolidated aeolianites since before 450 ka. Concerning the whole northern tip of the

island, our findings suggest that sand pathways were cut off by degree. Three main periods can be differentiated: I. around 180-170 ka, II. around 135 ka and III. at latest around 50 ka. As the last period has so far not been described, further investigation is needed to validate or falsify the existence of that period. Finally, given that volcanism affects the relationship between sand supply and sea level changes, the palaeo dune sequences should be interpreted cautiously.

Keywords: palaeosol, Pleistocene, Fuerteventura, aeolianite

4.2 Introduction

The formation of aeolianite archives has been of scientific interest for several decades (Inman, et al., 1966; Kruse and Meyer, 1970; Ward et al., 1979, Gardner et al., 1983; Warren, 1983, El-Asmar, 1994). Besides local influences which make each of these systems individual, these worldwide distributed archives can store information about global pattern by their relationship to sea level changes (Schofield, 1975; Pye and Tsoar, 2009).

Over the last few decades several studies have investigated the palaeo dune fields on northern Fuerteventura (Coudé-Gaussen and Rognon, 1988; Edwards and Meco, 2000; Ortiz et al., 2006; Faust et al, 2015; Roettig et al., 2017; Struck et al., 2018). Their formation as coastal dunes paved the way for generations of unconsolidated carbonate aeolianites situated in the transition band between terrestrial and marine systems. Thereby the carbonate sands originate from the shallow shelf, which, in its extent, depends on sea level changes. Following the basic assumptions during falling sea level we have to expect periods of highest supply of carbonate sands, whereby rising sea level should be accompanied by reduced supply (Schofield, 1975; Roettig et al., 2019).

In addition to the aeolian dynamics, several local factors contribute to the complexity of these archives (Coudé-Gaussen and Rognon, 1988; Roettig et al., 2017). On the Canary Islands local volcanism plays an important role. Meco et al. (2002) described vast volcanic activity of the Late Pleistocene forming the chain of volcanoes situated on the northern tip of the island. The associated lava flow covered a wide area and shifted the northern coastline further northwards. Roettig et al. (2019) described a strongly reduced supply of carbonate sands for the dune fields of the Barranco de los Encantados (marked in red in Fig. 4.1-A) and the Barranco del Jable (marked in blue in Fig. 4.1-A) as a result of that volcanic period around 135 ka.

To the south of the Montaña Los Apartaderos (located close to the eastern coastline, see Fig. 4.1-A) a further palaeo dune field is situated on the northern flanks of the Montaña Roja. Criado et al. (2004) reported an age of 173 ka of the Montaña Los Apartaderos. On the one hand the palaeo dune field of Montaña Roja seems to yield best conditions to advance the investigations on the interlacing of sediment pathways and volcanism. On the other hand the dunes of Montaña Roja enable extension of the existing correlation of Northern Fuerteventura's dune palaeosurface sections by Roettig et al. (2017). So far, the stratigraphic correlation encompasses the two neighbouring catchments of the Barranco de los Encantados and the Barranco del Jable, both situated close to the eastern coastline. Solely the correlation of Ortiz et al. (2006) includes additional areas located on the Eastern Canary Islands. This correlation is based on amino acid racemization data and has often been a subject of debate (e.g. Meco et al., 2011, von Suchodoletz et al., 2012) as the datings by Ortiz et al. (2006) seem to underestimate the ages. The here presented extended correlation is the first one spanning sites from the east to sites close to the western coast of Fuerteventura. The correlation is based on sedimentologic investigations accompanied by IRSL datings. First attempts at dating palaeosurface material of dune generations on Fuertevenura revealed methodological challenges. As part of this study we aim to initiate a discussion about the mismatch of IRSL ages performed on pure carbonate sands and IRSL ages performed on palaeosurface material. Finally, the findings of the dune field on the northern flanks of Montaña Roja initiated the idea that the Late Pleistocene volcanism history of northern Fuerteventura derived from findings of the investigated dune sections.

4.3 Geographical setting and state of research

The palaeo dune fields of the Barranco de los Encantados and Barranco del Jable are already well known from studies by Coudé-Gaussen and Rognon (1988), Edwards and Meco (2000), Bouab and Lamothe (1997), Damnati et al. (1996), Yanes et al. (2004), Faust et al. (2015), and Roettig et al. (2017). Both catchments are deeply incised by gully systems providing a vast number of outcrops of dune palaeosurface sequences (Roettig et al., 2019). These sequences are mainly composed of carbonate sands, Saharan dust, and material of volcanic origin. Carbonate sands originate from the shallow shelf, consist of more than 95% $CaCO_3$ (dominated by calcite and aragonite), and are dominated by the middlesand fraction. Deposits of carbonate sands supposedly come from the north (Criado et al., 2004; Roettig et al., 2019). The admixed Saharan dust is dominated by silt fraction but also

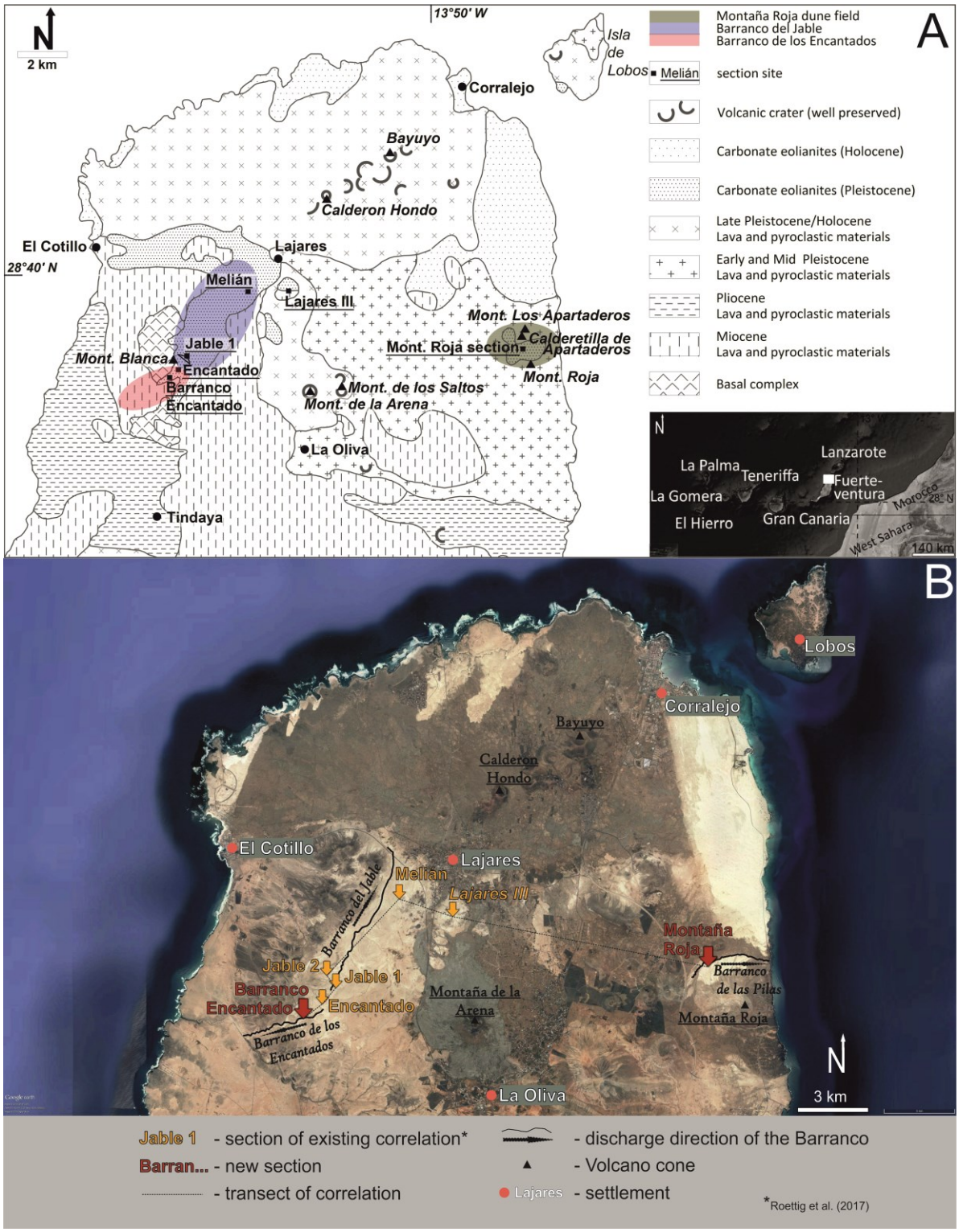

Fig. 4.1. A) Main geological units according to Rothe (1996), modified. B) Satellite image of northern Fuerteventura, based on Google earth (modified).

contains grain sizes of up to more than 125 µm (Menendez et al., 2013). The allochthonous origin is indicated by the content of quartz (Coudé-Gausson et al., 1987; Coudé-Gausson and Rognon, 1988; Herrmann et al., 1996; Varga and Roettig, 2018), because on the Eastern Canary Islands only the Basal Complex bear very small amounts of quartz. Thus,

evidently, silt sized quartz and even feldspar is of aeolian origin (Jahn, 1988; Misota and Matsuhisa, 1995). A third ingredient of the dune archives is the material of volcanic origin, which is admixed as tephra material, Lapilli, or basaltic rock fragments. Generally, the island of Fuerteventura was formed by different periods of volcanic activity (Fig. 4.1-A). The beginning of the formation is still under debate. For example, Muñoz et al. (2005)

discuss an Oligocene age, whereas Balogh et al. (1999) and Le Bas et al. (1986) postulate Cretaceous to Palaeogene ages of the so-called Basal Complex. Remnants of a huge volcano of Miocene age are situated in the northern part of the island, close to the western coastline. Also, during the Pleistocene age several periods of volcanic activity formed the relief of the island. Famous representatives of the Early to Middle Pleistocene are the Montaña de Blancas and the Montaña Roja (the latter one dated 1.7 Ma, reported by Criado et al., 2004). The whole northern tip is dominated by Late Pleistocene lava flows of the chain of volcanoes, including the Calderon Hondo and the Bayuyo, dated 134 ka (Meco et al., 2002) and 135 ka (reported by Casilla Ruíz and Torres Cabrera et al., 2012). Regarding the Montaña de la Arena located in the north of the village of La Oliva, Edwards and Meco (2000) reported an age of 185 ka, possibly related to the first eruption of the Arena, whereas the latest eruption is much younger, as Rando et al. (2008) concluded an eruption of Holocene age (younger than 2 ka).

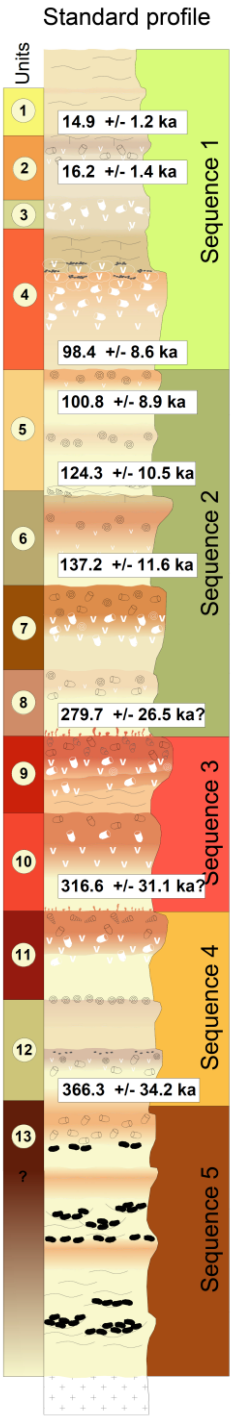

Fig. 4.2. Standard profile of dune palaeosurface sequences according to Roettig et al. (2017).

A first attempt to correlate dune sequences of Faust et al. (2015) was extended to sections further south by Roettig et al. (2017) (Fig. 4.1). The correlation of dune palaeosurface sequences by Roettig et al. (2017) spans the area from the upper reaches of the Barranco de los Encantados (Encantado section) to the Barranco del Jable (Jable 1 and 2 and Melián section) to the section of Lajares III, which is situated to the southeast of the village of Lajares (Fig. 4.1). Thus, Roettig et al. (2017) established a standard profile of 5 sequences encompassing 13 units (Fig. 4.2). These sequences and units differ in the intensities of sand accumulation, the occurrence of features of humidity, and indications of volcanic imprint. One of the most prominent units is Unit 9, being a widely distributed well preserved stratigraphic unit dividing most of the dune palaeosurface sections into two main parts. The part below Unit 9 tends to indicate drier conditions and shows locally very huge sand accumulations bearing only one

stratigraphic position of clear imprint of tephra material (Fig. 4.2, Unit 12). The part above Unit 9 features several periods of volcanic imprint. Furthermore, the characteristics indicate changes in moisture conditions accompanied by decreasing accumulation of carbonate sands in the uppermost parts.

Although the middle reaches of the Barranco de los Encantados are strongly incised and wider parts are eroded, several remnants containing important features are preserved. These are mainly located on the southern and southeastern slopes of the Barranco de los Encantados. The sampled section is situated on the northwestern flank of *Morro Encantado* (Fig. 4.1).

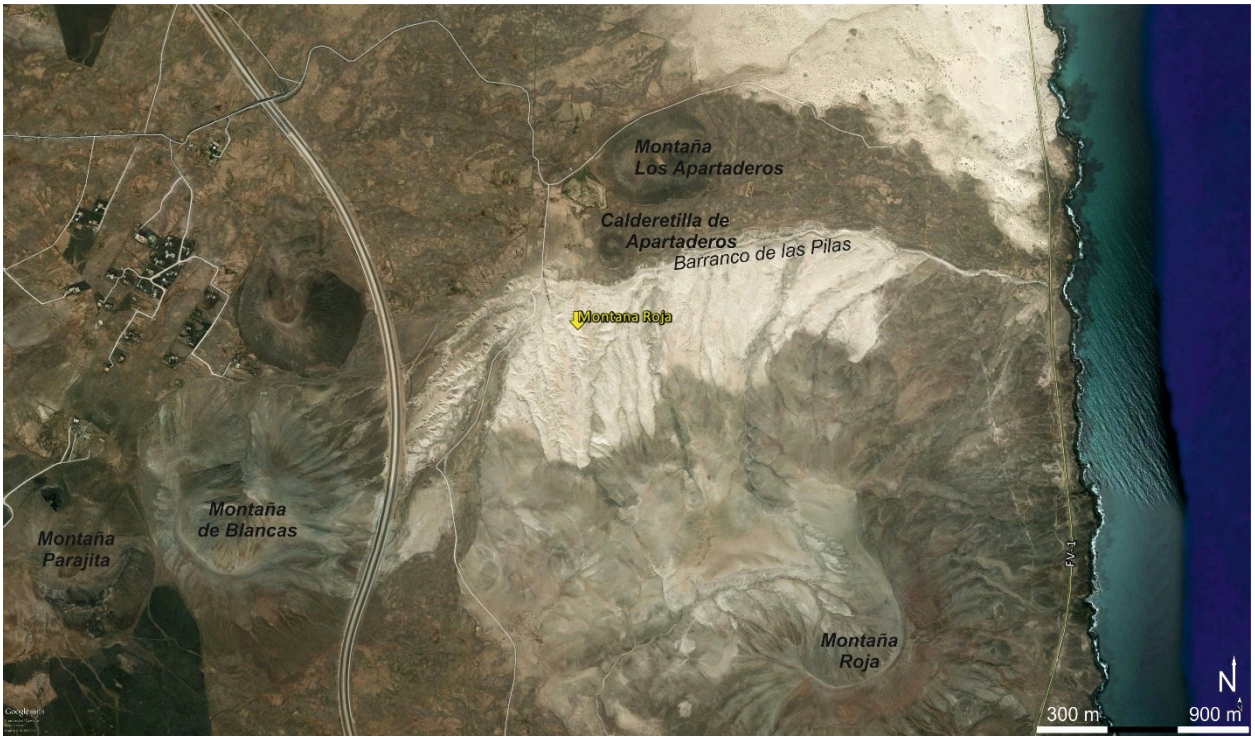

Fig. 4.3. Satellite image of the palaeo dune field on the northern flank of Montaña Roja (sampled Montaña Roja section is marked with a yellow arrow). Based on Google earth (modified).

The easternmost section (Montaña Roja section) is part of the palaeo dune field on the northern flank of Montaña Roja, which is bordered to the north by the Barranco de las Pilas and the lava flows of the Montaña de los Apartaderos and the Calderetilla de Apartaderos. The Montaña Los Apartaderos is dated 173 ka (Criado et al., 2004). The intersection of the mentioned lava flows to the Barranco de las Pilas is characterised by a steep inclination with a height offset of about 20 m. The Barranco de las Pilas is widely incised. The inclination of the depression lines of the gully systems eroding the palaeo dune field is in line with the inclination of the northern slopes of the Montaña Roja. The closer to Montaña

Roja, the steeper the inclination and the thinner the palaeo dune layers. Here the gullies are less incised, respectively. The sampled section "Montaña Roja" is located in the area with best preserved conditions, where the sequence is most complete.

4.4 Methods

4.4.1 Fieldwork

After a thorough investigation of the study area we selected one location in the Montaña Roja dune field for sediment sampling and Luminescence sampling and another location for Luminescence dating in the middle reaches of the Barranco de los Encantados. In the field both profiles were examined for features of sediment composition, soil forming processes, and trace fossils.

4.4.2 Grain size distribution

We suspended the air-dried samples with sodium pyrophosphate for 24 hours. Neither calcium carbonate nor organic material was removed. Each sample was measured consecutively 5 times. The plotted values correspond to the medians of measured values of 80 grains size classes between 0.058 and 2500 µm. The grain size distributions were performed at GFZ Potsdam using the Horiba LA-950 laser diffraction particle sizer.
The grain size plots were created with the software R. Grain size distributions were plotted as a heatmap (Schulte, 2016). Colours represent the percentage of each class. The attribution of colour is logarithmic for three single matrices (see bottom of the grain size figure of Fig. 4.4). The first matrix represents the clay fraction, ranging from 0.058 to 1.981 µm. The second matrix represents the silt fraction, ranging from 1.981 to 58.953 µm. The third matrix encompasses the grain sizes from 58.953 to 2500 µm, representing the sand fraction. To provide the sum of clay, silt, and sand fractions samplewise, we present the cumulated percentages of the three matrices (per sample) at the top of the grain size figures (Fig. 4.4). .

4.4.3 Elemental composition and $CaCO_3$ content

The measurements of elemental composition were performed in the Geographic Laboratory of the TU Dresden. After pressure digestion with concentrated nitric and hydrofluoric acid, the samples were measured for total elemental composition by atomic adsorption spectrometry. To measure the pedogenic iron content the samples were

extracted by dithionite (Schlichting et al., 1995). The content of $CaCO_3$ was determined using a Scheibler apparatus by treating the samples with hydrochloric acid (Schlichting, 1995).

4.4.4 Colours

Colours were determined using the Munsell scale (Munsell Color, 1975). The colours were identified in dry and wet conditions of each sample. The colour of wet conditions is used for all descriptions in the text.

4.4.5 Profile Figures

The profile figures were created through AutoCAD Civil software. The bar plots of elemental composition and the heatmap image of grain size distributions were created using the software R and transferred to AutoCAD Civil 2017.

4.4.6 Luminescence dating

For this study, a total of 42 luminescence samples from the polymineral fine grain (4-11 µm) fraction were considered to determine regional chronology in our research area. All samples were taken at night using opaque plastic bags. They were prepared under subdued red light conditions (640 +/- 20 nm) following standard procedures (e.g., Fuchs et al., 2010). After wet sieving to various grain size fractions, (< 38 µm, 38-63 µm, 63-90 µm, 90-200 µm) carbonates and organic material were removed by applying hydrochloric acid (10%) and hydrogen peroxide (10%), respectively. For the fine grained material < 38 µm, the pH-value was constantly monitored during the procedure to avoid coagulation of clay sized particles in the low pH-region of < 3. After this chemical treatment, the polymineral fine grain fraction (4-11 µm) was separated by settling the remaining material from the < 38 µm fraction in Atterberg cylinders and applying specific settling times according to Stoke's law.

All luminescence measurements were carried out in the luminescence laboratory of the University of Bayreuth using automated Risø-Reader TL/OSL-DA-15 systems, equipped with built-in $^{90}Y/^{90}Sr$ β-sources for artificial irradiation and infrared light LEDs (875+/- 80 nm) for stimulation. The luminescence signal was detected using a Thorn-EMI 9235 photomultiplier, combined with a 3-mm Chroma Technology D410/30x interference filter, restricting the detection window to the blue-violet wavelength band.

Following the advice of Huot & Lamothe (2003), Preusser (2003), and Rother et al. (2010), we applied a modified single aliquot regenerative-dose (SAR) protocol that has already been described in detail by Faust et al. (2015) and Roettig et al. (2017). The aim of applying such a modified protocol was to minimise the effects of anomalous fading in feldspars and to avoid severe age underestimations. For equivalent dose determination, the first 5 seconds of the measured IRSL signals were used after subtracting a background which was derived from the last 20 seconds. Only aliquots with a recycling ratio of 0.9 - 1.1, a recuperation of ≤ 5% of the natural sensitivity corrected signal intensity (Murray and Wintle, 2000), and a signal not lower than 3 times the background were accepted for equivalent dose calculation. All data analysis was done by using an R-script based on various analysis functions provided by the R package 'Luminescence' (e.g., Kreutzer et al. 2012, 2016).

After determining the U- and Th-concentrations by thick source alpha-counting and the K-contents by ICP-OES, sample specific dose rates were calculated by applying the conversion factors given by Guerin et al. (2011). Cosmic dose rates were considered following Prescott & Hutton (1994). Derived from present-day water contents and considering sedimentological properties and the specific geographical settings of the various sampling locations, interstitial water contents of either 10 +/- 5% or 5 +/- 3% were assumed to be representative for the burial period (except for samples BT 1517, BT 1570, and BT 1571 for which 15 +/- 5% were used due to a significantly higher amount of clay and silt sized particles). Since all measured samples were non-etched fine grain samples, alpha efficiency correction has to be taken into account. Therefore, a common regional specific a-value of 0.1 +/- 0.02 was used for dose rate determination. This value was calculated as average derived from a-value measurements which had been done for various samples originating from different locations of the study area.

For this study, ages derived from 22 new samples were compiled with data already published in previous publications (e.g., Faust et al. 2015, Roettig et al. 2017). With respect to these later samples, we would like to point out that there are some slight differences concerning the presented ages of the study in hand. These differences are due to the consideration of additional measurements that were not yet available at the time when the ages were originally published. However, we would also like to stress that these differences in age assessment are not significant, nor do they affect the interpretation of results given in the cited studies. For example, Roettig et al. 2017 reported IRSL ages of 121.3 +/- 10.4 ka and 171.2 +/- 15.4 ka for the uppermost samples originating from the Jable 2 section.

IRSL ages for these samples were recalculated for the study in hand and now reveal values of 124.5 +/- 10.7 ka and 173.2 +/- 16.1 ka respectively and are thus within errors identical to the already published ages

4.5 Results

4.5.1 Montaña Roja section

The Montaña Roja sequence encompasses 13 sediment layers (SL). The lowermost part of the section starts with SL 13 – SL 11, which are characterised by a strong admixture of rock fragments from the Montaña Roja (Fig. 4.4). These red to purple rocks (hence the name "Montaña Roja") are widely distributed in SL 12, whereas in SL 13 and especially in SL 11 these rock fragments are concentrated close to the palaeosurface of the layers. Generally, these three lowermost layers are dominated by features of water-induced relocation that can be considered as slope deposits. The top positions of SL 13 and 12 present truncated palaeosurfaces, respectively. Only SL 11 shows an in situ palaeosurface indicated by trace fossils on the very top. The $CaCO_3$ contents of SL 13 - 11 are more or less the same (>80 %), bearing just a slight decrease in SL 11. Interestingly, SL 11 features the highest Mg content of the whole section, maybe caused by volcanic imprint from Montaña Roja, providing a high content of Mg.

SL 10 shows the palaeosurface with the most intense colour (7.5 YR 5/6 - strong brown) and features the hightest Fe_t- and Fe_d-value (18.71 g/kg of Fe_t and 5.74 g/kg of Fe_d) in combination with one of the lowest $CaCO_3$ contents (56.4%). SL 9 presents one of the lowest sand contents and few traits of water-induced relocation. Besides the dominance of relocation features, SL 8 is strongly influenced by tephra material. This layer shows a block-like structure and is well exposed due to its higher morphologic resistance. SL 7 is characterised by nearly pure carbonate sands as parent material, showing more than 95 % sand, more than 80 % $CaCO_3$, and 1886 mg/kg of Sr. On top of SL 6 a stronger influence of volcanic material is recognisable, underlined by the highest Zn content, with 49 mg/kg (sample 25) of the entire section. SL 5 shows relocation features containing broken pieces of *Cochlicella sp.* (compare Yanes et al., 2004). Above this, SL 4 is the only layer consisting of pure carbonate sands without any fine material, whereas the palaeosurface on top of SL 4 features the imprint of dust and indicates in situ features including trace fossils. SL 3 again shows features of erosion by water and some individual Pomatias lanzarotensis were found on top of that layer. Besides slight features of water-induced

relocation, SL 2 shows patchy enrichments of gypsum. SL 1 indicates recalcification and water-induced relocation with a $CaCO_3$ crust formed by overflow. A silty layer covers the $CaCO_3$ crust.

There are two conspicuous features at the section of Montaña Roja. Firstly, the whole section is characterised by a vast number of brood cells but they are difficult to detect because they are not calcified. In general, the de- and recalcification features are very weak, except on the very top of the section showing a $CaCO_3$ crust also including calcified brood cells (compare Edwards and Meco, 2000; Roettig et al., 2017).

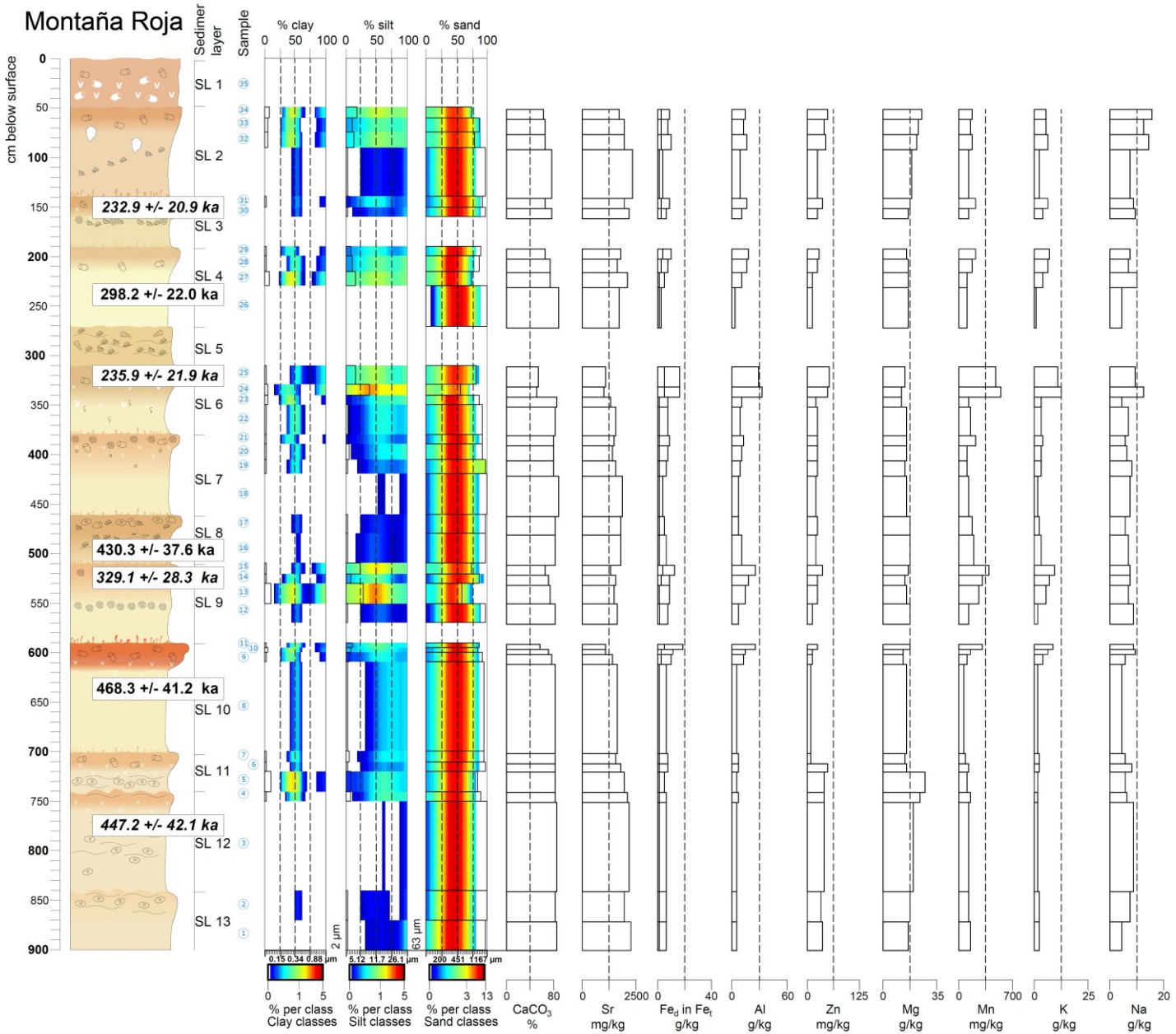

Fig. 4.4. Montaña Roja section – italicised IRSL ages are datings performed on palaeosurface material

Secondly, the entire section is interspersed by rhizoconcretions made of gypsum. With varying intensities in gypsum concentration/enrichment the rhizoconcretion occurs more or less ubiquitously. They reach lengths of several metres, whereby characteristically their top end is always linked to a palaeosurface layer.

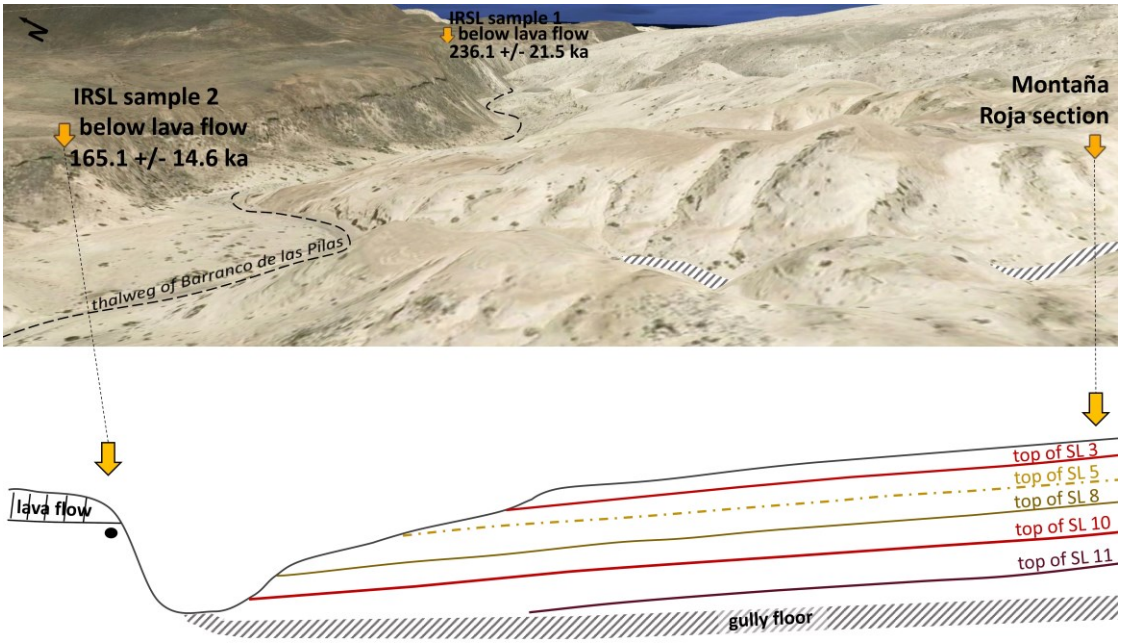

Fig. 4.5. North-south transect of the main layers on the northern flanks of Montaña Roja, including the location of luminescence sampling below the lava flow of the Montaña Los Apartaderos and the neighbouring Calderetilla. The lava flow itself was K-Ar dated 173 ka, reported by Criado et al. (2004).

Figure 4.5 shows an oblique view from the east, presenting the dune palaeosurface layering on the northern flanks of Montaña Roja. The main sediment layers are well exposed over long distances because of subsequent erosion processes and gully formation. Below the lava flow of the Montaña Los Apartaderos and the Calderetilla de Apartaderos (for location also compare Fig. 4.3) we dated the sediments to 236.1 +/- 21.5 ka (Fig. 4.5, IRSL sample 1 below lava flow) and to 165.1 +/- 14.6 ka (Fig. 4.5, IRSL sample 2 below lava flow). These datings are in good agreement with the K-Ar dated age of 173 ka (Criado et al., 2004).

Barranco Encantado section

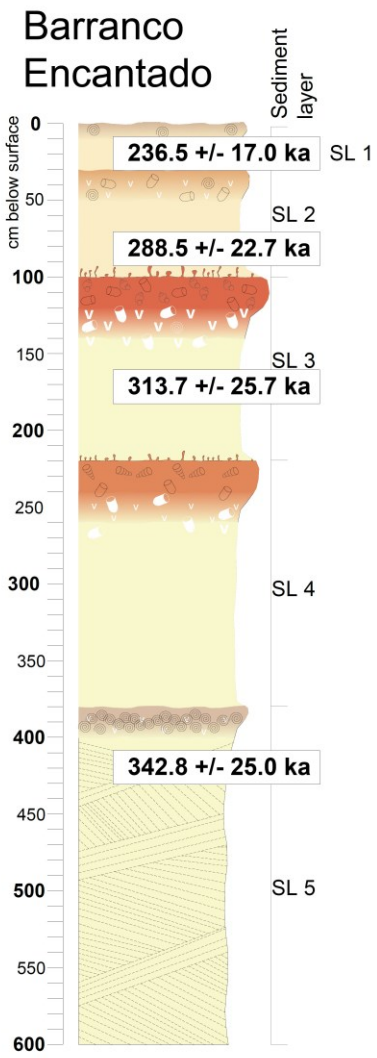

Fig. 4.6. Barranco Encantado section (see Fig. 4.4 for key)

The Barranco Encantado section within the westernmost part of the palaeo dune fields on Northern Fuerteventura serves to complete the stratigraphic correlation. The lowermost part of this section (Fig.4.6, SL 5) shows middle to coarse carbonate sand of very pale brown (10 YR 8/4) colour and cross bedding features. In some areas this sediment layer is up to 6 metres thick. At some places close to the section these sands are abraded by wind and consequently are bizarrely shaped. SL 5 capped off with a greyish palaeosurface and some admixed mafic minerals accompanied by an abundance of molluscs (predominantly *Theba sp.*). SL 4 consists of nearly pure carbonate sands topped by a reddish yellow (7.5 YR 6/6) coloured palaeosurface with weak re- and decalcification features like calcified brood cells. One characteristic feature is the remarkable occurrence of individual *Cochlicella sp.* The border with the overlying carbonate sands indicates an in situ preservation by trace fossils. The carbonate sands of SL 3 show on the top the strongest re- and decalcification features of the entire section. The respective palaeosurface stands out by being the one with the most intense colour (YR 7.5 5/6). The very top of the palaeosurface is interspersed by individual *Pomatias lanzarotensis*, the border with the overlying sediments is characterised by trace fossils. SL 2 and SL 1 feature some admixed mafic minerals and even the related palaeosurfaces are influenced by volcanic imprint. The palaeosurface of SL 2 shows very weak de- and recalcification features, whereas the palaeosurface of SL 1 is free of such characteristics, just showing some molluscs but additionally being dominated by the imprint of volcanic material.

4.6 Discussion

4.6.1 IRSL ages performed on palaeosurface material

Overall, the determined luminescence ages for the major part of the analysed samples are in stratigraphic order and support a reasonable interpretation of the examined sediment sequences and also a suitable correlation of exposures. However, for some samples the calculated IRSL ages indicate apparent age inversions (compare Fig. 4.7). Specifically this is the case for some samples originating from palaeosurface material of the Montaña Roja section, the Encantado section, and the Jable 1 section. Therefore, in Figure 4.7 ages for palaeosurface-related samples are indicated by star symbols. We assume that all samples taken from palaeosurface material have been exposed for prolonged periods. Compared with the sandy layers building up the rest of the profiles, palaeosurface sediments reveal significantly higher amounts of clay and silt-sized particles. It is known that thorium and potassium can easily be adsorbed by such fine grain particles (e.g., Kemski et al., 1996) and stored in the respective soils or sediment layers. Thus, we assume a more or less continuous accumulation of thorium and potassium during the burial period for those sediment layers in our research area that reveal increased proportions of clay and silt-sized particles. As a result, the radionuclide concentrations determined for the samples originating from the palaeosurface layers may not be representative of the entire burial period. The present day concentrations of radionuclides have to be interpreted as the final point of a long lasting accumulation process. Therefore, the determined dose rates for these samples might be strongly overestimated, resulting in a severe underestimation of the calculated luminescence ages. Since the processes responsible for accumulation and re-mobilisation of radionuclides are complex and depend on various environmental conditions, there is no easy way to assess appropriate values of the dose rates representative of the whole period of interest. Thus, we conclude that ages derived from the palaeosurface samples should be treated cautiously and can only be interpreted as minimum age estimates, significantly underestimating the true deposition ages of the respective sediment packages. Finally, we argue that these ages do not represent reliable age estimations and should not be considered for palaeoenvironmental interpretation.

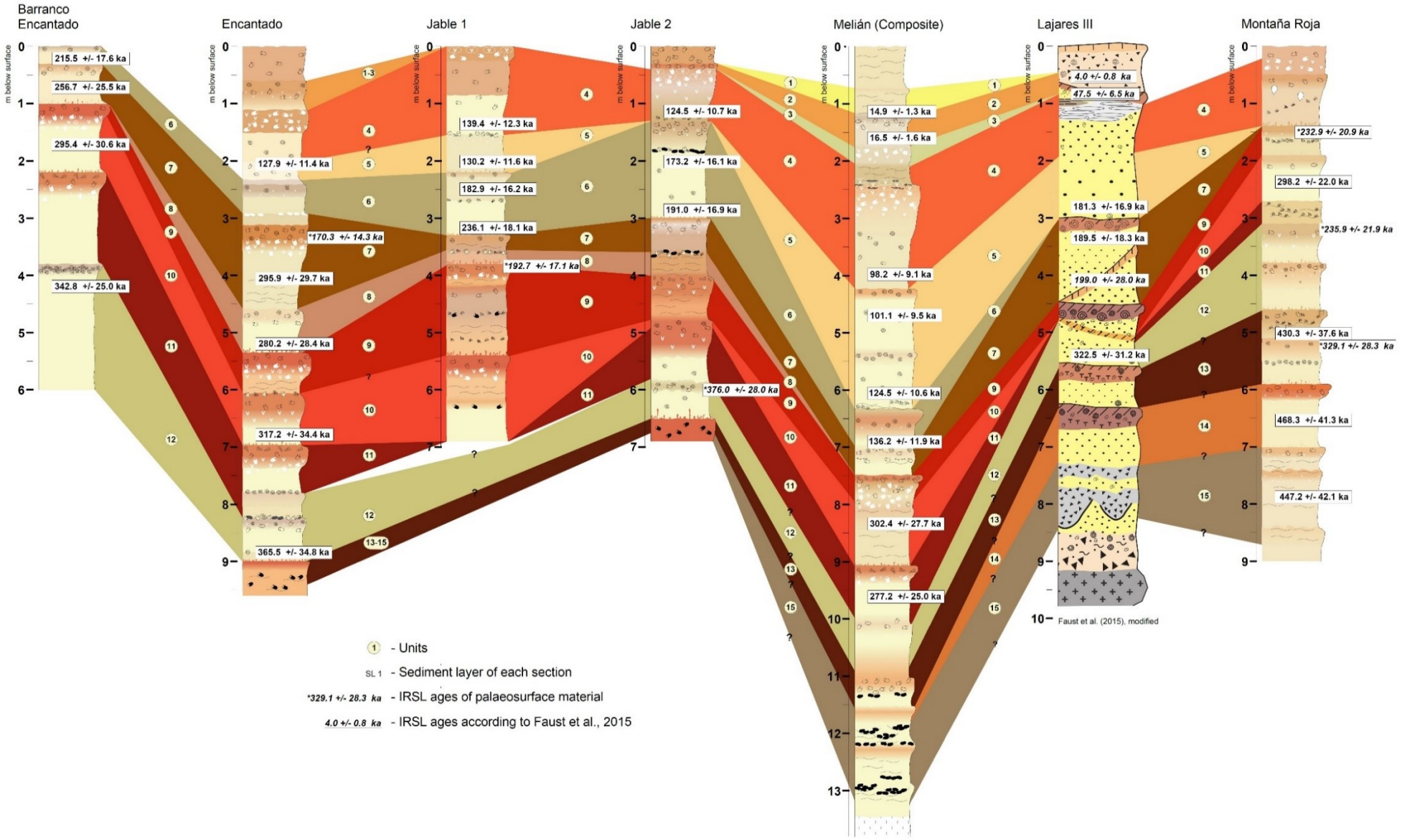

Fig. 4.7. Extended correlation of dune palaeosurface sequences on northern Fuerteventura (according to Roettig et al., 2017, modified). See Fig. 4.4 for key.

4.6.2 Extending the stratigraphic correlation

The Barranco Encantado section features in its lowermost part huge accumulations of carbonate sands dated 342.8 +/- 25.0 ka with a corresponding palaeosurface being characterised by slight volcanic imprint correlating with Unit 12 (Fig. 4.7). In the part above, just slight de- and recalcification features correspond to Unit 11 with the occurrence of *Cochlicella sp.* Unit 9 at the Barranco Encantado section is of strong brown colour (7.5 YR 5/6) combined with strong de- and recalcification features. The occurrence of *Pomatias lanazarotensis is* also *a* characteristic feature of that unit (Roettig et al., 2017). The correlation is underpinned by the IRSL age 295.4 +/- 30.6 ka. As above for Unit 9 we assume that strongly reduced sediment supply is responsible for just thin deposits of carbonate sands. This is followed by a period when sand supply was cut off at the very top.

The Montaña Roja section provides a much deeper insight into the periods older than Unit 9 (Fig. 4.7). Thus, it mainly encompasses Units 9 – 13 of the existing correlation (Roettig et al., 2017). Additionally, the section supports the designation of two further units older than Unit 13. Therefore we added Units 14 and 15 (Fig. 4.7) to the existing correlation.
Unit 15 shows strong features of water-induced relocation. At Montaña Roja, Unit 15 presents rock fragments originating from Montaña Roja itself. These deep red to purple coloured rock fragments are incorporated into slope deposits, which were transported by sheet flow or in small fluvial channel beds. These traits are also detectable in the lowermost parts of Lajares III and in the Melián section (Faust et al., 2015). At these locations the stratigraphic sequences contain numerous black basaltic rock fragments being transported and concentrated in small channel beds.
Above Unit 15 the carbonate sands of Unit 14 revealed an age of 468.3 +/- 41.3 ka. Besides IRSL dating we have to mention that the strong brown (7.5 YR 4/6) coloured palaeosurface of Unit 14 from Montaña Roja could also correlate with the palaeosurface on top of Unit 13 at the Melián section. A correlation along these lines would mean a tremendous hiatus above Unit 13 at Lajares III section. The lack of available data for the lowermost parts of the sections of Melián and Lajares III complicates the correlation. Therefore at these positions we added question marks to the correlation figure, respectively. With regard to the Encantado and Melián sections, Unit 12 of the Montaña Roja section clearly shows strong imprint of tephra material besides just slight de- and recalcification features. As

discussed before, IRSL dating of 235.9 +/- 21.9 ka seems to underestimate the age of the palaeosurface (Unit 9).

At the Montaña Roja section Unit 11 shows evidence of strong relocation. The correlation of Unit 11 is supported by the occurrence of some individual *Cochlicella sp.* that is restricted to a specific and relatively narrow time frame, in which *Cochlicella sp*. occurred. At the Montaña Roja section the IRSL age of 298.2 +/- 22.0 ka of Unit 10 dates the latest accumulation of pure carbonate sands originating directly from the shallow shelf. Unit 9 shows strongest gypsum rhizoconcretion comparable to those we noted in the same stratigraphic position in the surrounding Encantado section. On top of the Montaña Roja section the characteristic gypsum patches above indicate the relation to Unit 4. Hence, we also correlated these sediments to Unit 4. Moreover, the area-wide distributed crust of calcium carbonate on top of the Montaña Roja section correlates with Unit 4. Thus, we cannot differentiate Units 8 – 5 at the Montaña Roja section.

Generally, the Montaña Roja section also shows strongly reduced or even ceased sediment supply above Unit 9. Solely thin deposits of reworked material were accumulated. The reduction in sand supply ocurred with the eruptions of the Montaña Los Apartaderos and the Calderetilla de Apartaderos, suggesting a cut-off from the sediment pathway by the lava outflows. The close range of the uppermost IRSL age of 232.9 +/- 20.9 ka of the Montaña Roja section and the 173 ka dated lava flow by Criado et al. (2004) underlined by the here presented IRSL ages of 236.1 +/- 21.5 ka and 165.1 +/- 14.6 ka from below the lava flow support the cut-off scenario. Similarly, these findings underline the assumption of sand supply coming from the north.

The aforementioned ubiquitous appearance of gypsum rhizoconcretions at the Montaña Roja section accompanied by nearly absent $CaCO_3$ crystallisation cause a higher impact of sea spray in comparison to the other sections in palaeo dune fields of northern Fuerteventura. Therefore the site-specific ubiquitous appearance of gypsum rhizoconcretions supports a consistent positioning close to the coast and supports the assumption of a prevailing northern wind direction for the last ~500 ka, presumably resulting in constant sea spray supply for longer periods.

4.6.3 Interplay of sand supply and volcanic activity on a larger scale - Different periods of volcanism cutting off the sand pathway gradually

As many studies revealed the dependency of the supply of carbonate sands and sea level changes, there is a certain availability of sediments building up coastal dune systems during all periods. Nevertheless, in turn, there are certain periods of maxima and minima in sediment supply. For the Canary Islands we have to assume highest sand availability during starting regression after sea level highstands and lowest supply during rising sea level (Roettig et al., 2019). The study area shows a site-specific deposition pattern of carbonate sands, allowing the assumption that sites were cut off from sand supply for distinct periods. Thus, we assume the relationship between carbonate sand supply and sea level changes was cut off gradually too. The different site-specific accumulation patterns correlate with incipient volcanic activity above Unit 9 of the stratigraphic correlation. Hence, the relationship between carbonate sand supply and changing sea level seems to be generally interrupted by the local volcanism of the island (compare Roettig et al., 2019). The findings of the Montaña Roja dune field support this assumption. The stratigraphic results combined with the IRSL ages (compare Fig. 4.5) indicate that by the eruption of Montaña Los Apartaderos and Calderetilla de Apartaderos the dune field on the northern flanks of Montaña Roja was cut off from carbonate sand pathways reaching the island from the north. At the same time the lava flow initiated the formation of a depression line against the slope of Montaña Roja, forming the Barranco de las Pilas. A more detailed description about the assumed formation stages of the Montaña Roja dune field and its drainage system is given in the supplementary material.

In the following we discuss a succession of three main periods of volcanism and the effect on the supply of carbonate sands. We assign the three main periods of Late Pleistocene volcanic activity as follows:

a) around 180 – 170 ka

b) around 135 ka

c) around 80 – 50 ka

By linking these volcanic periods to the dune palaeosurfaces of northern Fuerteventura, including the sections of the present study and the palaeo dune fields of Barranco del Jable and Barranco de los Encantados studied by Faust et al. (2015) and Roettig et al. (2017), a distinct pattern of carbonate sand deposits becomes visible (shown in Fig. 4.8).

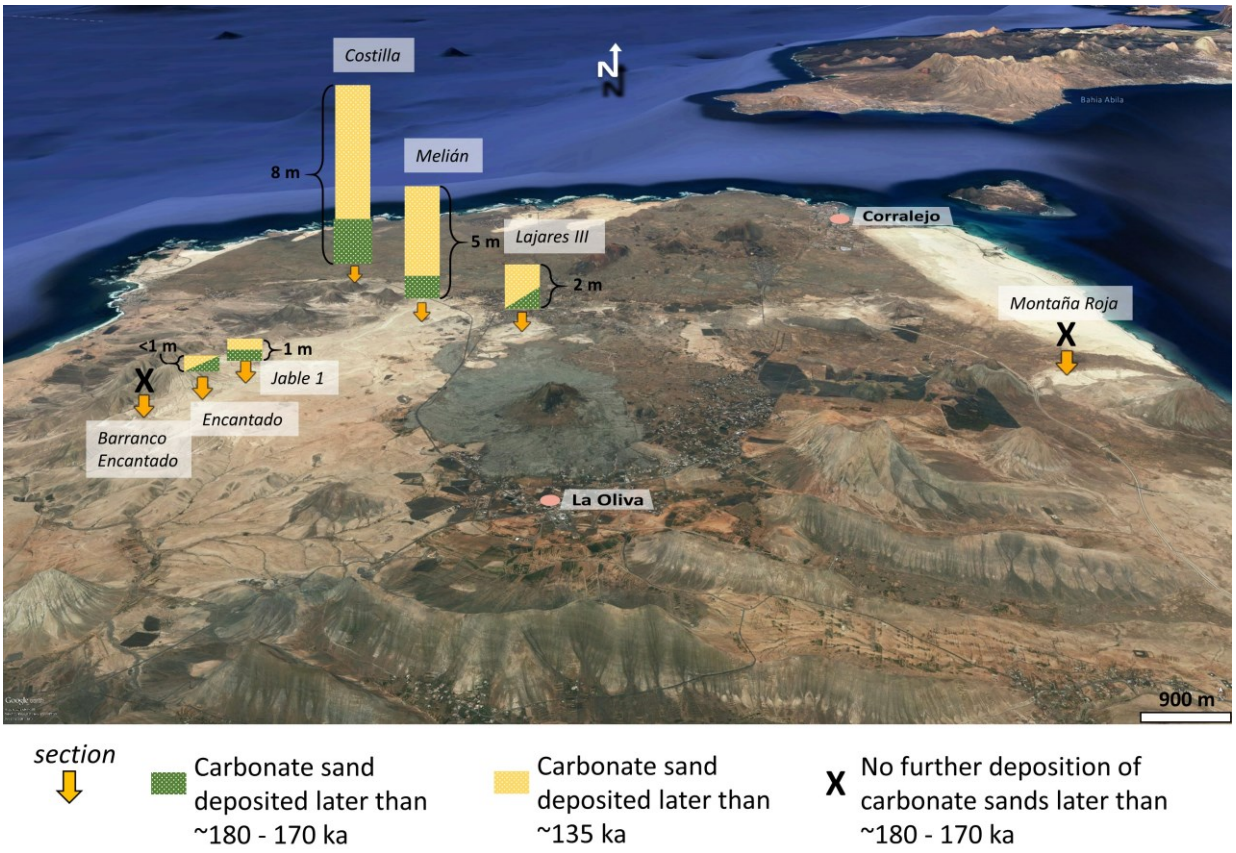

Fig. 4.8. Thicknesses of carbonate sands deposited above Unit 9

Period a)

As described above, the palaeo dune field of Montaña Roja was severely impacted by volcanic activity around 173 ka (reported by Criado et al., 2004). Some kilometres to the west, the Montaña de la Arena was dated to 185 ka, reported by Edwards and Meco (2000). This age had often been discussed (e.g. Meco et al., 2011) because of the discrepancy of the freshness and appearance of the Montaña de la Arena conveying an explicit younger age. Rando et al. (2008) indirectly dated the last eruption of the Montaña de la Arena resulting in >2 ka. Possibly the dating of 185 ka corresponds to the first eruption of the Montaña de la Arena. Furthermore, the neighbouring Montaña Los Saltos is assigned as being of Late Pleistocene age (Balcells Herrera et al., 1990), but datings of the Montaña los Saltos are so far not available.

In accordance to our findings in the here presented sections, the whole study area indicates stronger volcanic imprint above Unit 9, supporting volcanic imprint around 180 - 170 ka. We assume those eruptions were responsible for a decreased or even ceased sand supply

of the southernmost sites (located in the Barranco de los Encantados) and the easternmost site (Montaña Roja section).

Period b)

A next period of volcanic activity is related to the chain of volcanoes including the Calderon Hondo and the Bayuyo. The latter was dated 134 ka by Meco et al. (2002). Casillas Ruíz and Torres Cabrera (2012) reported an age of 135 ka of the Bayuyo volcano. These studies implied a lava flow related to eruptions covering almost the whole northern tip of the island from the western to the eastern coastline. In general, our sections support the impact of volcanic activity during this period. The corresponding stratigraphic position of this volcanic event is dated best within the Meliàn section (Unit 6) (compare Fig. 4.7). The corresponding lava flow of the chain of volcanoes including the Bayuyo blocked the main pathway of carbonate sands reaching the island presumably from the north. Additionally, the lava flows shifted the northern shoreline further northwards and covered larger parts of the former shallow shelf area. Consequently, they locked a larger part of the former source area of carbonate sands. Undoubtedly, parts of former sand seas were also covered. Following that event, merely less than one metre of carbonate sand was deposited at the sections of Encantado and Jable 1.
Concerning the volcanic activity around 135 ka it is important to mention that Meco et al. (2002) reported an age of 134 ka concerning a lava flow covering marine deposits at the "El Cotillo site" (for location of El Cotillo see Fig. 4.1). Meco et al. (2011) referred to that dating describing a site of an aeolian sand section with palaeosols covered by lava close to the village of "Los Lajares". Therefore the location of sampling seems to be unclear.

Period c)

In contrast to the effect of strongly reduced or even ceased sediment availability at the Barranco de los Encantados and the southern part of the Barranco del Jable after the periods around 180 – 170 ka and around 135 ka, Roettig et al. (2019) described further sedimentation after these periods at the three northernmost sections of the Barranco del Jable. Not only do these sections show further deposited carbonate sands after ~135 ka but they also reveal a gradient in thickness of deposited carbonate sands. Thereby, the thicknesses of deposited carbonate sands decrease from a northwestern to southeastern direction. Hence, Roettig et al. (2019) assumed the possibility of sediment supply after 135 ka. This pathway allowed further sand supply to reach the island from a northwestern

direction until a further eruption (possibly related to the Montaña del Coto Camachos) finally sealed off that last sediment pathway. The corresponding volcanic eruption appeared after 100 ka and at latest around 50 ka. After that event there was no further deposition of carbonate sands originating from the shelf in the entire study area and the dune fields became “palaeo” dune fields.

Roundup a) – c)

The distribution of site-specific accumulation of carbonate sands suggests the presented scenario. This compilation of Mid- to Late Pleistocene volcanism on northern Fuerteventura allows us to assume a cut off from carbonate sand pathways gradually. In Fig. 4.9 we illustrate in a very simplified manner the main periods of volcanic activity (given as “counterclockwise sequenced sectors”, for illustration purposes only). The Late Pleistocene cut-off scenario started around 180 - 170 ka in the eastern part (sector I) of northern Fuerteventura and ‘proceeded’ via the north, around 135 ka (sector II) to the northwest (sector III) latest at around 50 ka. The studied sections of dune palaeosurface sequences of the study in hand in compilation with the sections investigated by Faust et al. (2015) and Roettig et al. (2017, 2019) reflect the stages of the reduction in sand supply. Thus, the impact of volcanic activity around 180 -170 ka cut off the southernmost (Barranco de los Encantados) and easternmost (Montaña Roja) areas, followed by volcanic activity around 135 ka cutting off the southern part of Barranco del Jable. An assumed period, latest around 50 ka (after 100 ka), finally completed the cut-off from sand supply concerning all studied sections.

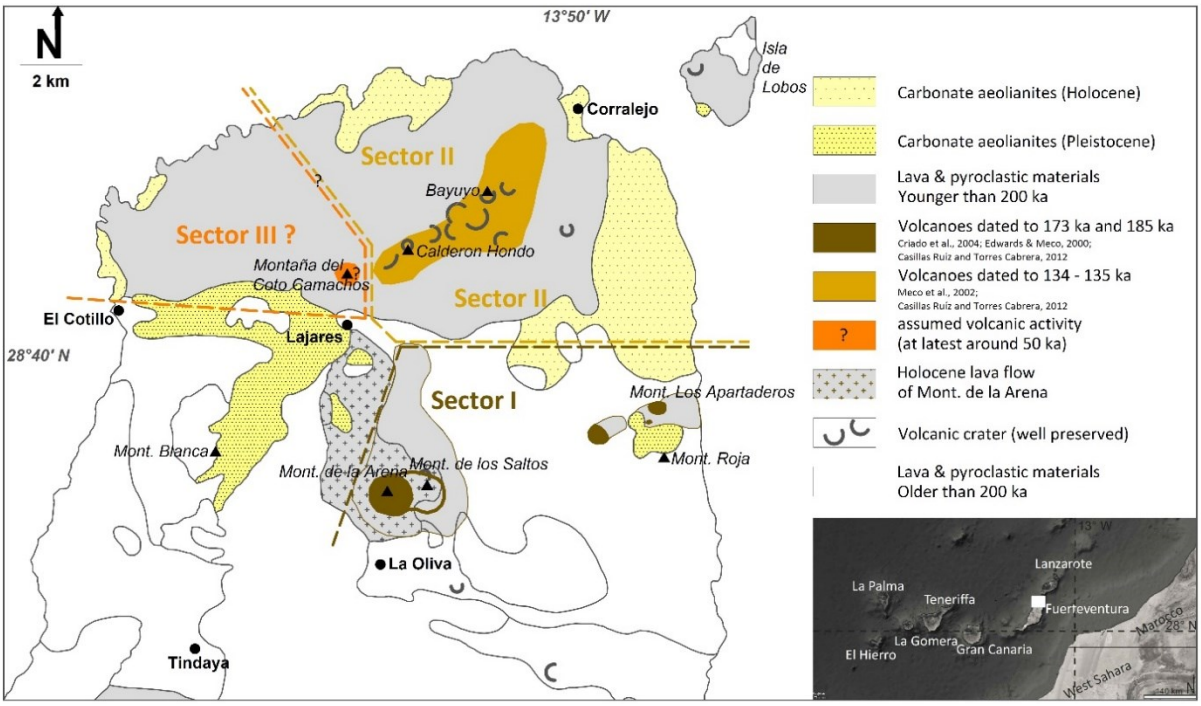

Fig. 4.9. Periods of volcanic activity blocking the sediment pathways, gradually (counterclockwise). The borders of sectors are generalised and simplified.

4.7 Conclusion

This is the first study to provide a chrono-stratigraphic correlation of dune palaeosurface sequences encompassing sites from both the eastern coastline and sites of dune fields near the western coastline. The chrono-stratigraphy dates back to about 450 ka. IRSL ages performed on palaeosurface material seem to systematically underestimate the chronology as the radionuclide concentrations determined for the samples originating from the palaeosurface sediments may not be representative of the entire burial period.

The Montaña Roja dune field indicates a complex interlacing of volcanic activity and the deposition of carbonate sands originating from the shallow shelf.

Findings of the dune fields of the Barranco Encantado, Barranco del Jable, and the dune field of Montaña Roja suggest that three different volcanic periods reduced the sand supply on northern Fuerteventura gradually, until finally the complete cut-off from the sand pathways at latest around 50 ka.

In conclusion we clearly have to differentiate between absent or reduced sediment supply caused by global sea level changes and reduced or even ceased sediment supply caused by local volcanic activity. Thus, volcanic activity not only built the basement for dune deposits but was also able to cut off the sand supply. Furthermore, the study in hand points out the necessity of site-specific strategy and interpretation.

4.8 Acknowledgements

Special thanks to Dr. Michael Dietze for coordinating the grain size measurements at the GFZ Potsdam and to Beate Winkler who did the measurements at the laboratory of the TU Dresden. Many thanks for all advices from Assist. Prof. Dr. Yurena Yanes (University of Cincinnati). For many valuable hints and discussions, many thanks to PD Dr. Michael Zech and Dr. Sascha Meszner. Special thanks to Elizabeth Kelly for proofreading. This work was supported by the German Research Foundation (FA 239/18-1).

4.9 References

Balcells Herrera, R., Barrera Morate, J. L., Gómez Sainz de Aja, 1990. Mapa Geológico de España 1:25.000 (La Oliva). Instituto Geológico y Minero de España, Madrid.

Balogh, K., Ahijado, A., Casillas, R., Fernández, C., 1999. Contributions to the chronology of the Basal Complex of Fuerteventura, Canary Islands. Journal of Volcanology and Geothermal Research 90, 81– 101.

Bouab, N., Lamothe, M., 1995. Geochronological framework for the Quaternary paleoclimate record of the Rosa Negra section (Fuerteventura – Canary Islands, Spain). Clim. Past 2-7 (1995), 37–42.

Casillas Ruíz, R., Torres Cabrera, J. M., 2012. Inventario de recursos vulcanológicos de Fuerteventura. Cabildo de Fuerteventura.

Coudé-Gaussen, G., Rognon, P., Bergametti, G., Gomes, L., Strauss, B., Gros, J. M., Le Coustumer, M. N., 1987. Saharan dust on Fuerteventura Island (Canaries): Chemical and mineralogical characteristics, air mass trajectories, and probable sources. Journal of Geophysical Research 92, 9753–9771.

Coudé-Gaussen, G. and Rognon, P., 1988. Origine Eolienne de Certains Encroutements Calcaires sur l'ile de Fuerteventura (Canaries Orientales). Geoderma 42, 271-293.

Criado, C., Guillo, H., Hansen, A., Hansen, C., Lillo, P., Torres, J. M., Naranjo, A., 2004. Geomorphological evolution of Parque Natural de Las Dunas de Corralejo (Fuerteventura, Canary Island). In: Benito, G., Díez Herrero, A. (Eds.), Contribuciones Recientes sobre Geomorfología. SEG y CSIS, Madrid.

Damnati, B., Petit-Maire, N., Fontugne, M., Meco, J., Williamson, D., 1996. Quaternary paleoclimates in the Eastern Canary Islands. Quat. Int. 31, 37–46.

Edwards, N. and Meco, J., 2000. Morphology and palaeoenvironment of brood cells of

Quaternary ground-nesting solitary bees (Hymenoptera, Apidae) from Fuerteventura, Canary Islands, Spain. Proceedings of the Geologists' Association 111, 173-183.

El-Asmar, H. M., 1994. Aeolianite sedimentation along the northwestern coast of Egypt: Evidence for middle to late quaternary aridity. Quaternary Science Reviews, Vol. 13, 699-708.

Faust, D., Yurena, Y., Willkommen, T., Roettig, C., Richter, Dan., Richter, Dav., Suchodoletz, H.v., Zöller, L., 2015. A contribution to the understanding of late Pleistocene dune sand-paleosol-sequences in Fuerteventura (Canary Islands). Geomorphology 246, 290–304.

Fuchs, M., Fischer, M., Reverman, R., 2010. Colluvial and alluvial sediment archives temporally resolved by OSL dating: Implications for reconstructing soil erosion. Quaternary Geochronology 5, 269-273.

Gardner, R .A. M., Goudie, A. S., Pye, K., 1983. Aeolianite. Chemical Sediments and Geomorphology: Precipitates and Residua in the Near-surface Environment. Academic Press, 265–300.

Guerin, G., Mercier, N., Adamiecz, G., 2011. Dose rate conversion factors update. Ancient TL 29, 5–8.

Herrmann L., Jahn R., Stahr K., 1996. Identification and Quantification of Dust Additions in Perisaharan Soils. In: Guerzoni S., Chester R. (eds) The Impact of Desert Dust Across the Mediterranean. Environmental Science and Technology Library, Vol. 11. Springer, Dordrecht.

Huot, S., Lamothe, M., 2003. Variability of infrared stimulated luminescence properties from fractured feldspar grains. Radiat. Meas. 37, 499–503.

Inman, D. L., Ewing, G. C., Corliss, J. B., 1966. Coastal sand dunes of Guerro Negro, Baja California, Mexico. Bull. Geol. Soc. Am. 77, 787–802.

Jahn, R., 1988. Vorkommen, Genese und Eigenschaften von Böden aus Vulkaniten im semiariden Klima Lanzarotes (Kanarische Inseln). Hohenheimer Arbeiten, Ulmer, Stuttgart.

Kemski, J., Klingel, R. Siehl, A., 1996. Die terrestrische Strahlung durch natürlich radioactive Elemente in Gesteinen und Böden. In: Siehl, A. (Ed.): Umweltradioaktivität. Ernst & Sohn, Berlin.

Kreutzer, S., Schmidt, C., Fuchs, M. C., Dietze, M., Fischer, M., Fuchs, M., 2012. Introducing an R package for luminescence dating analysis. Ancient TL 30, 1–8.

Kreutzer, S., Dietze, M., Burow, C., Fuchs, M. C., Schmidt, C., Fischer, M., Friedrich, J., Mercier, N., Smedley, R. K., Durcan, J., King, G., 2016. Luminescence: Comprehensive Luminescence Dating Data Analysis. CRAN version 0.7.3, http://CRAN.R-project.org/package=Luminescence.

Kruse, W. and Meyer, B., 1970. Untersuchungen zum Prozeß der Rubefizierung (Entkalkungsrötung) mediterraner Böden am Beispiel kalkhaltiger marokkanischer Küsten - Dünen. Göttinger Bodenkundlichen Berichte, Bd. 13, 77 – 140.

Le Bas, M. J., Rex, D. C., Stillman, C. J., 1986. The early magmatic chronology of Fuerteventura, Canary Islands. Geological Magazine 123, 287– 298.

Meco, J., Guillou, H., Carracedo, J-C., Lomoschitz, A., Ramos, A. J. G., Rodríguez-Yánez, J. J., 2002. The maximum warmings of the Pleistocene world climate recorded in the Canary Islands. Palaeogeography, Palaeoclimatology, Palaeoecology 185, 197-210.

Meco, J., Muhs, D. R., Fontugne, M., Ramos, A. J. G., Lomoschitz, A., Patterson, D., 2011. Late Pliocene and Quaternary Eurasian locust infestations in the Canary Archipelago. Lethaia 44, 440–454.

Menéndez, I., Pérez-Chacón, E., Mangas, J., Tauler, E., Engelbrecht, J. P., Derbyshire, E, Cana, L., Alonso, I., 2013. Dust deposits on La Graciosa Island (Canary Islands, Spain): Texture, mineralogy and a case study of recent dust plume transport. Catena 117, 133-144.

Misota, C., Matsuhisa, Y., 1995. Isotopic evidence for the eolian origin of quartz and mica in soils developed on volcanic materials in the Canary Archipelago. Geoderma 66, 313–320.

Muñoz, M., Sagredo, J., de Ignacio, C., Fernández-Suárez, J., Jeffries, T. E., 2005. New data (U-Pb, K-Ar) on the geochronology of the alkaline-carbonatitic association of Fuerteventura, Canary Islands, Spain. Lithos 85, 140-153.

Munsell Color (Firm), 1975. Munsell soil color charts. Baltimore.

Murray, A. S., Wintle, A. G., 2000. Luminescence dating of quartz using an improved single aliquot regenerative dose protocol. Radiation Measurements 32, 57-73.

Ortiz, J. E., Torres, T., Yanes, Y., Castillo, C., de la Nuez, J., Ibáñez,M., Alsonso, M. R., 2006. Climatic cycles inferred from the aminostratigraphy and aminochronology of Quaternary dunes and palaeosols from the eastern islands of the Canary Archipelago. J. Quat. Sci. 21, 287–306.

Prescott, J. R. & Hutton, J. T., 1994. Cosmic ray contribution to dose rates for

luminescence and ESR dating: Large depths and long-term time variations. Radiation Measurements 23, 497-500.

Preusser, F., 2003. IRSL dating of K-rich feldspars using the SAR protocol: comparison with independent age control. – Ancient TL 21, 17-23.

Pye, K., Tsoar, H., 2009. Aeolian Sand and Sand Dunes. Springer-Verlag, Berlin Heidelberg.

Rando, J. C., Alcover, J. A., Navarro, J. F., garcía-Talavera, F. Hutterer, R., Michaux, J., 2008. Chronology and causes of the exteinction of the Lava Mouse, Malpaisomys insularis (Rodentia: Muridae) from the Canary Islands. Quaternary research, 70, 141-148.

Roettig, C-B., Kolb, T., Wolf, D., Baumgart, P., Richter, C., Schleicher, A., Zöller, L., Faust, D., 2017. Complexity of aeolian dynamics (Canary Islands). Palaeogeography, Palaeoclimatology, Palaeoecology 472, 146–162.

Roettig, C-B., Varga, G., Sauer, D., Kolb, T., Wolf, D., Makowski, V., Recio Espejo, J. M., Zöller, L., Faust, D., 2019. Characteristics, nature, and formation of palaeosurfaces within dunes on Fuerteventura. Quaternary Research Volume 91, Issue 1, 4-23.

Rothe, P., 1996. Kanarische Inseln. Sammlung Geologische, Führer 81, Gebrueder Borntraeger, Stuttgart.

Rother, H., Shulmeister, J., Rieser, U., 2010. Stratigraphy, optical dating chronology (IRSL) and depositional model of pre-LGM glacial deposits in the Hope Valley, New Zealand. Quat. Sci. Rev. 29, 576-592.

Schlichting, E., Blume, H.-P., Stahr, K., 1995. Bodenkundliches Praktikum. Blackwell, Berlin, Wien.

Schofield, J. C., 1975. Sea level fluctuations cause periodic post-glacial progradation, South Kaipara barrier, North Island, New Zealand. N.Z. J. Geol. Geophys. 18, 295-316.

Schulte, P., Lehmkuhl, F., Steininger, F., Loibl, D., Lockot, G., Protze, J., Fischer, P., Stauch, G., 2016. Influence of HCl pretreatment and organo-mineral complexes on laser diffraction measurement of loess–paleosol-sequences. Catena 137, 392–405.

Struck, J., Roettig, C-B., Faust, D., Zech, R., 2018. Leaf waxes from aeolianite–paleosol sequences on Fuerteventura and their potential for paleoenvironmental and climate reconstructions in the arid subtropics. E&G Quaternary Sci. J. 66, 109-114.

Von Suchodoletz, H., Blanchard, H., Hilgers, A., Radtke, U., Fuchs, M., Dietze, M., Zöller,

L., 2012. TL and ESR dating of Middle Pleistocene lava flows on Lanzarote island, Canary Islands (Spain). Quaternary Geochronology 9, 54-64.

Varga, G., Roettig, C-B., 2018. Identification of Saharan dust particles in Pleistocene dune sand-paleosol sequences of Fuerteventura (Canary Islands). Hungarian Geographical Bulletin 67, 121-141.

Ward, W. T., Little, I. P., Thompson, C. H., 1979. Stratigrapy of two sandrocks at Rainbow Beach, Queensland, Australia, and a note on humate composition. Palaeogeography, Palaeoclimatology, Palaeoecology 26, 305-316.

Warren, J. K., 1983. On pedogenic calcrete as it occurs in the vadose zone of Quaternary calcareous dunes in coastal South Australia. J. Sediment. Petrol. 53, 787–796.

Yanes, Y., Castillo, C., Hutterer, R., De la Nuez, J., Quesada, M., Torres, T., Ortiz, J. E., Alonso, M.R., Ibáñez, M., 2004. Valoración patrimonial de las formaciones dunares cuaternarias del Barranco de los Encantados y Cantera de Melián de la isla de Fuerteventura (Islas Canarias). Geogaceta 36, 195–198.

4.10 Supplementary material

4.10.1 Montaña Roja dune field - catchment development / formation of depression lines

The satellite image of the palaeo dune field on the northern slopes of Montaña Roja (compare Fig. 4.3) let assume a complex formation especially with regard to its drainage system. Generally, the eastern part (near the coastline) of the dune field is characterised by less relief intensity whereas the western part of the dune field shows higher relief intesities. Between these areas there is no gradual shift but there are distinct borders. The map of slope inclinations (Fig. 4.10) provides a deeper insight into the development of depression lines and water induced erosion up to the nowadays gully system of the palaeo dune field (concerning Fig. 4.10 please note that the largest areas of highest slope inclination are related to the inner part of the crater of the Montaña Roja and do not belong to the area of the dune field deposits). Accordingly, we differentiate the dune field into three main areas in order of being tapped subsequently.

During a first period (Fig. 4.10, AREA I) the system was captured in western direction by degree, draining directly into the ocean. As AREA I is situated closest to the coastline its relief is more eroded and more leveled in comparison to the western parts of the dune field. Accordingly, the depression lines of AREA I are straight and elongated at all. A clear diffenerence in morphology becomes visible by comparing AREA I and AREA II. AREA II is less leveled and shows a higher density of steeper slopes. That means a higher relief intensity characterised by winding and less elongated depression lines in comparison to AREA I. Assumingly the lava flow of the Calderetilla de Apartaderos retarded the development of the westward capturing. In accordance, a level step (roughly 1.5 metres in height) located in the thalweg of the Barranco de las Pilas indicates a fixed position of longer duration (marked blue in Fig. 4.10). The level step is formed in basaltic solid rock. Even the clearing of the obstacle and the ongoing capturing further westward seem to took place by degress as in a first step AREA II was captured. In contrast to AREA I and II the depression lines of AREA III feature dendritic pattern. Therwith we assume that AREA III was not captured until the passage to the south of the Calderetilla de Apartaderos was cleared, completely.

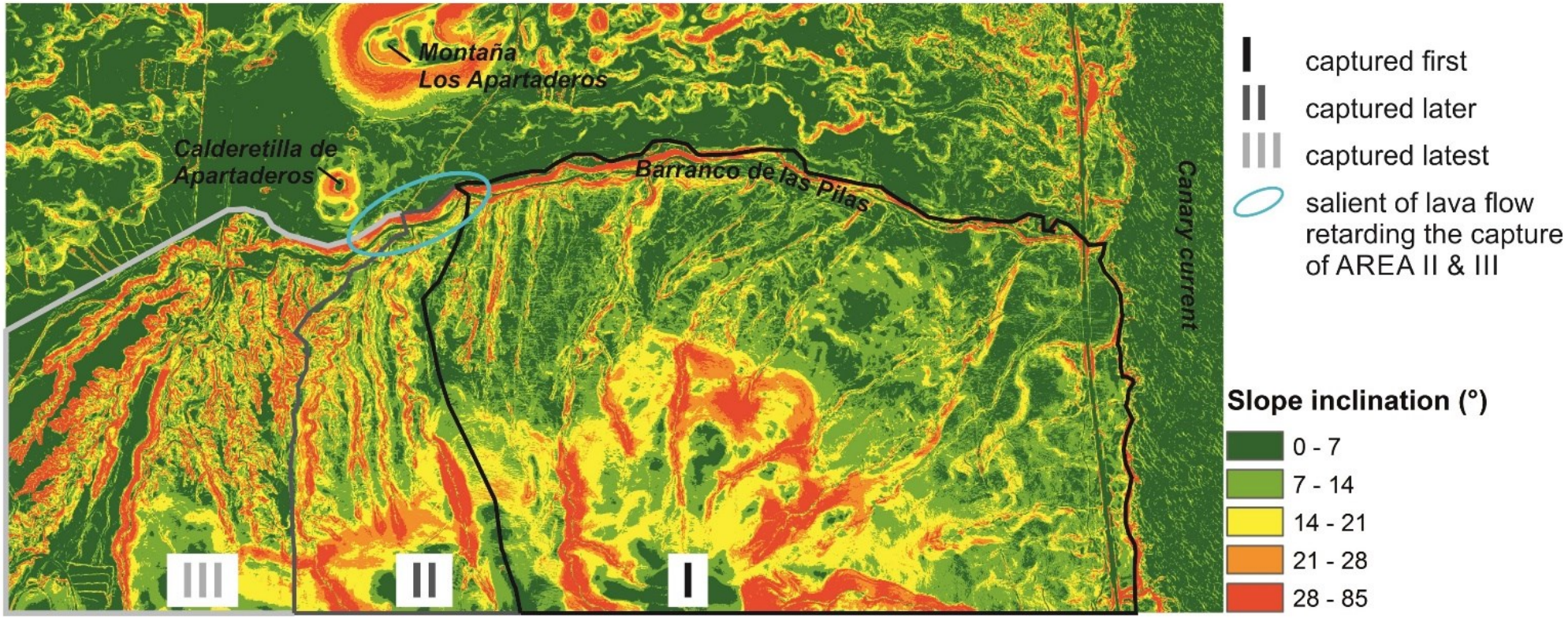

Fig. 4.10. Slope inclination – relief intensity, based on LIDAR data provided by IDE Canarias (area comparable to satellite image of Fig. 4.3)

Generally, we interprete the stages of development/formation of the Montaña Roja dune field as follows:

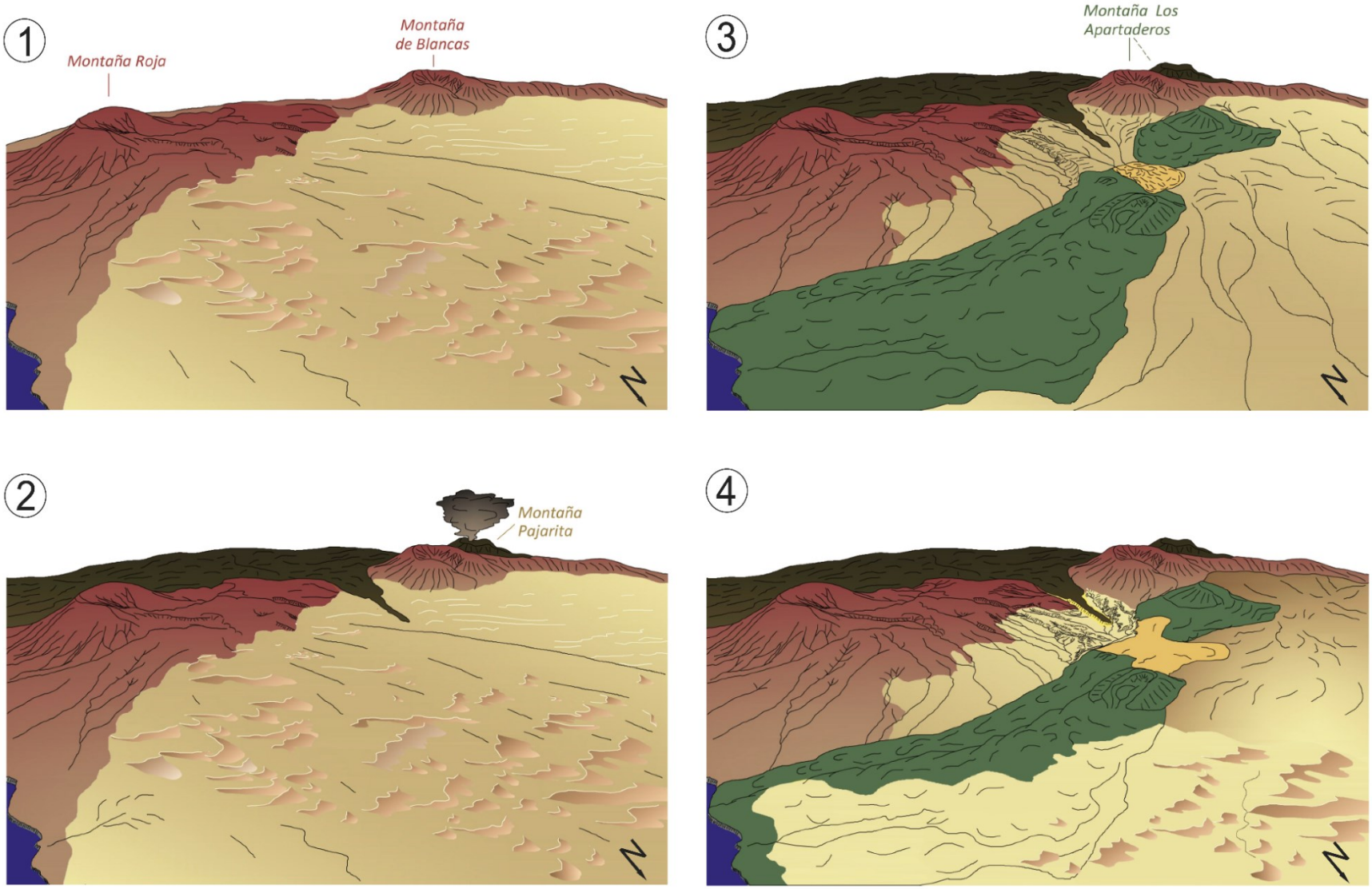

Fig. 4.11. Montaña Roja dune field – stages of development

4.10.2 Montaña Roja dune field –interaction of sand supply, volcanic activity and water induced erosion on a smaller scale

Stage 1 (Fig. 4.11 - 1):

After a period of high slope dynamics (compare Unit 15 of the correlation) dune sands (bearing barchanes) reached the northern and northeastern flanks of Montaña Roja and Montaña de Blancas. That formation started at latest in correspondance to Unit 14 (dated to 468.3 +/- 41.3 ka). We assume less intense shaped relief as in that stratigraphic position there is no indication concerning the formation of deep incision which should be visible by channel fillings or the like.

Stage 2 (Fig. 4.11 - 2):

A small tongue of the lava flow of Montaña Parajita (dated to 400 ka, Criado et al., 2004) passed the ridge between Montaña Roja and Montaña de Blancas covering a narrow part of the dune field. The lava flow covered a leveled relief. Below the leveled relief a palaeosurface features a vast abundance of Cochlicella sp. (Yanes et al., 2004). We assume the age of 400 ka overestimate the age of the lava flow as the abundance of Cochlicella sp. is clearly linked to Unit 11 (Roettig et al., 2017). The lava flow devided the surrounding dune field into two parts and initiated a first formation of a depression line between the lava tongue and the Montaña de Blancas situated in western direction.

Stage 3 (Fig. 4.11 - 3):

The eruption of Montaña Los Apartaderos and of the Calderetilla de Apartaderos blocked the sediment pathway from northern direction. The lava flow in relation to the Montaña Los Apartaderos is dated to 173 ka (Criado et al., 2004). Our IRSL ages below the lava flow (Fig. 4.5, 236.1 +/- 21.5 ka and 165.1 +/- 14.6 ka) support that chronology. The lava flow broadly covered the dune field, flowing in eastern direction reaching the coastline,

finally. This lava flow blocked the before mentioned depression line between lava tongue (400ka) and the Montaña de Blancas (compare *stage 2*) and the lava flow itself initiated the formation of a depression line on its southern border (at the nowadays position of the Barranco de las Pilas). Assumingly, the lava flow of the Calderetilla de Apartaderos caused an obstacle which laterally devided the dune field in an early captured eastern (AREA I as discussed before) and a later captured western (AREA II & III) part. While the eastern part was captured by degree and formed the Barranco de las Pilas draining in eastern direction into the ocean, the western part drained into a basin to the southwest of the Montaña Los Apartaderos where the sediments were accumulated, respectively. We assume the nowadays visible basin deposits had been accumulated during Unit 4 as Unit 4 is characterised by more moisture conditions (in accordance to widely distributed $CaCO_3$-crust of Unit 4).

Stage 4 (Fig. 4.11 - 4):

The periodic waters of Barranco de las Pilas cleared the sediments by degree. Finally, the depression line break through the obstacle initiated by the lava of the Calderetilla de Apartaderos and captured the western catchment. The basin sediments which had been accumulated during Stage 3 underwent erosion, as currently visible. We have to assume the final depth of incision of the gully system is related to human pressure, mainly grazing of goats (comparable to reports by Granados Corona et al., 1988 and Santana-Cordero et al., 2016).

4.10.3 References

Criado, C., Guillo, H., Hansen, A., Hansen, C., Lillo, P., Torres, J. M., Naranjo, A., 2004.

Geomorphological evolution of Parque Natural de Las Dunas de Corralejo (Fuerteventura, Canary Island). In: Benito, G., Díez Herrero, A. (Eds.), Contribuciones recientes sobre geomorfología. Sociedad Espanola de Geomorfología, Madrid.

Granados Corona, M., Vicente, A. M., Garcia Novo, F., 1988. Long-term vegetation changes on the stabilized dunes of Doñana National Park (SW Spain). Vegetatio 75, 73-80.

IDE Canarias (Infraestructura de datos especiales de Canarias): LIDAR 2010-2011. http://tiendavirtual.grafcan.es/visor.jsf?currentSeriePk=263585792 , retrieved 2018.

Santana-Cordero, A. M., Monteiro-Quintana, M. L., Hernández-Calvento, L., 2016. Reconstruction of the land uses that led to the termination of an aridcoastal dune system: The case of the Guanarteme dune system(Canary Islands, Spain), 1834–2012. Land Use Policy 55, 73–85.

Yanes, Y., Castillo, C., Hutterer, R., De la Nuez, J., Quesada, M., Torres, T., Ortiz, J.E., Alonso, M. R., Ibáñez, M., 2004. Valoración patrimonial de las formaciones dunares cuaternarias del Barranco de los Encantados y Cantera de Melián de la isla de Fuerteventura (Islas Canarias). Geogaceta 36, 195–198.

5 Extended summary

5.1 An attempt towards a comparison with regional archives

Site specificity proved to play a very important role within the palaeo dune systems on Fuerteventura (compare Chapter 2.6.3 & 3.7.2). The studied sequences often showed site-specific characteristics, e.g. in sediment colour, thickness of deposits, or elemental composition within one and the same stratigraphic position. These differences point to site-specific deposition of carbonate sands and site-specific palaeosurface formation (and relocation) as well. Nevertheless, the dune archives suggest a general pattern of cyclicity. The cyclicity is characterised by subsequent sand accumulation, palaeosurface formation (including dust imprint and weak soil forming processes), and water-induced erosion (Chapter 3.7.2). Finally, the distribution of site-specific characteristics in combination with the deduced cyclicity allowed conclusions about the relation of the studied archives to sea level changes and led to the deduction of a conceptual approach (discussed in Chapter 3.7.4).

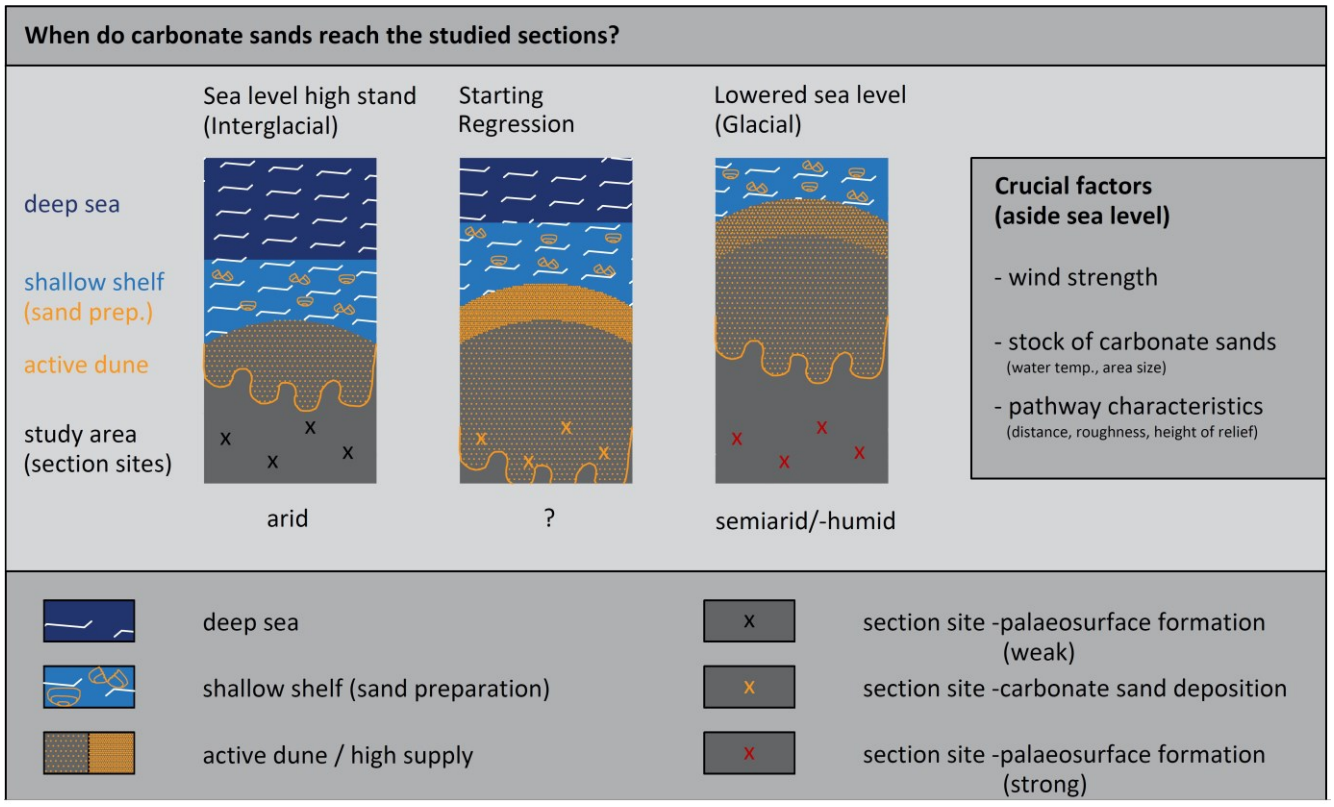

Fig. 5.1. Relationship of of sand deposition and sea level changes

According to Chapter 3.7.4 and illustrated by Fig. 5.1, sea level high stands result in moderate sand supply, too little to be transported over longer distances landwards. During starting regression we assume the highest sand supply accompanied by further landward progradation (comparable to findings of Fletcher III, 2005). The lower the sea level the longer the distance between the sand source area and the studied sections, resulting in a lack of sand accumulation at the study sites. Thus, during lowered sea level the study sites show an increased potential of longer duration of surface exposure. Furthermore, the conceptual approach by Roettig et al. (2019) (CAR) is based on the assumption that lower sea level enables more precipitation to reach the Canary Islands (Chapter 3.7.4, cf. Fig. 3.11). Based on the CAR, Figure 5.2 shows a comparison to further regional archives. Thus, the figure includes findings from Meco et al. (2011) as well as conclusions deduced from archives on Lanzarote (by Zöller et al., 2003 and von Suchodoletz et al., 2013) and results from marine sediment cores from the Canary Basin (Moreno et al., 2001).

Meco et al. (2011) described periods of dune deposition and periods of palaeosol formation. The time frame of their study is based on dated volcanic eruptions. Zöller et al. (2003) and von Suchodoletz et al. (2013) (the latter one is based on findings of von Suchodoletz et al., 2010) interpreted colluvial sequences on Lanzarote in terms of alternating moist and dry periods, whereas Moreno et al. (2001) concluded changing intensities of wind strength (on the basis of Si/Al-values) and differing dust supply (based on variations in Al content).

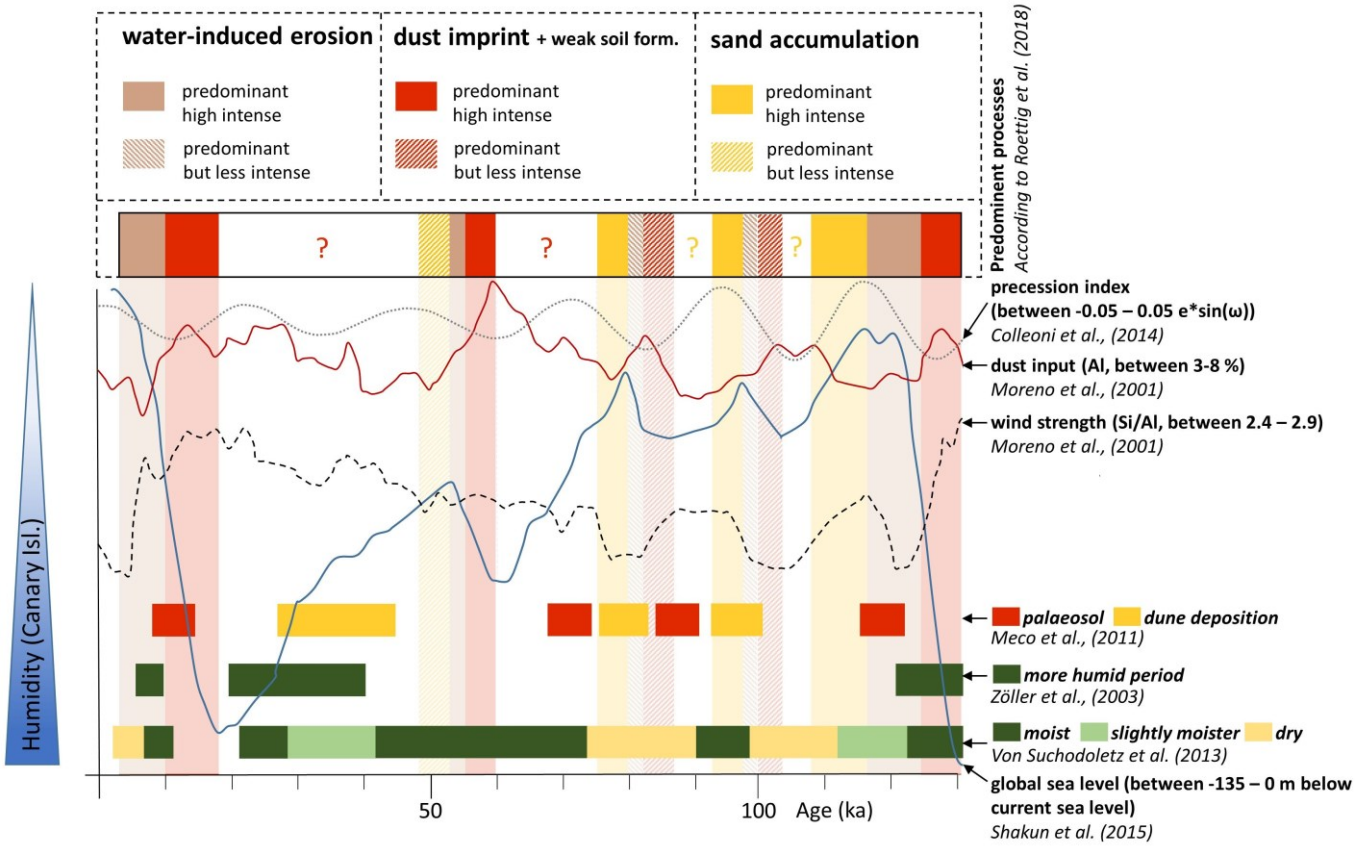

Fig. 5.2. Data of Canarian archives on the backdrop of the conceptual approach according to Roettig et al. (2019), modified

The CAR is in good agreement with the marked dune accumulations after 100 ka and around 80 ka according to Meco et al. (2011) (Fig. 5.2). Additionally, the periods of palaeosurface formation of the CAR seem to match the palaeosol formations according to Meco et al. (2011) around 90 ka and around 15 ka. The period around 120 ka by Meco et al. (2011) does not contradict the period of palaeosurface relocation drawn by the CAR. Generally, the underlying assumption of the CAR, whereby lower sea level means that more precipitation reaches the Canary Islands (discussed in Chapter 3.7.5) is supported by the studies of Zöller et al. (2003) and von Suchodoletz et al. (2013) (cf. Fig. 5.2). Fittingly, the main period of increased moisture started around 70 ka, whereas three dry periods according to von Suchodoletz et al. (2013) (around 110 – 100 ka, 90 – 70 ka and after 8 ka) occurred during periods of raised sea level. Von Suchodoletz et al. (2010) interpreted a relation of dry periods (namely "pedogenis minima" within Vega deposits on Lanzarote) to obliquity maxima. The periods of less intense palaeosurface formation of the CAR (between 105 and 100 ka and 90 and 80 ka) do not contradict that assumption. The study

by von Suchodoletz et al. (2013) also included data from the Mala dune section on the eastern coast of Lanzarote (see Apendix Mala section). The "palaeosol (Bv8)" in the uppermost part of the Mala dune section resulted in 95 ka (ESR dating). Possibly that "Bv8" correlates with the palaeosurface around 100 ka of the CAR (supported by two IRSL ages of the Melián section 101.1 +/- 9.5 ka at the top of Unit 5 and 98.2 +/- 9.1 ka at the bottom of Unit 4, according to Chapter 4, Fig. 4.7).

Generally, periods of palaeosurface formation according to the CAR (marked red in the upper bar of Fig. 5.2) are in very good agreement with periods of increased dust input interpreted by Moreno et al. (2001). Consistently, the "palaeosols" as early indicators of Interglacials according to Meco et al., (2011) support those periods. Moreno et al. (2001) deduced a precessional dependent dust availability. In accordance with this, minima in precessional index led to high seasonality with increased weathering because of enhanced monsoon during boreal summer but increased dust supply during boreal winter. Thus, during boreal summer, enhanced weathering caused high quantities of fine material to be transported by enhanced winds during boreal winter. Besides the mentioned enhanced seasonal winds at precessional minima, of course we cannot exclude a relation of changes in wind strengths (on millenial scale) to either sand deposition or dust input, but the Si/Al-ratio (as indicator of wind strength) according to Moreno et al. (2001) just suggests increased wind strength at terminations which means changes in glacial-interglacial time scale (compare also Moreno et al., 2002).

5.2 Synthesis

Chrono-stratigraphic correlation and standard profile

This thesis made available a universal stratigraphy of dune palaeosurface sequences derived from different dune fields on northern Fuerteventura (cf. Chapter 2.6.2). The correlation of different sections is mainly based on stratigraphic findings and could be worked out to a chrono-stratigraphy by means of IRSL dating. During the study we were able to extend the correlation that has been developed for the Barranco de los Encantados and the Barranco del Jable to the dune field of Montaña Roja (cf. Chapter 4.6.2). Now the correlation spans from sites located near the eastern coast to sites close to the western coastline. The sedimentary characteristics within these archives are very site-specific as they are defined by the position related relief and the connectivity to erosion pathways (cf.

Chapter 2.6.3). Indicators like colour within a specific stratigraphic position vary strongly within close distances. The colour seems less appropriate to distinguish different intensities of soil formation but proved to be useful in differentiating mineral compositions (cf. Chapter 2.6.1). According to the extended correlation the derived standard profile encompasses 15 Units which we divided into 5 main sequences. These sequences mainly differ in sand supply and accumulation, in features of changing moisture conditions, and in the indication of volcanic activity (cf. Chapter 2.6.3). The chrono-stratigraphy dates back to roughly 450 ka. The chronology is mainly based on IRSL datings performed on dune material, whereas dating results performed on palaeosurface material point to a systematical underestimation of those ages (cf. Chapter 4.6.1). Generally, the measured IRSL ages contribute to the discussion of dating within dune archives on Fuerteventura as these ages support the assumption of Middle to Late Pleistocene formation of the studied sections. Malacological results indicate that maxima in occurrence of *Obelus pumilio*, *Cochlicella sp.*, *Pomatias lanzarotensis* and *Rumina decollata* correspond to stratigraphical order (cf. Chapter 2.6.1).

Palaeosurfaces (dust imprint and soil-forming processes)

Generally, within the carbonate sand dominated sequences in-situ processes are restricted to de- and recalcification and to recrystallisation of iron and manganese (cf. Chapter 3.7.1). The high content of $CaCO_3$ hampers stronger intensities of soil-forming processes. Values of SiO_2 and quartz measurements indicate high dust content within palaeosurface layers (cf. Chapter 3.7.1). Additionally, hematite is carried by dust pathways. Being a component of dust deposits, hematite contributes to the reddening of palaeosurface layers. Possibly, reddening is also produced by a combination of dust deposition and recrystallisation of allochthonous iron. Ultimately, the palaeosurface layers are predominantly influenced by the imprint of dust than by in-situ processes.

Periods of sand accumulation and periods of palaeosurface formation

The findings indicate a cyclicity of alternating I. sand accumulation, II. dust imprint and weak soil formation and III. water-induced relocation (cf. Chapter 3.7.2). Sand supply and accumulation seem to control the possibility of palaeosurface formation in terms of longer duration of surface exposure. Thus, periods of high sand supply and accumulation hampered the formation of palaeosurfaces, whereas decreased supply and accumulation of carbonate sands allowed the formation of palaeosurfaces. Changes in wind direction as

controlling factor of sand availability could be excluded. The study supports prevailing winds coming from northern directions during the last 400 - 450 ka. Highest sand supply seems to occur right after sea level maxima, whereas terminations (going ahead with transgression phases) suggest best conditions for palaeosurface formation (cf. Chapter 3.7.4). Generally, changes in moisture conditions and dust availability seem to control the intensity of palaeosurface formation. Referring to Moreno et al. (2001), dust supply depends on changes in precessional index (cf. Chapter 5.1). Accordingly, highest dust availability is in line with precessional minima. The CAR derived from the findings within the dune archives on Fuerteventura seem to reflect this relation of increased dust imprint during periods of palaeosurface formation against the backdrop of minima in precession index. Thus, the dune archives on northern Fuerteventura seem to store information about sea level changes, moisture conditions, and changes in precessional index.

Local volcanism

Local volcanic activity is clearly influenced by the formation of dune archives on northern Fuerteventura (cf. Chapter 4.6.3 and 4.10.1). Firstly, lava flows were able to cut off the sand pathways. Secondly, lava flows covered (former) sand source areas. The study suggests a gradual cut off from sand pathway. Accordingly, there are three main periods of volcanic activity: first period around 180 – 170 ka, second period around 135 ka, and a suggested third period no later than 50 ka. Thus, we were able to deduce from findings within the dune archives an idea of how the northern tip of Fuerteventura was formed and shaped during the Late Pleistocene. For this area the third period of volcanic activity has not been described so far. In turn, the studied dune archives need to be interpreted carefully against the backdrop of the interplay of volcanic activity, sea level changes, and changing distances to sand sources.

5.3 Applied methods and used terms

The here presented thesis reflects the development of ideas, of indication, and growing experience. With each field trip over the last few years the interpretability has become broader and has in turn enabled a deeper insight into the dune archives of Fuerteventura. This also becomes visible by the development in the usage of terms. At first we started by using the term “aeolianite” to refer to consolidated and also unconsolidated carbonate sands. Over time we decided to use the term “carbonate sands” (cf. Chapter 3) as we

realised during scientific discussions that the meaning of the term "aeolianite" in its strict sense (as consolidated deposits) is confusing. A similar development became apparent in reference to the usage of the term "soil formation". Even if already in the first publication (cf. Chapter 2.7) we determined just de- and recalcification as the most prominent in-situ soil forming processes we decided over time to avoid the term "soil formation" because of its general association. Especially the use of "strong soil formation" was misleading as we tried to use it for specific systems. In the end we ceased to use these terms and instead employed the term "palaeosurface formation".

Similarly, the application of different methods portrays a development over time. Firstly, XRD test measurements were not promising. Therefore, in consequence, we began to indicate the imprint of Saharan dust by the content of Si (XRF measurements) (cf. Chapter

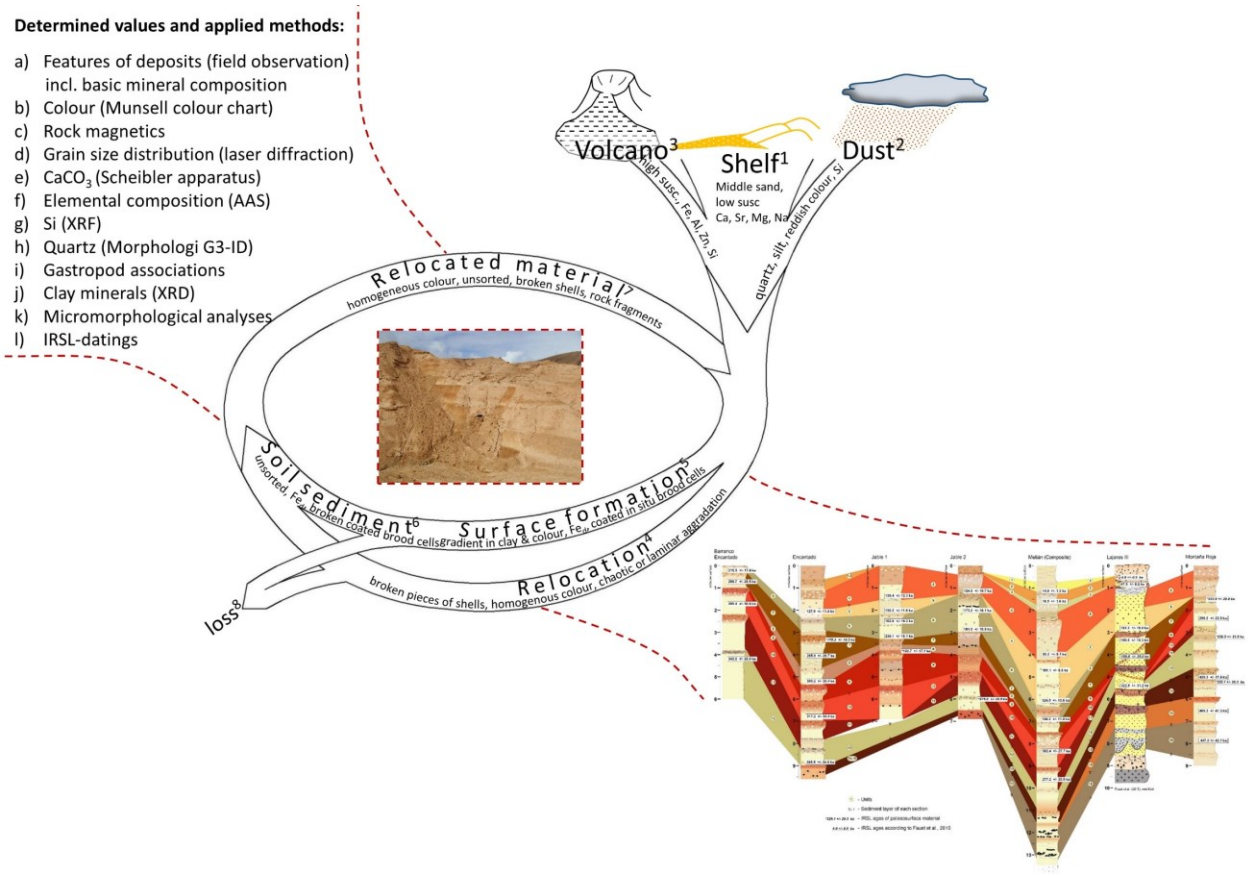

Fig. 5.3. Applied methods according to Roettig et al. (2017), modified

2.6.4). On Fuerteventura the content of Si within the studied archives depends on dust imprint as well as on volcanic imprint (Fig. 5.3 - g, 2). Finally, the Morphologi G3-ID measurements allowed the determination of Quartz contents (Fig. 5.3 – h) and therefore, massively extended the possibility to indicate the imprint of dust (cf. Chapter 3.5.4 and 3.11.1). Deeper insight into in-situ soil forming processes, which at first were deduced

from field observations via differing intensities of coatings of brood cells, became much more evident by micromorphological analyses, enabling the clear definition of processes taking place within the studied dune archive (Fig. 5.3 - a, k and cf. Chapter 3.7.1).

At first, we standardly avoided taking dating samples of palaeosurface near sediments. The chronology in terms of the chrono-stratigraphy (Fig. 5.3 – l and cf. Chapter 2.6.2, 4.6.2) is mainly based on ages performed on layers dominated by carbonate sands. Nevertheless, in contrast to the low content of allochthonous dust material in carbonate sand layers, the increased Saharan dust imprint (enriched in datable minerals) of palaeosurface layers immediately suggested the attempt of dating palaeosurface material too. The corresponding measurements showed a systematic underestimation of IRSL datings performed on palaeosurface material (cf. Chapter 4.6.1). Despite these discussed discrepancies, the measured IRSL ages allowed us to work out a reliable chrono-stratigraphy for the palaeo dune fields of northern Fuerteventura.

The highly promising field measurements of magnetics led to extended rock magnetic measurements at the laboratory (Fig. 5.3 - c). The rock magnetic data revealed such high potential that we decided to exclude these results (Master thesis by Florian Schneider, TU Dresden) from the here presented thesis in favour of a separate manuscript (submitted to the Journal of Quaternary Science; corresponding author: Florian Schneider; for further detail see Chapter 10.4).

We took the same decision in view of the terrific results concerning gastropod associations (Master thesis by Christiane Richter, TU Dresden). Besides the mentioned occurrence of gastropod associations which correspond to stratigraphic positions (cf. Chapter 2.6.1), the ecological interpretation of the different gastropod associations are excluded from this thesis in favour of being subject of a separate manuscript (published in Quaternary Science Reviews; corresponding author: Christiane Richter; for further detail see Chapter 5.4).

5.4 Further publications in close cooperation

Richter, C., Roettig, C-B., Wolf, D., Groh, K., Kolb, T., Faust, D. (2019). Changes in Pleistocene gastropod faunas on Fuerteventura (Canary Islands) and implications on shifting palaeoenvironmental conditions. Quaternary Science Reviews 209, 63-81.

Varga, G., Roettig, C-B. (2018). Identification of Saharan dust particles in Pleistocene dune sand-paleosol sequences of Fuerteventura (Canary Islands). Hungarian Bulletin 67 (2), 121-141.

Struck, J., Roettig, C-B., Faust, D., Zech, R. (2018). Leaf waxes from aeolianite–paleosol sequences on Fuerteventura and their potential for paleoenvironmental and climate reconstructions in the arid subtropics. E&G Quaternary Sci. J., 66, 109–114.

Lerch, M., Bliedtner, M., Roettig, C-B., Schmidt, J-U., Szidat, S., Salazar, G., Zech, R., Glaser, B., Kleber, A., Zech, M., 2018. Lipid biomarkers in aeolian sediments under desert pavements – potential and first results from the Black Rock Desert, Utah, USA, and Fuerteventura, Canary Islands, Spain. E&G Quaternary Sci. J., 66, 103-108.

Schneider, F., Roettig, C-B., Wolf, D., Baumgart, P., Hambach, U., Faust, D., (in review). Rock magnetics of carbonate systems – Investigating paleo-dune-archives on Fuerteventura (Canary Islands). Journal of Quaternary Science.

5.5 Master and Bachelor theses within the context of the thesis

Master theses

Makowski, V.	Mikromorphologische Untersuchungen zu Bodenbildungen in den Paläodünen im Norden Fuerteventuras (Micromorphological analyses to investigate soil forming processes within palaeo dunes on northern Fuerteventura)
Richter, C.:	Study of Quaternary environmental conditions based on gastropods and their stable isotope signals in aeolianite-palaeosol sequences on Fuerteventura, Canary Islands (master thesis was written in English)
Schneider, F.:	Magnetische Eigenschaften quartärer Äolianite auf Fuerteventura (Magnetic properties of Quaternary aeolianites on Fuerteventura)

Bachelor theses

Gille, J.:	Altersangaben und Elementgehalte der Vulkane Fuerteventuras und Lanzarotes (Ages and elemental compositions of volcanos on Fuerteventura and Lanzarote)
Lorenzen, L. M.:	Tonminerale in Böden und Sedimenten Fuerteventuras (Clay minerals of soils and sediments of Fuerteventura)
Scheffler, C.:	Endmemberanalyse an Sedimenten pleistozäner Paläodünen im Norden Fuerteventuras

(Endmember analysis of Pleistocene palaeo dune sediments on northern Fuerteventura)

5.6 Continuation/outlook:

In view of the postulated Late Pleistocene volcanic period, generally, only further dating of volcanic lava flows would be able to bring the formation history of northern Fuerteventura to light. In addition, as the dune archives on northern Fuerteventura were cut off from sand pathways at latest around 50 ka, the sequences are too old for precise luminenscence dating. Thus, there is still a need for further IRSL dating for two reasons. Firstly, double or triple wise sampling and measurement could possibly compensate the uncertainty by an error of 10%. Secondly, in view of dating performed on palaeosurface material further dating has to be carried out as samples should be taken vertically in very close intervals (e.g. 5 cm). Perhaps this provides a deeper insight into the duration of periods of surface formation and into the assumed underestimation of those ages. Additionally, a comparison with further dating methods would be useful. The first ESR test measurements are currently in progress (by Dr. P. Schielein (Köln). Again in view of the cut-off from sand supply, the study area needs to be enlarged to close the gap between lacking sand accumulation periods. A promising study area seems to be the area of El Jable on Lanzarote. The first sections have already been sampled and dating is currently still in progress (project supervisor: Prof. D. Faust; funded by the DFG, FA-239/23-1). In the backdrop of the new sections on Lanzarote we also expect further advance by studies of gastropod associations in order to compare ecological demands and stratigraphic correspondance of the associations to those investigated on Fuerteventura. Besides the mentioned ESR test measurements, the gastropod studies have opened further new possibilities through the highly considered cooperation with Dr. Eric Walliser (Mainz). Dr. Walliser carried out tests to derive information from isotopic analyses about differing seasonality via multi-sampling of individual *Theba sp.* The first test measurements have provided an indication of differences in $\delta^{18}O$ values, suggesting higher seasonality (boreal summer vs. boreal winter) referring to Unit 11 in comparison to Unit 9. Further such measurements will allow us to gain deeper insight into changes on an annual scale. To bring forward the discussion about a possible combination of dust deposition and recrystallisation of allochthonous iron, we sent samples of present dust material (kindly provided by Dr. Inmaculada Menéndez, ULPCG Gran Canaria) to Dr. Andreas Gärtner

(Senckenberg, Dresden). In the use of raster electron microscopy Dr. Gärtner will answer the question if the samples include coated iron particles. Furthermore, the composition of "pure" carbonate sands against the backdrop of differing proportions within carbonate-producing communities could potentially reveal important findings in terms of changes within the marine environment. We are hopeful that with further investigation within the Canarian dune archives and comparable archives of other regions, a transregional correlation will become feasible.

6 Apendix

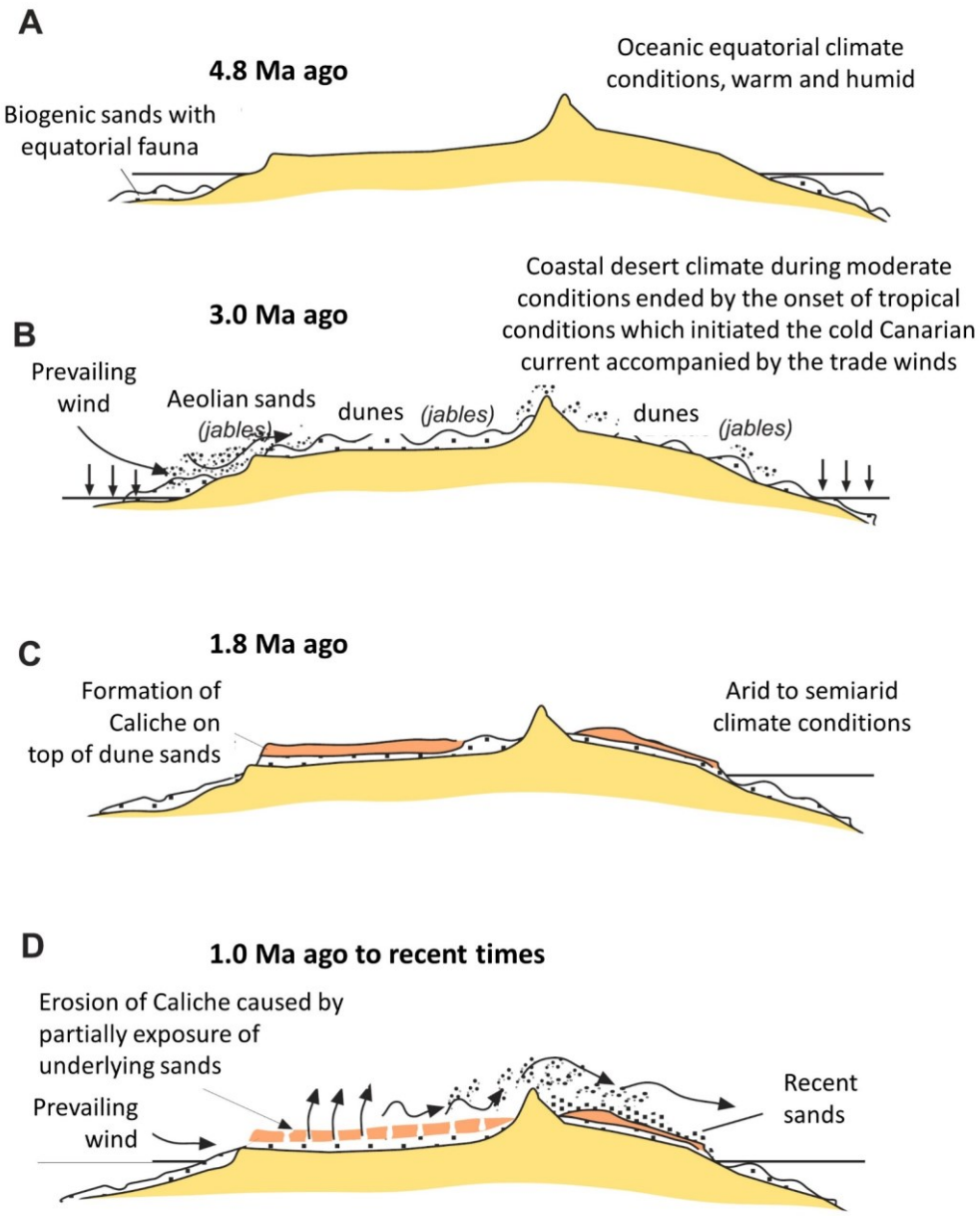

Fig. 6.1. Dune formation according to Meco et al. (2008), modified/translated

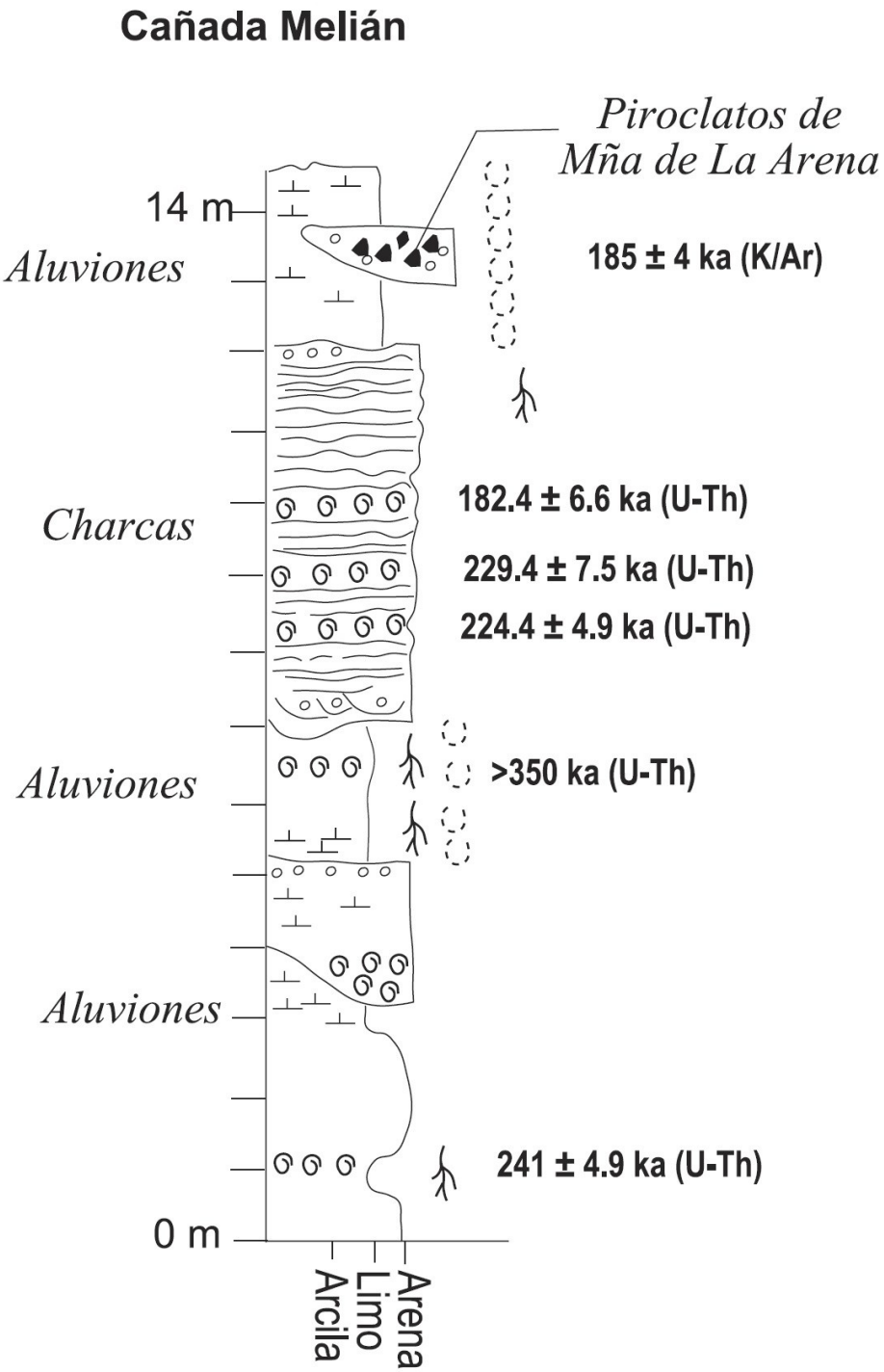

Fig. 6.2. Dune formation according to Meco et al. (2008), modified

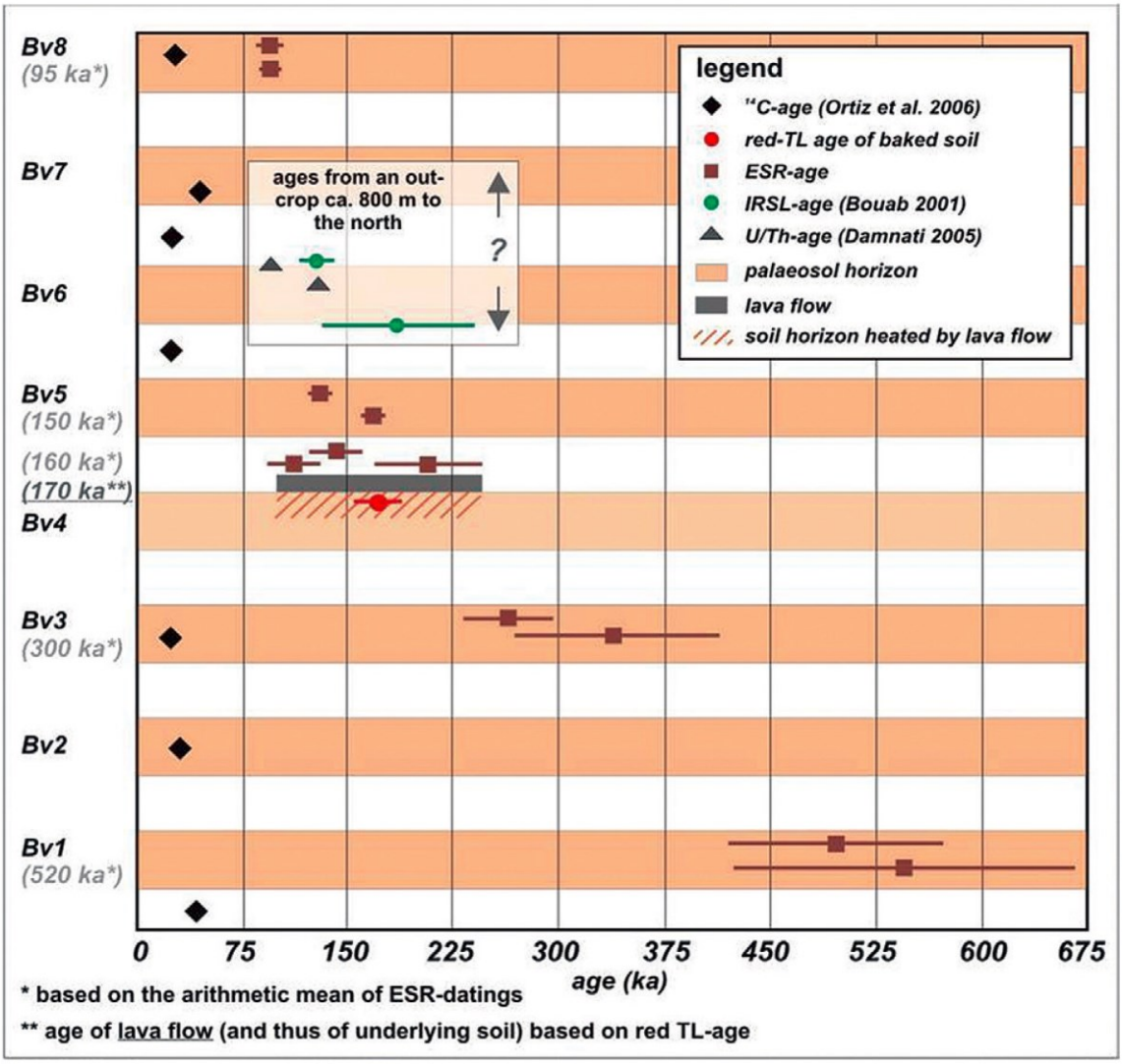

Fig. 6.3. Compiled dating of Mala section, according to von Suchodoletz et al. (2013)

7 References (of Chapters 1, 5 and 6)

Alcántara-Carió, J., Fernández-Bastero, S., Alonso, I., 2010. Source area determination of aeolian sediments at Jandia Isthmus (Fuerteventura, Canary Islands). Journal of Maine Systems 80, 219–234.

Anguita, F., Hernán, F., 1975. A propagating fracture model versus a hot-spot origin for the Canary Islands. Earth Planet. Sci. Lett. 27, 11-19.

Araña, V., Ortiz, R., 1986. Marco geodinámico del volcanismo canario. An. Física 82, 202-231.

Anguita, F. Hernán, F., 2000. The Canary Islands origin: a unifying model. Journal Volcanology and Geothermal Research 103, 1-26.

Ball, M. M., 1967. Carbonate sand bodies of Florida and the Bahamas. Journal of Sedimentary Petrology 21, 85-104.

Balogh, K., Ahijado, A., Casillas, R., Fernanández, C., 1999. Contributions to the chronology of the Basal Complex of Fuerteventura, Canary Islands. Journal of Volcanology and Geothermal Research 90, 81 – 101.

Beck, H. E., Zimmermann, N. E., McVicar, T. R., Vergopolan, N., Berg, A., Wood, E. F., 2018. Present and future Köppen-Geiger climate classification maps at 1-km resolution. Science Data 5:180214.

Bouab, N., Lamothe, M., 1995. Geochronological framework for the Quaternary paleoclimate record of the Rosa Negra section (Fuerteventura – Canary Islands, Spain). Climate of the Past 2-7 (1995), 37–42.

Brooke, B., 2001. The distribution of carbonate eolianite. Earth-Science Reviews 55, 135–164.

Coudé-Gaussen, G., Rognon, P., 1988. Origine Eolienne de Certains Encroutements Calcaires sur l'ile de Fuerteventura (Canaries Orientales). Geoderma 42, 271–293.

Criado, C., Naranjo, A., 2011. Geomorfología y Paisaje en La Oliva. In: Lobo Cabrera, M. (Ed.), La Oliva Historia de un pueblo de Fuerteventura. Ayuntamiento de La Oliva, La Oliva, Spain, 13–44.

Dash, B. P., Bosshard, E., 1969. Seismic and gravity investigations around the western Canary Islands. Earth and planetary science letters 7, 169-177.

Del Arco Aguilar, M. J., Rodríguez Delgado, O., 2018. Vegetation of the Canary Islands. Springer International Publishing.

DWD (German Meteorological Service), 2019. ftp://ftp-cdc.dwd.de/pub/CDC/

observations_global/CLIMAT/multi_annual/ (accessed 31.03.2019)

Edwards, N.,Meco, J., 2000.Morphology and palaeoenvironment of brood cells of Quaternary ground-nesting solitary bees (Hymenoptera, Apidae) from Fuerteventura, Canary Islands, Spain. Proceedings of Geologists Association 111, 173–183.

Einsele, G., 2000. Sedimentary basins: evolution, facies and sediment budget. Springer-Verlag, Berlin Heidelberg.

Fairbridge, R.W. and Teichert, C., 1953. Soil horizons and marine bands in the Coastal Limestones of Western Australia. Journal and Proceedings of the Royal Society New South Wales 86, 68–87.

Fairbridge, R.W., Johnson, D.L., 1978. Eolianite. In: Fairbridge, R.W., Bourgeois, J. (Eds.), The Encyclopedia of Sedimentology. Encyclopedia of Earth Sciences Series, Volume VI. XVI. Dowden, Hutchinson and Ross, Stroudsburg, 279–282.

Faust, D., Yurena, Y., Willkommen, T., Roettig, C., Richter, Dan, Richter, Dav, Suchodoletz, H.v., Zöller, L., 2015. A contribution to the understanding of late Pleistocene dune sand-paleosol-sequences in Fuerteventura (Canary Islands). Geomorphology 246, 290–304.

Ferrer-Valero, N., Hernández-Calvento, L., Hernández-Cordero, A. I., 2019. Insights of long-term geomorphological evolution of coastal landscapes in hot-spot oceanic islands. Earth surface processes and landforms 44, 565–580.

Fletcher III, C. H., Murray-Wallace, C. V., Glenn, C. R., Sherman, C. E., Popp, B., Hessler, A., 2005. Age and Origin of Late Quaternary Eolianite, Kaiehu Point (Moornomi), Molokai, Hawaii. Journal of Coastal Research 42, 97-112.

IDE Canarias (Infraestructura de datos especiales de Canarias): https://visor.grafcan.es/visorweb/# , retrieved 2019.

Maud, R.R., 1968. Quaternary geomorphology and soil formation in coastal Natal. Zeitschrift für Geomorphologie - Supplement Band 7, 155–199.

MacFarlane, D. J., Ridley, W. I., 1969. An interpretation of gravity data for Lanzarote, Canary Islands. Earth and planetary science letters 6, 431-436.

McCarthy, M. J., 1967. Stratigraphical and sedimentological evidence from the Durban region of major sea-level movements since the late tertiary. South African Journal of Geology 70, 135 – 165.

McKee, E. D., Ward, W. C., 1983. Eolian environment. In: Scholle, P.A., Bedout, D.G.,

Moore, C.H. (Eds.), 1983. Carbonate Depositional Environments, AAPG Memoir, vol. 33. American Association of Petroleum Geologists, Tulsa, 132–169.

Meco, J., 1993. Testimonios paleoclimáticos en Fuerteventura. Tierra y Technología 6, 41-48.

Meco, J. (Ed.), 2008. Historia geológica del clima en Canarias (Las Palmas de Gran Canaria).

Meco, J., Muhs, D.R., Fontugne, M., Ramos, A.J.G., Lomoschitz, A., Patterson, D., 2011. Late Pliocene and Quaternary Eurasian locust infestations in the Canary Archipelago. Lethaia 44, 440–454.

Medwenitsch, W., 1970. Zur Geologie und regionalen Stellung der Canarischen Inseln. Mitteilungen der Geologischen Gesellschaft in Wien 63, 160-184.

Moreno, A., Targarona, J., Henderiks, J., Canals, M., Freudenthal, T., Meggers, H., 2001. Orbital forcing of dust supply to the North Canary Basin over the last 250 kyr. Quaternary Science Reviews 20, 1327-1339.

Moreno, A., Nave, S., Kuhlmann, H., Canals, M., Targarona, J., Freudenthal, T., Abrantes, F. F., 2002. Productivity response in the North Canary Basin to climate changes during the last 250000 yr: A multi-proxy approach. Earth and Planetary Science Letters 196, 147-159.

Müller, G., 1964. Frühdiagenetische allochthone Zementation mariner Küsten-Sande durch evaporitische Calcit-Ausscheidung im Gebiet der Kanarischen Inseln. Beiträge zur Mineralogie und Petrographie 10, 125–131.

Müller, G., Tietz, G., 1975. Regressive diagenesis in Pleistocene eolianites from Fuerteventura, Canary Islands. Sedimentology 22, 485-496.

Pye, K., Tsoar, H., 2009. Aeolian Sand and Sand Dunes. Springer-Verlag, Berlin.

Reynolds, J. F., Stafford Smith, D. M., Lambin, E. F., Turner II, B. L., Mortimore, M., Batterbury, S. P. J., Downing, T. E., Dowlatabadi, H., Fernández, R. J., Herrick, J. E., Huber-Sannwald, E., Jiang, H., Leemans, R., Lynam, T., Maestre, F. T., Ayarza, M. Walker, B., 2007. Global Desertification: Building a Science for Dryland Development. Science 316, 847-851.

Rivas-Martínez, S., 2009. Ensayo geobotánico global sobre la Macaronesia. In: Beltrán Tejera, E., Afonso Carrillo, J., García Gallo, A., Roedríguez Delgado, O. (eds.), 2009. Homenaje al profesor Dr. Wolfredo Wildpret de la Torre. Instituto de Estudios Canarios, La Laguna (Tenerife, Islas Canarias).

Roettig, C-B., Varga, G., Sauer, D., Kolb, T., Wolf, D., Makowski, V., Recio Espejo, J.

M., Zöller, L., Faust, D., 2019. Characteristics, nature, and formation of palaeosurfaces within dunes on Fuerteventura. Quaternary Research Volume 91, Issue 1, 4-23.

Rothe, P., 2008. Kanarische Inseln. Sammlung Geologische, Führer 81, Gebrueder Borntraeger, Stuttgart.

Sayles, R.W., 1931. Bermuda during the ice age. Proceeding of the America Academy of Arts and Science 66, 381–467.

Short, A. D., 2005. Carbonate sandy beaches. In: Schwartz, M. (Ed.). Encyclopedia of Coastal Science. Springer Netherlands. 218 – 220.

Sperling, C.H.B., Goudie, A.S., 1975. The Miliolite of western India. A discussion of the aeolian and marine hypotheses. Sedimentary Geology 13, 71–75.

Sunding, P., 1979. Origins of the Macaronesian flora. In: David Bramwell (ed.), 1979. Plants and Islands. Academic Press, London. 13-40.

Von Suchodoletz, H., Oberhänsli, H., Hambach, U., Zöller, L., Fuchs, M., Faust, D., 2010. Soil moisture fluctuations recorded in Saharan dust deposits on Lanzarote (Canary Islands) over the last 180 ka. Quaternary Science Reviews 29, 2173–2184.

Von Suchodoletz, H., Zöller, L., Hilgers, A., Radtke, U., Faust, D., 2013. Vegas and dune-palaeosoil- sequences – two different palaeoenvirnmental archives on the Eastern Canary Islands. In: Fernández-Palacios, J. M., de Nascimento, L., Hernández, J. C., Clemente, S., González, A., Díaz-González, J. P. (Eds.), 2013. Climate change perspectives from the Atlantic: past, present and future. Servicio de Publicaciones, Universidad de La Laguna de Tenerife, 249-264.

Ward, W.C, 1973. Influence of climate on the early diagenesis of carbonate eolianites. Geology 1, 171-174.

Warren, J.K., 1983. Pedogenic calcrete in Quaternary calcareous dunes in coastal Southern Australia. Journal of Sedimentary Petrology 53,787-796.

Yaalon, D. H., 1967. Factors affecting the lithification of eolianite and interpretation of its environmental significance in the coastal plain of Israel. Journal of Sedimentary Petrology 37, 1189–1199.

Zarei, M. (1989): Verwitterung und Mineralneubildung in Böden aus Vulkaniten auf Lanzarote (Kanarische Inseln). Verlag B. Schulz, Berlin.

Zöller, L., von Suchodoletz, H., Küster, N., 2003. Geoarchaeological and chronometrical evidence ofearly human occupation on Lanzarote (Canary Islands). Quaternary Science Reviews 22, 1299–1307.

8 Acknowledgements

Professor Dominik Faust

Dominik, ich danke Dir sehr für Dein Vertrauen auf dessen Grundlage Du mir die Möglichkeit gabst, mich im Gelände Fuerteventuras beweisen zu dürfen, für Deine beeindruckende Offenheit, mit der Du mir, trotz Deiner klar überlegenen Erfahrung, bei manch intensiver Diskussion immer wieder Raum gabst und natürlich danke ich Dir für viele viele geöffnete Türen! Du hast mir nicht nur ermöglicht, auf vielen Tagungen dabei sein zu können, sondern Du hast mich zur Teilnahme ermutigt und mir den Stellenwert der öffentlichen Diskussion klar gemacht; bishin zum internationalen Symposium auf Fuerteventura, mit dem Verantwortung und Vertrauen nochmals anwuchsen. Eine sehr bereichernde Zeit verdanke ich in großem Maße Dir und freue mich auf das was kommt!

Professor Ludwig Zöller

Ludwig, hab großen Dank für Dein Vertrauen, Deinen Zuspruch und Deine Hilfe!

Professorin Daniela Sauer,

Daniela, ich danke Dir sehr, dass Du seinerzeit Dein Einverständnis gabst, so dass ich diese Arbeit überhaupt antreten konnte und Du darüber hinaus zur Zusammenarbeit auf den Kanaren bereit warst! Es waren gute Tage im Gelände, gepaart mit hilfreichen Diskussionen und Resultaten. Hab auch Dank für alle ausgiebigen Telefonate für die Du Dir stets Zeit freihieltest!

PD Dr. Michael Zech,

ich danke Dir sehr für allen gegebenen Freiraum, viele Diskussionen, Deine wertvollen Meinungen und Ratschläge und Deinen Rückhalt!

Dr. Thomas Kolb

Thomas, es war eine super Zeit mit Dir im Gelände und ebenso während aller Diskussionen! Ich danke Dir vor allem auch für den Einblick in Deine Methodenwelt! Was für eine angenehme und fruchtbare Zusammenarbeit –vielen vielen Dank!

Dr. Daniel Wolf

Daniel, hab großen Dank für alle schweißtreibende Arbeit im Gelände, alle Diskussionen währenddessen und im Nachgang!

Dr. Sascha Meszner

Sascha, wenn ich eine Idee habe, ist Deine Tür meist die erste –hab Dank für alle aufgebrachte Zeit, Deine Meinungen und alle Diskussionen!

Rico Hübner

Rico, ich war stets froh Deine Meinung zu hören, da Du auf Dinge zu achten vermagst, die ausserhalb meiner Sensoren liegen – hab großen Dank! …natürlich auch für alle Hilfe bei den „Abkürzungen“ in der Arbeit mit „R“ (ohne Dich hätte ich bei manchen Schritten dreimal so lang gebraucht)

Herzlichen Dank für alle Zeit und Anregungen an Hans von Suchodoletz! Besonderer Dank gilt Professor Ulrich Hambach, der alle Magnetikmessungen betreute und somit großer Rückhalt war. Ebenso ganz herzlichen Dank an Anja Schleicher & Andrea Gotzsche für die reibungslose und effektive Zusammenarbeit! Vielen Dank an Professor Bernd Ullrich für die XRF-Messungen und Auswertung und an Michael Dietze für die Möglichkeit sämtliche Korngrößenmessungen am GFZ Potsdam durchführen zu können, ebenso für alle Diskussionen! Natürlich auch großen Dank für die Zeit vor und während des Symposiums auf Fuerteventura an Ramona Winter, Yesmine Trigui und Amelie Demmer! Weiterhin vielen Dank an Andreas Scheffler, Philipp Baumgart, Clara Scheffler, Christiane Richter, Florian Schneider, Vera Makowski, Jakob Labahn, Lena Lorenzen, Patrick Schielein und Eric Walliser. Ein großes Dankeschön an Sibylle Fruhstorfer für allen Verwaltungsaaufwand in Sachen Dienstreisen, Abrechnungen etc.!

Beate Winkler & Sieglinde Gerstenhauer, habt großen Dank für alle Laborarbeit und Euren Rückhalt! Allen Kollegen (weiblich wie männlich) des Instituts danke ich für das sehr angenehme Miteinander!

Dr. György Varga

Gyuri, many thanks for our fruitful cooperation! You really pushed the studies forward - it is a blessing and pleasure to work with you –thanks a lot!

Many many thanks to Maria Tarquis Gongora & Don Manuel! You always permitted access to our main sections and welcomed us cordially and obliging – I am deeply in your dept!

Victor, thanks a lot for your great hospitality – I loved to stay in Villaverde!

Concha, you are something like the mother and the good soul of La Oliva – many thanks for welcoming us and our international guests to the symposium!

Inmaculada Menéndez & Laura Cabrera, many thanks to you for staying with us in field, for all discussions and the good time we had together!

José Mangas and Ignacio Alonso, many thanks for welcoming us with open arms and for your great help during the symposium on Fuerteventura – I learned a lot!

Professor José Manuel Recio-Espejo, many thanks for the fruitful cooperation!

Ganz herzlichen Dank der DFG – ohne solch eine großartige Möglichkeit der Förderung von Grundlagenforschung wären dieserlei Arbeiten schwer möglich!

Den Gutachtern danke ich für alle aufgebrachte Zeit und für das Hineindenken in die Darstellungen der Arbeiten der vergangenen Jahre!

Meinen Eltern danke ich stets
und
Stefanie & Noah & Anna – ohne Euch wäre das alles nicht halb soviel wert
– DANKE!